IJASST
International Journal of
Applied Sciences and Smart Technologies

Volume 07
Issue 01
June 2025

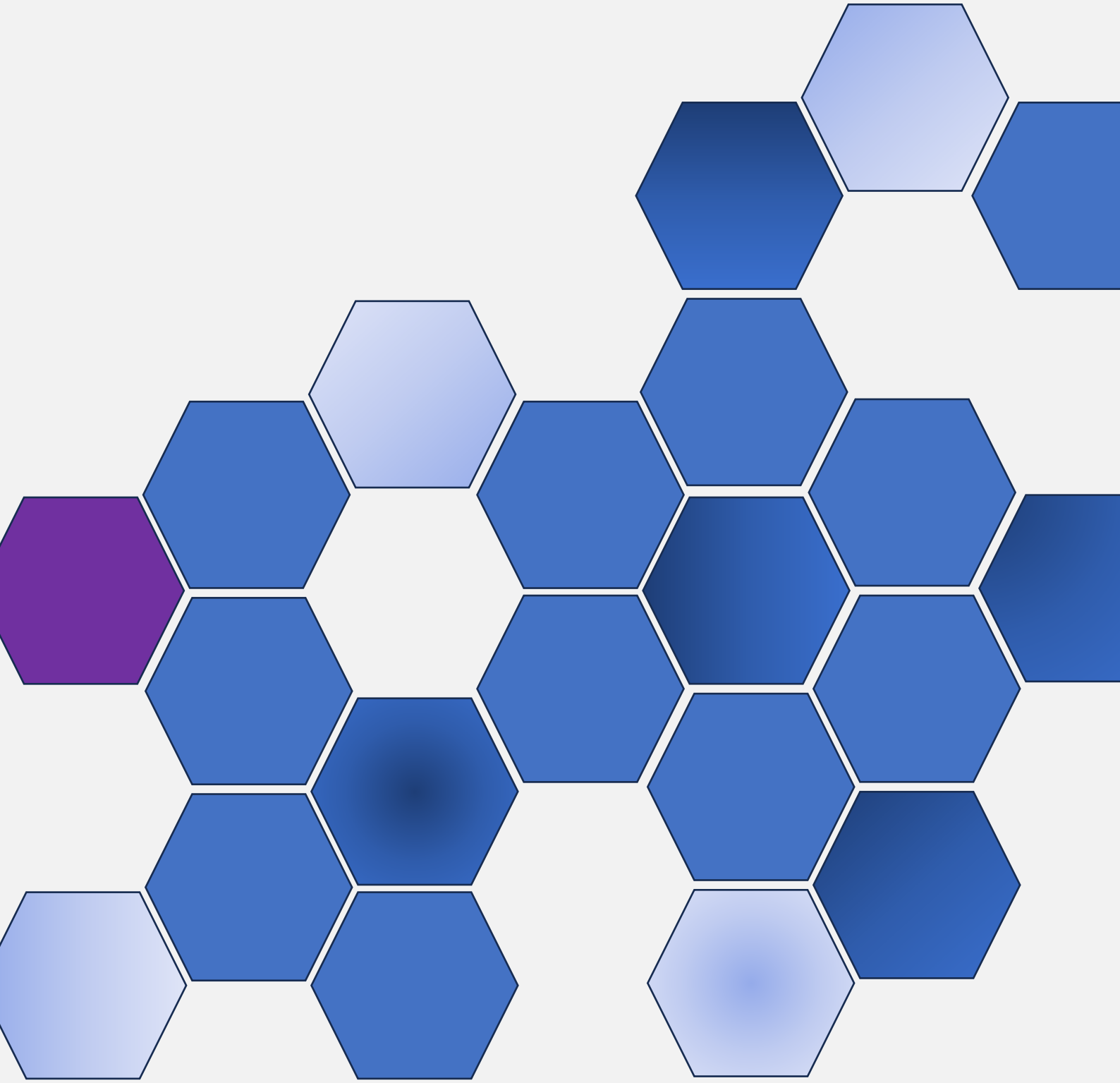

Faculty of Science and Technology
Universitas Sanata Dharma

IJASST
International Journal of
Applied Sciences and Smart Technologies
p-ISSN 2655-8564, e-ISSN 2685-943, 2024

Volume 07
Issue 01

CONTENTS

IJASST
International Journal of
Applied Sciences and Smart Technologies
p-ISSN 2655-8564, e-ISSN 2685-943, 2024
Volume 07
Issue 01

IJASST
International Journal of
Applied Sciences and Smart Technologies
p-ISSN 2655-8564, e-ISSN 2685-943

PREFACE

Dear readers, we are delighted to serve you Volume 07, Issue 01 of *International Journal of Applied Sciences and Smart Technologies* (IJASST), which is managed and published by the Faculty of Science and Technology, Universitas Sanata Dharma. IJASST is an open-access peer-reviewed journal that mediates the dissemination of research and studies conducted by academicians, researchers, and practitioners in science, engineering, and technology. Its scope also includes basic sciences which relate to technology, such as applied mathematics, physics, and chemistry.

In this edition, we have fifteen papers authored by researchers from Indonesia, Bangladesh, Nigeria, and South Africa. Submitted papers are reviewed fairly using the open journal system (OJS) of IJASST. After the review process, accepted papers of the journal are publicly available for free at the website of IJASST. For future issues, we are looking forward to your contributions to IJASST.

Dr. I Made Wicaksana Ekaputra
Editor in Chief
IJASST

IJASST International Journal of Applied Sciences and Smart Technologies

Volume 07
Issue 01

p-ISSN 2655-8564, e-ISSN 2685-943, pp. 1-14, 2025

Cluster Change Analysis to Assess the Effectiveness of Speaking Skill Techniques Using Machine Learning

Nunik Herani Wulandari[1], Vega Purwayoga [2*]

[1]*University of Muhammadiyah Tasikmalaya, Indonesia*
[2] *Department of Informatics, Faculty of Engineering, Siliwangi University, Indonesia*
[*]*Corresponding Author: vega.purwayoga@unsil.ac.id*

(Received 30-08-2024; Revised 22-09-2024; Accepted 07-10-2024)

Abstract

Students have different characteristics in the learning process, especially in developing speaking skills. So it requires the right learning method. This study aims to compare effective teaching methods for speaking using machine learning. The classes used in this study consisted of three classes: conventional, vlog project, and picture series. The data used were students' pre-test and post-test scores. The machine learning algorithm used is K-Means. K-Means clusters the pre-test and post-test data. The results of K-Means clustering on the pre-test and post-test identified the differences in student groups between the pre-test and post-test. Students who experienced the most cluster movement were those in the vlog project class, the conventional class, and the picture series class.

Keywords: Clustering, K-Means, Machine Learning, Speaking Skill

1 Introduction

Speaking is one way to communicate with someone. The main components of speaking include fluency, comprehension, grammar, vocabulary, and pronunciation [1]. Speaking skills do not appear instantly, so regular practice is needed. One of the places to practice speaking skills is at school with the help of teachers [2]. Intensive learning can improve speaking skills, especially in English lessons [3].

Based on research [4], students need to develop skills in speaking English. The earlier students learn English, the easier it is for them to understand English. Learning English is an investment for a bright future. Speaking English allows us to easily access and obtain information because Most people write information in English.

This work is licensed under a Creative Commons Attribution 4.0 International License

Some effective teaching techniques for learning to speak include vlog projects and picture series [5]. The picture series technique allows educators to see the development of students' speaking skills. The picture series learning model positively impacts speaking ability [6]. There is a significant difference between classes that use conventional learning methods and classes that use the picture series learning method [7]. Vlog projects can improve speaking skills by an average of 27%. Vlog projects are the preferred learning method, and a student's level of desire for the method is 89% [8]. Like previous research, research [9] also revealed that vlog projects are an effective learning method to improve students' speaking skills.

Some previous studies have discussed the effectiveness of picture series and vlog project learning methods to improve students' ability to speak English [6]. Few discuss which comparison is more effective than the picture series and vlog project. Research that compares picture series and vlog project learning methods is research [5]. The study's results [5] stated that the vlog project was more effective than the picture series. Comparing effective learning methods in speaking skills can be done with machine learning techniques [10]. Research [11] applied a machine learning algorithm, K-Means, to evaluate effective learning methods. K-Means effectively cluster and evaluate student performance [12]. This research continues the research conducted by previous research [5]. Since K-Means works effectively and few studies compare the learning methods of picture series and vlog projects, this research aims to group students based on pre-learning and post-learning results. This research has contributed in terms of verifying cluster changes that have not been carried out by previous studies. Grouping children is expected to determine the changes or consistency of children's groups when Educators use the picture series or vlog project learning method.

2 Material and Methods

Study Area and Research Data

This research was conducted on the eighth-grade students at MTs Negeri 13 Ciamis located at Jalan Cipancur No. 6 Sirnabaya, Rajadesa, Ciamis Regency, West Java, in the even semester of 2020 / 2021. The researcher conducted research from January to April 2021. This research has several stages as presented in Figure 1.

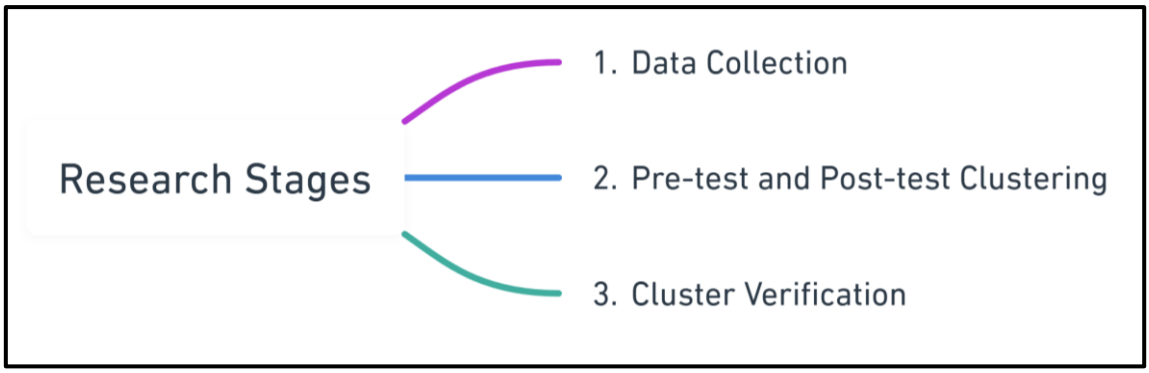

Figure 1. Research Stages

Data Collection

Data collection in the study was to collect pre-test and post-test scores of students from three classes, namely, conventional, vlog project, and picture series classes. The pre-test data collection process was carried out before the learning process, while the students took the post-test after the learning process. The learning process is carried out based on each class. In conventional classes, the English language subject teachers at the school carry it out.

Pre-test and Post-test Clustering

The K-Means cluster is applied using R programming. R Programming is a high-level language easily applied to data mining techniques [13]. K-Means is a popular clustering algorithm. The way K-Means works is to partition data into several groups based on the characteristics of the data. The first object in a cluster can be used as the cluster center point. The K-Means algorithm will repeat the following steps until the center point of a cluster does not change [14]. The stages of the K-Means algorithm can be seen in Figure 2.

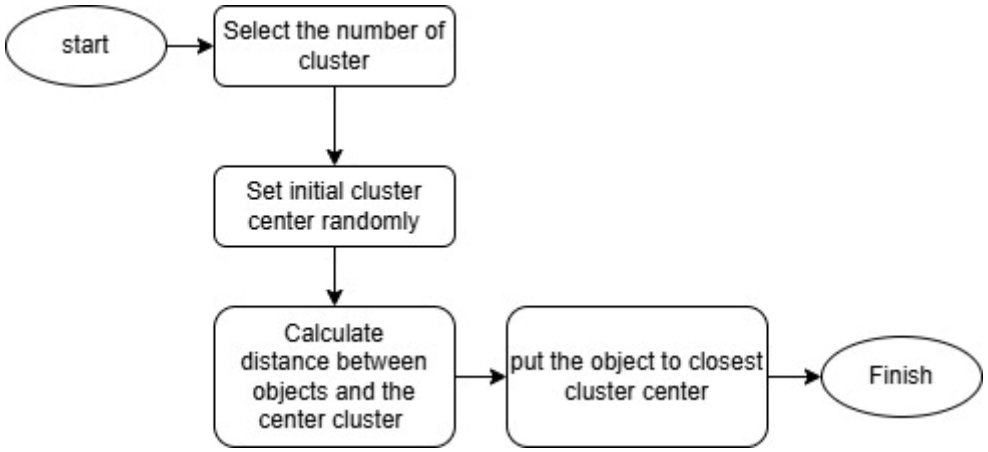

Figure 2. The stages of the K-Means algorithm [15][16]

Cluster Verification

Cluster verification is conducted to determine whether there is a shift or change in a student group after the treatment of each learning technique.

3 Results and Discussions

Data Collection

Data was collected by taking pre-test and post-test data from all classes. The classes consisted of a vlog project class, a picture series class, and a class that applied conventional techniques. The number of students in a class has been presented in Figure 3. The results of the pre-test and post-test data collection from the vlog project, picture series, and conventional classes are presented in Table 1, Table 2, and Table 3, respectively.

Figure 3. Number of students

Figure 2 is a histogram that explains the number of students in each class. The number of students in the conventional class consists of 20 students, the picture series class is 18, and the vlog project class consists of 19 students.

Table 1. Pre-test and post-test of vlog project class

No.	Student	Pre-test	Post-test
1	V1	44	66
2	V2	46	67
3	V3	46	67
4	V4	46	67
5	V5	44	65
6	V6	48	70
7	V7	45	60
8	V8	50	71
9	V9	52	72
10	V10	48	71
11	V11	45	66
12	V12	45	70

13	V13	48	70
14	V14	44	66
15	V15	50	71
16	V16	50	72
17	V17	50	72
18	V18	44	67
19	V19	47	67
	Average	47	68

As presented in Table 1, the average pretest score obtained by students is 47, while the posttest score is 68. There is an increase in value between the pretest and posttest scores found in the vlog project class.

Table 2. Pre-test and post-test of picture series class

No.	Student	Pre-test	Post-test
1	P1	48	67
2	P2	44	61
3	P3	47	66
4	P4	46	63
5	P5	48	66
6	P6	46	64
7	P7	44	60
8	P8	46	65
9	P9	49	67
10	P10	48	66
11	P11	50	70
12	P12	50	69
13	P13	52	71
14	P14	52	71
15	P15	44	63

16	P16	45	63
17	P17	44	60
18	P18	48	68
	Average	47	66

In Table 2, the average pretest score obtained by students is 47, while the posttest score is 66. Similar to the vlog project class, the picture series class also experienced an increase between the pretest and posttest scores.

Table 3. Pre-test and post-test of conventional class

No.	Student	Pre-test	Post-test
1	C1	44	59
2	C2	46	61
3	C3	44	59
4	C4	48	63
5	C5	50	68
6	C6	50	66
7	C7	44	60
8	C8	50	66
9	C9	49	65
10	C10	48	62
11	C11	44	59
12	C12	45	61
13	C13	48	64
14	C14	50	68
15	C15	46	61
16	C16	48	65
17	C17	47	62
18	C18	46	61
19	C19	50	66

20	C20	45	60
	Average	47	63

In Table 3, the average pretest score obtained by students is 47, while the posttest score is 63. The learning process increased the performance of all classes.

Clustering Pre-test

The method section explains that the R programming language assists this research. The libraries and functions used to apply K-Means are the cluster library and the kmeans() function. Each class will be grouped into three groups: cluster 1 = group of students with low pre-test scores, cluster 2 = group of students with medium pre-test scores, and cluster 3 = group of students with high pre-test scores. The results of student clustering for pre-test scores have been presented in Table 4.

Table 4. Pre-test clustering results

Class	Cluster	Student	Average student grades
Vlog Project	Cluster 1	V1, V2, V3, V4, V5, V7, V11, V12, V14, V18	45
	Cluster 2	V6, V10, V13, V19	48
	Cluster 3	V8, V9, V15, V16, V17	50
Picture Series	Cluster 1	P2, P4, P6, P7, P8, P15, P16, P17	45
	Cluster 2	P10, P3, P5, P9, P11, P18	48
	Cluster 3	P12, P13, P14	51
Conventional	Cluster 1	C1, C2, C3, C7, C11, C12, C15, C18, C20	45

	Cluster 2	C4, C9, C10, C13, C16, C17	48
	Cluster 3	C5, C6, C8, C14, C19	50

Clustering Post-test

As with pretest scores, post-test scores were also grouped to determine any differences between groups formed based on the pretest and based on post-test scores. The results of student grouping for post-test scores have been presented in Table 5.

Table 5. Post-test clustering results

Class	Cluster	Student	Average student grades
Vlog Project	Cluster 1	V7	60
	Cluster 2	V1, V2, V3, V4, V5, V11, V14, V18, V19	66
	Cluster 3	V6, V8, V9, V10, V12, V13, V15, V16, V17	71
Picture Series	Cluster 1	P2, P4, P7, P15, P16, P17	62
	Cluster 2	P1, P3, P5, P6, P8, P9, P10, P18	66
	Cluster 3	P11, P12, P13, P14	70
Conventional	Cluster 1	C1, C2, C7, C11, C20	59
	Cluster 2	C2, C4, C10, C12, C15, C17, C18	62
	Cluster 3	C5, C6, C8, C9, C13, C14, C16, C19	66

Table 4 and Table 5 show a difference between the average pre-test and post-test scores. Table 5 shows that the number of students included in Cluster 1 is less than the other clusters in all classes. The highest average post-test score for cluster 3 is in the vlog project class. The vlog project class has an average post-test score of 71, the picture series score of 70, and the conventional class has a score of 66.

Cluster Verification

Each student is identified in cluster verification to see if there is a change after the learning process. The identification process is done by looking at changes in student clusters based on pre-test and post-test scores. The results of cluster verification can be seen in Table 6.

Table 6. Cluster verification

Class	Student	Cluster origin	Move to cluster
Vlog Project	V1	Cluster 1	Cluster 2
	V2	Cluster 1	Cluster 2
	V3	Cluster 1	Cluster 2
	V4	Cluster 1	Cluster 2
	V5	Cluster 1	Cluster 2
	V11	Cluster 1	Cluster 2
	V12	Cluster 1	Cluster 2
	V14	Cluster 1	Cluster 2
	V18	Cluster 1	Cluster 2
	V6	Cluster 2	Cluster 3
	V10	Cluster 2	Cluster 3
	V13	Cluster 2	Cluster 3
Picture Series	P6	Cluster 1	Cluster 2
	P8	Cluster 1	Cluster 2
	P11	Cluster 2	Cluster 3
Conventional	C3	Cluster 1	Cluster 2
	C12	Cluster 1	Cluster 2
	C15	Cluster 1	Cluster 2
	C18	Cluster 1	Cluster 2

C9	Cluster 2	Cluster 3
C13	Cluster 2	Cluster 3
C16	Cluster 2	Cluster 3

In Table 6, the class that experienced the most cluster changes was the vlog project class. Students who experience cluster movement make up 12 or approximately 63% of the students in the vlog project class. In the picture series class, students who experienced cluster changes were three students, and for conventional classes, there were as many as seven classes.

4 Conclusions

This study has successfully analyzed the best learning method to improve speaking skills by using the K-Means algorithm. The results of the cluster verification show that the vlog project is the class whose students have the most cluster changes compared to the other classes. That can be a reference to the fact that the vlog project is one of the effective learning techniques for improving speaking skills. This study only uses two assessment parameters to determine the best learning method. It is hoped that subsequent studies can use other parameters to strengthen the results of this study.

Acknowledgements

The author would like to thank the staff of MTs Negeri 13 Ciamis who have supported this research so that this research can be completed.

References

[1] A. E. Warliati, Z. Rafli, and D. Darmahusni, “Discussion and Think-Pair-Share Strategies on the Enhancement of EFL Students’ Speaking Skill: Does Critical Thinking Matter?,” *Journal of English Language Studies*, vol. 4, no. 2, p. 120, Sep. 2019, doi: 10.30870/jels.v4i2.6100.

[2] Riris Nurkholidah Rambe, Andini Syahfitri, Aini Humayroh, Nadila Alfina, Putri Azkia, and Tania Dwi Rianti, "Upaya Meningkatkan Keterampilan Berbicara Di Depan Umum," *Jurnal Pendidikan dan Sastra Inggris*, vol. 3, no. 2, pp. 11–24, Jun. 2023, doi: 10.55606/jupensi.v3i2.1966.

[3] H. Hotmaria, "Upaya Meningkatkan Keterampilan Berbicara Bahasa Inggris pada Materi Pengandaian Diikuti Perintah/Saran Menggunakan Strategi Pembelajaran Three Step Interview," *Journal of Education Action Research*, vol. 5, no. 1, Jan. 2021, doi: 10.23887/jear.v5i1.31558.

[4] I. Hikmawan, I. L. Damayanti, and S. Setyarini, "Integrating Traditional Games into EFL Speaking Class: A case of English for Young Learners," *Journal of English Language Studies*, vol. 8, no. 2, p. 249, Sep. 2023, doi: 10.30870/jels.v8i2.19432.

[5] N. H. Wulandari and A. Ashadi, "Vlog Project or Picture Series: Examining Effective Techniques in Teaching Speaking Skills," *Jurnal Pendidikan Progresif*, vol. 11, no. 2, pp. 275–289, 2021, doi: 10.23960/jpp.v11.i2.202111.

[6] Ana Sri Lestari and N. I. Sholichah, "Improving Speaking Ability By Using Picture Series," *Jurnal Penelitian Ilmiah INTAJ*, vol. 6, no. 1, pp. 22–41, Apr. 2022, doi: 10.35897/intaj.v6i1.728.

[7] Chairani Annisa, Reflinda Reflinda, Melyan Melani, and Veni Roza, "The Effect of Using Picture Series toward Students' Speaking Skill at the Second Grade in MTSS Nagari Binjai," *Populer: Jurnal Penelitian Mahasiswa*, vol. 1, no. 4, pp. 19–33, Dec. 2022, doi: 10.58192/populer.v1i4.248.

[8] Z. Zubaidi, R. P. Suharto, and E. L. Rahayu, "Improving Students' Speaking Skill through Students Vlog Project as PBL Output on Online Speaking Class," *Briliant:*

Jurnal Riset dan Konseptual, vol. 6, no. 4, p. 764, Nov. 2021, doi: 10.28926/briliant.v6i4.757.

[9] K. Febianti, S. Wahyuni, and I. Imadona, "Vlog Project In Enhancing Students' Speaking Achievement," *Esteem Journal of English Education Study Programme*, vol. 6, no. 2, pp. 353–360, Jul. 2023, doi: 10.31851/esteem.v6i2.12321.

[10] B. Wu and C. Zheng, "An Analysis of the Effectiveness of Machine Learning Theory in the Evaluation of Education and Teaching," *Wirel Commun Mob Comput*, vol. 2021, pp. 1–10, Oct. 2021, doi: 10.1155/2021/4456222.

[11] S. Anwar, T. Suprapti, G. Dwilestari, I. Ali, P. Studi Rekayasa Perangkat Lunak Jln Perjuangan No, and B. Kesambi Kota Cirebon, "Pengelompokkan Hasil Belajar Siswa Dengan Metode Clustering K-Means Program Studi Sistem Informasi Jln Perjuangan No 10B Kesambi Kota Cirebon 4)," *Jurnal Sistem Informasi dan Teknologi Informasi)*, vol. 4, no. 2, pp. 60–72, 2022.

[12] S. N. Br Sembiring, H. Winata, and S. Kusnasari, "Pengelompokan Prestasi Siswa Menggunakan Algoritma K-Means," *Jurnal Sistem Informasi Triguna Dharma (JURSI TGD)*, vol. 1, no. 1, p. 31, Jan. 2022, doi: 10.53513/jursi.v1i1.4784.

[13] V. Purwayoga and B. Susanto, "Pengelompokkan Daerah Berdasarkan Ketersediaan Masjid Muhammadiyah Dengan Algoritma K-Means," vol. 13, no. 1, 2021, doi: 10.24853/jurtek.13.1.75-80.

[14] V. Purwayoga, "Optimasi Jumlah Cluster pada Algoritme K-Means untuk Evaluasi Kinerja Dosen," *Jurnal Informatika Universitas Pamulang*, vol. 6, no. 1, p. 118, Mar. 2021, doi: 10.32493/informatika.v6i1.9522.

[15] H. Gunawan and V. Purwayoga, "Data Mining Menggunakan Algoritma K-Means Clustering Untuk Mengetahui Potensi Penyebaran Virus Corona Di Kota Cirebon,"

Jurnal Sisfokom (Sistem Informasi dan Komputer), vol. 11, no. 1, pp. 1–8, Jan. 2022, doi: 10.32736/sisfokom.v11i1.1316.

[16] P. Pangestu, S. Maarip, Y. Nur Addinsyah, and V. Purwayoga, "Clustering and Trend Analysis of Priority Commodities in the Archipelago Capital Region (IKN) using a Data Mining Approach," *International Journal of Applied Sciences and Smart Technologies*, vol. 6, no. 1, Jun. 2024, doi: 10.24071/ijasst.v6i1.7798.

IJASST International Journal of Applied Sciences and Smart Technologies

Volume 07
Issue 01

p-ISSN 2655-8564, e-ISSN 2685-943, pp. 15-28, 2025

Assessing Motorcycle Helmet Usage Rates and Road Safety Laws Awareness Among Motorcyclists in Bangladesh

Md. Tanjil Mahmud Khan[1*]

[1]*Department of Civil Engineeirng, Daffodil International University, Bangladesh*
[*]*Corresponding Author: tanjildiu@gmail.com*

(Received 03-10-2024; Revised 30-10-2024; Accepted 02-11-2024)

Abstract

This study examines helmet use and motorcyclists' awareness about road safety laws regarding helmet usage in Darial union of Bakerganj Upazila in Bangladesh. For this study I have used Quantitative research methodology and used JASP statistical software for descriptive analysis and Chi-square tests. I have collected data from 100 participants that representing various age groups and professions. Then after data analysis it was revealed that, youngest age group of (15-20); here 33.33% people do not believe that wearing helmet is important and 66.67% are not aware about road safety laws regarding helmet usage. And older age groups (41-50 and 51 or above) here 100% aware of road safety laws regarding helmet usage. By profession here 60.61% "motorcycle driver" do not agree with motorcycle helmet wearing is important. In Darial Union, here it is the only category "student" who are used helmet during accident time is 0%. Middle age and older aged groups people helmet using rate is high comparing to other, (31-35) age group is 69.57%, 80% for the 41-50, 100% for those aged 51 and above. But few extra-ordinary groups like teachers, doctors, retired persons, and government job holders, had a helmet usage rate of about 100% during accident time. And here younger people, especially students, shows very low interest in wearing helmet and road safety training, while 100% of those aged 41+ and all government employees, teachers, doctors, and retirees have received it.

Keywords: motorcycle helmet, helmet use, road safety, awareness among motorcyclists

1 Introduction

Bangladesh, like many other low- and middle-income nations, has seen a sharp rise in the number of motorcycle riders. On the other hand, practically little is known about motorcycle riders' use of helmets. Only 53% of those who regularly used safety helmets were among the 45.3% of people who reported wearing one. And, according

This work is licensed under a Creative Commons Attribution 4.0 International License

to the report, young, single motorcyclists in Bangladesh's rural areas do not wear helmets [1]. In Bangladesh, there are more than 1.1 million registered motorcycles, or approximately 57% of all registered motor vehicles [2]. Especially in areas where public transportation is not easily accessible, motorbikes are a common form of transportation in developing countries. Driving without a helmet increases one's risk of being involved in an accident by three times (OR: 3.423, p value < 0.05). Research shows that, Helmet use is proven to be a critical component in preventing traffic crashes in Noakhali, Bangladesh [3]. It was also found that people who wear helmets and survive motorbike accidents in the United States have lower hospitalization costs than people who don't wear helmets [4]. Cochrane did a systematic study in 2009 and found that motorcycle helmets lower the risk of death and injury for riders who crash [5].

Motorcycle accidents are a significant cause of injury and fatalities in Bangladesh. Especially in rural areas, wearing a helmet and knowing traffic safety laws are often neglected. Wearing a helmet has been shown to have numerous benefits. But many motorcycle riders in these areas still disregard this crucial safety measure. In the event of an accident, this behavior increases their risk of suffering severe injuries or passing away. A significant segment of the populace either needs more awareness of or disregards road safety regulations mandating the usage of helmets. A world study by Abbas et al. found that not wearing a helmet was the most important thing that affected the death rate of motorcyclists in an RTI and that helmets lower the risk of death in a crash [6].

In Hai Duong province in 2006, Hung et al. did an observational study and found that 29.9% of riders wore helmets. Men and adults were more likely to be wearing helmets than women and children. Throughout 37 road locations, 16,560 motorcycle riders were monitored (which includes 5 road classifications). Motorcycle riders used helmets on average 29.94% of the time. Men were more likely than women to wear helmets (odds ratio (OR) 1.64, 95% confidence interval (CI) 1.53 to 1.76) [7]. In a survey conducted in the USA with 445 participants, 68.4% said they always wore a helmet. The motorcyclists who did not always wear a helmet had higher odds of being male, having less education, and having a history of motorcycle accidents and injuries

compared to those who did. In this state where riding instruction is required, less than half of riders obtained their riding skills from rider education courses, and 44% of those who do not wear helmets stated they would only do so if required by law [8]. After adjusting for a number of potential confounders, a recent analysis conducted in California revealed that motorcycle helmets were associated with a significantly lower risk of head injuries (RR 0.40, 95% CI 0.31–0.52), fatal injuries (RR 0.44, 95% CI 0.26–0.74), and slightly lower but statistically significant chance of injuries to the neck (RR 0.63, 95% CI 0.40–0.99) [9]. As far as lessening the severity of head injuries sustained, motorcycle safety helmets are an effective way to increase safety. People working in manufacturing or on the land, those without a college degree, and those with a history of significant traffic infractions may find training programs especially beneficial [10]. However, a significant percentage of Malaysian riders (44%), claimed that they began riding without a valid license [11]. On highways and major metropolitan routes, as well as in the mornings and on weekdays, helmet usage is higher. The usage of safety helmets is higher among longer-distance travelers, regular riders, and motorcyclists with powerful engines [12].

According to the study of a researcher, M.F. Hasan in Bangladesh, 33.91% of respondents said in the response that they use helmets every day. About 52.87% of respondents said here they wore helmets most of the time, with 9.77% saying they did so occasionally. And, here Merely 1.72% of respondents acknowledged that they never use a helmet, and the same proportion said they wear one very infrequently when riding a motorcycle. Several rates of helmet use have been seen during field observations on various cities, highways, and regional roads. According to his observational survey, Dhaka has the highest average rate of helmet wearers—98.6% (drivers: 99.8% and passengers: 91.8%). Helmet use on regional roads such as the Barisal-Patuakhali Highway and the Bakerganj-Barguna regional road is extremely low, with just 45.7% and 17.5%, respectively. As per the statement, here most people don't wear helmets when they go on short rides, especially in hot weather when they don't expect to encounter law enforcement when riding on a local route. When riding for a brief distance, nearly 63% of respondents said to him, they typically avoid wearing helmets or don't wear them at all [13]. Only 54.6% of the 350 motorcycle riders knew about

road signs and safety requirements, while 16.9% needed more information. Furthermore, just 50.6% of respondents adhered to good road safety procedures, whereas 23.4% did not. Although most motorcycle riders were aware of specific signs and laws, their general road safety knowledge and practice needed to improve [14]. Helmets are extremely successful in preventing this kind of trauma, and the use of them is higher and the risk of head injuries among motorcycle riders is lower in areas where wearing one is mandatory [15].

Wearing a helmet dramatically lowers the risk of head and neck injuries by 53% and lowers the risk of death by 72% [16]. The best way to prevent or decrease the severity of injuries sustained in an accident is to wear a motorcycle helmet. According to the current meta-analysis, helmet use among motorcycle riders and passengers can rise significantly as a result of safety initiatives [17]. An analysis of accident data showed that from 2000 to 2014, there were 460 motorbike accidents in the Dhaka Metropolitan Area, resulting in 581 fatalities. Riding made up about 56.45% of the victims, followed by passengers (24.61%) and pedestrians (24.61%). Over 50% of deaths occurred among people under the age of thirty, while roughly 32% and 14%, respectively, occurred in people between the ages of 31 and 40. In the research area, the percentage of rear-end crashes was high (53.5%). The study also showed that 94% of incidents did not include the use of helmets [18].

Previous research study show that motorcycle accident is a very serious issue and, in those cases, using helmet is one of the best options that can help to reduce serious injury. And, there is no previous research work based on this selected area, darial Union of Bakerganj Upazila in Bangladesh. Like many rural places, the Darial Union of Bakerganj Upazila faces challenges related to road safety, particularly for motorcycle riders. This growing issue results from several factors, including a need for more knowledge about road safety laws, a lax attitude toward helmet use, and inadequate enforcement of existing regulations.

Here the exact problem is People are ignoring to wearing helmet, and then badly injured in motorcycle accident & facing even death, they have lack of awareness and knowledge about road safety laws regarding helmet usage. So, this research goal is to assessing the helmet using rates & understanding the percentage of motorcycle users

is concern about road safety law regarding helmet use in Darial Union of Bakerganj Upazila. And, after getting the data insights it will be easier for decision makers to take any decisions or steps.

2 Material and Methods

This study used a quantitative research method to investigate helmet usage rates among motorcyclists and their awareness of road safety laws. A structured questionnaire was implemented here to collect data from motorcycle users of different professions and ages in the Darial Union of Bakerganj Upazila, Bangladesh. Few years back there was no pitch road in this union, but recently developed the union with pitch road and increased motorcycle percentage. The reason of selecting this study area is, here I have physically seen and noticed, occurred several horrible motorcycle accidents and died all of them every time and observed none of them used helmet during that accident time, because I think they have lack of knowledge and awareness about it. The survey gathered information on their helmet usage habits and frequency, motorcycle ownership, involvement in motorcycle accidents, whether they wore a helmet during the accident, their awareness of road safety laws related to helmet usage, and whether they had received any training or lessons on the importance of wearing a helmet.

2.1 Instruments

At first, a structured survey was designed as the primary instrument for gathering data for this research. The survey included only closed-ended questions to allow quantitative analysis that focused on motorcycle helmet usage rates and road safety laws awareness among motorcyclists in darial union. The survey was carefully prepared to ensure clarity and avoid opacity, with questions formatted as yes/no options, Likert scales, and multiple-choice answers. Also, a pilot test was conducted with a small group of people to validate the instrument's effectiveness and make any necessary adjustments before full deployment.

2.2 Data Collection

To manage the scope of the research effectively, data collection was focused on the Darial Union, one of the 14 unions within Bakerganj Upazila, comprising 172 villages. The Darial Union, consisting of 15 villages, was selected as the study area. Data was gathered through a Google Form that was created and distributed online to residents of Darial Union. In addition to the online distribution, I visited the area to raise awareness about the study and to share the Google Form directly with individuals. For participants who did not have access to social media and email addresses, I conducted face-to-face interviews. I manually completed the Google Form on their behalf. This approach ensured inclusivity and a more comprehensive data collection process. Data was collected from 105 respondents with full consent, representing a diverse range of ages and professions.

2.3 Data Analysis

Firstly, the data collected through the structured questionnaire were cleaned by the process of manually checking including missing information in forms to ensure accuracy, and 100 samples were used from a total of 105 data samples for missing information of participants profession. Then entered the data into Microsoft Excel using coded values for efficiency. The dataset was then saved in .CSV format and imported into JASP (version 0.18.3) software, JASP is used for statistical analysis, where the coded values were converted back into string values for clarity during analysis. Here, at first descriptive statistics test was completed using JASP software to get mean, median, percent, frequency to summarize helmet usage patterns, motorcycle ownership, accident involvement percentage, justifying awareness level percentage, and the rate of trained persons. The study revealed varying levels of helmet usage, with notable differences based on ownership, profession, age, training, and awareness level. Then used chi-square tests to examine associations between categorical variables. This tests also explored the relationships between wearing helmets at accident time with the comparing age, profession, and motorcycle ownership factors.

3 Results & Discussions

After analyzing data from 100 participants, including 7 age groups and 10 professional categories, it was found that the youngest age group, those between 15 to 20 years old, had 33% who did not believe that wearing a helmet was important. The study also showed that within this age group, 66.67% were not aware of road safety laws regarding helmet usage. In Fig. 1; From the seven age groups, two groups (15-20 and 36-40) did not 100% believe that wearing a helmet was important. The other age groups generally recognized 100%, the importance of helmet use for motorcyclists. The study showed that only two age groups (41-50 & 51 or above), comprising the other participants, were 100% aware of road safety laws regarding helmet usage. In the youngest age group (15-20 years old), only 33.33% were aware of these laws. The second lowest awareness level was found in the 36-40 age group, where only 45% of participants were aware of road safety laws.

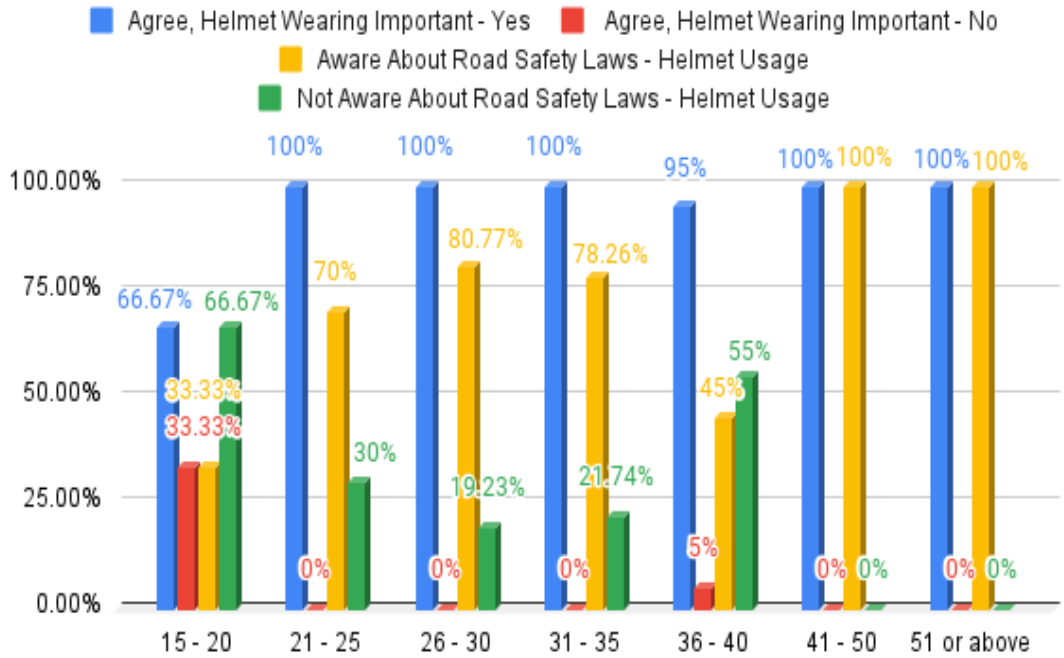

Figure 1. Helmet Wearing & Awareness rate about Road Safety by Age.

By profession, 60.61% of motorcycle drivers did not agree that wearing a helmet is important, which was the highest percentage among all groups. Among students, 50% were unaware of road safety laws regarding helmet usage, and 100% of unemployed individuals were not aware of these laws. Private job holders, unemployed individuals, and motorcycle drivers were the top categories not aware of road safety laws related to helmet usage, included in Fig. 2.

In Fig. 3; Middle-aged and older individuals had high helmet-wearing rates during accidents. Specifically, the rate was 69.57% for the 31-35 age group, 80% for the 41-50 age group, and 100% for those aged 51 and above. The only category with a 0% helmet usage rate during accidents was students. Highly educated individuals, such as teachers, doctors, retired persons, and government job holders, had a helmet usage rate of about 100% during accidents, data from Fig. 4. The lowest helmet usage rates during accidents were found among unemployed individuals and motorcycle drivers.

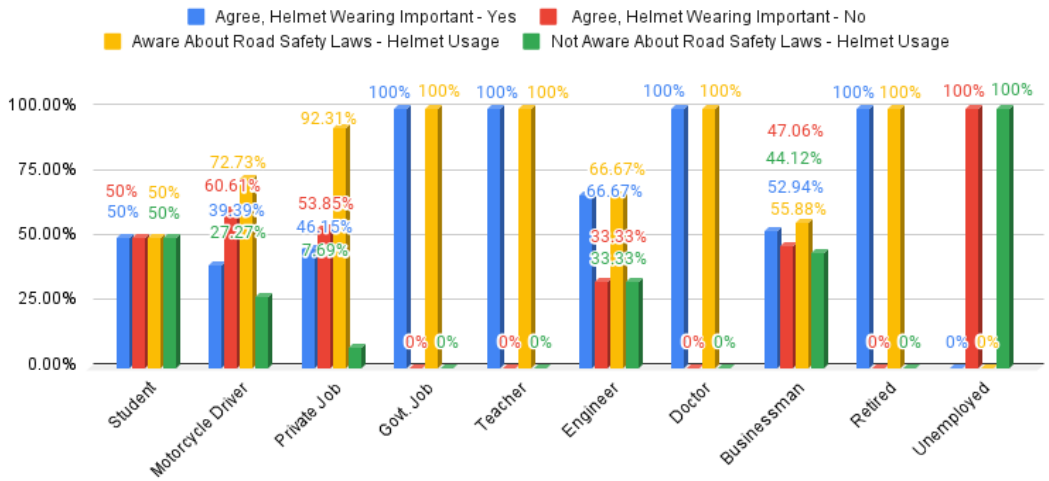

Figure 2. Helmet Wearing & Awareness rate about Road Safety by Age.

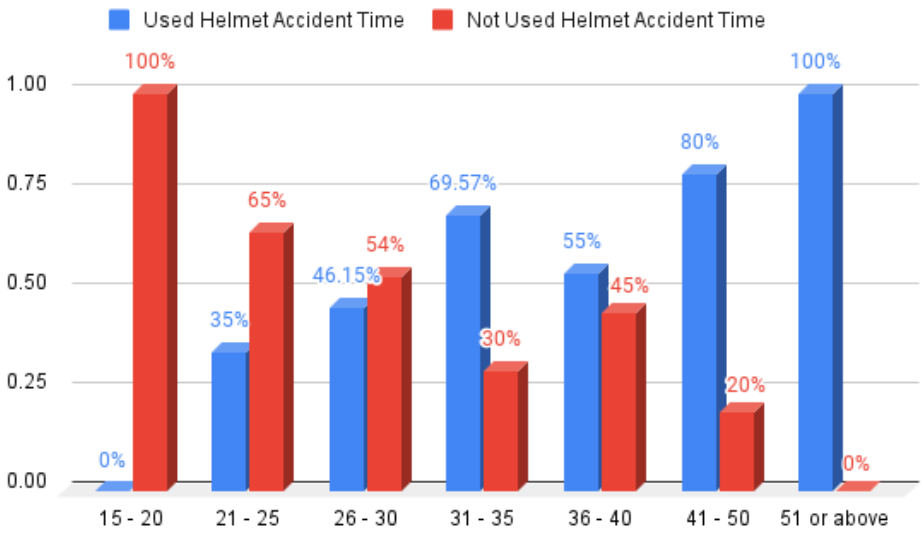

Figure 3. Helmet using rate at accident time by Age.

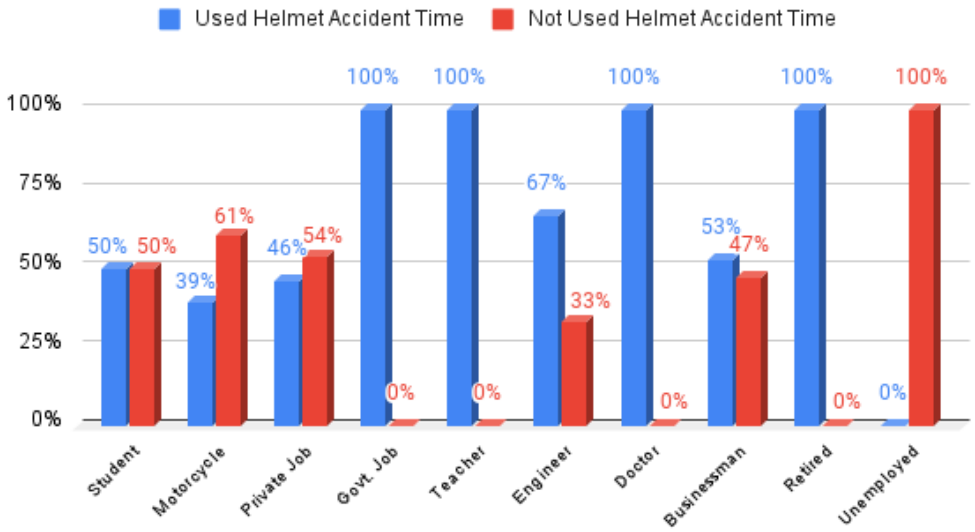

Figure 4. Helmet using rate at accident time by Profession.

This study shows that in Figs. 5 and 6; younger individuals, particularly students, are very less interested in taking lessons or training on motorcycle helmet use and road safety laws. And, 100% people of aged 41-50 and those aged 51 and above have taken such lessons or training. Everyone (100% participants) who works for the government, teaches, doctors, and retirees has taken part in lessons or training on these subjects.

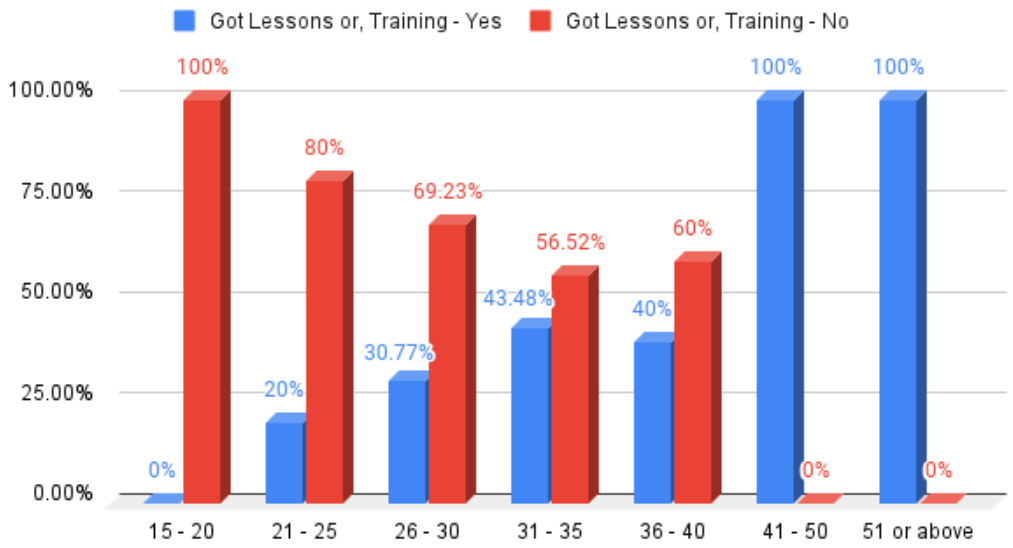

Figure 5. Got lessons or Training by Age.

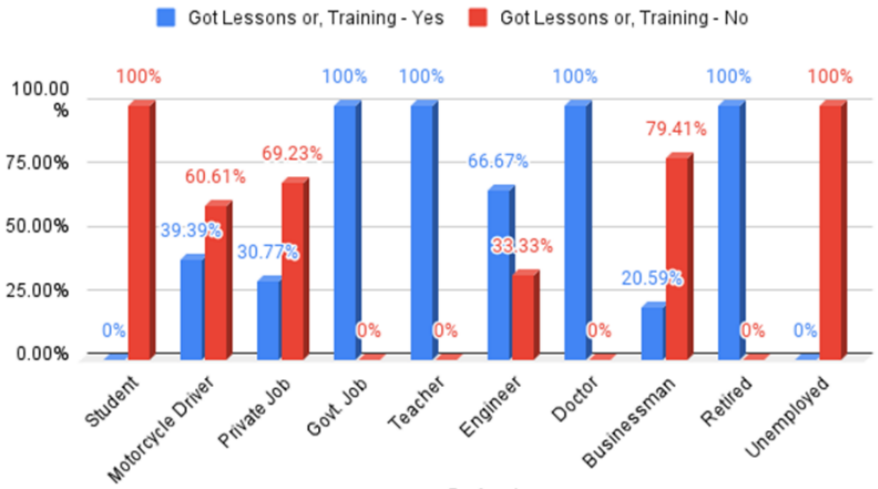

Figure 6. Got lessons or Training by Profession.

4 Conclusion

This research identifies significant gaps in helmet use and road safety awareness among motorcyclists in the Darial Union of Bakerganj Upazila. Here younger people, mainly those aged 15-20, exhibited low helmet usage and inadequate understanding of road safety laws, rendering them highly vulnerable to accidents. The 36-40 age group likewise needed more awareness to reach 100%. On the other hand, older age groups,

particularly those aged 41-50 and 51 and up, used helmets frequently and were well-versed in road safety laws. These groups were also more likely to take part in safety training. Motorcycle drivers, students, and the unemployed had the lowest helmet use and safety knowledge levels. It is especially alarming for motorcycle drivers, who face the most significant risk. On the other hand, government employees, teachers, doctors, and pensioners demonstrated the highest levels of safety compliance, with nearly all receiving relevant lessons or training. The findings highlight the importance of focused awareness campaigns and instructional initiatives, particularly among younger riders and high-risk professional groups. The study argues that resolving these gaps will considerably enhance traffic safety in rural areas, especially in the Darial Union of Bakerganj Upazila in Bangladesh. Due to the lack volunteers, for data collection process, this study conducted on only single union of Bakerganj. But the future study may focus on the location of rest of the union of Bakerganj Upazila and may try to apply both quantitative and qualitative methods and may include also several things in their survey questions about cultural attitudes, economic constraints for getting more better insights.

Acknowledgment

I am deeply grateful to my thesis supervisor, Khondhaker Al Momin, for his generous support, valuable time, information, resources, and expert guidance during this research work.

References

[1] F. N. Rahman, "Determinants of Non-compliance in Motorcycle Helmet Use in Bangladesh," *Injury Prevention*, vol. 18 (Suppl 1), 2012.

[2] M. M. Hoque, M. S. Hossain, M. A. Rahman and S. M. A. B. A. Islam, "Safer Motorcycling and Safer Roads: The Context of Bangladesh," in *SEARSS*, Bali, Indonesia, October 2014.

[3] M. M. Miah, B. Chakma and K. Hossain, "Analyzing the Prevalence of and Factors Associated with Road Traffic Crashes (RTCs) among Motorcyclists in Bangladesh," *The Scientific World Journal,* vol. 2024, 09 May 2024.

[4] M.-M. Brandt, K. S. Ahrns, C. A. Corpron, G. A. Franklin and W. L. Wahl, "Hospital Cost is Reduced by Motorcycle Helmet Use," *Journal of Trauma and Acute Care Surgery,* vol. 53(3), pp. 469-71, 2002 Sep.

[5] B. C. Liu, R. Ivers, R. Norton, S. Boufous, S. Blows and S. K. Lo, "Helmets for Preventing Injury in Motorcycle Riders," *Cochrane Database of Systematic Reviews,* January 2008.

[6] A. F. H. F. M. A.-Z. Alaa K. Abbas, "Does Wearing Helmets Reduce Motorcycle-related Death? A Global Evaluation," *Accident Analysis & Prevention,* vol. 49, pp. 249-252, November 2012.

[7] D. V. Hung, M. R. Stevenson and R. Q. Ivers, "Prevalence of Helmet Use among Motorcycle Riders in Vietnam," *Injury Prevention,* pp. 409-13, December 2006.

[8] M. L. Ranney, M. J. Mello, J. B. Baird, P. R. Chai and M. A. Clark, "Correlates of Motorcycle Helmet Use among Recent Graduates of a Motorcycle Training Course," *Accident Analysis & Prevention,* pp. 2057-62, October 2010.

[9] T. M. Ricea, L. Troszaka, J. V. Ouelleta, T. Erhardta, G. S. Smitha and B.-W. Tsaia, "Motorcycle Helmet Use and The Risk of Head, Neck, and Fatal Injury: Revisiting The Hurt Study," *Accident Analysis & Prevention,* pp. 200-207, May 2016.

[10] M. Q. Haqverdi, S. Seyedabrishami and J. A. Groeger, "Identifying Psychological and Socio-Economic Factors Affecting Motorcycle Helmet Use," *Accident Analysis & Prevention,* pp. 102-110, September 2015.

[11] R. Ramli, N. L. Siang, N. F. Chi, N. A. Rahman and J. Oxley, "Helmet Use amongst Injured and Non-injured Motorcyclists in Malaysia," *Journal of the Australasian College of Road Safety,* vol. 22, no. 2, 2011.

[12] P. M. Sharif, S. N. Pazooki, Z. Ghodsi and A. Nouri, "Effective Factors of Improved Helmet Use in Motorcyclists: A Systematic Review," *BMC Public Health,* 05 January 2023.

[13] M. F. Hasan, S. M. S. Mahmud, M. A. Raihan, A. Akter and A. Bhattacharjee, "Motorcyclist Safety Risk And Attitude To Using Helmet," *Journal of Engineering Science,* vol. 13(2), pp. 11-20, January 2023.

[14] S. K. Das, T. Tamannur, A. Nesa, A. A. Noman, P. Dey, S. K. Kundu, H. Sultana, B. K. Riaz, A. S. Islam, G. Sharower and B. K. Dhar, "Knowledge and Practice

of Road Safety Measures among Motor-Bikers in Bangladesh: A Cross-sectional Study," *Injury Prevention,* November 2023.

[15] L. Buckleya, C. R. Binghama, C. A. Flannagana, P. M. Carterb, F. Almania and J. B. Cicchino, "Observation of Motorcycle Helmet Use Rates in Michigan after Partial Repeal of The Universal Motorcycle Helmet Law," *Accident Analysis & Prevention,* pp. 178-86, 2016 Jul 21.

[16] S.-H. Keng, "Helmet Use and Motorcycle Fatalities in Taiwan," *Accident Analysis & Prevention,* vol. 37, no. 2, pp. 349-355, March 2005.

[17] M. Akbari, K. B. Lankarani, R. Tabrizi, M. Vali, S. T. Heydari, S. A. Motevalian and M. J. Sullman, "The Effect of Motorcycle Safety Campaign on Helmet Use: A Systematic Review and Meta-Analysis," *IATSS Research,* May 2021.

[18] T. Akter and S. Pervaz, "Assessing Motorcycle Accident And Injury Characteristics In Dhaka Metropolitan City," in *International Conference on Urban and Regional Planning (ICURP)*, Dhaka, October 2019.

This page intentionally left

IJASST
International Journal of
Applied Sciences and Smart Technologies
p-ISSN 2655-8564, e-ISSN 2685-943, pp. 29-56, 2025
Volume 07
Issue 01

Geocoding and Implementation of a Web-Based Water Distribution Geospatial Information System for Ilorin Metropolitan City, Kwara State, Nigeria

O.T. Amoo[1]*, H.A. Salami[2], O.G. Okeola[3], A. Sunday[3], T.S. Abdulkadir[3], and A.W. Salami[3]

[1]*Centre for Global Change, Walter Sisulu University, Private Bag X1 UNITRA 5117, Mthatha, South Africa.*
[2]*CIWAT Engineering Consultant, No 9 Umar Audi Road, Fate, Ilorin Kwara State, Nigeria*
[3]*Department of Water Resources and Environmental Engineering, Faculty of Engineering and Technology. University of Ilorin, PMB 1515, Kwara State, Nigeria*
**Corresponding author's email: oamoo@wsu.co.za; oseni@wsmgroup.co.za*

(Received 21-10-2024; Revised 23-11-2024; Accepted 02-12-2024)

Abstract

Water is essential for human life and activities, but its supply depends on the proximity and interconnection network with the populations or cities that need it. Moreso, the proper functioning of water supply systems (WSS) relies on the expertise and experience of field workers who rely on information from maps or field surveys, whose processes and mapping methods are labour-intensive, time-consuming, and are done relatively infrequently. The study aims to utilised a spatial-based online Map plugin in the Quantum Geographic information system (QGIS) environment to host a web-based GIS platform to view the transmission, and delivery of Drinking Water Distribution (DWD) network in the Ilorin township, from source to household users. It explores modern spatial information and Web-GIS capabilities in managing water infrastructure for an expanding metropolitan city. The resultant comparison results range from 60% to 75% in meeting users' needs for pipe network, road connection, DWD layout, catchment boundary, slope, and sub-catchment geometric properties demonstrate GIS technological web-based tools as a data management, scenario analysis, and decision support tool in managing water infrastructure for an expanding metropolitan city. Our configured web-based system offers real-time accessibility and user-friendly interaction that significantly support the decision-making process.

Keywords: Geocoding, QGIS, water distribution network, water supply systems, web-based

This work is licensed under a Creative Commons Attribution 4.0 International License

1 Introduction

Sustainable access to drinking water is one of the problems of Third World cities [1]. Demographic growth and the extension of cities make it more and more difficult to supply drinking water to the populace. The topographical contrasts and the anarchy in land use reinforce the difficulties of water distribution. As a result, the distribution companies of the drinking water supply (DWS) network face technical, logistical, and intricate service provider problems mostly from lack and sometimes inadequate modern spatial databases for meaningful progress to be made to water supply schemes (WSS). The study focused on the transmission and delivery of drinking water from the source to household users according to the capacities planned for the DWD system. It responds to research questions on the users' requirement and purpose of the web-based QGIS; which web development framework will be used and examines the extent to which present existing water infrastructure assets could be digitized for future expansion support. The implementation could aid in geocoding a web-based platform in viewing the transmission, and delivery of the DWD network by WSS for meaningful technical progress in managing water infrastructure assets for an expanding metropolitan city like Ilorin, Kwara State.

Ilorin city is immense in increasing water demands to meet the needs of its rapidly growing and urbanizing population, changing lifestyles, and economic growth [2]. The city is challenged with a water crisis caused by inadequate water asset documentation, insufficient infrastructure maintenance, digitalization and investment in water network distribution, inequities in water access, and a lack of skilled water practitioners who rely on outdated maps in this era of a rapidly changing environment. In many instances of these problems, the proper functioning of water supply systems (WSS) relies on the expertise and experience of field workers, a good organization structure with an adequate digital database containing all the key hydraulic infrastructure, to support its management and operational guidelines, to be able to perform optimally. However, most of this essential information is either inadequate or quite staggering for successful implementation of the WSS. At most, much of the existing information is in old maps or antiquated sketches which are too difficult to

update and to keep up with modern times. This development calls for a decision-support tool for sustainable water transmission schemes (WTS), and water distribution networks (WDN) to enhance the efficient management of these infrastructures.

Geographical Information System (GIS) allows the creation and management of spatially referenced data to be useful in many fields or situations [3,4]. The significant expansion of the internet and growing public interest in accessing online geospatial information bore the fore need to investigate water distribution networks(WDN), and water transmission schemes (WTS) to enhance the efficient management of these infrastructures and ensure functional water supply monitoring. GIS has proven to be an effective and powerful tool in the water distribution industry [5]. It could aid the preservation and delivery of water infrastructure from the source to the end users. Thanks to their various spatial representation in the cloud. The use of modern spatial remote-sensing data and integration into GIS web-based has progressed over the past years for water supply, water allocation, water management, and flood estimation [6-14]. Thus, the application of spatial remote sensing data and visualization of WTS is essential in an expanding, dense population and increasing demand for accessible portable water supply for the teaming populace.

GIS-remote sensing has provided numerous solutions and convenience to characterizing biophysical and geophysical land surface processes and properties, many of which are well related to hydrologic and hydraulic science systems [15-17]. Satellite data have emerged as a viable alternative or supplement to in-situ observations due to their easier accessibility and applicability over vast areas in a catchment [18]. Spatial representation of WDN can provide surface data relevant to specific WTS to help alleviate some of the prolonged bottlenecks in resolving the water supply problems. Amongst these are: to enhance the efficient management of these infrastructures; highlight the need for alternative water supply routes; quantify surface water transmission links; evaluate water conservation measures and fair water allocation policies and provide guidelines for future non-traditional water supply projects. Maintaining data integrity has led to the development of web mapping applications like QGIS Cloud, geo-server, and map-server for the betterment of society.

Today, many models are used in different climatic zones to aid and enhance decision support systems (DSS) for water transmission. These range from the customization and integration of an open-source WebGIS system, and PostgreSQL/PostGIS as the relational database for dissemination, extraction, and analysis of water utility information online [19-23]. The extension works by [24] explored the combined application of GIS as a framework for data management and optimization of hydraulic parameters alongside three other hydraulic plugins: Ghydraulics, OpenLayer, and Qgis2threejs through hydraulic simulation in EPANET for the possible route, terrain navigation, least pipe network and spatial topographic profile representation is of immense benefit while literature work by [25] on the integration of free-of-charge open-source software, e.g. QGIS and EPANET, and engineering practices applicable to water distribution network design have expanded the space for more innovation and expansion of knowledge.

[25,26] use a QGIS 3.14 version alongside the Environmental Protection Agency Network (EPANET 2.2) to analyze the design of a water distribution network for the Agiliti community in the Kosofe Local Government Area of Lagos State, Nigeria. [28] dwell on new expansion using the plugin GHydraulics of QGIS and the MapBasic language of MapInfo. Despite the significant challenge of ensuring optimal water delivery to multiple locations with appropriately sized infrastructure compatible with existing systems, antiquated and manual drawings are still employed in this modern era. As useful as most of these invented tools and models have proved to be, the use of an intuitive web-based approach linking urbanization with human analysis in assessing water distribution networks(WDN), and water transmission schemes (WTS) is limited to few studies or has not received much attention in this clime. Hence, this study combined the use of in-situ measurements and remotely sensed data in digitizing physiographic information for Ilorin water supply, distribution network assessment, and water transmission schemes to the different end users in a fast, safe and convenient mode in resolving many bottlenecks associated with technical WSS challenges in real-time.

The study acknowledges and benefits from the works of literature while further on the intuitive usage of spatial data in meeting both the supply and demand side in

solving water distribution and network problems in third-world countries. Therefore, this study sought to establish the applicability of a web-based in-situ PostgreSQL database to host spatial data and visualize the city water distribution networks in real-time. The study presents a digitalized and secure database for Ilorin's water infrastructure, ranging from its storage reservoirs to the end-user distribution network in digital format. Other necessary information entails water infrastructure and utilities such as pipes, fire hydrants, washouts, water meters, pumps could be easily displayed without printing as a softcopy map. The study would assist decision-makers in upgrading the existing water distribution system with spatial data and ensure future expansion with updated information for effective redesigning, planning, and management for near-future increasing users. The study would also be useful for people who know nothing about GIS due to its simplicity, and ease of supporting multi-user interface requirements.

1.1 Study Area Description

The study area (Ilorin) has 3 Local Government Areas (LGAs) namely the Ilorin West, Asa, and Moro LGA. As one of the most densely populated areas, Ilorin City occupies most state assets [29]. Ilorin is situated in Kwara state North Central region of Nigeria. It is located between latitudes 8°30'N and 4°33'E (Figure 1). The study area occupies a land area of 765km² and an estimated population of 732,199 [30]. It harbours the State Ministry of Water Resources and Sanitation which is responsible for developing policies, strategies, and plans for water resources management and executing water supply projects within the state's boundaries while the Kwara State Water Corporation (KWWC) manages, controls, and operates water supply

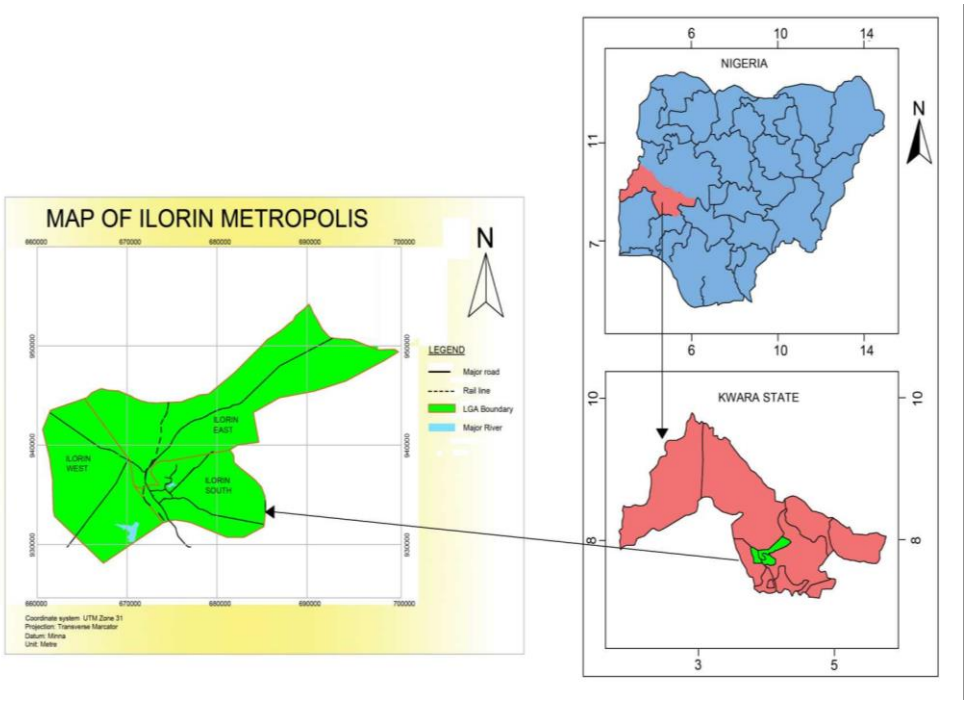

Figure 1. Map of Ilorin showing its three local government areas in relation to Nigeria

infrastructure within urban areas and suburb towns in the state. Fig. 1 depicts the Map of the study area in relation to Nigeria.

The study area WDS consists of the sources, dams, water treatment plants, transmission and distribution networks, and reservoirs(tanks). The Ilorin water scheme consists of 3 Nos of dams namely Asa Dam, Agba Dam, and Sobi Dam, 5 Nos of water treatment plants (WTPs), 13 Nos of elevated reservoirs, 5 Nos of ground reservoirs, 2 weirs, and 1 underground reservoir, all located in the city of Ilorin metropolis, the state capital.

2 Materials and Methods

To address the objective, the aggregated views of stakeholders within the Water management sector were solicited through questionnaires which gives the expertise side to the expected web-based development for verification. The content of the questionnaire instrument was structured in the modified Likert fashion 1 being the

lowest and 5-point being the largest. Participants were then instructed to respond to their degree of agreement with the statements contained in the instrument. These questions were sufficient in answering users' requirement features for a web-based water distribution system users wanted to be held on the internet. At various spatial and temporal scales, the relevant datasets framework needed to create and compile the old and new database for the study area description (Ilorin water supply scheme) evolved, and a centralized spatial database for all the water infrastructures was identified, digitized updated new data-based inventory was set up for the study area. Thereafter, analyses and querying of the developed database management system were embarked on before evaluating the performance of the developed web-based monitoring system for the area water supply and distribution networks which enriched the data visualization techniques used in the web mapping interface. Details of the applied procedural step are hereby presented.

2.1 Sample design, and rationale

Due to the nature of this research, which requires the insights of experts, and scientists who are well-grounded in GIS, geocoding, and water management. The non-probability, snowball sampling method was adopted in selecting the participants. In non-probability sampling, elements do not have an equal chance of being selected [31] while in snowballing, a researcher collects data from a few people (participants) whom he or she can find, then asks the same people (participants) to recommend where potential participants may be found or people whom such participants relate with. Hence, the researcher continuously solicits referrals for other potential participants till all the contacts have been exhausted [32,33].

29 employees at the State Ministry of Water and Environmental Sanitation (MWES), Ilorin, and an expert consultant (CIWAT) were consulted. Amongst these 29 employees, the researcher retrieved 25 completed questionnaires. The remaining questionnaires were either not filled out or filled out incompletely (which makes them void). The questionnaire design was done in such a simple way that elucidates worthwhile information from respondents. Table 1 presents the respondents' demographic data responses.

Table 1 shows a fair proportion of the respondents' responses were from informed sources who understand the research subject. The respondents were knowledgeable enough to state their desired function requirement for web hosting of water distribution network systems. Also, the stakeholder input through questionnaires shows the respondents' experience ranged from 2 to 20 years, which the researcher considered fit for the study. Most of the respondents had more than six years of work experience. This is significant, as their insightful comment guide in pipe layout and geometry consideration in data gathering to ensure that collected data is reliable. Also, their input serves as the reference point in validating the web design criteria consideration Hence, the research design and adopted method are well-suited and robust for the data collection.

2.2 Data Collection and Datasets

Historical data and Information were sourced from the Kwara State Water Cooperation and CIWAT consultants on the expansion project [34]. The data source includes sketches of the very old network layout for installing AC pipes in late 1976. For ease of delineating places where future expansion for supply will be needed,

Table 1. Respondents' years of experience and experts' field

Year of experience/Expert field	**1-5yrs**	**6-10yrs**	**11-15yrs**	**16-20yrs**	**Over 20yrs**	**Total**	**Mean**
Soil expert	0	0	1	2	2	5	1.0
GIS-coding	2	0	3	5	1	11	2.1
Water supply	0	2	1	1	1	5	1.0
Irrigation	**0**	**1**	**2**	**1**	0	**4**	**0.8**
Total	**2**	**3**	**7**	**9**	**4**	**25**	

and due to the constant surge in household population, the three local governments (Asa, Moro, and Ilorin West) boundaries are included as one unit as Ilorin township cities. Also, since most sketches and existing drawings were done with old software, their accuracy and positioning were slightly doubtful. Hence, we embarked on a Field survey with Garmin GPS 78sc to pick different points for the existing water infrastructure including pipes, Fire hydrants, washouts, valves, etc. Google Earth aided in the realignment of the expanded distribution network for Ilorin township. The realigning of the following pipe sizes (100mm,150mm,200mm, and 250mm Upvc) from new waypoints is necessary. This was due to some newly made shift road construction to avoid rock blasting and keep the project within budget, without jeopardizing its geometry slope grade that allows for gravity flow. Although, major rehabilitation and expansion works have been done in Ilorin West.

The site reconnaissance survey was done with the assistance of senior Kwara State Water Corporation staff, it was confirmed that sketches made with hard copy coordinates documentation are mostly accurate using Garmin GPS. The major updated works included in this study are the expansion of rising mains of 800mm/600mm/400mm diameter pipes and ductile Iron pipes of about 38km. Older pipe networks constructed in the 70s are now mostly located in the middle of roads due to dualization works, especially in Ilorin West. Even though some of these pipes are in use, they should all be replaced at most in the next 20 years. All pipes laid were asbestos cement pipes ranging from 80mm to 350mm, and they all have a lifespan of just over 50 years. Furthermore, the distribution pipe network included 500mm, 450mm, 400mm 350mm, 300mm, 250mm, 200mm, and 100mm ductile iron/Upvc pipes totaling over 100km were equally and adequately digitized and geoprocessing. Thereafter, the new coordinates for all the pipe layouts were noted and are well reprocessed in the new web-based in-situ PostgreSQL database to host the spatial data and visualize the city water distribution networks in real-time. The new spatial data are met to enhance the easy accessibility of information and future expansion scheme studies for researchers.

The GPS was also used in picking the storage tanks around the Ilorin metropolis some are not presently in use, but these are well documented in the GIS software with

their attribute. However, it must be noted that there exist some potential drawbacks in GPS measurement, accuracy, and difficulties experienced during data gathering and how we overcome these challenges. Since GPS signals are at terrestrial receivers which tend to be relatively weak, acquiring and tracking the satellite signals may be difficult or impossible. The field data gathering was done under open-clear sky conditions which enhanced calibration precision and helped to navigate obstacles and fitness tracking.

Furthermore, both random and systematic errors were mitigated by taking several measurements of the object in question. Random error mainly affects precision, which is how reproducible the same measurement is under equivalent circumstances. In contrast, to systematic error. Even though GPS satellites broadcast their signals in space with a certain accuracy, the receiver design features/quality may inhibit its accuracy especially when these devices must travel through remote areas. Thus, to mitigate this, the GPS was constantly checked so as not to lose its signal and recalibrated repeatedly to ensure correct measurement was picked or when picking the auxiliary water infrastructure features. However, most of these challenges could be minimal through repeatability, and constant calibration and revalidation of the instrument when not in use. Table 2 lists the various tools used in the system development while Table 3 states the applied attributes in the database creation.

Table 2. presents applied software and its function.

No.	Tools	Function
1.	Quantum GIS 3.26	Spatial data creation
2.	PostgreSQL 13.5.2	Spatial database creation
3.	Post GIS	Data Conversion/Visualization
4.	CAD2 Shape Version 8	Conversion of AutoCAD file to Shapefile
5.	Global Mapper 22	Georeferencing

6.	GIS Cloud	An online platform for hosting, publishing, editing, and sharing maps, data, and services on the internet.

2.3 Spatial Data Creation and Analysis

The installed Quantum GIS 3.26 software was used for spatial data processing. This interfaced with Google Earth, Global Mapper, and CAD to create and import vector layers in digitizing the pipe network. GPS was used to map accurate coordinates for the distribution network while realigning to digitized area maps on Google Earth. All created shapefiles were imported on QGIS for further conversion into their corresponding relational tables for processing in the PostgreSQL database. PGadmin 4 v 7 and PostGIS 3.4 in the PostgreSQL database were used in creating the new Ilorin water Supply Scheme database. This process was repeated for each vector layer created for the entire study area. Table 3 presents the summary of all available field data collected.

Table 3. Summary of the attribute field data details on QGIS

	Pipe	Valve	Hydrants	Air Valve	Washout	Endcaps	Tanks
Installation date	A	A	A	A	A	A	A
Length	A	N/A	N/A	N/A	N/A	N/A	N/A
Route Name	A	A	N/A	N/A	N/A	N/A	A
Manufacturer	A	A	A	A	A	A	A
Material	A	A	A	A	A	A	A
Maintenance	A	A	A	A	A	A	A
Diameter	A	A	N/A	N/A	N/A	N/A	A

Volume/Capacity	N/A	N/A	N/A	N/A	N/A	N/A	A

*Where A = APPLICABLE N/A =NOT APPLICABLE

Moreso, the thought processes that go into selecting/arriving at a technique employed go beyond the periphery parameter measurement. Existing field data for area, perimeter, or length for a GIS data file need to be recalculated to verify the unprojected data set for a new geometry feature. It is also important to note that before any water asset calculations are made, the data must be projected, and units must be set, and when performing field calculations, the edition of the data must be done within an editing session, by so doing, the coordinate system of the data source or the data frame is on and helps in better precision measurement. Field mapping information on pipe network, road connection, drinking water distribution layout, catchment boundary, and sub-catchment geometric properties consideration was well documented and geo-reference in QGIS. Table 4 depicts the attributes' detailed representation in the QGIS environment.

Table 4. Data set used for the study of their attributes

No.	Data Type	Data Subtype		Geometry Type
1.	Boundary	i)	Local government boundary	Polygon Polyline
		ii)	Roads	Polyline
2.	Topographical Features	i)	River	Google satellite
		ii)	Buildings	Google Satellite
		iii)	Railway line	Polyline
3.	Water Network	i)	Air Valve	Point
		ii)	End Cap	Polyline
		iii)	Fire hydrants	Point
		iv)	Meter	Point
		v)	Reducer	Point

		vi)	Sluice/Gate Valves	Point
		vii)	Washout	Point
		viii)	Water Tanks	Polygon

Table 4 depicts the dataset attributes used to create the QGIS database for the Ilorin township water supply scheme. The created table contains all the shape files including the original coordinates and geometry feature that define each. This process identified all previous pipe network layouts in the city (Ilorin) created and digitized new features to update the water supply network schemes. The subsequent sessions highlighted how the developed database management system was used to create a centralized spatial database for all water infrastructures which were later hosted in the developed web-based platform in updating the spatial information system, before analyses and querying their performance.

3 Results and Discussions

3.1 Web-Based Development and Data Upload

To have a QGIS database web page for the Ilorin township water supply scheme, the spatial data was made available online using QGIS Cloud, a powerful Web-GIS platform built for sharing maps, data, and services online. It supports all QGIS functionalities, enabling users to create and edit maps directly within the platform. QGIS Cloud acts as a spatial data infrastructure on the Internet, which could enable the publication of QGIS projects, maps, and vector data to be hosted on the Internet[35]. One of its key features is the ability to share spatial data with others. QGIS Cloud was selected for this project due to its user-friendly interface, freely accessible by anyone, and the fact that its online output closely mirrors the experience of working on the desktop version. It does not require a local server where the uploader must always be online, another advantage over other types of platforms is that it does not require technical knowledge to understand its basic infrastructure. Once conversant with QGIS Desktop, transitioning to using QGIS Cloud is straightforward. Fig. 2

presents the QGIS assets database which includes information on pipe layout network, road connection, catchment boundary, slope, and sub-catchment geometric attribute properties, which can easily be retrieved, stored, and reclassified. Fig. 2 shows the attribute table of a typical pipe size which is the 300mm DI pipe, this attribute was also done for all pipe sizes to geocode all Ilorin water assets while Figure 3 depicts the QGIS Attribute table showing all the created fields table. The spatial datasets and their attributes created in Fig. 3 are useful for smart asset management and retrieval of spatial data layers as shown in Fig. 4 with their entire network connection.

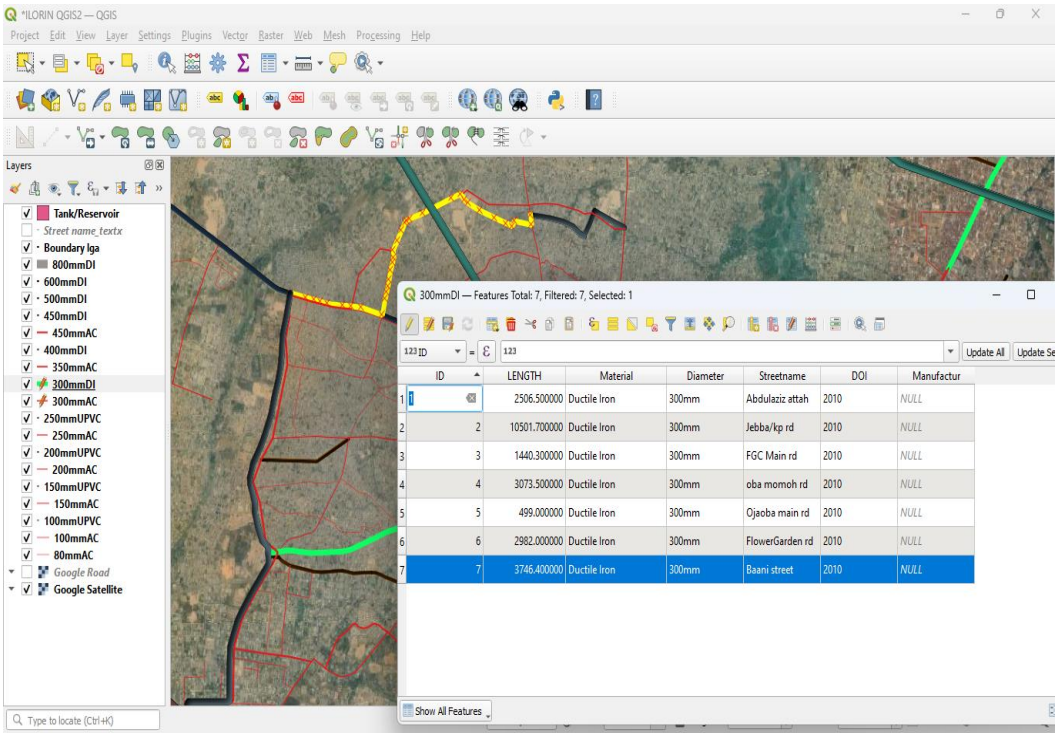

Figure 2. QGIS Attribute table showing details of 300mm DI

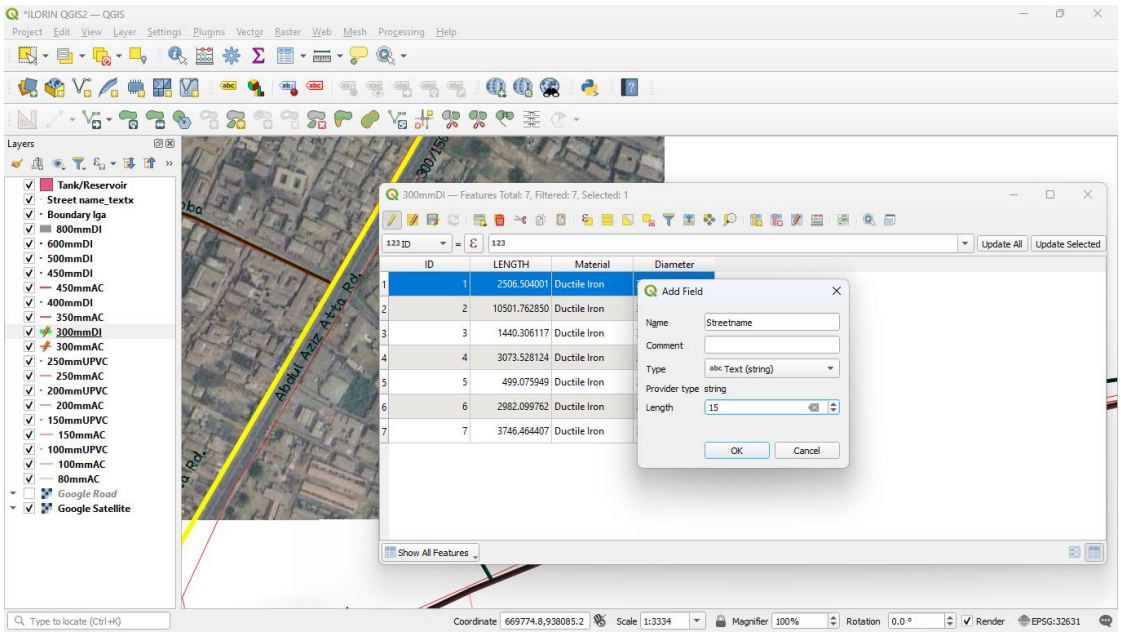

Figure 3. QGIS Attribute table showing the creation of field table

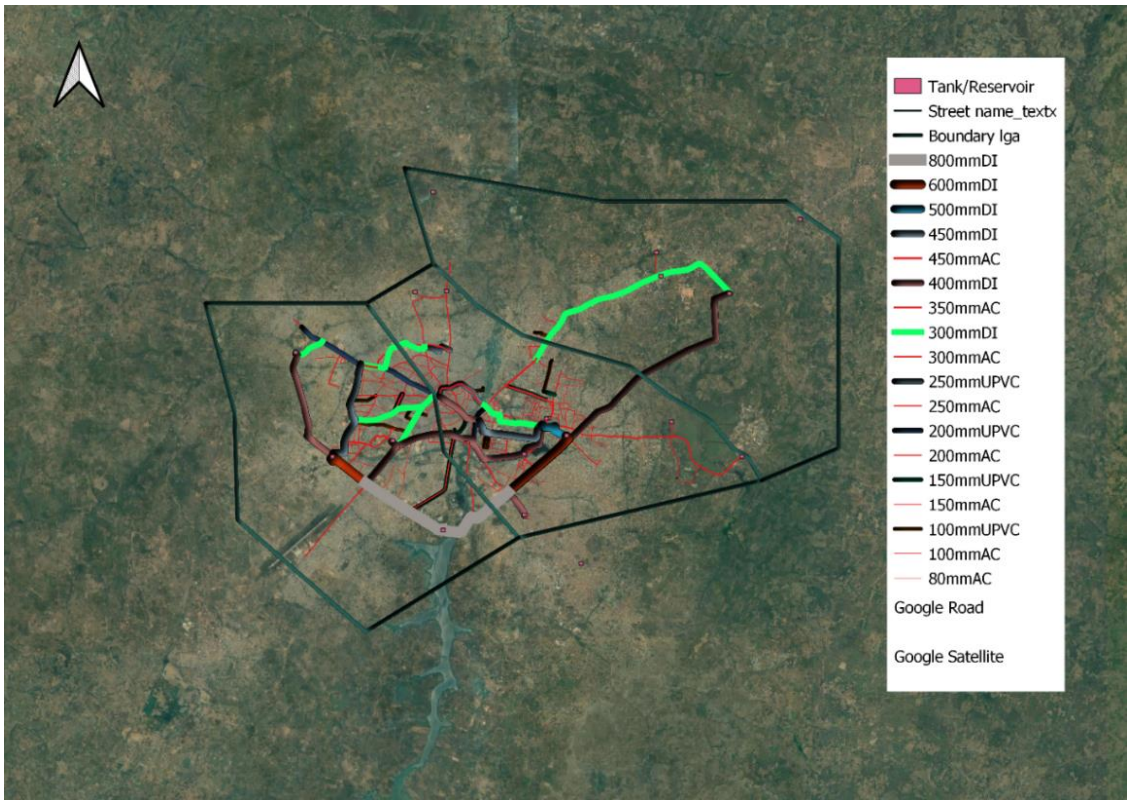

Figure 4. Spatial Pipeline network connection and distribution in Ilorin

Fig. 4 depicts the developed integrated water information system (IWIS) useful for detailing analysis and risk mitigation projection from the proposed water supply network that can match population growth based on various map queries and interactions exported and imported from another platform compatible with the query search engine. The figure shows the different pipeline network connections and distribution layouts in Ilorin. These pipes range from 800mm to 80 mm AC/UPVC, etc.

3.2 Findings Discussion

The employed geocoding skills and innovative geospatial integration of water supply assets and digitalization of water distribution infrastructure play a critical role in developing and implementing geospatial hydrology and remote sensing methodologies that enhance water management and productivity. To address the water asset documentation issues, the user must be smart with all this available information. Table 5 depicts the averaged response summary on how the developed web-based features meet users' requirements.

Table 5. Significant features that users wanted the web system to be capable of.

No.	Desired Function	Average
1	General view and layout region	3
2	Interaction with maps	4
3	Accessibility to Internet	3
4	Adding new pipes	4
5	Adding new bulk meters & appurtenances	3
6	Location of new network	3
7	Pipe attributes illustration	4

8	Indicate property boundaries	3
9	Print/export maps	5
10	Perform searches(query)	4

From Table 5, the designed web system effectively met these needs. From the analysis, system users expected the web hostage to be able to support querying/viewing and updating spatial data(4/5). Users also wanted the web hosting to be able to add new bulk meters and their appurtenances(4/5), be flexible in locating new water networks(3/5), enrich map creation with detail attributes(4/5), perform and analyze water supply flow rate distribution(3/5). Hence, an overall performance of 75% in meeting users' needs is a good rating between the user expectations and the Web-GIS capabilities testing.

No doubt, the stakeholder and expert inputs help shape the overall configuration and preference testing of the performance of the QGIS Cloud server in generating and hosting the maps on the internet. Fig. 5 depicts the results of the various attributes for the sub-catchment surface layer feature. Fig. 5 depicts a search query on each local layer database showing the attribute layer features while the results obtained through interacting with the developed web-based are diagrammatically illustrated in Fig. 6.

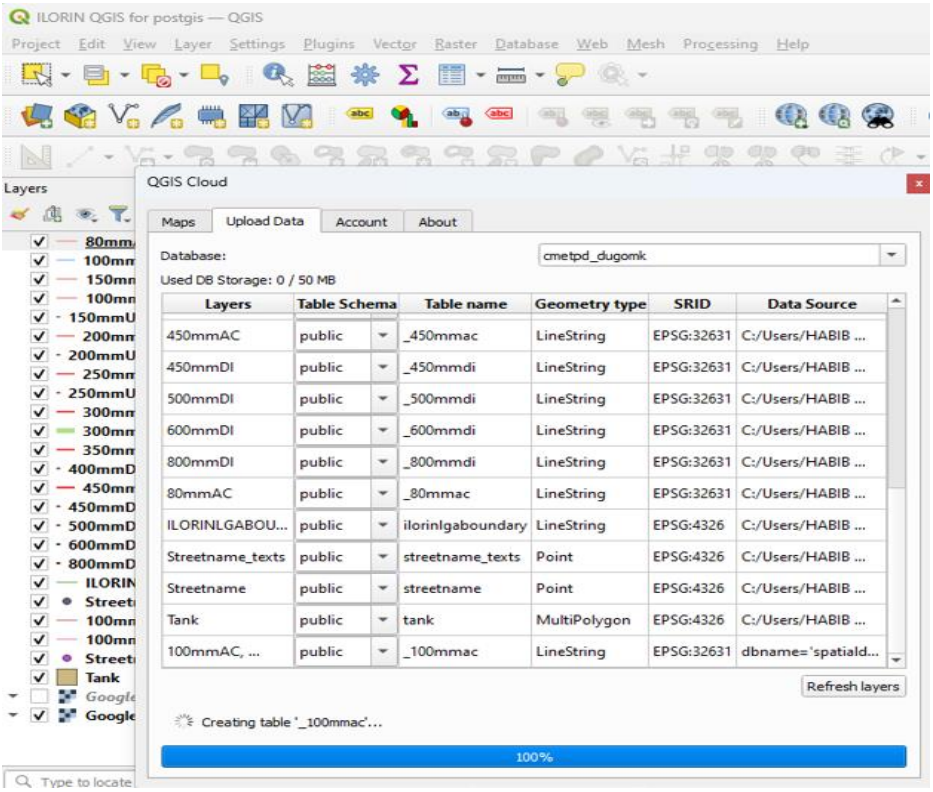

Figure 5. Local layers databased being uploaded

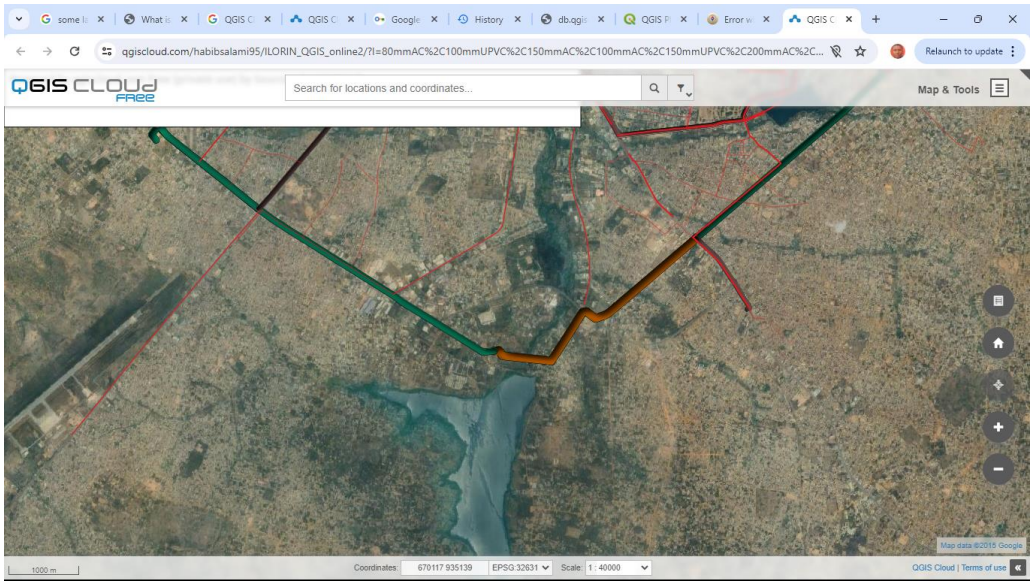

Figure 6. Uploaded file now on the internet

Fig. 6 shows the local layers being uploaded to the database in the QGIS Cloud database. These layers include all the different pipe sizes, tanks, reservoir modules; weirs and pumps; pressurised pipes; street names; pumps and storage. These data are now imported from the local shapefiles into the QGIS Cloud PostgreSQL database. Figure 6 shows evidence and potential change in the city network with a view of slow pace to rapid-onset long-term change in extreme events. The design and host web-based QGIS Cloud PostgreSQL database retrieval query and other high-performance computing simulation systems depict what the future landscape holds for the city expansion in real-time, on-site maintenance, and innovative criticism to achieve a sustainable urban water distribution network. It was important to know that these data sources in the project could be exchanged while the original shape files would no longer be visible, but instead, the data from the QGIS database would be displayed. Hence, the water supply distribution layout, network design, and operation module are embedded in the QGIS Cloud services which are interfaced with complex WDNs in geographic map layers. Thus, providing easy access to visualize and retrieve its spatial database over the internet within limited nano-speed time intervals. The link for the cloud data now is https://qgiscloud.com/habibsalami95/ILORIN_QGIS_online2/. After it was uploaded the link was revisited as shown in Fig. 7.

3.3 Web-System connection to the QGIS cloud

Figure 7 illustrates the created Postgresql database using the spatial extension in pgadmin by importing all vector layers from QGIS to connect to the database, all components of the system in the post-GIS and Postgresql assist the QGIS Cloud server in generating the maps on the internet. The WSS problems generally require intensive evaluation of spatial information and analysis to hold the dataset, thus we use the database “cmetpd_dugomk,” as shown in Fig. 7 to randomly generate and display the map on the internet.

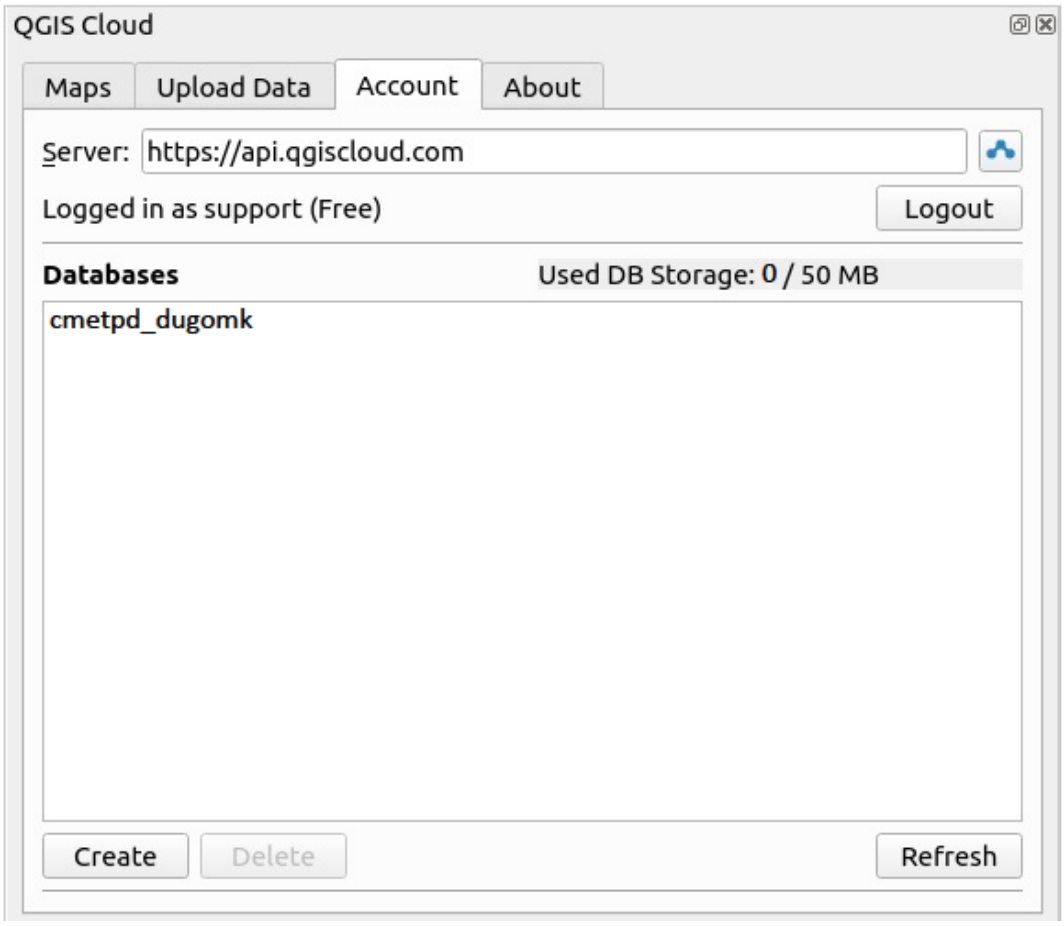

Figure 7. The created Database cmetpd_dugomk files

By default, the data is loaded into the database schema public. In the default list, the local layers are listed. However different schemas can be selected for different databases. Since only one database was used and only one schema was employed. Only one database was used for the entire distribution network. Among the many different available server services providers like Map Server or Geoserver. The QGIS Cloud server was chosen because it offers a more friendly environment as against the alternative drawback of hosting and publishing maps with more complex map definitions. The QGIS Server understands the projects created in the QGIS PC environment, so there's no need for additional map definitions. The map will appear exactly as it does on the desktop. In case where a raster file was used, it is important to create another database.

3.4 Performance Evaluation

To evaluate the success of this research work, user testing and performance were done. Users wanted the web hosting to be able to add new bulk meters and their appurtenances(4/5), be flexible in locating new water networks(3/5), enrich map creation with detail attributes(4/5), accessibility of the deploy web-GIS on the internet (3/5), perform and analyze water supply flow rate and distribution(3/5) among other. Hence, an overall performance of 75% in meeting users' needs is a good rating for the user expectations and the Web-GIS capabilities testing. Most QGIS Cloud server could empower a broad range of data users that permeate across disciplines to produce new and meaningful research and insights work across different field.

In the development stage, geocoding and utilization of PostgreSQL9.4, GeoQuery and webGIS may be challenging without sufficient training and experience. Also, the identification, and leveraging upon the right data usage for a particular task and bid can be difficult without expert input and insight. In all, continuous guardian from expert and literature works documentation [36,37] help overcome the technical challenge around a high-performance, computing environment and flexible data framework that could be interface with web-GIS. Also, the web- GeoQuery's codebase and post processing methodologies are open source, thereby reducing the barriers of finding and accessing geospatial data, thereby reducing processing time to a few or less minutes .

4 Conclusions

The utilization of various QGIS geocoding platforms for hosting a digitized web-based spatial information for water transmission and distribution layout in Ilorin township was carried out in this study. The study employed QGIS Cloud services interface with PGadmin 4 v 7 and PostGIS 3.4 in the PostgreSQL geocoding database in creating the new digitized Ilorin water supply scheme database. The implementation of a web-based QGIS hostage makes a valuable contribution to supporting future expansion programmes. provides a practical framework that can be adapted to any other context in decision-making. The application of various spatial physiographic

information for the transmission, and delivery of drinking water from sources to household users has helped minimize resources spent on data collection, aided time spent in tracing faults and could helped make informed database design. The web-based GIS information hosted on the internet presents a centralized storage database that is useful for both present and near-future users. Thus, loss of data is not an excuse in today's cloud-range database storage. The study contributes to advancing the field of applied sciences and smart technologies in improving water distribution systems.

The cumulative result shows effectiveness in meeting users' requirement of a QGIS web-server capable of integrating many plugins in functionality that enrich the general web view, support created maps in different format, flexible in adding new pipes, bulk meters and appurtenances, capable of uploaded map creation with attributes that is internet friendly. The uploaded created map illustrates water geo-reference properties and geometry boundaries, which could enable data filtering and query, overlay data from external sources, and enrich attributes dataset tables in carrying out spatio - temporal analysis which could be deploy in determining the rate of infrastructure development. Most web GIS applications have built-in plugin support services necessary for large-scale project expansion and infrastructure development.

Despite the potential transmission lag-period shortcomings in viewing the hosted web-based imagery, the employed QGIS Cloud PostgreSQL database toolkits have been able to act as prototypes that will guide large-scale development of a web-based GIS application for Ilorin water assets information documentation which can aid future expansion. Also, the limited preferred spatial data format, was overcome through application of updated PostGIS databases which can do a lot of editing for ease of use by many stakeholders and decision-makers.

Georeferencing the dataset has help minimize GPS satellite broadcast signals in measurement thereby eliminate both random and relative errors in calculating and storing important attributes of Ilorin WDN and assets coordinate reference. This asset includes the length of pipes, Manufacturers, Date of installation, storage capacities of the tank, etc. Future water supply and distribution network modelling can be easily undertaken. The study effectively shows how QGIS's built toolkit aids in creating a

spatial database for water network mapping and storage of many out-of-position features such as reservoirs, tanks, and pipe distribution networks.

The study provided a secure database for spatial documentation of Ilorin's water infrastructure. In addition to documenting and visualizing the water distribution network, the study offers a thorough and easily accessible platform that could enhance the sustainable development of the city's water infrastructure and water distribution network system. The employed QGIS web-based helps to visualize the spatial data attributes that is too numerous and critical for water distribution networks and application modification. Overall, the web system's effectiveness demonstrates spatial data storage and queries to help improve the presently existing system and provide real-time monitoring of services. The Web-QGIS interface can effectively present spatial information and analyze query map layers. It has provided a report module to illustrate data in many ways and facilitate decision analyses in coordinating geo-referenced database.

The open-source GIS toolkit provides a framework for the digitalization of all water supply infrastructures in Ilorin water distribution schemes. The centralized dataset performs well for different entities' users ranging from regional managers, engineers, distribution supervisors, meter testing supervisors, customer care supervisors, credit controller supervisors, and GIS officers, to provide real-time monitoring of services. We suggest the Kwara State Water Cooperation Board the statutory agency responsible for drinking water supply (DWS) services in the city would find the developed in-situ PostgreSQL application useful in resolving many of the existing bottlenecks related to the distribution and supply of drinking water. The board and any other relevant agencies would find it useful to adopt the built Web-based GIS interface as a data management, scenario analysis, and decision support tool in managing water infrastructure for an expanding metropolitan city like Ilorin, Kwara State.

Acknowledgements

We are grateful to all those who participated in the survey, and to the students who helped with the georeferenced data entry. The authors acknowledge the Tertiary Education Trust Fund TETFUND (National Research Fund, NRF) for sponsoring this study through the TETFUND/DR & D – CE/NRF/2020/SETI Grant and the University of Ilorin, Ilorin for providing the enabling environment.

Author Contributions

Conceptualization, OG, H.A.;
Analysis, H.A., O.T.;
Initial Draft. A.W,
writing-review and editing, OG, O.T, T.S.;
Funding Acquisition, A.W.;
Project Administration, AW.

Ethical approval and consent to participate

Ethical clearance letters were collected from the University ethics committee for both the study participants and the researchers. During the survey, confidentiality was maintained by giving codes to each respondent rather than recording their name. The participants were informed to have full right to discontinue or refuse to participate in the study and all participants were fully informed of the objective of the study. They all gave their consent and participated freely in the research.

Declaration of interest

The authors declare that they have no competing interests in this manuscript.

References

[1] Beker, B.A. and Kansal, M.L., 2024. Complexities of the urban drinking water systems in Ethiopia and possible interventions for sustainability. *Environment, Development and Sustainability*, *26*(2), pp.4629-4659.

[2] Agaja, T.M. and Towobola, D.O., 2022. Impact of Urban Land Use on Rainwater Quality: Case Study in Ilorin Metropolis, Nigeria. *Journal of Environmental Geography*, *15*(1-4), pp.31-37.

[3] Mohanlal, C., Nagarajan, K. and Narwade, R., 2019. Applications of 4D GIS Model in Construction Management. *International Journal of Innovative Technology and Exploring Engineering (IJITEE),(July-2019) ISSN*, pp.2278-3075.

[4] Breunig, M., Bradley, P.E., Jahn, M., Kuper, P., Mazroob, N., Rösch, N., Al-Doori, M., Stefanakis, E. and Jadidi, M., 2020. Geospatial data management research: Progress and future directions. *ISPRS International Journal of Geo-Information*, *9*(2), p.95.

[5] Asli, K.H. and Asli, K.H., 2023. Smart Water System and Internet of Things. *Journal of Modern Industry and Manufacturing*, *2*.

[6] Zeng, Y., Cai, Y., Jia, P. and Jee, H., 2012. Development of a web-based decision support system for supporting integrated water resources management in Daegu City, South Korea. *Expert Systems with Applications*, *39*(11), pp.10091-10102.

[7] Saravani, M.J., Saadatpour, M. and Shahvaran, A.R., 2024. A web GIS-based integrated water resources assessment tool for Javeh Reservoir. *Expert Systems with Applications*, *252*, p.124198.

[8] Chen, W., He, B., Ma, J. and Wang, C., 2017. A WebGIS-based flood control management system for small reservoirs: a case study in the lower reaches of the Yangtze River. *Journal of Hydroinformatics*, *19*(2), pp.299-314.

[9] Shrivastava, V., Jaiswal, A., Thakur, P.K., Agarwal, S.P., Kumar, P., Kota, G.K., Carrera, D., Dhasmana, M.K., Sharma, V. and Singh, S., 2018. Application of GIS for the design of potable water distribution system in IIRS. *ISPRS Annals of the Photogrammetry, Remote Sensing and Spatial Information Sciences*, *4*, pp.87-94.

[10] Pérez-PadilPérez-Padillolo, J., Morillo, J.G., Poyato, E.C. and Montesinos, P., 2021. Open-source application for water supply system management: Implementation in a water transmission system in southern Spain. *Water*, *13*(24), p.3652.

[11] Kadhim, N.R., Abdulrazzaq, K.A. and Mohammed, A.H., 2021, May. The management of water distribution network using GIS application case study: AL-Karada area. In *Journal of Physics: Conference Series* (Vol. 1895, No. 1, p. 012038). IOP Publishing.

[12] Luo, B., Zhang, F., Liu, X., Pan, Q. and Guo, P., 2021. Managing agricultural water considering water allocation priority based on remote sensing data. *Remote Sensing*, *13*(8), p.1536.

[13] Dastres, R. and Soori, M., 2022. Advances in web-based decision support systems. *International Journal of Engineering and Future Technology*, 2021. hal-03367778f; Volume 19; Issue No. 1; ISSN 2455-6432

[14] Shah, D. and Shete, D., 2022. Attaining optimal sustainability for urban wastewater management using open-source tools like QGIS, EPANET and WATERNETGEN. In *Water Resources Management and Sustainability* (pp. 489-514). Singapore: Springer Nature Singapore.

[15] Schultz, G.A. and Engman, E.T. eds., 2012. *Remote sensing in hydrology and water management*. Springer Science & Business Media.

[16] Girgis, K., Clouse, N., Mushe, O., Morgan, P., Brooks, T. and Mahmoud, M., 2022, December. The applications of GIS in water resources. In *2022 International Conference on Computational Science and Computational Intelligence (CSCI)* (pp. 1515-1520). IEEE.

[17] Mamai, L.M., Gachari, M. and Makokha, G. 2017. Developing a Web-Based Water Distribution Geospatial Information System for Nairobi Northern Region. *Journal of Geographic Information System*, **9**, 34-46 https://doi.org/10.4236/jgis.2017.91003

[18] Sheffield, J., Wood, E.F., Pan, M., Beck, H., Coccia, G., Serrat-Capdevila, A. and Verbist, K.J.W.R.R., 2018. Satellite remote sensing for water resources management: Potential for supporting sustainable development in data-poor regions. *Water Resources Research*, *54*(12), pp.9724-9758.

[19] Costantino, D.M.G.A., Angelini, M.G., Alfio, V.S., Claveri, M. and Settembrini, F., 2020. Implementation of a system WebGIS open source for the protection and sustainable management of rural heritage. *Applied Geomatics*, *12*, pp.41-54.

[20] Martinho, N., Almeida, J.P.D., Simões, N.E. and Sá-Marques, A., 2020. UrbanWater: Integrating EPANET 2 in a PostgreSQL/PostGIS-based geospatial database management system. *ISPRS International Journal of Geo-Information*, *9*(11), p.613.

[21] La Guardia, M., Koeva, M., D'ippolito, F. and Karam, S., 2022, October. 3D Data integration for web-based open source WebGL interactive visualisation. In *17th 3D GeoInfo Conference* (pp. 89-94).

[22] Sadoun, B., Al-Bayari, O. and Al-Tawara, S., 2022. "Open-Source GIS Solution: An Overview of the Architecture of Free Open-Source Web GIS".

[23] Xia, J., Huang, Q., Gui, Z. and Tu, W., 2024. Relational Databases. In *Open GIS* (pp. 97-141). Cham: Springer International Publishing.

[24] Nagarajan, K. and Charhate, S.B., 2018. Water Distribution Network: A Remote Sensing and GIS Approach. NFiCE, 2018, IIT Bombay, Author ID: ABC_1234

[25] Muller, A.L., Gericke, O.J. and Pietersen, J.P.J., 2020. Methodological approach for the compilation of a water distribution network model using QGIS and EPANET. *Journal of the South African Institution of Civil Engineering*, *62*(4), pp.32-43.

[26] Rawlings, A. and Seghosime, S. (2022a) Design of a Water Distribution Network Using QGIS in Combination with EPANET: A Case Study of Agiliti Community in Kosofe LGA, Lagos State, Nigeria. USEP Journal of Research in Civil Engineering, Vol.18, No.4, 2021 4254-4280

[27] Rawlings, A. and Seghosime, S., 2022b. Evaluation of water supply, sanitation and hygiene facilities in Ekosodin community of Ovia North-East LGA, Benin City, Edo State, Nigeria. *Nigerian Journal of Technology*, *41*(4), pp.632-643.

[28] Kah, E., Therry, N.T. and Innocent, N.M., 2019. GIS-Based Multi-Criteria Decision Analysis for the Sustainable Management of the Nkong Zem Pipe-Borne Water Network: West Region of Cameroon. *Journal of Geographic Information System*, *11*(06), p.727.

[29] Solihu, H. and Bilewu, S.O., 2022. Assessment of anthropogenic activities impacts on the water quality of Asa River: A case study of Amilengbe area, Ilorin, Kwara state, Nigeria. *Environmental Challenges*, *7*, p.100473.

[30] Kofo, A.A., 2012. Significance of 2006 head counts and house census to Nigerian sustainable development. *International Journal of Academic Research in Economics and Management Sciences, 1*(3), p.45.

[31] Etikan, I. and Bala, K. 2017. Sampling and sampling methods. *Biometrics & Biostatistics International Journal,* 5**,** 00149.

[32] Mitchell, A. and Education, A. E. A review of mixed methods, pragmatism, and abduction techniques. Proceedings of the European Conference on Research Methods for Business & Management Studies, 2018. 269-277.

[33] Sharma, G. 2017. Pros and cons of different sampling techniques. *International journal of applied research,* 3**,** 749-752.

[34] CIWAT (2024) Infrastructure report draft on water supply and sanitation master plan for Kwara State January 2024.

[35]Hammerle, R.J., 2001. *The design of a Web-based distributed Geographic Information System*. The University of New Brunswick.

[36]Pathak, D., Varde, A.S., De Melo, G. and Alo, C., 2020. Hydroinformatics and the web: Analytics and dissemination of hydrology data for climate change and sustainability. *ACM SIGWEB Newsletter, 2020*(Autumn), pp.1-17.

[37] Netek, R., Pohankova, T., Bittner, O. and Urban, D., 2023. Geospatial analysis in Web Browsers—Comparison study on WebGIS process-based applications. *ISPRS International Journal of Geo-Information*, *12*(9), p.374.

IJASST International Journal of Applied Sciences and Smart Technologies

Volume 07
Issue 01

p-ISSN 2655-8564, e-ISSN 2685-943, pp. 57-66, 2025

Assessing Impact of Public Transportation Services on Traffic Jam in Dhaka City

Md. Tanjil Mahmud Khan[1*]

[1]*Department of Civil Engineeirng, Daffodil International University, Bangladesh*
[*]*Corresponding Author: tanjildiu@gmail.com*

(Received 03-10-2024; Revised 30-10-2024; Accepted 02-11-2024)

Abstract

This study used JASP Software for descriptive analysis and Chi-square tests. I surveyed 100 people of different backgrounds and age for their opinions. It determined that 56% of respondents were dissatisfied with the public transportation service, and 69% used public transportation daily. According to this study, 82% of people regularly experience traffic jams because it is hard to get to places, especially in places like Mirpur. Even though 64% of those who responded used buses as public transport, but only 18% wanted more buses to help ease traffic. They would rather see digital transportation systems, awareness and safety improvements. Notably, 80% of those who answered think improving public transportation services could help reduce the traffic jams in Mirpur, Dhaka city.

Keywords: traffic jam, public transportation, traffic jam of dhaka city

1 Introduction

Traffic jams on roads are getting worse around the world. One toxic effect of traffic jams is that they hurt the economy and the quality of life in numerous cities [1]. There is a significant problem with traffic congestion, In the city of Makassar, Indonesia, when fire trucks are on route and face heavy traffic jams, then they are usually forced to reduce speed, hindering their ability to respond quickly and facing problem for traffic jam [2]. But it is not only impacting the general public but also negatively impacts the interests of commercial activity. Even though no statistics indicate the economic loss caused by traffic congestion in Hong Kong, there is some proof from countries in the United States and Europe that traffic congestion entails substantial financial damage. The United States of America, according to a report that

This work is licensed under a Creative Commons Attribution 4.0 International License

was published in 2014, spent 124 billion dollars in a single year due to traffic congestion [3].

The most crowded city in the world overall is Dhaka, the capital of Bangladesh. Dhaka has a population of more than twelve million, and the count is rising daily; much of Dhaka suffers from severe traffic jams most of the day [4]. Traffic jam is a prevalent issue in all cities in Bangladesh. Major metropolitan areas such as Dhaka, Chittagong, Khulna, and Rajshahi are confronting this issue, particularly in Dhaka, where it has become a significant challenge in addition to fundamental demand shortages [5]. Traffic jams are a big problem in Dhaka. According to the study of an author, most people drive in the city for more than two hours daily. And just because of traffic jams, they lose an average of one hour of work each day [6].

Nineteen million of Bangladesh's 55 million registered cars are in Dhaka. And, in Dhaka, there are more than five times as many cars on the road as lanes are not enough to meet the demand [7]. Another author from Bangladesh completed a survey in 2019 and suggested several steps to reduce traffic jams. These include executing traffic management strategies, strictly following traffic laws and rules, and inspiring people to use public transportation [8]. The highest traffic congestion in that region is caused by a combination of factors, including the signaling failure in the Dhaka traffic system and people's lack of awareness. This problem costs the economy a significant amount of money daily [9].

Overall, we are experiencing a massive problem due to traffic jams in Dhaka city. Researchers have suggested various solutions to the traffic congestion issues in Dhaka. Enhancing public transportation options is widely acknowledged as reducing traffic jams [10]. According to an author, Primary objective of the accessibility assessment for public transportation is to improve the connectivity between people and locations throughout the system, reducing traffic congestion on highways [11]. Therefore, I am eager to work on this matter by assessing the impact of public transportation accessibility on traffic jams in Mirpur 1 to 10 at Dhaka city, evaluating public transportation availability, accessibility, and usage, and analyzing commuter behavior and satisfaction. Then, finally, I want to share proposed recommendations to improve public transportation and reduce traffic jams.

2 Material and Methods

This study applied a quantitative research approach to look at the impact of public transportation networks on traffic jam in the Dhaka city of Bangladesh. Participants were asked about their own vehicle percentage, frequency of public transportation use, most often used public transportation, public transportation accessibility rate, satisfaction rate of using public transportation, what they are thinking about improving public transportation can help to lower traffic jam.

2.1 Instruments

At first, the primary instrument for data collection in this investigation was a structured survey. Only closed-ended questions were included in the survey to facilitate quantitative analysis that concentrated on the influence of public transport services on traffic congestion in the Mirpur region in Dhaka. Questions were formatted as yes/no options, Likert scales, and multiple-choice answers to ensure clarity and prevent opacity in the survey using google form. In addition, a pilot test was implemented with a limited number of individuals to verify the instrument's efficacy and implement any required modifications prior to its complete deployment.

2.2 Data Collection

To effectively administer the research's scope, I concentrated data collection on the Mirpur 2 and Mirpur 10 areas of Dhaka, Bangladesh. Then I developed a Google form and disseminated it online to residents of Mirpur 2 and 10. Data was collected through this form. In addition to the online distribution, I personally visited the region to distribute the Google Form to individuals. I conducted face-to-face interviews with people who lacked access to email addresses and social media. I manually completed the Google Form on their behalf. This method guaranteed inclusivity and a more thorough data collection process. A total of 105 participants, spanning a wide variety of ages and occupations, provided informed consent for data collection.

2.3 Survey Design

The survey questions were set up to get a wide range of information about how people use public transport and how that affects traffic in Dhaka city. Questions about age, occupation, and vehicle ownership helps to put answers in context because these

things often affect how people move. I have asked how frequently and which types of public transport peoples used most to find out how usually and how much people relied on it. To rate the quality of the service, people were also asked to rate how easy it was to use and how satisfied they were with the current public transport choices. Also, asked people about their experiences with traffic jams and their thoughts on possible solutions that can help to understand how they think better public transport could help ease traffic jam problem.

2.4 Data Analysis

At first, I remove the missing data from the structured questionnaire data set for correctness, and finally 100 samples were chosen from the 105 data sets. To maximize efficiency, data was entered into Microsoft Excel using coded values. The dataset was saved in .CSV format using Microsoft Excel and loaded these into JASP (0.18.3 version) software. Then the coded values were changed to string values for analytical clarity. And after that here, descriptive statistics and Chi-square tests were used. For this study, I have used here descriptive statistics and also Chi-square tests to understand the relationships and trends within the dataset. Here descriptive statistics provided an overview of the data distribution, allowing me to assess central tendencies and variability across responses. This initial analysis gave a clearer picture of general patterns in public transportation usage, satisfaction levels, and perceptions regarding traffic congestion. The Chi-square test was then employed to examine relationships between categorical variables, such as age, profession, vehicle ownership, and attitudes toward public transportation.

3 Results and Discussions

After analyzing 100 participants' data, including 10 professions and 7 age groups, from Fig. 1; it was found that 42% of participants are students and those aged between 21-25. This research study revealed a few crucial facts these are daily public transportation is used in Mirpur 1, 2, and 10 by 69% of people; here always and often – a total of 82% of people face traffic jams; using public transportation - dissatisfied and the very dissatisfied rate is 56%; study showed most using public transit by people - 64% is bus; having no own vehicle of people is 88%, in these areas public

transportation accessibility rate is very lower, research showed it is only 41%, and exactly 80% of people telling improving public transportation can help to reduce this traffic jam.

Research shows that people using public transportation daily have a satisfaction level of only 4.29%, a neutral level of 31.43%, and a dissatisfaction level of 37.14%, mentioned in Figs. 2 and 3. The very dissatisfied level is 27.14%. Then, for people who are using weekly public transportation, their satisfaction portion is 11.77%, neutral is 17.65%, dissatisfied is 52.94%, and very dissatisfied is 17.65%. After that, the third category is people who rarely use public transportation; their satisfaction rate is 7.69%, neutral is 23.08%, dissatisfied is 38.46%, and very dissatisfied is 30.77%. People with their own vehicles still use public transportation; the daily used percentage is 58.33%. On the other hand, people without an own vehicle use public transportation more than those with it; the daily use percentage is 71.59%. But in the third category, 'rarely,' people with a vehicle are using public transportation more than those without a vehicle; if we look at the daily using public transportation data, the percentage is 33.33%.

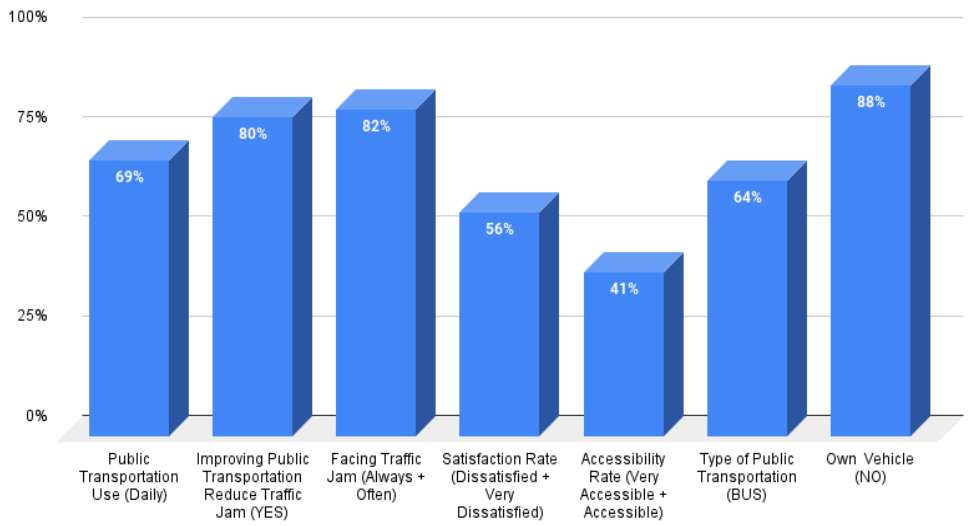

Figure 1. Important facts about public transportation.

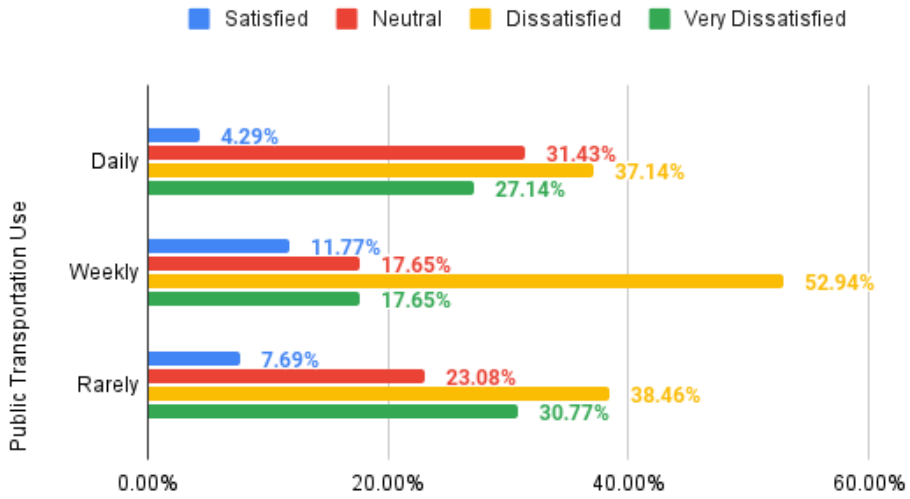

Figure 2. Public transportation use & satisfaction level.

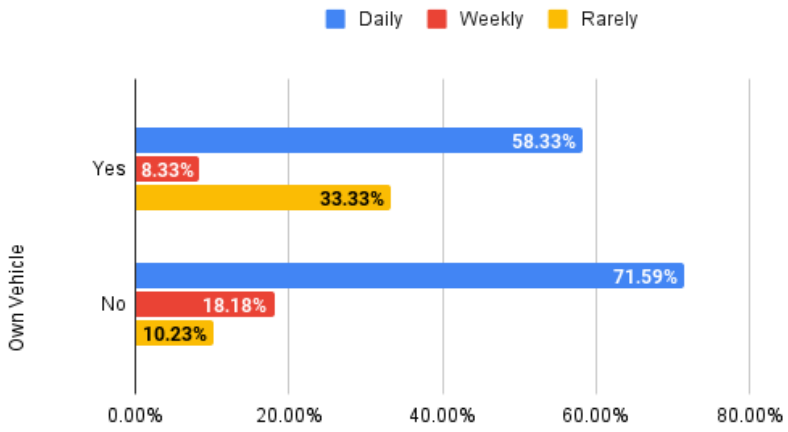

Figure 3. Own Vehicle & Public Transportation Using Ratio.

Now, the data on public transportation accessibility and their records of facing traffic jams, here analysis showed in Fig. 4; people who are in the ‘very accessible’ category face a very lowest amount of traffic jams daily than all others, which is 28.57%. The only category named ‘accessible’ here is that 2.94% of people never faced a traffic jam. In the ‘neutral’ category, 40.91% of people always face traffic jams.

But, in ‘inaccessible’ and ‘very inaccessible,’ people here interestingly always face 66.67% traffic jams and, in the category, ‘often’ for 33.33%.

This study showed that in Fig. 5; 80% of people say that improving public transportation may reduce traffic jams in Dhaka. Here 64% of people used the bus as a public transport and data says only 18% chose ‘more buses’ as an option that may reduce traffic jams, this was the lowest voted option. Then, the area with the highest improvement selected by participants is the digital transport service. Others are lower fares 23%, more routes 39%, better schedule 32%, improved safety 46%, and raising awareness campaigns 59%.

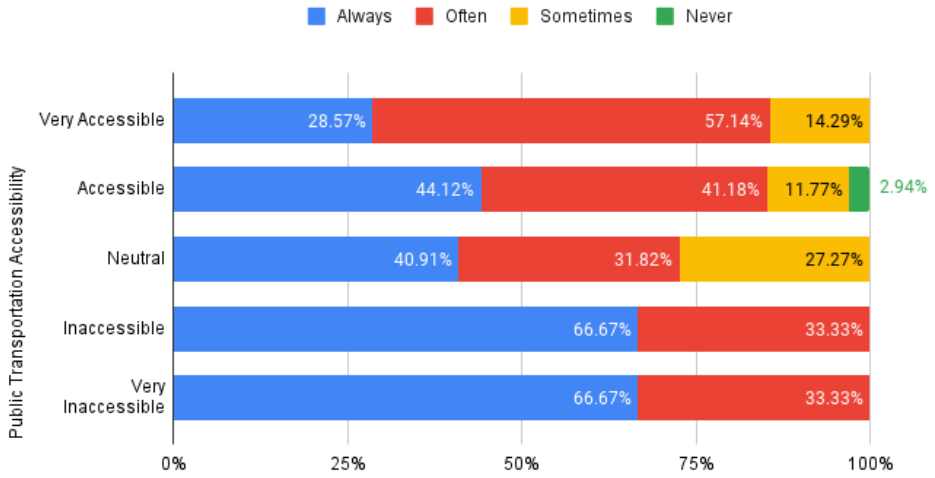

Figure 4. Public transportation accessibility and records of facing traffic jam.

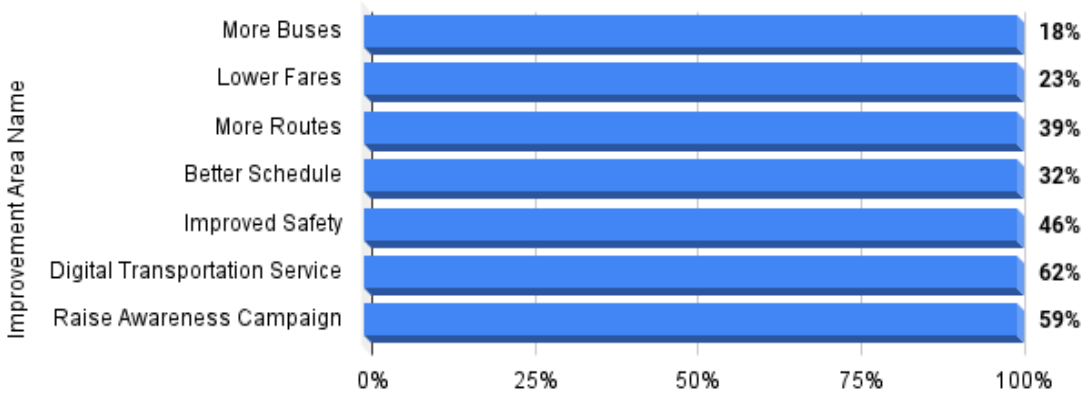

Figure 5. Most wanted improvement area.

4 Conclusion

In Mirpur-Dhaka, this research study illustrates that traffic jam is substantially exacerbated by inadequate public transportation and traffic management. In Mirpur, public transit is extensively utilized by most commuters, particularly students aged 21-25, with 69% using it daily. The public transportation system suffers from low accessibility (41%), high dissatisfaction rate (56%), and frequent traffic jams (82%). And 80% of participants believe that improving public transportation services can free up traffic jams. Here 64% of people who use public transit say they take the bus. We need digital transportation services, more lines, and better safety measures to reduce traffic jams. To fix the city's terrible traffic jam problems, we must also make public transportation more accessible. A future study may focus on more areas in dhaka city, using mixed methods, and longitudinal studies that can help to reach more better results.

Acknowledgment

I want to thank my respected undergraduate thesis supervisor, Khondhaker Al Momin, for his invaluable guidance, support, and encouragement, which significantly helped me to successfully reach this research publication.

References

[1] T. Bokaba, W. Doorsamy and B. S. Paul, "A Comparative Study of Ensemble Models for Predicting Road Traffic Congestion," *Applied Sciences*, 2022.

[2] M. Friaswanto, E. A. Lisangan and S. C. Sumarta, "The Simulation of Traffic Signal Preemption using GPS and Dijkstra Algorithm for Emergency Fire Handling at Makassar City Fire Service," *International Journal of Applied Sciences and Smart Technologies*, vol. 3, no. 2, pp. 185-202, 2021.

[3] F. Guerrini, "Traffic congestion costs Americans $124 billion a year," Forbes, 2014.

[4] K. Mahmud, K. Gope, S. Mustafizur and S. Chowdhury, "Possible Causes & Solutions of Traffic Jam and Their Impact on the Economy of Dhaka City," *Journal of Management and Sustainability,* vol. 02, 2012.

[5] T. Chowdhury, S. M. Raihan, A. Fahim and M. A. Bhuiyan, "A Case Study on Reduction of Traffic Congestion of Dhaka City: Banani Intersection," in *International Conference on Agricultural, Civil and Environmental Engineering (ACEE-16),* Istanbul, Turkey, April 18-19, 2016.

[6] M. Z. Haider and R. S. Papri, "Cost of traffic congestion in Dhaka Metropolitan City," *Public Transport,* 11 May, 2021.

[7] M. M. Ali, M. A. H. Didar, A.-U. Hosna, M. N. Nobi and S. A. Moni, "Traffic Jam in Bangladesh: An Analysis Focusing the Economic Impact," *Global Mainstream Journal of Business, Economics, Development & Project Management,* vol. 01, no. 04, December, 2022.

[8] U. T. T. J. P. M. M. R. N. J. Shila, "Traffic Congestion in Dhaka City - A Case Study in Mirpur 1 to Mirpur 10," in *Proceedings of International Conference on Planning, Architecture and Civil Engineering*, 12 - 14 October 2023.

[9] M. S. Hossain, M. Ahmad, M. M. Islam and M. Asadujjaman, "Traffic Scheduling Simulation: The Case of Dhaka City," *Journal of Modern Science and Technology,* vol. 5, pp. 89-101, September 2017.

[10] Y. Ali, M. Rafay, R. D. A. Khan, M. K. Sorn and H. Jiang, "Traffic Problems in Dhaka City: Causes, Effects, and Solutions (Case Study to Develop a Business Model)," *Open Access Library Journal,* 2023.

[11] I. Y. (Jackiva), E. B. (Budiloviča) and V. Gromule, in *10th International Scientific Conference Transbaltica 2017: Transportation Science and Technology*, 2017.

This page intentionally left

IJASST
International Journal of
Applied Sciences and Smart Technologies
p-ISSN 2655-8564, e-ISSN 2685-943, pp. 67-82, 2025

Volume 07
Issue 01

Efficient Design of Reinforced Columns: Insights into Lateral Confinement and Performance

Badhon Singha[1 *], Nafis Niaz Chowdhury [1,]

Mohammad Atiqur Rahman Sakib[1]

[1]*Graduate Student, Ahsanullah University of Science and Technology, Dhaka, 1215, Bangladesh*
[*]*Corresponding Author: badhon10776@gmail.com*

(Received 10-11-2024; Revised 03-12-2024; Accepted 06-12-2024)

Abstract

In this research, the effects of hoop spacing on load-carrying capacity and deformation behaviour are examined in relation to the structural performance of reinforced concrete columns subjected to seismic strain rates. The study incorporates properties from analytical and experimental methods to simulate the stress-strain behaviour of constrained concrete using ABAQUS finite element modelling. To optimize hoop spacing, parametric research is carried out with the goal of balancing material cost and structural performance. To assess how different hoop spacing affects column performance, the load vs. displacement relationships is examined. The findings show that while optimal configurations improve load capacity and deformation resilience, excessive hoop spacing causes early spalling and decreased structural strength. This study contributes to safer and more effective structural systems by offering useful insights into the economical design of reinforced concrete columns with enhanced seismic performance.

Keywords: Confined concrete, Finite model, Lateral reinforcement, Mander model, and Unconfined concrete.

1 Introduction

A column, a fundamental vertical structural member in the realms of structural engineering and architecture, serves as the primary support for compressive loads. In the intricate fabric of a building or structure, columns play a multifaceted role with crucial functions such as load-bearing, providing support to horizontal components like beams and slabs, imparting height and stability, and facilitating the systematic distribution of loads to the foundation. The resistance of columns to compressive forces is paramount

This work is licensed under a Creative Commons Attribution 4.0 International License

for the overall stability and integrity of the structure, preventing any risk of structural failure.

Spiral columns, characterized by their cylindrical structure with continuous spiral bars, embody a specialized design with helical reinforcement. The helical reinforcement, also known as spiral reinforcement, contributes to transverse support, preventing lateral expansion of the concrete. Spiral columns, particularly suited for situations requiring flexibility or cost-effective enhanced strength under high loads, showcase the intricacies of structural engineering design.

On the other hand, tied columns, constituted by longitudinal bars connected by narrower bars at regular intervals, represent a predominant structural form in non-seismic locations. The ties, often transverse bars of smaller diameter, provide crucial lateral confinement, ensuring the verticality of longitudinal bars during construction and contributing to buckling resistance. The failure of a tied column leads to the crushing and shearing of concrete in all directions.

The focal point of this discourse extends to the behavior of reinforced concrete (RC) columns under lateral confinement, a critical consideration in earthquake-resistant design. The application of lateral confinement, achieved through confining reinforcement such as ties or spirals, is pivotal in understanding and enhancing the structural performance of columns, particularly in seismic regions.

Examining the relationship between force and displacement is foundational to comprehending structural behavior. Structural stiffness, a defining factor in how a structure or structural element deforms under applied force, plays a central role in ensuring safety and performance. The selected research on lateral confinement behavior in integrated concrete columns holds significant implications for determining load-carrying capacity, deformation behavior, and the application of the Mander model in both unconfined and confined concrete columns.

2 Background Studies

Numerous studies have explored the modeling of confined and unconfined concrete behavior, as well as the confinement effect in column strengthening. The schematic of concrete column shown in Fig. 1. The stress-strain relationship in concrete is well-

understood up to its maximum strength, but recent research has mainly focused on the post-peak phase and high-strength concrete characteristics. A key area of investigation is establishing an effective stress-strain relationship for confined concrete, achieved through strategic placement of transverse reinforcement. In low-stress conditions, transverse reinforcement experiences minimal strain, causing the concrete to behave similarly to unconfined concrete. As stress approaches the uniaxial strength, internal fracturing leads to dilation, resulting in a confining effect, which significantly enhances concrete strength and ductility.

Unconfined concrete

Kent and Park (1971) [1] proposed stress-strain equations for both confined and unconfined concrete, expanding upon Hognestad`s (1951) [2] formulations to more comprehensively depict the post-peak stress-strain patterns. Subsequently, Popovics (1973) [3] introduced an equation designed to characterize the stress-strain behaviour specifically for unconfined concrete. Thorenfeldt et al. (1987) [4] later modified Popovics' (1973) [3] model to incorporate adjustments accounting for the descending branch of the specific stress-strain connection. Seeking enhanced control over the post-peak segment of the stress-strain relationship, Tsai (1988) [5] presented a generalized iteration of the Popovics (1973) [3] equation.

The evolution of these stress-strain equations reflects a progressive refinement in modeling concrete behaviour under various conditions. Kent and Park's (1971) [1] extension of Hognestad's (1951) [2] work suggests a desire for a more nuanced understanding of post-peak stress-strain phenomena. Popovics (1973) [3] contributes with a specialized equation catering to the unconfined concrete scenario, and subsequent modifications by Thorenfeldt et al. (1987) [4] address nuances in the descending branch of the specific stress-strain connection. Tsai's (1988) [5] generalized version further emphasizes the need for precise control over the post-peak behavior, underlining a continuous pursuit of accuracy and applicability in stress-strain modeling for concrete.

These developments, rooted in the pioneering work of Kent, Park, Hognestad, Popovics, Thorenfeldt, and Tsai, collectively advance the understanding of concrete behavior across various loading conditions. The iterative refinement of stress-strain equations contributes to the ongoing quest for comprehensive and accurate

representations of concrete response, essential in the field of structural engineering and materials science.

Confined concrete

The stress-strain model formulated by Kent and Park (1971) [1] underwent modifications, prompted by findings from Roy and Sozen's (1964) [6] tests on small square columns, which demonstrated the inefficacy of confinement by rectangular or square rings in appreciably increasing the compressive strength of concrete. Desayi et al. (1978) [7] addressed this by developing a unified equation-based stress-strain model, incorporating insights from tests conducted on circular columns with lateral spiral reinforcement, to elucidate both pre- and post-peak behavior of confined concrete.

Scott et al. (1982) [8] conducted a study involving square concrete columns, laterally braced by stacked arches and reinforced longitudinally, to explore the effects of lateral reinforcement configurations, especially under high strain rates common in seismic loading. Unlike the Kent and Park (1971) [1] model, calibrated for small-scale testing, Scott et al. (1982) [8] observed a significant increase in strength with robust confinement reinforcement. To accommodate this enhanced compressive strength at high strain rates, minor adjustments were made to the Kent and Park model.

Mander et al. (1988a) [9] expanded the scope by evaluating full-sized square, rectangular, and circular columns at seismic strain rates, investigating diverse lateral reinforcement configurations. Their subsequent model (Mander et al., 1988b) [10] incorporated a fracture criterion based on the five-parameter model of William and Warnke (1975) [11] combined with insights from Schickert and Winkler (1979) [12], resulting in a widely used, generalized multiaxial confinement model. However, the model exhibits limitations with the rise in usage of high-performance materials, necessitating potential revisions.

Yong et al. (1989) [13] proposed a stress-strain relationship specifically for linearly confined high-strength concrete, utilizing two polynomial equations defining the ascending and post-peak branches. Bjerkeli et al. (1990) [14] explored the ductility of high-strength, stress-resistant, reinforced concrete columns subjected to axial loads, identifying factors such as cross-section shape, reinforcement confinement ratio, and concrete compressive strength as key influencers in the stress-strain relationship. Li et al.

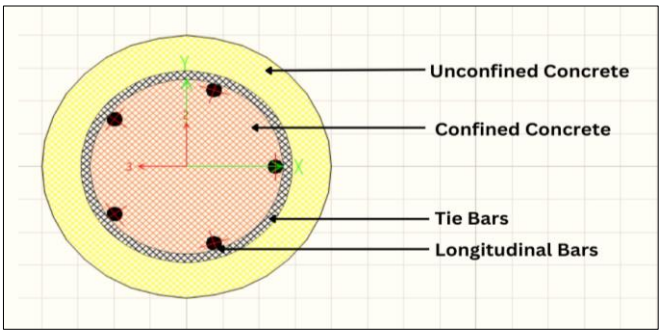

Figure 1. Specifications of concrete column

(2000) [15] conducted experimental tests on high-strength concrete columns confined by various transverse reinforcements, concluding that the stress-strain curve's shape is strongly influenced by confining reinforcement characteristics. Building upon this, Li et al. (2001) [16] developed a three-branch stress-strain model for high-strength concrete under normal- and high-yield-strength transverse reinforcement, based on their comprehensive experimental study. These sequential refinements underscore a continuous pursuit of precision and applicability in stress-strain modeling for confined concrete structures in the realm of structural engineering.

3 Analysis Methodology

The fundamental principle in ABAQUS is the step-by-step breakdown of issue history, where each useful period, encompassing dynamic transients, creep holds, or thermal transients, is denoted as a step. A step in ABAQUS/Standard may range from a basic static analysis of a load shift to more intricate scenarios.

In explicit dynamics processing, a multitude of tiny time increments is effectively executed using the explicit central-difference time integration method. Each increment, owing to the absence of simultaneous equation solutions, is relatively economical compared to the direct-integration dynamic analysis process in ABAQUS/Standard. The velocity and displacement solutions are advanced in time by utilizing accelerations

computed at time 't,' satisfying dynamic equilibrium equations through the explicit central-difference operator.

In the context of field output, ABAQUS/CAE permits the request of full sets of fundamental variables (e.g., components of strain or stress), showcased in X-Y data plots for reasonably frequent output requests in specific model areas.

The concept of embedded regions involves embedding model regions within their host regions or throughout the entire model using embedded region constraints. Here, reinforcement is embedded within the host region, which is concrete. Coupling constraints prove beneficial when a collection of coupling nodes is constrained to the rigid body motion of a single node. Such constraints find practical applications in providing model loads or boundary conditions. Two types of boundary conditions are employed, particularly for fixing one end of the column.

The analysis involves the utilization of six different models as listed in Table 1. each demonstrating significant differences as shown in Figs. 2-7. These differences primarily lie in the hoop distance or pitch distance between consecutive models. This approach allows for a comprehensive exploration of the impact of varying parameters on the structural behavior within the analytical framework.

Table 1. Description of the Models (for Abaqus FE analysis)

Model No.	Height (mm)	Diameter (mm)	Longitudinal Rebar length (mm)	Main Rebar	Hoop Size
1	2000	254	1898.4	5#5 bar	12#5 bar
2	2000	254	1898.4	5#5 bar	7#3 bar, 2#4 bar
3	2000	254	1898.4	5#5 bar	12#3 bar
4	2000	254	1898.4	5#5 bar	12#3 bar
5	2000	254	1898.4	5#5 bar	13#3 bar
6	2000	254	1898.4	5#5 bar	13#3 bar

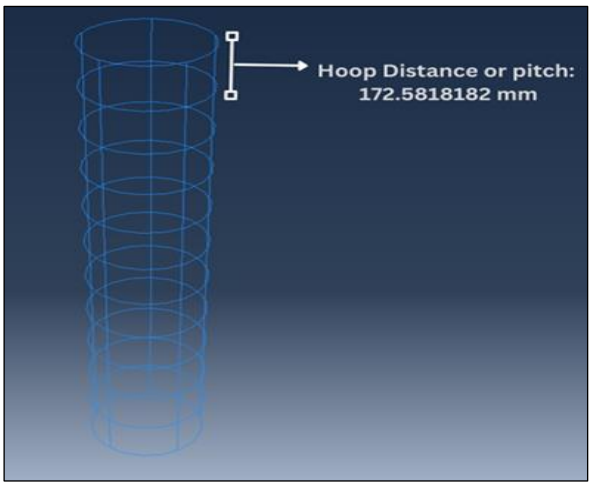

Figure 2. Model-1

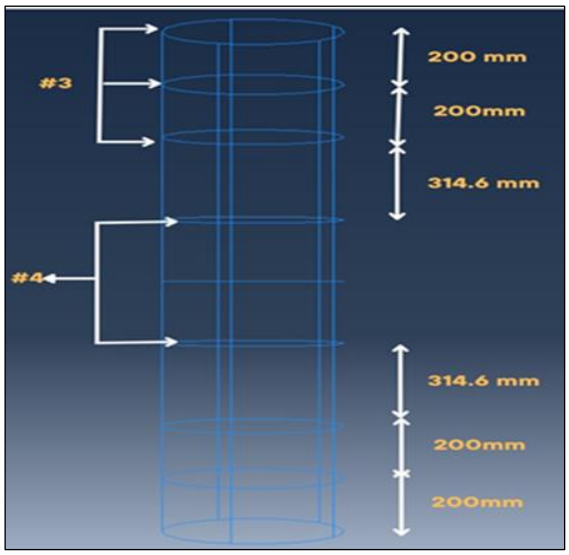

Figure 3. Model-2

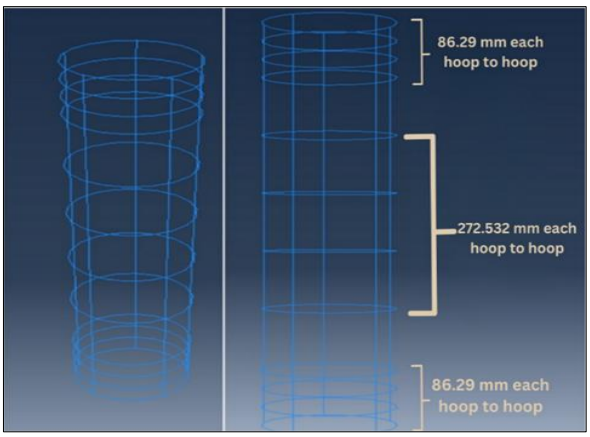

Figure 4. Model-3

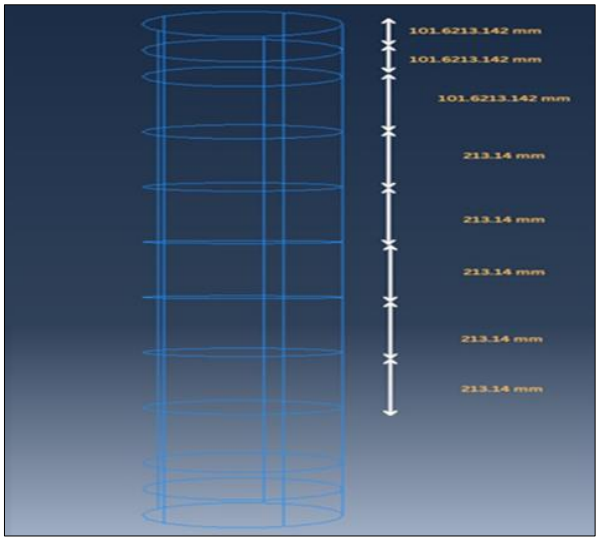

Figure 5. Model-4

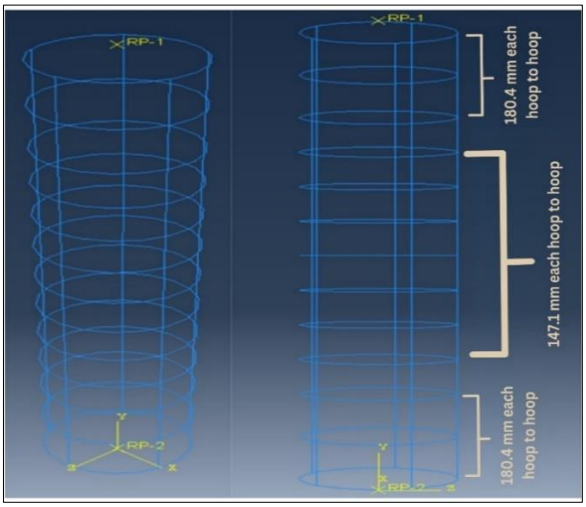

Figure 6. Model-5

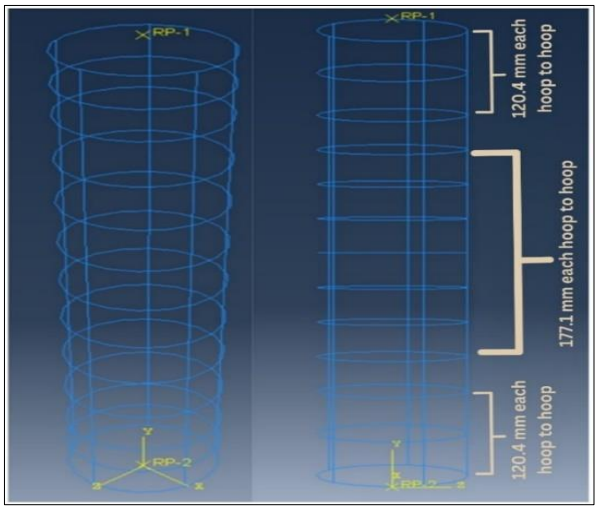

Figure 7. Model-6

4 Model Validation

The validation of the Abaqus model references the experimental work of Guadagnuolo et al. (2020) [17], focusing on concrete column behavior with varying transverse reinforcement details. The process involves defining input parameters like material properties, geometry, meshing, and loading conditions to mirror the experimental setup. Comprehensive data from the reference study, including dimensions, material properties, loading conditions, and force-displacement data, ensures accurate alignment with the physical model. The final model of concrete column shown in Fig. 8. Validation focuses on peak force values, disregarding post-ultimate force data. A rigorous comparison with a database of experimental and simulation results establishes the finite element (FE) model's reliability and accuracy for reinforced concrete columns.

The key material, as well as geometrical characteristics about the experimental data, has been summarized in Table 2. The column dimension of the reference work has been given in Table 2. The simulation in Abaqus produced a force vs. displacement graph, enabling a detailed comparison of the ultimate force obtained through finite element (FE) analysis with experimental results as shown in Fig. 9. The ultimate force from the FE analysis is 2953.03 kN, while the corresponding value from the reference experiment (Guadagnuolo et al. (2020) [17]) is 2990.09 kN. This comparison, conducted entirely through software simulation, shows a close agreement with a marginal difference of 1.24%, emphasizing the model's accuracy. The validation process in Abaqus involved replicating experimental setups, defining material properties, geometry, meshing, and

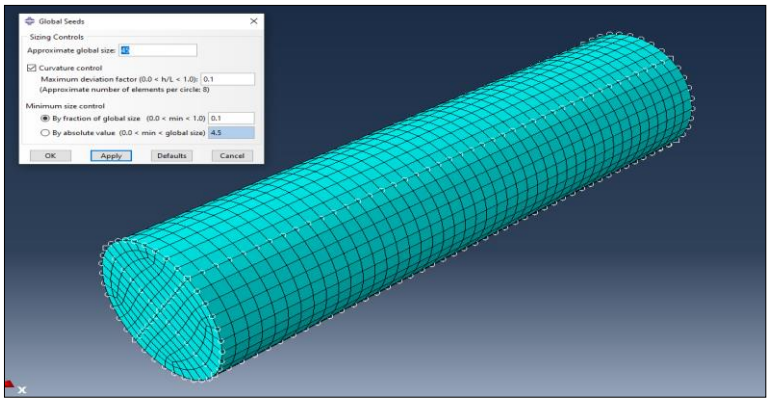

Figure 8. Fine meshing for FE simulation

Table 2. Reference and test specimen details

Research Name	Column Specimen	Concrete, fcu (MPa)	Column dimensions (mm x mm x mm x mm)	Steel reinforce-ment long bars	fy (MPa)		Hoop Size
					Long .Bars	Tie Bars	
Guadagn-uolo et al. (2020)	Column-58	27.80	300 × 300 × 1300	8Φ12 mm	450	450	Φ8@ 150 mm

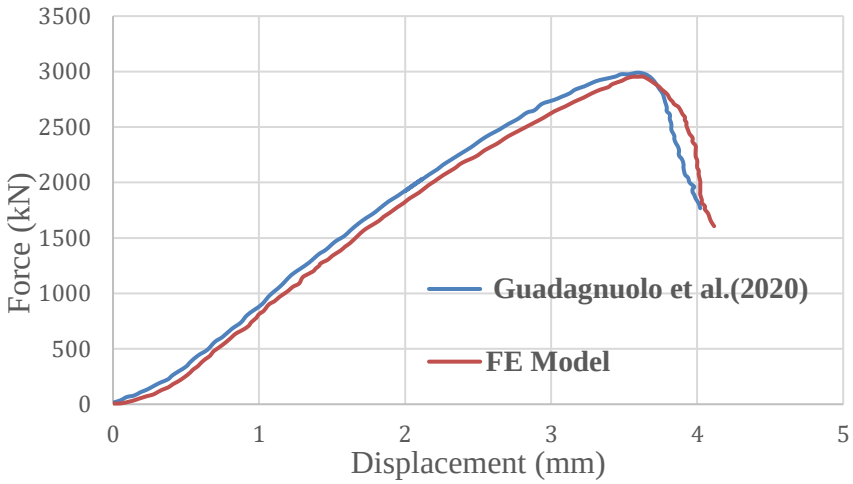

Figure 9. Force vs Displacement graph

loading conditions to ensure precise alignment. The close match between simulated and experimental results highlights the reliability of the FE model in capturing the structural response of reinforced concrete columns.

5 Results and Discussions

Finding the effectiveness of confinement in reinforced column:

This simulation in SAP 2000 for figure out the effectiveness of hoop distance in the column stress strain capacity. The hoop distance is decreased linearly in columns. Several Columns in different pitch conditions has been simulated in this research. At the end of the simulation, it has been seen that different models have different ultimate forces at

different displacements. The ultimate force that a column can bear is governed by a number of parameters, including its size, material qualities, and kind of loading. The diameter or hoop-to-hoop spacing of a column can impact its capacity to withstand axial loads (compression or tension), lateral loads (bending), and other forces. In general, increasing the diameter of a column while holding other elements constant improves the column's capacity to carry axial stresses and resist buckling.

A sample column has been Simulated on the SAP2000.Where are eight different pitch distances as listed in Table 3. For those, the different stress vs strain graphs have been found (shown in Fig. 10).

Table 3. Stress-Strain observation of different pitch distances

Hoops Spacing	Strain	Stress (Ksi)
6 inches	0.0182	4.7843
7 inches	0.0187	4.5730
8 inches	0.0186	4.3893
9 inches	0.0187	4.2940
10 inches	0.0192	4.1961
11 inches	0.0198	4.0872
12 inches	0.0204	4.0563
Without Hoop	0.0022	0.0050

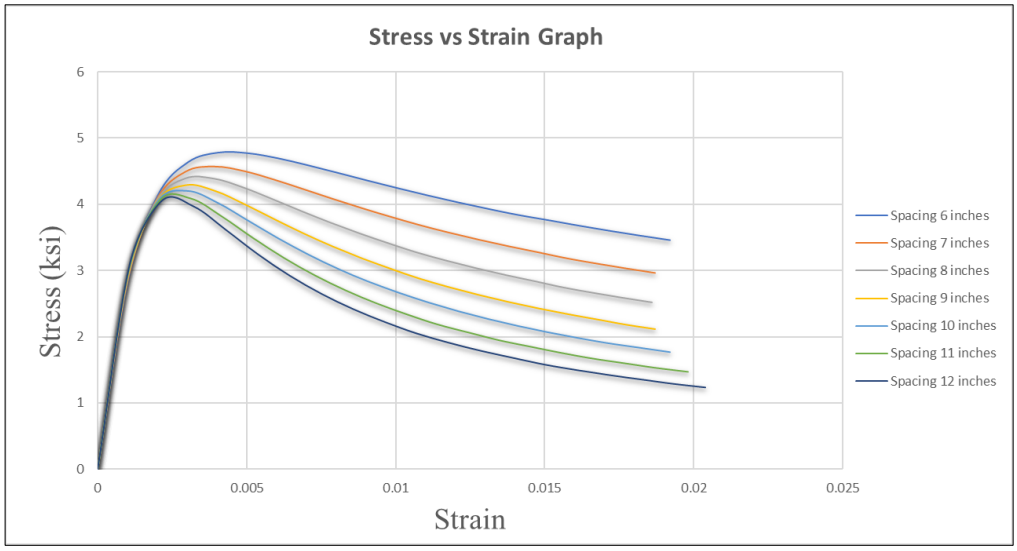

Figure 10. Stress-Strain graph for different pitch conditions

Finding the effective orientation of confinement in reinforced column:

Here for finding the effective confinement orientation in reinforced column there are six different models have been used in Abaqus FE simulation. Each model has significant difference to each other. The difference of the consecutive models has not only in their hoops distance (not necessarily in linear way) but also in their hoops number and orientation, the analytical results are presented in Table 4. and also characterized by Fig. 11.

Table 4. Combined table from the analysis result

Model name	Ultimate Force (kN)	Displacement at Ultimate Force (mm)	Area of Rein. (mm2)	Force/Reinforcement (kN/mm2)
01	4667.718	4.50	851.6112	5.481
02	4541.295	4.65	754.8372	6.016
03	4497.565	4.20	851.6112	5.281
04	4506.795	4.00	851.6112	5.292
05	4737.519	4.70	922.5788	5.135
06	4659.881	4.75	922.5788	5.050

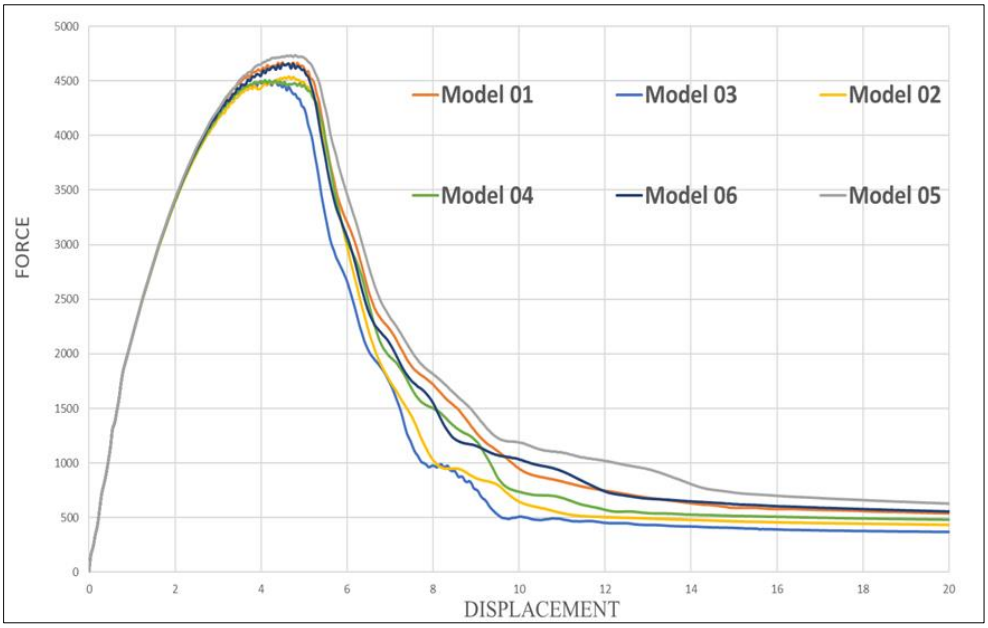

Figure 11. Combined Force vs Displacement graph

Change in reinforcement distribution, with greater spacing in certain regions and increased area in others, may reflect an optimization based on the column's individual load and performance requirements. This improved distribution may result in more efficient load transfer mechanisms and, as a result, larger peak forces per hoop.

Model 02 achieves the highest force-to-reinforcement ratio (6.016 kN/mm²), indicating the most efficient use of reinforcement material. Although its ultimate force (4541.295 kN) is not the highest, the smaller reinforcement area (754.8372 mm²) ensures that the material is utilized effectively. This makes Model 02 the most economical choice when balancing structural performance with resource utilization. Model 01 demonstrates the highest ultimate force (4667.718 kN) with low displacement (4.50 mm), showcasing strong load-carrying capacity and minimal deformation. However, its force-to-reinforcement ratio (5.481 kN/mm²) is lower than Model 02, indicating less efficient material usage. Model 05 delivers the second-highest ultimate force (4737.519 kN) but requires the largest reinforcement area (922.5788 mm²), resulting in a lower efficiency ratio of 5.135 kN/mm². While it provides strong capacity, it is less economical compared to Model 02. Model 06, with a similar ultimate force, exhibits the highest displacement (4.75 mm) and the lowest force-to-reinforcement ratio (5.050 kN/mm²), making it less

effective in both performance and material usage. Models 03 and 04 offer moderate performance but are outperformed by Model 02 in efficiency and by Model 01 in strength.

Overall, Model 02 is the most efficient design with the highest force-to-reinforcement ratio (6.016 kN/mm²), while Model 01 excels in strength for applications prioritizing ultimate load capacity.

The strength and ductility of the column can be improved by adjusting the distribution of reinforcement. While some regions might benefit from greater ductility, others might need more reinforcement to withstand higher loads. Optimization seeks to use materials efficiently, avoiding overdesign in areas where loads are lower. This approach is crucial for economic reasons and sustainability, as it minimizes the use of materials without compromising safety.

To achieve strain compatibility throughout the column, the distribution of reinforcement can be adjusted. It guarantees that the column's various sections deform in unison, encouraging ductile behavior and averting untimely failure.

6 Conclusions

Lateral reinforcement is integral in confining concrete within a column, enhancing both strength and ductility by preventing premature spalling or crushing. This confinement allows the column to deform more ductility before failure and prevents buckling of longitudinal reinforcement (main bars), crucial for maintaining their stability under high axial loads. The study highlights the importance of optimizing reinforcement distribution to improve the strength, ductility, and efficiency of columns. By strategically varying the spacing and area of reinforcement, it is possible to enhance the load transfer mechanisms within the column, allowing it to achieve higher peak forces with better material utilization. Regions subject to higher stresses may require denser reinforcement, while areas experiencing lower stresses can have reduced reinforcement, ensuring a balanced design that avoids overdesign in less critical zones. This approach is not only economical but also promotes sustainability by minimizing material usage without compromising structural safety.

Among the models studied, Model 02 stands out with the highest force-to-reinforcement ratio (6.016 kN/mm²), indicating the most efficient use of materials. While

its ultimate force (4541.295 kN) is not the highest, its smaller reinforcement area (754.8372 mm²) reflects a well-optimized design. On the other hand, Model 01 demonstrates the highest ultimate force (4667.718 kN) with minimal displacement (4.50 mm), making it ideal for applications where maximum load capacity is critical, albeit at a slightly lower efficiency.

Optimizing reinforcement distribution also ensures strain compatibility across the column, encouraging uniform deformation and ductile behavior. This reduces the risk of premature failure, making the column safer and more reliable under varying load conditions. Increasing the hoops area in the middle zone of a reinforced concrete column positively influences both load-carrying and deformation capacities. This practice enhances the performance of columns where ductility is a critical consideration, allowing for a more economical design by utilizing smaller and cost-effective structural members, thereby reducing material and construction.

Acknowledgements

The Authors would like to thank The Almighty and everyone who supported and contributed to the completion of this work.

References

[1] D. C. Kent and R. Park, “Flexural Members with Confined Concrete,” *Journal of the Structural Division,* vol. 97, no. 7, 1971, doi: 10.1061/jsdeag.0002957.

[2] E. Hognestad, “A Study of Combined Bending and Axial Load in Reinforced Concrete Members,” *Bulletin Series No. 399,* 1951.

[3] S. Popovics, “A numerical approach to the complete stress-strain curve of concrete,” *Cem Concr Res,* vol. 3, no. 5, 1973, doi: 10.1016/0008-8846(73)90096-3.

[4] A. Thorenfeldt, E., Tomaszewicz and J. Jensen, “Mechanical properties of high-strength concrete and application in design,” in *Proceedings of the symposium utilization of high strength concrete,* 1987.

[5] W. T. Tsai, “Uniaxial Compressional Stress-Strain Relation of Concrete,” *Journal of Structural Engineering,* vol. 114, no. 9, 1988, doi: 10.1061/(asce)0733-9445(1988)114:9(2133).

[6] H. E. H. Roy and M. A. Sozen, “Ductility of Concrete,” *Symposium Paper*, vol. 12, pp. 213–235, Jan. 1965.

[7] P. Desayi, K. T. Sundara Raja Iyengar, and T. Sanjeeva Reddy, “Equation for stress-strain curve of concrete confined in circular steel spiral,” *Matériaux et Constructions*, vol. 11, no. 5, 1978, doi: 10.1007/BF02473875.

[8] B. D. Scott, R. Park, and M. J. N. Priestley, “Stress-Strain Behavior of Concrete Confined by Overlapping Hoops at Low And High Strain Rates.,” *Journal of the American Concrete Institute*, vol. 79, no. 1, 1982, doi: 10.14359/10875.

[9] J. B. Mander, M. J. N. Priestley, and R. Park, “Observed Stress-Strain Behavior of Confined Concrete,” *Journal of Structural Engineering*, vol. 114, no. 8, 1988, doi: 10.1061/(asce)0733-9445(1988)114:8(1827).

[10] J. B. Mander, M. J. N. Priestley, and R. Park, “Theoretical Stress-Strain Model for Confined Concrete,” *Journal of Structural Engineering*, vol. 114, no. 8, 1988, doi: 10.1061/(asce)0733-9445(1988)114:8(1804).

[11] K. J. Willam and E. P. Warnke, “Constitutive Model for the Triaxial Behavior of Concrete,” in *IABSE} Proceedings, Vol 19*, 1975.

[12] G. Schickert and H. Winkler, “Results of test concerning strength and strain of concrete subjected to multi-axial compressive stress,” pp. 123–123, 1977.

[13] Y. Yong, M. G. Nour, and E. G. Nawy, “Behavior of Laterally Confined High-Strength Concrete under Axial Loads,” *Journal of Structural Engineering*, vol. 114, no. 2, 1988, doi: 10.1061/(asce)0733-9445(1988)114:2(332).

[14] L. Bjerkeli, A. Tomaszewicz, and J. J. Jensen, “Deformation properties and ductility of high-strength concrete,” in *American Concrete Institute, ACI Special Publication*, 1990. doi: 10.14359/2844.

[15] L. Bing, R. Park, and H. Tanaka, “Constitutive behavior of high-strength concrete under dynamic loads,” *ACI Struct J*, vol. 97, no. 4, 2000, doi: 10.14359/7427.

[16] L. Bing, R. Park, and H. Tanaka, “Stress-strain behavior of high-strength concrete confined by ultra-high- and normal-strength transverse reinforcements,” *ACI Struct J*, vol. 98, no. 3, 2001, doi: 10.14359/10228.

[17] M. Guadagnuolo, A. Donadio, A. Tafuro, and G. Faella, “Experimental Behavior of Concrete Columns Confined by Transverse Reinforcement with Different Details,” *The Open Construction & Building Technology Journal*, vol. 14, no. 1, 2020, doi: 10.2174/1874836802014010250.

IJASST International Journal of Applied Sciences and Smart Technologies

Volume 07
Issue 01

p-ISSN 2655-8564, e-ISSN 2685-943, pp. 83-98, 2025

Bubble Flow Configurations Generated by Ejector Type Bubble Generator

IGNB. Catrawedarma [1*], Sefri Ton [2], Dadang Dwi Pranowo [3], Fredy Surahmanto [4], Achilleus Hermawan Astyanto [5,6]

[1]*Department of Mechanical Engineering, Politeknik Negeri Banyuwangi, Jalan Raya Jember Km. 13, Kabat, Banyuwangi 68461, Indonesia*
[2]*Department of Agribusiness, Politeknik Negeri Banyuwangi, Jalan Raya Jember Km. 13, Kabat, Banyuwangi 68461, Indonesia*
[3]*Department of Civil Engineering, Politeknik Negeri Banyuwangi, Jalan Raya Jember Km. 13, Kabat, Banyuwangi 68461, Indonesia*
[4]*Department of Mechanical Engineering Education, Universitas Negeri Yogyakarta, Yogyakarta 55281, Indonesia*
[5]*Department of Mechanical Engineering, Universitas Sanata Dharma, Kampus III USD Maguwoharjo, Yogyakarta 55282, Indonesia*
[6]*Center for Smart Technology Studies, Universitas Sanata Dharma, Kampus III USD Maguwoharjo, Yogyakarta 55282, Indonesia*
[*]*Corresponding Author: ignb.catrawedarma@poliwangi.ac.id*

(Received 18-12-2024; Revised 05-01-2025; Accepted 06-01-2025)

Abstract

Bubble flow configurations generated by an ejector bubble generator were captured using a high-speed video camera and extracted into several images. The air flow and nozzle diameter were varied during the test in ranges of 0.1-1.5 lpm and 1.17-3.5 mm, respectively. The results reveal that in general the bubble flow structure coming out from the bubble generator is divided into three regions, namely the entrance, bubble swarm, and bubble dispersed region. It is found that there is a higher time delay of bubble production when the air flow and the nozzle diameter decrease. On the other hand, the bubble production time is longer, if the air flow and the nozzle diameter increase.

Keywords: Bubble swarm and dispersed regions, bubble delayed dan generated times

1 Introduction

Microbubble generators are a new and emerging technology with extensively potential applications in numerous industries, such as medicine, where they are utilized

This work is licensed under a Creative Commons Attribution 4.0 International License

as a contrast agent in ultrasound examinations to improve the appearance of tissues or organs [1], [2]. In addition, airlift pump systems use microbubbles to lift water and sediment [3]–[6], while wastewater treatment employs them to diminish oil, heavy metals, and tiny particulates in water via the flotation processes [7], [8]. Here, microbubbles possess a high surface area, enabling them to expedite molecular interactions in the chemical industry [9]. Therefore, microbubbles are frequently employed to cleanse fresh products, disinfect food items, and sanitize equipment within the food sectors [10], [11]. On the other hand, microbubbles in the shipping sector also minimize drag on the ship's outer surface, thereby reducing fuel consumption [12].

However, several problems associated with microbubbles' utilization encompass sustaining stability across diverse conditions and attaining a reliable cost-effective manufacturing scale for specific applications. Consequently, various researchers persistently engage in research and development to enhance the utilization of microbubbles and address current issues. They have innovated bubble formation methods, such as reducing the channel cross-section to increase the flow velocity, which in turn increases the shear force and breaks the bubble into a smaller diameter. Included in this method are orifice [13]–[15], venturi [16]–[24], and spherical body [25] types of microbubble generators. Another innovation employs swirl flow to harness centrifugal force for enhancing shear force [26]–[29].

The orifice type features a design characterized by an abrupt decrease in cross-section to enhance fluid velocity, which concurrently elevates the loss of flow energy. Meanwhile, the design of the spherical body, minimizing the cross-section at the channel's periphery instead of its center, poses issues in both production and maintenance. On the other hand, the swirl flow configuration leads to considerable energy dissipations, requiring a pump with substantial capacity to transport water. Therefore, Basso et al. [30] and Terasaka et al. [31] designed a venturi type with a stepwise cross-sectional reduction to minimize flow energy losses, hence enhancing its economic efficiency. Moreover, the venturi type offers the benefits of simple installation and maintenance [32], and it generates bubbles with a smaller diameter while maintaining the same operational parameters as other types [33], [34]. In a mean time, the incorporation of air gap and porous pipes on the air inlet side was executed to achieve a reduced bubble size

distributions [14], [35]–[37]. Additionally, researchers have also used multistage venturi and swirl-venturi combinations to achieve a smaller bubble diameter [27], [28], [38].

Next, Huang et al. [32] synthesized the effects of diverse geometric and operational parameters on venturi-type microbubble generators. The results enhance that the bubble size is inversely proportional to the water discharge, but it is proportional to the air discharge as also implied on several reports [16], [17], [36], [39]. Here, the air discharge has a smaller effect on the size and distribution of bubbles than the water discharge because the bubble rupture is highly dependent on the flow turbulence. Another, augmenting the throat length and divergence angle or reducing the throat and outlet diameters in a venturi-type bubble generator results in a reduction of the bubble diameter [40]. Here, the convergence angle, diameter, and number of air holes have almost no effect on the bubble diameter as also reported by several others [19], [41]. Therefore, the throat diameter and divergence angle play an important role in the performance of the venturi bubble generator.

The present study employs an ejector bubble generator, a variant of the venturi bubble generator in which a similar ejector's working principle was briefly described on the report of Mardikus [42]. Here, the ejector bubble generator utilizes a tapered cross-section at the water input to reduce flow energy loss, and includes supplementary air space prior to the amalgamation of air and water to increase bubbles' production. Investigations toward the detailed characteristics of the bubble generator were carried out by varying the input air flow as a part of the operational parameters and the nozzle diameter as particular geometric parameters. The configuration of the bubble flow emerging from the bubble generator was examined utilizing a high-speed camera. Changes in the time delay and the duration of bubble formation were investigated to determine the optimum value of the pair of the air flow and nozzle diameter.

2 Material and Methods

In the present investigation, a procedure on the experiment, conducted at the Mechanical Engineering Workshop of Politeknik Negeri Banyuwangi, commencing with the assembly of an ejector bubble generator, is schematically illustrated in Fig. 1(A). The water input diameter of the bubble generator, D, was 7 mm, while the nozzle diameter, d,

was adjusted from 1.17 to 3.50 mm. The ejector bubble generator was positioned 5 cm above the base of the test pool, exactly at the midpoint of its width. The test pool was 100 cm in length, 50 cm in width, and 50 cm in height; it was constructed from transparent glass and filled with water to a depth of 45 cm, as depicted in Fig. 1(B).

The data collection was initiated by activating a 12 VDC water pump to supply water to the bubble generator. The water discharge was constantly set at 5.0 liters per minute (lpm) using a water flowmeter. The air discharge flowing from the aerator was regulated from 0.1 to 1.5 lpm through an air flowmeter for each nozzle diameter. Subsequently, the amalgamation of water and air in the ejector bubble generator produced bubbles that were expelled and integrated with the water in the test pool. The bubble flow was captured with a Sony ZV-1 high-speed camera at 1000 frames per second (fps), with a shutter speed of 1/12800, an aperture of f8.0, and an ISO of 4000. The distance from the lens to the central output of the ejector bubble generator was 30 cm. A series of 50 W LED lamps was mounted behind the test pool to enhance the illumination, with a diffused

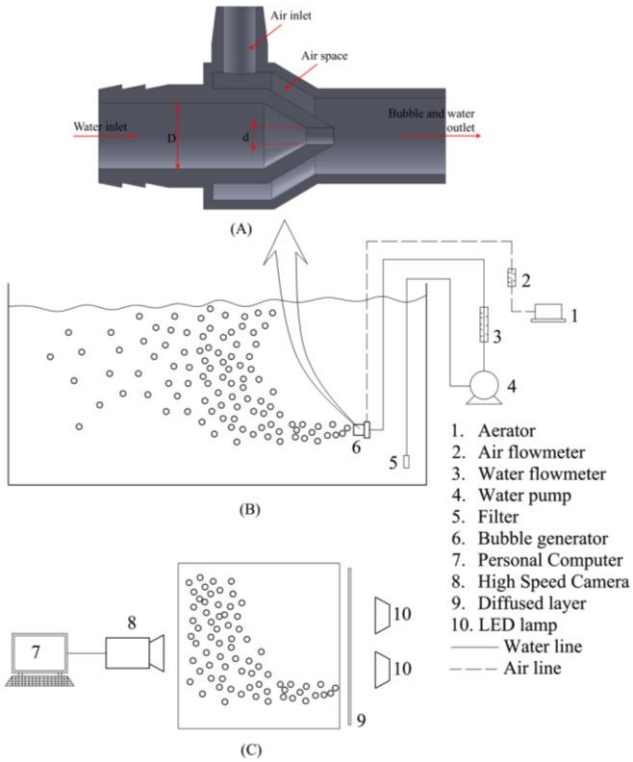

Figure 1. (A) Detail of ejector MBG, (B) Apparatus schematic, (C) Image capturing schematic

layer to achieve a uniform lighting, as depicted in Fig. 1(C). The video of the bubble flow emitted from the bubble generator for each air discharge and nozzle diameter was subsequently recovered into multiple images using MATLAB software to analyze the flow structures, time delays, and created durations.

3 Results and Discussions

3.1. Bubble flow configurations

Fig. 2 illustrates the standard flow configurations when the bubble exits the bubble generator's outlet. Here, flow areas can be grouped into entrance, bubble swarm, and bubble dispersed regions. The entrance region is the closest area to the bubble generator outlet, and the influence of the turbulent flow (yellow line) is very strong on this particular area. This area is referred to a ligament as reported by Mawarni et al.[43] or a mixing shock by Cramers et al.[44]. Next, the flow regions that occur in the ejector include a configuration of jet flow, mixing shock and bubble flow. The jet flow area exhibits a low pressure which drastically increases when it enters the mixing shock area and tends to be stable in the bubble flow area. The mixing shock area has a high rate of energy dissipation, turbulence, and shear stress. It produces small bubbles and increases the interfacial area. Visually, it can be seen that if the air flow increases from Qg = 0.1 lpm to Qg = 1.5 lpm, there is an increase in the entrance length. When the bubble comes out of the outlet, there is another increase in the flow acceleration due to the changes in the momentum between the bubble and the water in the pool.

On the other hand, due to the influence of the hydrostatic force of the water, there is a deceleration in the flow of the previously produced bubble. It causes a high turbulent bubble flow to penetrate the bubble flow that has previously come out. Collisions, ruptures, and amalgamations of bubbles transpire during this penetration. Both, collisions between the bubbles, and also collisions between bubbles and water, respectively, cause an interface instability. Here, if a light fluid is configured below a heavier fluid in a gravitational field, the lighter fluid will press the heavier fluid so that the interface of the two fluids is unstable to small disturbances. However, Rayleigh–Taylor instability states that interface instability between two fluids occurs due to differences in the density. This

interface instability occurs when there is a constant acceleration that leads from the heavy fluid to the light fluid [45]. Additionally, Kelvin-Helmholtz instability also implies that the interface between two fluids becomes unstable if there is a jump in tangential velocity towards the interface. Here, the interface instability between two fluids is caused by differences in velocity [46].

Hence, in the bubble swarm region the influence of turbulent flow begins to decrease, and several bubbles start to separate for evenly distributed. The breaking and coalescing of bubbles begin to occur. The bubble fragments into smaller pieces as a result of the water's hydrodynamic force, which surpasses the bubble's surface tension. The hydrodynamic force of water is generated by the erratic motion of the water and the bubbles emanating from the bubble generator's output. The break of this bubble causes a smaller bubble diameter, which causes the surface tension to become more significant and the rising velocity to become lower. It flows to the red circle with the dotted line in the bubble dispersed area.

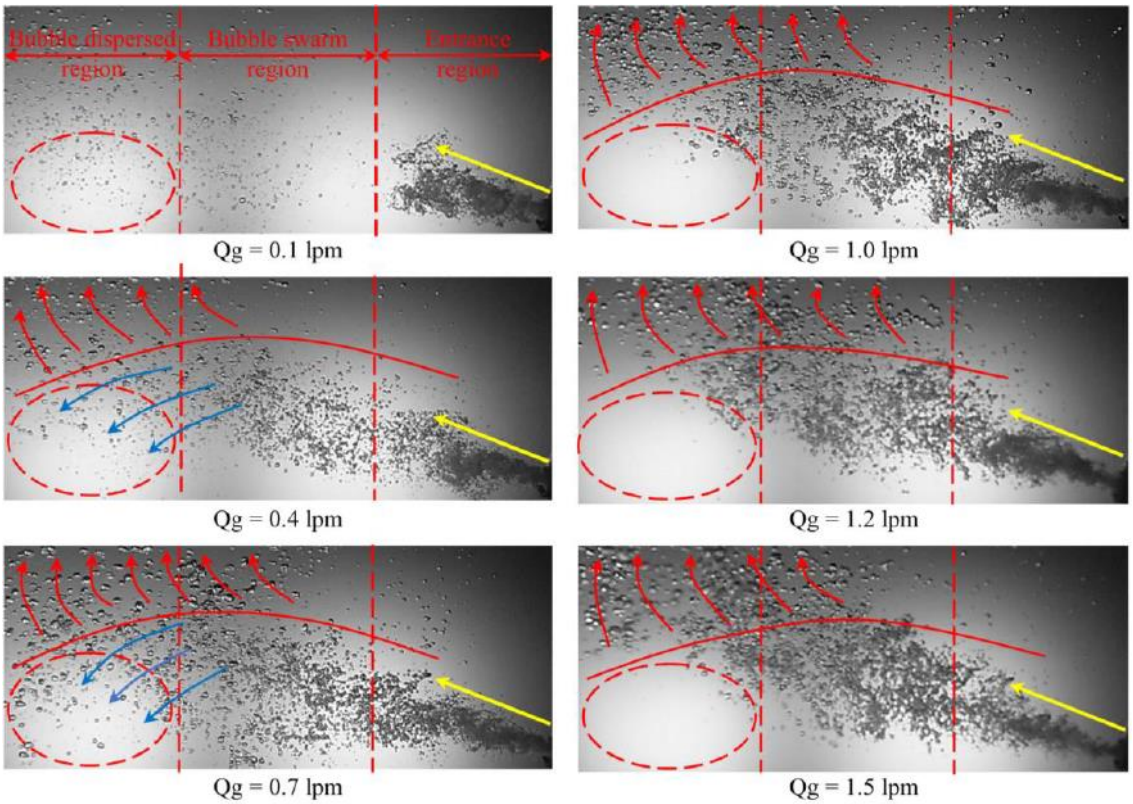

Figure 2. Flow structure in various air flow rate at d = 1.40 mm

Moreover, the bubble flows dispersed in the bubble dispersed region, characterized by the formation of larger bubbles flowing towards the top, as shown by the red arrow. In contrast, bubbles with smaller diameters flow towards the bottom, as indicated by the blue arrow. The circle with the dotted line shows the difference in the small bubble flow area in the bubble dispersed region. Here, the more air flow increases, the fewer bubbles are in the circle with the dotted line. It further shows that the greater the air flow, the larger the diameter of the bubble generated so that its volume is larger. This enhances a buoyancy and ascent velocity of the bubble while reducing its residence period, facilitating upward movement.

Fig. 2 shows that at the air flow Qg = 0.1 lpm, there is a stagnant bubble flow caused by a delay in bubble production time between the first bubble in the dispersed bubble region and the second bubble production in the entrance region. Different phenomena occur when the air discharge increases from Qg = 0.4 lpm to Qg = 1.5 lpm with a shorter bubble production delay time. The smaller water discharge causes this delayed time, and two-phase flow pressure at the outlet of bubble generator becomes lower due to a lower friction between the phases [47]. The low contact area between the phases causes the lower friction between phases due to the smaller bubbles formed when the air flow is lower. Thus, bubbles are smaller when the air flow is lower due to the lower inertial force. The bubble formation process is caused by ‘competition’ between inertial force and the bubble's surface tension. More bubbles are produced when the surface tension exceeds the inertial force.

3.2. Bubble-delay and Bubble-generation Times

One of the factors that affects the performance of the microbubble generator in increasing dissolved oxygen is the number of generated microbubbles. Therefore, when the time delay is longer, the number of bubbles generated is less so that the concentration of dissolved oxygen is lower. Fig. 4 shows the effect of air flow and nozzle diameter on waiting time for bubbles to come out from the ejector and time to produce bubbles. The intermittent nature of the bubble emanating from the ejector output results in a delay in bubble formation.

Fig. 3(A) illustrates the procedure for quantifying bubble-delay and bubble-generation's durations. The video of the bubble formation was extracted in several images, and then the bubble-delay and bubble-generation times were identified. Bubble-generation time is the time needed to produce bubbles or the initial time the bubble comes out from the outlet until it stops coming out. Here in the picture, when t = 0.99 s, the bubble started to flow out of the bubble generator's outlet and moved away until it was separated from the outlet as at t = 1.74 s. A bubble-generation time is determined by subtracting the final time of bubble formation from the initial time, so that here in particular, the bubble-generation time equals to 1.74-0.99 = 0.74 s. After t = 1.74 s, the bubble does not come out of the ejector outlet, and the bubble starts to come out again at t = 2.28 s. The time from t = 1.74 s to t = 2.28 s is called bubble-delay time. Therefore, bubble-delay time is the time to wait until a new bubble produces from the ejector outlet. Here, bubble-delay time is determined by the time of a new generated bubble minus the time of the last generated bubble, so from Fig. 3(A), we get bubble-delay time equals to 2.28-1.74 = 0.54 s.

Fig. 3(B) presents the influence of air discharge on generated and delayed times. The solid line shows the trend line of bubble-delayed time, and the dotted line depicts the bubble-generated time. The greater the air flow at a constant nozzle diameter, the more significant the decrease in bubble-delayed time and the increase in bubble-generated time. It is caused by the influence of the higher flow velocity when the air discharge is more significant. The higher velocity causes the inertial force to be greater, so the two-phase flow pressure at the bubble generator outlet is more significant. It causes the two-phase flow's ability to penetrate the water in the pool to be greater, and the waiting time for the bubble production becomes shorter. It shows that when the air flow supplied to the bubble generator increases, the bubbles form more smoothly without delay. The intersection of the trendline of delayed and generated time occurs at an air discharge of 0.5 lpm, which means that the generated water discharge and the delayed time are almost the same.

Fig. 3(C) shows the effect of nozzle diameter on bubble generated and delayed times. When the nozzle diameter is larger, there is a decrease in the delayed time and an increase in the bubble generated time. It is strongly influenced by a physical phenomenon in which the larger the nozzle diameter, the greater the contact angle between the fluid

and the outlet wall. The greater the contact angle, the smaller the throat area and the shorter the low-pressure area. It allows more bubbles to be sucked in and implicates the longer the bubble generated time. The intersection point of the generated trendline and delayed time occurs at a nozzle diameter of 1.75 mm, with the shortest time difference. It reveals that the nozzle diameter of 1.75 mm is the optimum dimension since there is no significant difference between the bubble-generation and the bubble-delay times.

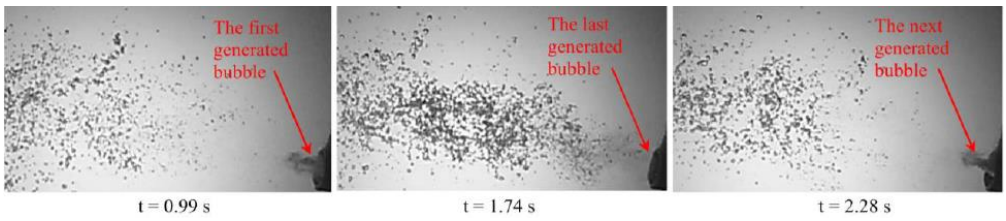

(A)

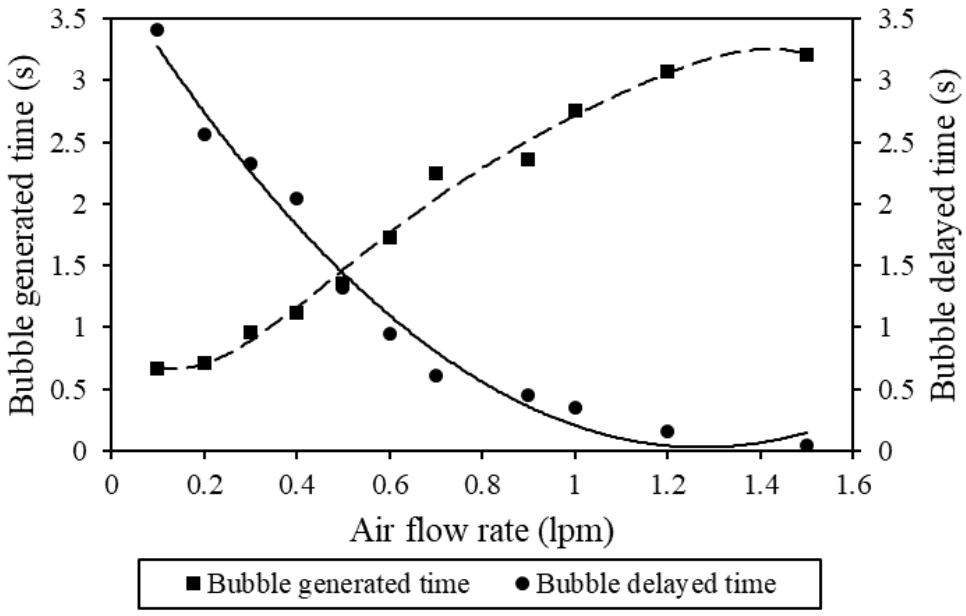

(B)

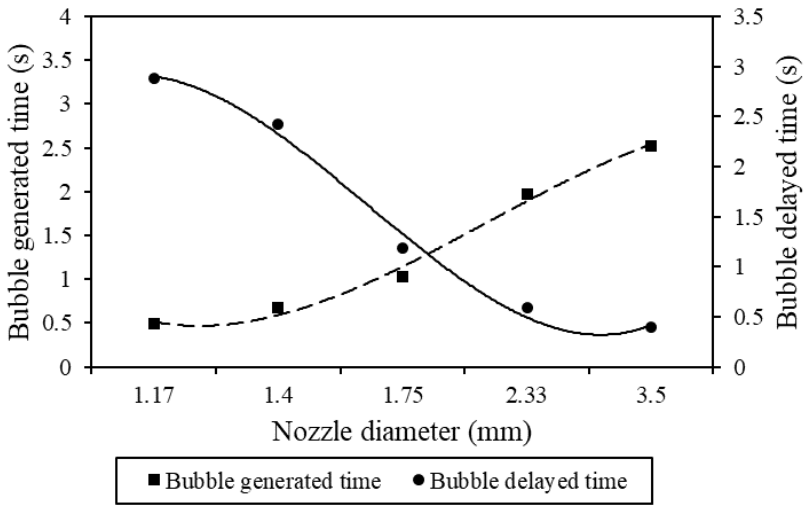

(C)

Figure 3. (A) Measurement of generated and delayed time, (B) Generated and delayed bubbles time for various air flow rate at d = 1.4 mm, (C) Generated and delayed bubbles time for various nozzle diameter at Qg = 0.1 lpm

4 Conclusions

The investigations on the bubble flow configurations generated by bubble generator-type ejectors were conducted to ascertain the bubble flow characteristics, the periods of bubble generation, and the delays in bubble formation for different air discharge rates and nozzle sizes. The results are as follows:

- The bubble flow from the ejector bubble generator is classified into the entrance, bubble swarm, and bubble-dispersed regions. The division of this area is based on the influence of the turbulent flow from the bubble generator outlet, which decreases as the bubble gets further away from the outlet.
- In the bubble formation process using an ejector bubble generator, it is revealed that the time delay in the bubble generated is shorter when the air flow rate is lower and the nozzle diameter is smaller. The duration of bubble generation increases with a higher airflow rate and a larger nozzle diameter. The condition with an air flow rate of 0.5 lpm and a nozzle diameter of 1.75 mm provides an optimum performance for bubble-delayed and bubble-generated times.

Acknowledgements

The authors would like to express a deepest gratitude to Indonesia Endowment Fund for Education Agency (Lembaga Pengelola Dana Pendidikan/LPDP) and Direktorat Pendanaan Riset dan Inovasi, National Research and Innovation Agency (Badan Riset dan Inovasi Nasional/BRIN) for the financial support through the Riset dan Inovasi untuk Indonesia Maju (RIIM-4) scheme with contract number 136/IV/KS/11/2023.

References

[1] S. S. Dastgheyb and J. R. Eisenbrey, Microbubble Applications in Biomedicine, in Handbook of Polymer Applications in Medicine and Medical Devices, Elsevier (2014) pp. 253–277, doi: 10.1016/B978-0-323-22805-3.00011-6.

[2] A. Sridharan, J. R. Eisenbrey, P. Machado, E. D. deMuinck, M. M. Doyley, and F. Forsberg, Delineation of Atherosclerotic Plaque Using Subharmonic Imaging Filtering Techniques and a Commercial Intravascular Ultrasound System, *Ultrason Imaging*, vol. 35, no. 1, pp. 30–44, Jan. 2013, doi: 10.1177/0161734612469511.

[3] IGNB. Catrawedarma, Deendarlianto, and Indarto, Statistical Characterization of Flow Structure of Air – water Two-phase Flow in Airlift Pump – Bubble Generator System, *International Journal of Multiphase Flow*, vol. 138, no. 103596, pp. 1–16, 2021, doi: 10.1016/j.ijmultiphaseflow.2021.103596.

[4] I. Catrawedarma, Deendarlianto, and Indarto, The performance of airlift pump for the solid particles lifting during the transportation of gas-liquid-solid three-phase flow : A comprehensive research review, *Proc IMechE Part E: J. Process Mechanical Engineering*, vol. 0, no. 0, pp. 1–23, 2020, doi: 10.1177/0954408920951728.

[5] G. Ligus, D. Zajac, M. Masiukiewicz, and S. Anweiler, A new method of selecting the airlift pump optimum efficiency at low submergence ratios with the use of image analysis, *Energies*, vol. 12, no. 4, 2019, doi: 10.3390/en12040735.

[6] P. Enany, O. Shevchenko, and C. Drebenstedt, Experimental Evaluation of Airlift Performance for Vertical Pumping of Water in Underground Mines, *Mine Water and the Environment*, vol. 40, no. 4, pp. 970–979, 2021, doi: 10.1007/s10230-021-00807-w.

[7] S. Khuntia, S. K. Majumder, and P. Ghosh, Microbubble-aided water and wastewater purification: a review, *Reviews in Chemical Engineering*, vol. 28, no. 4–6, Jan. 2012, doi: 10.1515/revce-2012-0007.

[8] C. Liu *et al.*, Effect of microbubble and its generation process on mixed liquor properties of activated sludge using Shirasu porous glass (SPG) membrane system, *Water Research*, vol. 46, no. 18, pp. 6051–6058, Nov. 2012, doi: 10.1016/j.watres.2012.08.032.

[9] R. Parmar and S. K. Majumder, Microbubble generation and microbubble-aided transport process intensification—A state-of-the-art report, *Chemical Engineering and Processing: Process Intensification*, vol. 64, pp. 79–97, Feb. 2013, doi: 10.1016/j.cep.2012.12.002.

[10] J. Lu, O. G. Jones, W. Yan, and C. M. Corvalan, Microbubbles in Food Technology, *Annu. Rev. Food Sci. Technol.*, vol. 14, no. 1, pp. 495–515, Mar. 2023, doi: 10.1146/annurev-food-052720-113207.

[11] H. Zhang and R. V. Tikekar, Air microbubble assisted washing of fresh produce: Effect on microbial detachment and inactivation, *Postharvest Biology and Technology*, vol. 181, p. 111687, Nov. 2021, doi: 10.1016/j.postharvbio.2021.111687.

[12] A. Hashim, O. B. Yaakob, K. K. Koh, N. Ismail, and Y. M. Ahmed, Review of micro-bubble ship resistance reduction methods and the mechanisms that affect the skin friction on drag reduction from 1999 to2015, *Jurnal Teknologi*, vol. 74, no. 5, pp. 105–114, 2015, doi: 10.11113/jt.v74.4650.

[13] N. Dietrich, N. Mayoufi, S. Poncin, N. Midoux, and H. Z. Li, Bubble formation at an orifice: A multiscale investigation, *Chemical Engineering Science*, vol. 92, pp. 118–125, Apr. 2013, doi: 10.1016/j.ces.2012.12.033.

[14] W. E. Juwana, A. Widyatama, O. Dinaryanto, W. Budhijanto, Indarto, and Deendarlianto, Hydrodynamic characteristics of the microbubble dissolution in liquid using orifice type microbubble generator, *Chemical Engineering Research and Design*, vol. 141, pp. 436–448, Jan. 2019, doi: 10.1016/j.cherd.2018.11.017.

[15] S. H. Marshall, M. W. Chudacek, and D. F. Bagster, A model for bubble formation from an orifice with liquid cross-flow, *Chemical Engineering Science*, vol. 48, no. 11, pp. 2049–2059, 1993, doi: 10.1016/0009-2509(93)80081-Z.

[16] A. Gordiychuk, M. Svanera, S. Benini, and P. Poesio, Size distribution and Sauter mean diameter of micro bubbles for a Venturi type bubble generator, *Experimental Thermal and Fluid Science*, vol. 70, pp. 51–60, 2016, doi: 10.1016/j.expthermflusci.2015.08.014.

[17] J. Huang *et al.*, A visualized study of bubble breakup in small rectangular Venturi channels, *Exp. Comput. Multiph. Flow*, vol. 1, no. 3, pp. 177–185, Sep. 2019, doi: 10.1007/s42757-019-0018-x.

[18] J. Huang *et al.*, An investigation on the performance of a micro-scale Venturi bubble generator, *Chemical Engineering Journal*, vol. 386, p. 120980, Apr. 2020, doi: 10.1016/j.cej.2019.02.068.

[19] C. H. Lee, H. Choi, D.-W. Jerng, D. E. Kim, S. Wongwises, and H. S. Ahn, Experimental investigation of microbubble generation in the venturi nozzle, *International Journal of Heat and Mass Transfer*, vol. 136, pp. 1127–1138, Jun. 2019, doi: 10.1016/j.ijheatmasstransfer.2019.03.040.

[20] L. Putri, W. Endra, and F. Martino, Performance of Porous-Venturi Microbubble Generator for Aeration Process, vol. 2, no. 2, pp. 73–80, 2017.

[21] A. Yadav, A. Kumar, and S. Sarkar, Performance evaluation of venturi aeration system, *Aquacultural Engineering*, vol. 93, p. 102156, May 2021, doi: 10.1016/j.aquaeng.2021.102156.

[22] A. Yadav and S. M. Roy, An artificial neural network-particle swarm optimization (ANN-PSO) approach to predict the aeration efficiency of venturi aeration system, *Smart Agricultural Technology*, vol. 4, p. 100230, Aug. 2023, doi: 10.1016/j.atech.2023.100230.

[23] L. Zhao, L. Sun, Z. Mo, J. Tang, L. Hu, and J. Bao, An investigation on bubble motion in liquid flowing through a rectangular Venturi channel, *Experimental Thermal and Fluid Science*, vol. 97, pp. 48–58, Oct. 2018, doi: 10.1016/j.expthermflusci.2018.04.009.

[24] L. Zhao *et al.*, Effects of the divergent angle on bubble transportation in a rectangular Venturi channel and its performance in producing fine bubbles, *International Journal of Multiphase Flow*, vol. 114, pp. 192–206, May 2019, doi: 10.1016/j.ijmultiphaseflow.2019.02.003.

[25] M. Sadatomi, A. Kawahara, K. Kano, and A. Ohtomo, Performance of a new micro-bubble generator with a spherical body in a flowing water tube, *Experimental Thermal and Fluid Science*, vol. 29, no. 5, pp. 615–623, 2005, doi: 10.1016/j.expthermflusci.2004.08.006.

[26] D. I. Mawarni *et al.*, Statistical Characterization of Bubble Breakup Flow Structures in Swirl-Type Bubble Generator Systems, *ASEAN J. Chem. Eng.*, vol. 23, no. 1, p. 62, Apr. 2023, doi: 10.22146/ajche.78558.

[27] X. Wang *et al.*, Performance comparison of swirl-venturi bubble generator and conventional venturi bubble generator, *Chemical Engineering and Processing - Process Intensification*, vol. 154, p. 108022, Aug. 2020, doi: 10.1016/j.cep.2020.108022.

[28] X. Wang *et al.*, Bubble breakup in a swirl-venturi microbubble generator, *Chemical Engineering Journal*, vol. 403, p. 126397, Jan. 2021, doi: 10.1016/j.cej.2020.126397.

[29] X. Xu, X. Ge, Y. Qian, B. Zhang, H. Wang, and Q. Yang, Effect of nozzle diameter on bubble generation with gas self-suction through swirling flow, *Chemical Engineering Research and Design*, vol. 138, pp. 13–20, Oct. 2018, doi: 10.1016/j.cherd.2018.04.027.

[30] A. Basso, F. A. Hamad, and P. Ganesan, Effects of the geometrical configuration of air–water mixer on the size and distribution of microbubbles in aeration systems, *Asia-Pacific Journal of Chemical Engineering*, vol. 13, no. 6, pp. 1–11, 2018, doi: 10.1002/apj.2259.

[31] K. Terasaka, A. Hirabayashi, T. Nishino, S. Fujioka, and D. Kobayashi, Development of microbubble aerator for waste water treatment using aerobic activated sludge, *Chemical Engineering Science*, vol. 66, no. 14, pp. 3172–3179, 2011, doi: 10.1016/j.ces.2011.02.043.

[32] J. Huang *et al.*, A review on bubble generation and transportation in Venturi-type bubble generators, *Experimental and Computational Multiphase Flow*, vol. 2, no. 3, pp. 123–134, 2020, doi: 10.1007/s42757-019-0049-3.

[33] A. Yoshida, O. Takahashi, Y. Ishii, Y. Sekimoto, and Y. Kurata, Water purification using the adsorption characteristics of microbubbles, *Japanese Journal of Applied Physics, Part 1: Regular Papers and Short Notes and Review Papers*, vol. 47, no. 8 PART 1, pp. 6574–6577, 2008, doi: 10.1143/JJAP.47.6574.

[34] S. Uesawa, A. Kaneko, and Y. Abe, Measurement of void fraction in dispersed bubbly flow containing micro-bubbles with constant electric current method, 2012, doi: 10.1016/j.flowmeasinst.2012.03.010.

[35] D. Deendarlianto, I. Indarto, W. E. Juwana, L. P. Afisna, and F. M. Nugroho, Performance of Porous-Venturi Microbubble Generator for Aeration Process, *JEMMME*, vol. 2, no. 2, Dec. 2017, doi: 10.22219/jemmme.v2i2.5054.

[36] L. Sun *et al.*, Characteristics and mechanism of bubble breakup in a bubble generator developed for a small TMSR, *Annals of Nuclear Energy*, vol. 109, pp. 69–81, Nov. 2017, doi: 10.1016/j.anucene.2017.05.015.

[37] L. Zhao *et al.*, A visualized study of the motion of individual bubbles in a venturi-type bubble generator, *Progress in Nuclear Energy*, vol. 97, pp. 74–89, May 2017, doi: 10.1016/j.pnucene.2017.01.004.

[38] G. Ding, Z. Li, J. Chen, and X. Cai, An investigation on the bubble transportation of a two-stage series venturi bubble generator, *Chemical Engineering Research and Design*, vol. 174, pp. 345–356, Oct. 2021, doi: 10.1016/j.cherd.2021.08.022.

[39] J. Huang, L. Sun, M. Du, Z. Mo, and L. Zhao, A visualized study of interfacial behavior of air–water two-phase flow in a rectangular Venturi channel, *Theoretical and Applied Mechanics Letters*, vol. 8, no. 5, pp. 334–344, 2018, doi: 10.1016/j.taml.2018.05.004.

[40] F. Reichmann, M.-J. Koch, and N. Kockmann, Investigation of Bubble Breakup in Laminar, Transient, and Turbulent Regime Behind Micronozzles, in *ASME 2017 15th International Conference on Nanochannels, Microchannels, and Minichannels*, Cambridge, Massachusetts, USA, Aug. 2017, p. V001T03A001. doi: 10.1115/ICNMM2017-5540.

[41] J. Li, Y. Song, J. Yin, and D. Wang, Investigation on the effect of geometrical parameters on the performance of a venturi type bubble generator, *Nuclear Engineering and Design*, vol. 325, pp. 90–96, Dec. 2017, doi: 10.1016/j.nucengdes.2017.10.006.

[42] S. Mardikus, Effects of Shock Wave Phenomenon on Different Convergent Lengths in the Mixing Chamber of the Steam Ejector, *International Journal of Applied Sciences and Smart Technologies*, vol. 3, no. 1, pp. 93–100, Jun. 2021, doi: https://dx.doi.org/10.24071/ijasst.v3i1.3249.

[43] D. I. Mawarni, W. E. Juwana, K. A. Yuana, W. Budhijanto, Deendarlianto, and Indarto, Hydrodynamic characteristics of the microbubble dissolution in liquid using the swirl flow type of microbubble generator, *Journal of Water Process Engineering*, vol. 48, p. 102846, Aug. 2022, doi: 10.1016/j.jwpe.2022.102846.

[44] P. Cramers, A. Beenackers, and van L. Dierendonck, Hydrodinamics and mass transfer characteristics of a loop-venturi reaktor with a downflow liquid jet ejector, *Chemical Engineering Science*, vol. 47, no. 13/14, pp. 3557–3564, 1992.

[45] I. Catrawedarma, D. Deendarlianto, and I. Indarto, Statistical Characterization of Flow Structure of Air–water Two-phase Flow in Airlift Pump–Bubble Generator System, *International Journal of Multiphase Flow*, vol. 138, no. 103596, 2021.

[46] D. H. Sharp, An overview of Rayleigh-Taylor instability, *Physica D: Nonlinear Phenomena*, vol. 12, no. 1–3, pp. 3–18, Jul. 1984, doi: 10.1016/0167-2789(84)90510-4.

[47] E. N. Sari, A. Fiveriati, N. Rusti, J. Rulianto, R. Bhiqman Susanto, and I. Catrawedarma, Visual and Pressure Signal Investigations on Bubble Produced by Ejector Bubble Generator, *E3S Web Conf.*, vol. 483, p. 03020, 2024, doi: 10.1051/e3sconf/202448303020.

This page intentionally left

IJASST International Journal of Applied Sciences and Smart Technologies

Volume 07
Issue 01

p-ISSN 2655-8564, e-ISSN 2685-943, pp. 99-108, 2025

Comparison of Laterite Nickel Deposit Levels on the Mining Front with Stockpile at PT Ceria Nugraha Indotama, Kolaka Regency

Anshariah[1], Muhammad Reza Ardhana Irwan[1],
Alam Budiman Thamsi[1*], Muhammad Aswadi[2]

[1] *Faculty of Industrial Technology, Muslim University of Indonesia, 455696, Indonesia*
[2] *Faculty of engineering, Tadulako University, Sekoarno Hatta KM.9, 94148, Indonesia*
[*]*Corresponding Author: alambudiman.thamsi@umi.ac.id*

(Received 20-11-2024; Revised 03-01-2025; Accepted 09-01-2025)

Abstract

PT Ceria Nugraha Indotama is a company engaged in mining laterite nickel ore in Wolo sub-district, Kolaka district, Southeast Sulawesi province. In lateritic nickel ore mining activities, there is often a difference in levels of laterite nickel ore when it is still in the mining front and after being transferred to the stockpile. This research is to determine the proportion of differences in the levels of Ni, Fe, MgO and SiO2 on the mining front with the stockpile and to determine the factors that influence changes in nickel content. The method used in this study is the grab sampling method in front mining and stockpile. The results of this study are based on the results of the analysis, obtained data on the levels of Ni, Fe, MgO and SiO2 on the mining front with a stockpile, the Ni content has a difference of 0.05% and the Fe content has a difference of 0.34%, the two minerals have the highest grades on the mining front. mining and MgO content has a difference of 2.68% and SiO2 content has a difference of 8.87%, the two minerals have the highest grade in the stockpile. Factors that influence changes in nickel content are the heterogeneous distribution of ore, the position of the waste above the ore and the rainy weather that occurs in the field, operator and sampling skills.

Keywords: Grade, Nickel Laterite, Front, Stockpile, Grab Sampling

1 Introduction

Indonesia is a country that has many special resources in eastern Indonesia [1].[2]. On the island of Sulawesi there is the Sulawesi Ofiolite Complex, which is the third largest Ofiolite Complex in the world [3]. In foreign languages, the Sulawesi Ofiolite

This work is licensed under a Creative Commons Attribution 4.0 International License

Complex is considered the East Sulawesi Ophiolite Belt (ESOB) or East Sulawesi Ofiolite lane. The formation of nickel deposits in the tropics occurs due to the weathering process of ultraalkaline rocks whose Ni content reaches 0.25% [4]. Currently, the mining industry is faced with a problem where its mining reserves are getting thinner and even depleted, causing companies to stop mining activities in an area. Mineral resources that have special properties are *Non Reneable Resources* which is if the mineral material will not be renewed or in other words, the mining industry means a large industry without recycling [5]. Topography is one of the factors that affect the availability of laterite nickel resources. The surrounding topography can affect water movement which can help the formation of laterite nickel deposits [6], [7]. Laterite nickel deposits are products derived from the advanced weathering process in Ni-Silicate-carrying ultramafic rocks, generally found in areas with tropical to subtropical climates. Indonesia is known to be one of the countries that produces mineral materials in the world, including nickel [8], [9]. Nickel laterite is a type of metallic mineral obtained through the chemical weathering process of ultraalkaline rocks, which makes residue enrichment and secondary origins of the elements Ni, Mn, Fe, and Co. Nickel laterite is characterized by containing metal oxides using a reddish-brown color and containing Ni and Fe [10]. There are two groups of laterite nickel ores, namely limonite zone nickel with low nickel content and saprolite zone nickel with high nickel content. The disparity that exists in these two types of ore zones is that the ore in the saprolite zone has a low Fe content and high Mg while the limonite zone has a high Fe content and low Mg [11]. Laterite nickel deposits are deposits due to the lateritic weathering process of ultramafic host rocks (perittite, dunit, and serpentinite) containing Ni using high levels, the weathering agents are in the form of rainwater, temperature, humidity, topography, and others. Generally, the formation of laterite nickel deposits occurs in tropical or sub-tropical areas [12], [13].

Changes in levels that occur on the mining and stockpile fronts must be identified as various possible causes so that with the knowledge of the causes of these changes in levels can be overcome to minimize their occurrence, because if not done this will continue so that the quality of the excavated material may decrease to not meet the specifications of the demand level for shipping needs and will have the potential to cause losses for the Ceria Nugraha company Indotama. The formulation of the problem in this

study is how much is the percentage difference in Ni, Fe, MgO and SiO2 levels on the mining front with the stockpile and what are the factors that affect the change in nickel levels. The purpose of this study is to find out the percentage difference in Ni, Fe, MgO and SiO2 levels on the mining front with the stockpile and to find out the factors that affect the change in nickel levels.

2 Material and Methods

The type of data used in this study consists of primary data and secondary data. Primary data is data collected by making direct observations in the field. The data that will be used in this study are documentation data, level data on the mining front, content data on the *stockpile* and the level analysis process using XRF equipment in the company's laboratory [14], [15]. Secondary data is data obtained from the company/agency based on the results of previous observations or research such as company archives, journals and reference books. Secondary data in this study are the map of the research location and the company's SOP (standard operating *procedure*). The data processing used in this study is quantitative data processing. General conclusion based on the results of the data analysis method In this study, the data analysis technique used is descriptive quantitative analysis. The author uses a descriptive method to obtain an overview of the results of data processing in the Excel application [16].

3 Results and Discussions

The levels of laterite nickel deposits often experience differences between *the mining front* and *the stockpile*, so the author analyzed the data on the levels of laterite nickel deposits on samples on the *mining front* with *the stockpile*. The samples used amounted to 300 samples on the *mining front* with stockpiles. Every 20 samples were analyzed using XRF equipment so that the author obtained 15 values of laterite nickel deposits in Ni, Fe, MgO and SiO2 minerals in the *mining front* with *a stockpile* while the factors that affect the change in nickel content are the distribution of heterogeneous ore, the position of impurities to *ore*, weather and operator and *sampling skills*.

Difference in Laterite Nickel Deposit Levels in *Mining Fornt* with *Stockpile*

To find out the difference in the levels of laterite nickel deposits, it is necessary to compare the levels in the *mining front* area with *the stockpile*. The values of nickel precipitation rates compared are Ni, Fe, MgO and SiO2 (shown in Table 1).

Based on Table 1, the author has data on the level of laterite nickel deposits on the *mining front* . The minerals compared by the author are nickel, iron, magnesium oxide and silica. The value obtained from the author comes from the award pit at PT Ceria Nugraha Indotama. The total level owned by the author is 15 levels.

Table 2 shows the value of laterite nickel deposits in the *stockpile*. The data owned by the author comes from *Dome* 172, *Dome* 174, *Dome* 176, *Dome179 and Dome* 182. The total levels owned by the author are 15 levels equal to the data on the level of laterite nickel deposits on the *mining front*.

Table 1. Data on Laterite Nickel Deposit Levels on *the Mining* Front

It	*Assay*				Qty	Location
	Ni	Fe	MgO	SiO2		
1	1.82	15.44	13.46	37.96	1	Pit Anugrah
2	1.74	15.25	13.31	38.40	1	Pit Anugrah
3	1.63	13.28	13.47	40.39	1	Pit Anugrah
4	1.68	22.57	7.56	27.71	1	Pit Anugrah
5	1.82	17.91	9.84	37.72	1	Pit Anugrah
6	1.68	14.50	12.23	42.65	1	Pit Anugrah
7	1.64	13.78	11.80	40.41	1	Pit Anugrah
8	2.03	15.43	12.31	37.89	1	Pit Anugrah
9	1.90	11.16	13.99	43.05	1	Pit Anugrah
10	1.84	13.28	11.90	41.10	1	Pit Anugrah
11	1.98	13.94	13.27	39.32	1	Pit Anugrah
12	1.56	13.52	11.47	47.32	1	Pit Anugrah
13	1.36	14.17	10.53	44.62	1	Pit Anugrah
14	1.34	12.80	11.95	44.56	1	Pit Anugrah
15	1.36	14.31	11.45	44.99	1	Pit Anugrah

Table 2. Data on Nickel Laterite Deposits on *Stockpile*

It	*Assay*				Qty	Location
	Ni	Fe	MgO	SiO2		
1	1.61	13.36	19.26	45.84	1	*Dome* 172
2	1.86	14.34	16.52	45.97	1	*Dome* 172
3	1.63	13.45	17.77	48.19	1	*Dome* 172
4	1.59	13.59	11.58	54.26	1	*Dome* 174
5	1.55	14.79	13.39	52.05	1	*Dome* 174
6	1.71	14.83	13.61	49.68	1	*Dome* 174
7	1.72	13.41	14.45	48.14	1	*Dome* 174
8	1.71	19.63	14.14	37.35	1	*Dome* 176
9	1.63	17.13	14.37	39.79	1	*Dome* 176
10	2.24	16.31	15.67	44.71	1	*Dome* 179
11	1.75	16.22	15.78	48.02	1	*Dome* 179
12	1.50	12.43	16.95	53.52	1	*Dome* 182
13	1.63	13.02	13.36	56.39	1	*Dome* 182
14	1.27	10.84	11.46	59.56	1	*Dome* 182
15	1.30	12.90	10.41	57.70	1	*Dome* 182

Fig. 1 shows the average rate value of laterite nickel deposits made in the form of a graph. In the graph there are 2 lines where the blue line is the rate value on the stockpile and the red line is the rate value on the mining front. At the nickel (Ni) level, the author obtained a difference in the value of 0.04% with the highest level on the mining front. At the iron content (Fe), the author obtained a difference in the value of 0.34% with the highest rate on the mining front. At the magnesium oxide (MgO) level, the author obtained a difference in the value of 2.68% with the highest level in the stockpile. at silica (SiO_2) level, the author obtained a difference of 8.87% with the highest value in the stockpile.

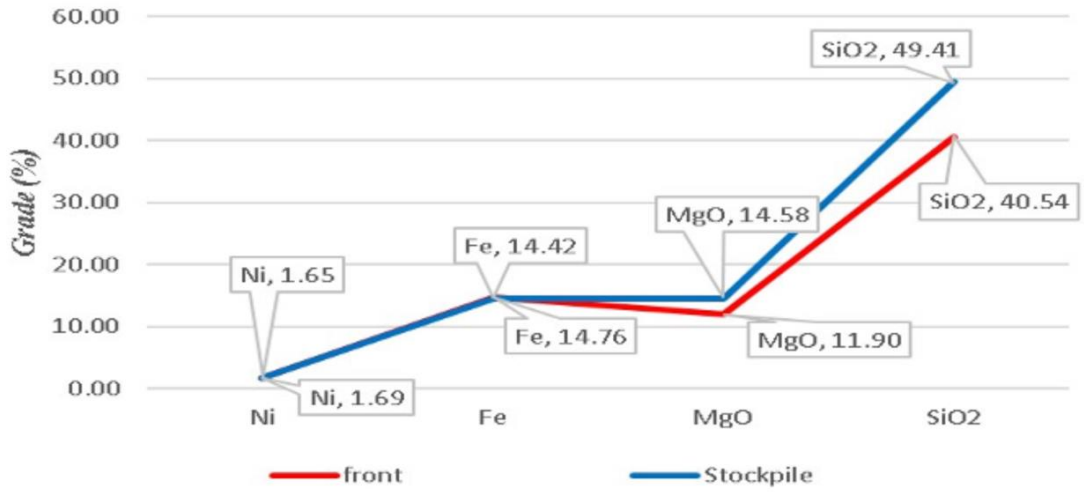

Figure 1. Comparison graph of the average levels of Laterite Nickel Deposits (Ni, Fe, MgO and SiO2).

Difference in Laterite Nickel Deposit Levels on *Mining Fronts* with *Stockpile*

Nickel has several factors that can cause the value of the rate to decrease. Based on Fig. 2, *non-homogeneous ore can cause changes in nickel levels because during* ore getting *activities, impurities* (waste) *can be included in the ore* product (Pranata et al., 2017). So that in carrying out *ore getting* activities, it is necessary to pay attention to grade *control* which functions to petrify operators in the implementation of *ore getting activities.*

In Fig. 3, it can be seen that in the *mining front* area, the *position of waste* and *ore* is always close together. This can cause changes in nickel levels. Nickel levels can be affected by rainy weather with rain can cause the *moisture content* content in ore products *to* increase so that this can cause *ore* products to be damaged or not meet *the needs of buyers.*

As shown in Fig. 4, *ore getting* is a very important activity. At the ore *getting* stage, impurities (*waste*) often occur in the *ore* product so that the presence of *waste* in *the ore* product can cause the nickel level to decrease. Therefore, it is necessary to carry out supervision at this stage which aims to maintain the stability of the rate on the *mining front*.

Figure 2. The distribution of *ore* is heterogeneous.

Figure 3. Waste position *relative* to *ore* and weather

Figure 4. Heterogeneous Ore Distribution

4 Conclusions

Based on the results of the analysis, data on Ni, Fe, MgO and Sio2 rates on the *mining front* with *stockpiles* were obtained, the Ni rate had a difference of 0.05% and the Fe rate had a difference of 0.34%, the two minerals had the highest rates on the *mining front* and the MgO rate had a difference of 2.68% and the SiO2 rate had a difference of 8.87%. Factors that affect changes in nickel levels are heterogeneous ore distribution, the position of *waste* above the *ore* and rainy weather that occurs in the field, operator and sampling skills.

Acknowledgements

The authors would like to thank the leadership of PT Ceria Nugraha Indotama for providing research opportunities.

References

[1] A. B. Thamsi, C. D. Sangadji, S. R. Nurhawaisyah, M. Aswadi, and L. O. M. Y. Amsah, "Analisis Perbandingan Kadar Nikel Hasil Pengeboran Dengan Hasil Penambangan di PT Mandiri Mineral Perkasa," *Jurnal Pertambangan*, vol. 6, no. 2, pp. 65–70, Dec. 2022, doi: 10.36706/JP.V6I2.1098.

[2] S. Bakri, M. Anas, M. H. Wakila, and C. A. Chalik, "Geochemical Characterization of Silica Sand in the Sidenreng Rappang Area Based on X-Ray Diffraction Analysis and X-Ray Fluorescence Analysis," *Journal of Geology and Exploration*, vol. 2, no. 1, pp. 1–7, Jun. 2023, doi: 10.58227/JGE.V2I1.36.

[3] A. S. Munir, N. Asmiani, N. Jafar, M. H. Wakila, and J. F. R. P. Gouw, "Analysis of Blasting Geometry on Blasting Production Results at PT Semen Bosowa Maros," *International Journal of Applied Sciences and Smart Technologies*, vol. 5, no. 2, pp. 195–212, Dec. 2023, doi: 10.24071/IJASST.V5I2.6423.

[4] S. A. A. S. H. Hutuba, A. Zainuri, and R. Hutagalung, "Karakteristik Endapan Nikel Laterit Pada Blok X Deposit Desa Watumbhoti, Kecamatan Palangga Selatan, Kabupaten Konawe Selatan, Provinsi Sulawesi Tenggara," *Jurnal Intelek Dan Cendikiawan Nusantara*, vol. 1, no. 5, pp. 7980–7993, Nov. 2024, Accessed: Nov. 20, 2024. [Online]. Available: https://jicnusantara.com/index.php/jicn/article/view/1409

[5] A. B. Thamsi and N. Jafar, "Estimation of Laterite Nickel Resources Using Ordinary Kriging Method in The Garuda Block PT Ceria Nugraha Indotama Southeast Sulawesi," *IJESCA*, 2024, [Online]. Available: http://pasca.unhas.ac.id/ojs/index.php/ijesca/article/view/5489

[6] N. Asmiani, A. B. Thamsi, S. Nompo, S. Bakri, "Model of Laterite Nickel Deposits Based on LGSO And HGSO Values PT Mitra Karya Agung Lestari," *JGE*, 2024, [Online]. Available: http://jge.eng.unila.ac.id/index.php/geoph/article/view/305

[7] L. O. Dzakir, M. K. Amir, Y. L. O. Prianata, and M. I. Kadar, "Analisis Perbandingan Kadar MgO Dan SiO2 Pada Nikel Kadar Rendah di Kabupaten Kolaka dan Kabupaten Kolaka Utara," *Jurnal Geomine*, vol. 10, no. 1, pp. 43–50, Jul. 2022, doi: 10.33536/jg.v10i4.1080.

[8] H. Bakri, A. B. Thamsi, and ..., "Efisiensi Kerja Pemboran Eksplorasi Pada PT Vale Indonesia: Efficiency of Exploration Drilling Work at PT Vale Indonesia," *Journal of ...*, 2023, [Online]. Available: https://ejournal.insightpublisher.com/index.php/JESTA/article/view/70

[9] S. Bakri, M. Anas, M. Hardin Wakila, C. Aulian Chalik, and S. Rappang, "Geochemical Characterization of Silica Sand in the Sidenreng Rappang Area Based on X-Ray Diffraction Analysis and X-Ray Fluorescence Analysis," *Journal of Geology and Exploration*, vol. 2, no. 1, pp. 1–7, Jun. 2023, doi: 10.58227/JGE.V2I1.36.

[10] A. Nawir, A. B. Thamsi, and M. F. W. MH, "Identification of Andesite Rock Distribution Using Resistivity Geoelectric Method in Tapalang Area of Mamuju District West Sulawesi Province," *IJESCA*, 2023, [Online]. Available: http://pasca.unhas.ac.id/ojs/index.php/ijesca/article/view/4894

[11] M. H. Wakila, N. Jafar, and A. Fiqriansyah, "Alteration and Mineralization in the Coppo Village, Barru District, South Sulawesi Province," *Journal of Geology and Exploration*, vol. 2, no. 1, pp. 24–31, Jun. 2023, doi: 10.58227/JGE.V2I1.50.

[12] M. Aswadi, J. R. Husain, A. Gazali, and A. B. Thamsi, "Spread Of Laterite Nickel Based on Drill Data at PT Manunggal Sarana Surya Pratama, Southeast Sulawesi Province," *Journal of Geology and Exploration*, vol. 1, no. 2, pp. 51–57, Dec. 2022, doi: 10.58227/JGE.V1I2.9.

[13] M. H. Wakila, N. Jafar, and A. Fiqriansyah, "Alteration and Mineralization in the Coppo Village, Barru District, South Sulawesi Province," *Journal of Geology and Exploration*, vol. 2, no. 1, pp. 24–31, Jun. 2023, doi: 10.58227/JGE.V2I1.50.

[14] A. Ilyas, A. R. Pasolo, and S. Widodo, "Analisis Karakteristik Mineralogi dan Geokimia Berdasarkan Zona Profil Endapan Nikel Laterit (Studi Kasus: Blok X PT Ang and Fang Brother, Site Lalampu, Kecamatan Bahodopi, Kabupaten Morowali, Provinsi Sulawesi Tengah," *Jurnal Geomine*, vol. 10, no. 1, pp. 01–12, Jul. 2022, doi: 10.33536/jg.v10i4.1165.

[15] A. Azarine, M. A. Azzaman, and A. Idrus, "Karakteristik Alterasi dan Mineralisasi Endapan Emas Tipe Carlin pada Blok Yance dan Leon, Kecamatan Ratatotok, Kabupaten Minahasa Tenggara, Provinsi Sulawesi Utara," *Jurnal Geomine*, vol. 9, no. 3, pp. 239–253, Feb. 2022, doi: 10.33536/jg.v9i3.1001.

[16] A. Nawir, A. B. Thamsi, H. Sanjaya, and M. Aswadi, "Resources Estimation of Laterite Nickel Using Ordinary Kriging Method at PT Mahkota Semesta Nikelindo District Wita Pond Morowali District," *International Journal of Applied Sciences and Smart Technologies*, vol. 5, no. 2, pp. 303–314, Dec. 2023, doi: 10.24071/IJASST.V5I2.6939.

IJASST International Journal of Applied Sciences and Smart Technologies
Volume 07
Issue 01
p-ISSN 2655-8564, e-ISSN 2685-943, pp. 109-128, 2025

Evaluating The User Experience of E-Commerce Platform Using Hassenzahl Framework

Sesaria Kikitamara[1], Stevanus Wisnu Wijaya [1*]

[1] *Department of Software Engineering, School of STEM, Universitas Prasetiya Mulya, Jln BSD Raya Utama, 15339, Indonesia*
[*]*Corresponding Author:wisnu.wijaya@prasetiyamulya.ac.id*

(Received 12-11-2024; Revised 01-02-2025; Accepted 08-02-2025)

Abstract

The Hassenzahl framework of UX provides an approach in measuring user experience of a product which covers such the following aspects : be goals, do goals, and motor goals. Yet the further approach for practical implementation in digital product like e-commerce platform is still insufficient. Another approach, the scenario model provides a journey mapping viewing from the user perspective. Thus, generally this method was used to portray the interaction process between user and product. Furthermore, the term of user journey is also commonly used by the UX designer in order to understand what actually the user needs, not just the user want. The solution offered to discuss within this paper is integrating three key elements of Hassenzahl method for every scenario in the e-commerce process. Hopefully the solution as presented on this paper will generate more credible properties and decent tools for developing an efficient, user friendly, and engaging e-commerce application.

Keywords: E-Commerce, User Experience, UX Evaluation, Hassenzahl Farmework

1 Introduction

Since the spread of the internet, many business models have changed a lot, especially the online business. Most company prefer to have a website or develop a mobile app to embrace the recent technology while promoting their products, even they choose not to build a physical store, rather than launch an online business only. However, many of them experience the business failures. The basic flaw is that the website do not deliver a simple, seamless and enjoyable experience for the user. The first impression of the platform was totally neglected. Therefore, there is no engagement for the user to use it multiple times and that makes them more likely to not trust the platform.

This work is licensed under a Creative Commons Attribution 4.0 International License

User Interface (UI), User Experiences (UX), and User Engagement are intertwined concept in which if one of them was poorly delivered then the other also experience the same thing. The definition of User Experience is the perceptions and responses a people will get from the use of product, system or service [1] while User Engagement is described as the quality of UX underline positive aspects from the interaction between user and product which lead to motivate the user to use it continually [2]. Logically speaking, it can be considered also that poor UX could bring poor user engagement as it could stimulate a periodic use of a product.

Marks Hassenzahl's Theory highlights an experience as user' perspective of which consist of three main aspects of why, what and how. That framework provides a holistic understanding of the way experience arouse when people interact with digital technology. Although this framework is widely adopted to assess UX of various platform, but according to our literature review, the implementation of this framework in e-commerce platform still need further investigation. In particular, there is a need to provide a measurement model of ecommerce platform which is able to assess the experience of users and provide a scale of successfulness of a UX design.

Another basic yet effective methodology is by creating a scenario-based method which depict the journey of the customer to use that technology. User scenario also can help designer to understand the user' motivation to interact with the product. It is partly responsible for determining the most critical area for user experience testing. Not to mention the guidance for testing can be derived from the scenario as well. By combining these two approach, hopefully could bring a new insight in order to enhance the way for creating a good user experience.

This paper proceeds as follows. First the background where the previous literature study has been taken also the methodology. The second part is the grounded theory to identify all of the theory and tools underpinning for chaping the UX evaluation framework. This will consist theory such as user experience, Hassenzahl approach, UX testing and scenario based methodology. The relationship among them also obviously explained in this section. The third part, where the implementation will be discussed, is the synthesis between Hassenzahl method and scenario based on e-commerce platform.

Lastly, the conclusion which discuss about the weakness, future challenge and further improvement for this paper.

The notion of user experience still has ambiguous meaning and closely related with usability and user-centric design [3]. Conversely, in a general perception, UX itself can be simplified as the good or bad feeling during interaction with a product or platform. Hence to give value whether it is good or bad, Hassenzahl gives more concise dimensions on why, what, and how. However, during the literature searching we found out that there is still limited sources which turn this concept into practice. Especially on e-commerce platform. The application of conceptual model like Hassenzahl framework, should be followed by the practical implementation for certain product. By transforming the theory into an action, basically it can generate more navigation to the real world problems, help to develop more professional skills also can predict the possible challenges for the future.

Recently, some papers which discuss the implementation of Hassenzahl mostly argue about the product design process. The meaning of product here is literally an actual or physical product, such as wearable activity trackers [4] electronic products [5] or information appliances [6]. Yet the digital product has a lot of differences from physical products, even from functionality or aesthetical perspectives. Digital products are products that incorporate information and communication technology. Common examples are desktop computers and mobile phones [7]. Furthermore, as today we could see that the digital product has evolved quickly from professional environment becomes personal, social, and even spiritual activities. The e-commerce platform is an example of digital product which in the present day becomes so important as people can order products or services at their own free will. It simply grows into compulsory to use for any transaction.

The UX evaluation method also differs clearly from usability evaluation method. In UX, it needs to assess the hedonic character as well as figured out the user's feelings during the interaction with the system [8] the type of product offered, also the type of platform it used. Besides, the UX evaluation method also ranging variously from academic and industrial perspective. It gives the UX researcher a broader set of factors before conducting UX evaluation, especially if the goal for the research is leveraging the user engagement. From an e-commerce platform, the heuristic UX evaluation mostly

derived from the functional requirement based on the accessibility [9] and problem solving aspect. So that it still does not cover the emotions of the user as mentioned by Hassenzahl method. Therefore, this paper also aims to fill in this gap by combining the emotional factor during the user journey experience an e-commerce platform depicted by scenario model.

2 Theoretical Foundation

The UX Framework

This part explores all the fundamental theory and tool for UX evaluation framework. Started from the notion of user experience, the elucidation of hassenzahl theory, UX testing, and scenario based methodology. Basically, the components written in this section are the valuable material we used to create a new model of user experience assessment for an e-commerce platform.

User Experience

Actually, the user experience term has broader concept than usability. Usability measure the user friendly readiness level from an interface, while UX covers ease of use and various subjective aspect of happiness while users intend to use the technology [10]. Designing a product or technology by following user experience concept give numerous benefits. One of them is bringing the persuasion architecture principles [11]. It could influence the user in such interactive way during storytelling based on the social psychological context [12]. Which means, we should able to persuade customer to use our website multiple times.

To put it simply, we also should know how to interpret the UX evaluation result into user engagement. Since it expresses the interactivity in a positive way so that the UX evaluation should delivers a positive result, particularly three aspects of Hassenzahl theory must be achieved in a satisfactory outcome. If using scoring method, it should be average upper score [39].

The Hassenzahl Theory

According to Hassenzahl, a user experience is a story or episode of human dialogue with interactive products. It comprises of subjective aspect of user satisfaction which covers various hedonic factors and the objective aspect of user measurement. The hedonic factor is commonly named as be-goals (why), which covers the motivation, intention and emotion to do an activity. Then, the pragmatic aspects is named do-goals (what) which capture concrete, expected result of activities and plan to reach them, and motor-goals (how), which looks into operation level for activities organization [13].

For future direction, Hassenzahl thinks that there should be transformation from technology-driven innovation to human-driven innovation. It means that human and social values causing the force to innovate through technology [37]. It will help the product to be full of inspiring stories and provide meaningful experience for the user. Through the experience design, a product can offer appealing, priceless and beautiful experiences in itself [13]. Additionally, a study found that preparing educators with adequate digital literacy skills will ensure the successfull integration of technology [40]. In the context of e-commerce, applying Hassenzahl's model of user experience, which emphasize both pragmatic and hedonic qualities, highloights how digital literacy and effective UI/UX design contribute to creating meaningful, engaging, and efficient online shopping.

The UX Testing

The current key to evaluate the user experience still based on user-centered design methodology [14]. This method was emphasizing on the urgency of testing the application to reflect the needs and user goals. Several benefits of involving user iteratively during the development process are minimize the development costs, make development time short and boost the productivity [15]. However, this concept also has some limitations: complience, recognition and incorporation; scarcity of resources; project definition adjustment; and what will be highlighted on this paper is the problem arises due to multidisciplinary team of the administration [16].

User-centered design, will involve a lot of designer which have plural area and diverse ideas. In order to accommodate those conflicts. Scenario - based testing will give

assistance to synchronize all of their views. By using scenario-based testing, both the designer and tester will be directed with the flow of the scenarios during the development process, so that they will have one side of look of their application.

Scenario Based Methodology

Scenarios describe the user views about usability, functionality and behavior of a software system [17]. This method has been an effective tool for validation and verification activities. It also brings a systematics ways to develop the test cases. Yet nowadays testing is often done in an unstructured, non-systematic way. The scenario testing usually consists of five phases as described below [18] :

1. **Planning :** First of all is defining all the components involved, like the target of participant and the type of product to be tested, can be a system or module, location or even cost. This step is very crucial for determining the complexity of the system before testing.
2. **Preparation :** After planning, what we must to do is choosing the instruments such as (interviews, questionnaire, observation, checklists and etc. The outcome are the test plan and tasks for the scenario test. For example, questionnaire method with bipolar likert scale using seven distinct categories. It also more suited to use through electronic distribution of inventories, such as via Google forms.
3. **Testing:** During the testing phase, it is critical to preserve the time and do the test following the order as stated on the schedule which included on the test plan and avoid the test from meddling with each other. Perhaps, some interventions are useful, for example the reaction if a problem arises during the testing process. The main task from this phase are distribute tasks to users, observe and collect data. The documentation of all deviation from the test plan also important to be output of this phase.
4. **Analyzing:** After doing testing and all the findings has been discovered, the it comes to the analyzing phase. During this phase, we have to divide the findings so that more important findings can be securely preserved first. Using a statistic method is a good

alternative both to calculate the data and present it. While the virtualization of the results can be demonstrated using charts, tables, or graphics.

5. **Documentation:** It is essential to document all the process and result and probably there are some anomalies from the test plan This documentation has several functions such as makes testing more accurate, easy and organized. Specially for any bigger companies like Microsoft, IBM, Oracle, their testing documents also can be a proper documentation for any user to understand their product. Usually they release periodically the technical documents that say what is works with the feature and what is not. This strategy is useful to maintain the user loyalty since user get update information about the latest version of the application they used.

In case of e-commerce website, the scenario basically will test the common scenarios which should be based on the user journey. User journey or customer journey is the stages which a customer goes through when interacting with a company or service that is represented on linier and time-based journey [19]. Generally, there are three stages of scenario testing as presented at Table 1[20] . First is the onboarding stage in which users depict the process for opening the website until the user see the home page. Second is the shopping journey process. In this stage, it requires input from the user to search and select a product. Lastly, the product selection and purchase, the shopping cart management and the checkout process. This last phase is a complex process to let user go through when checking out the items in the cart. It also will include choosing the preferences such as size, color, and etc.

Table 1. The General E-Commerce Scenario

No	E-commerce Scenarios
1.	The onboarding stage.
2.	The shopping journey process stage.
3.	The product selection and purchase stage.

3 Methodology

The research methodology used must precisely help us to get the solution to the problem. As the goal of this paper was to make further improvement for hassenzahl method in specific field like e-commerce, we decided to adopt a Systematic Literature Review approach. This will analyse existing research on Hassenzahl framework implementation for user experience measurement. Moreover, exploring and investigating all the potential research related to specific topics regarding the research questions have been the function of systematic review [21]. Accordingly, this brought to the aid for identifying the literature based on the current research topics in the field of user experience, e-commerce and customer engagement.

Research Question

The research question helps to focus when the research started. Indeed it was one of the fundamental elements to show what direction the research takes and serves as the catalysts for research to uncover the important discoveries. Consequently, due to its significant contribution to the research, we decided to mark only one primary research question as follow :

“What best approach to implement Hassenzahl method into an e-commerce platform”

Searching Process

During the searching process, we applied the search strategy including: scooping, searching, and analyze. In scooping process, we took the sources from the several keywords; user experience evaluation, e-commerce design, Hassenzahl implementation. For the time range, because the e-commerce platform has been created before the millenium era thus we also need to study the old paper. As a consequence, we decided not to give time frame for the sources. So that basically we only used the keywords and quality assessment to filter the sources. The output for this process is finding all the critical components that fit to the research question.

Quality Assessment

Quality is a complex process which implemented differently according to its theme. After the search process, all the scientific resources should be undergone through quality assessment to verify the effective ness of the findings.

Technically, we define the quality as an assessment tool to sorting out the literature by using specific questions as follows [21] ;

- Are the review's criteria appropriately described?
- Is the literature search likely to have covered all relevant studies?
- Did the reviewers assess the quality and validity of the studies?
- Were the basic data/studies adequately described?

4 Results and Discussions

As explained previously, we already define three basic scenarios for e-commerce platform. Those scenarios then should be integrated with Hassenzahl Method by classifying per scenario. In each scenario, we put the measurement properties based on three Hassenzahl method; be-goals, do-goals, and motor-goals. Thus, the result obtained from the combination of these two concept can be a guidance to generate properties in order to create the test cases in a UX assesment process. During the integration process, we follow the nature of meaning from each hedonic characters and intrepret them to the which specific scenario is being performed. As classified below are the outcome of this implementation, sequenced by the general scenario process of an e-commerce platform.

The onboarding stage

This initial step of a user journey usually must delivers a smooth process for the user, since executed only simply by typing the website URL on the browser, open a mobile application or clicking the advertising campaign. After entering the site, what people see for the first time is the home page. It has role as the entrance point and guide user to get to the next page. In such a way, the optimization and experience of a home page offers a significant factor for flourishing the user engagement. So that the creation of positive and desirable impression should begin from the visual design and content of a home page. Interestingly, a home page also gets the most views. There are many digital campaign which put a direct link to the home page.

Be-goal

This aspect indicates the motivation and emotion which must be clearly expressed through the home page. Regarding that matter, the design should be convenient for the user to enjoy window shopping [22]. More importantly, the persuasive characterictics of e-commerce design needs to be applied. For example, attractively presenting products, using sales and promotion techniques, suggesting related products based on each customer profile, and simplifying the purchase mechanism [23].

Do-goal

The product information displayed should not be too complex and overload of information [24]. The basic building blocks for a homepage of e-commerce website mostly the same with the general website; Container (the frame for the page), logotype (the sites identity), navigation (how the users can use the site), content (anything from images, text or video that can be found on the webpage), footer (the bottom on the page) and white space (areas without illustrations or typing) [25]. Furthermore, four important things that must exist in an e-commerce site are navigation, search, contact us and shopping cart [26].

Motor-goal

The customer of e-commerce website tend to make sure that the image displayed resembles its concrete appearance. Thus the visualization technique to present must be accurate, consistent and comprehensive. Precise and full view of the product should be provided [27]. This can be done using high quality image and image interactivity. By clicking and moving the object around, they can interact with it and view from many angle as if they are in the real store [28]. Currently, the introduction of Augmented Reality (AR) for e-commerce website also offers a unique experience for the customers so that it can be another strategies to gain customer engagement [38].

The shopping journey process stage

The way the user discover a product reflects the valuable opportunity to raise user engagement for e-commerce platform. The biggest challenge for this process is to help them discover the product or service they need. Knowing the customer that is actually matter, because it helps to establish a guarantee that the e-commerce website is the preferred destination to shop at. But sometimes, the navigation process has poor

performances. It can be due to lots of image with minimum quality and information, lack of categorization for product collection, or difficulties or lenghty process to find the right product. Thus by enabling the Hassenzahl principle into its navigation design, it forges the supervision to prevent such inferior user experience during browsing and product discovery process.

Be-goal

User journey on this process has specific motivation and emotion to find something what they really need. There are at least two types of user during this process. Type one, the user knowing their desired product then searching though search bar the categories /subcategories menu to find out the product. Second type, the user does not have a clear picture of the product they are looking for, still full of doubts thus they have to look at the entire product display available. Of course this is risky, since it will lead the user to be bewildered and get lost in the website maze [29]. Therefore, the e-commerce website should accommodate these two types of users.

Do-goal

The product categorization, grouping, and organizing are the key technique to deliver success process for browsing product through search bar or catalogue. To that extent, the taxonomy of the product should be systematically organized. It was implied with the following rules [30]:

- Make a group for similar product
- Make sure that the categorization based on the product type instead of brand or application
- For kits, sets, components, and assortments should be created on separate categories
- Make grouping name more general at the highest level and specific at the lowest level
- The name of the product should be understandable and simple

It is possible to turn browsers into buyer once the product display page able to capture the customer’s love. The addition feature like customer ratings and reviews can

help to boost the branding of the product. Nowadays most e-commerce platform always put this feature under the product image. More advanced feature like recommendation featured product also boost the platform capability by using data analytics based on customer preserences. From the visualization of product display, it has to fit all type of mobile platform or browsers.

Motor-goal

Effective navigation is a basic technique used during this process. The essential parts to build such strong yet meaningful navigators are clear meaningful categorization, clear label, and good visual design. If the product categorization is confusing enough or ambiguous, the customers will struggle then lead them to leave the application. It will happen for stores which having such broad assortment of products [31]. The principle of effective navigation can be measured by the amount of time a user has spent to find their desirable product. If the platform let the user to scrolling and suffer through all the product page, it means that it has poor experience in term of catalogue browsing and product discovery.

The Product Selection and Purchase Stage.

The checkout process is a mandatory process and becoming standard process for e-commerce website, with clear and expected outcome. Usually this process includes choosing product, adding to cart, filling some form about detail of the order, user payment system, and shipping information. The flow of this process is the longest part compare to the previous scenario. Actually, the biggest challenge to measure user engagement is by observing this part. Not a few people who really does have intention to buy, beside they just have a desire to do window shopping, a behaviour of people who like to only looking at the product displayed without intending to buy anything. Or maybe some people at first truly has objective to buy, so they easily adding the chosen product in their cart, but still it could not be guaranteed until they finish the payment process. Even the product has been placed under the cart management system, they can anytime cancel it or maybe just ignore it until the expiration time for the payment process has passed.

Be-goal

Derived from functionality and hedonic motivations of shopping, there are several types of customer during check out process: 1) determined to do an online purchasing 2) sales, discount and price promotion hunters, 3) attained personal entertainment value of using the cart, 4) just want to organize items of interest, and 5) information-seekers [36]. To support these various intents, the e-commerce platform should provides some features such as add to cart for direct purchase or wishing list that enough to accommodate the seeking behaviour of the user.

Do-goal

In order to deliver a smooth process during the check out mechanism, the information architecture concept should come first. Following are the information architecture which can be applied for this process [32] :

1. The shopping cart must be visible, handy, accessible and rich functionality
2. Keep the ordering option clear and simple
3. Put a display about related items available during the checkout process
4. Provide features such as wishlist or favorite items then put it near the shopping cart for the future process
5. Give advance notice of what the checkout process involves
6. Simplicity and neatness is the key for creating such efficient order form
7. Secure transaction is a must for each step during the checkout process

Another general guideline which help to improve the concept of checkout is by changing the mandatory step for registration to be optional. Because it can takes more effort as well as time also create hassle for the user. If the registration form was placed in the initial stage on the checkout process, user might just drop the idea to buy.

Motor-goal

Basically, there are two types of checkout process. i) a single one-page checkout process that contains all the necessary information for performing the purchase in a single page; and ii) a guided step-by-step checkout process in which users have to fill out their information in multiple steps, usually across multiple pages [33]. There is mothing wrong with both types of checkout design. What actually matter is the optimization principle

should be carried out during this process. With all of the items like cart, whising list or basket, the key is to keep it as simple as it can. Not only by creating the attractive front end-design, but also the content should include the review of what the user has put to their cart and provide a very obvious next step as well as options to make attribute changes to the order. The platform performance must be take into consideration also. There are a lot of reports from the user experiencing the crashed platform, mostly it happen when they gone through payment process. Thus it is important to remove unnecessary items such as advertisement links.

The Evaluation Step

It is crucial to define some steps for broader view of evaluation process. This also help in organizing and managing the work before we use mix method of scenario and Hassenzahl framework. In implementing this step, we summarize what the tester' phase of work and detail of implementation in Table 2.

Table 2. The Evaluation Steps

No.	Step	How to
Step 1	Define the goal of the platform	The website should represent either informational design (for digital catalogue display only) or online/transactional design [34]
Step 2	Define the user journey	Define the steps in which user interact with the website to perform any feature
Step 3	Develop the scenario test	There are three basic scenarios for e-commerce website
Step 4	Evaluate the Hassenzahl properties	Using be-goals, do-goals, and motor-goals principle. As illustrated on the Table 3.
Step 5	Result	Summary from the overall evaluation result

In the following paragraph, we propose a model for evaluating user experience of e-commerce platform. This model is presented at Table 3 which integrate the scenario and Hassenzahl framework of user experience evaluation. Specifically, we propose a model which enable UX engineer to examine the successfulness of e-commerce platform UX design through examine three main dimension of Hassenzahl UX successfulness criteria into each stage of user journey.

Table 3. The Integration of Hassenzahl and Scenario Based

Stage 1 : The onboarding stage	
Be-goal	• Convenient for window shopping • Persuasive design
Do-goal	• Product information clear and concise (not too complex or overload) • Comply with the standard feature of e-commerce homepage
Motor-goal	• Precise and full view of the product • High quality image • Image interactivity
Stage 2 : The shopping journey process stage	
Be-goal	Accommodate two types of user : the one who already now what he is looking for, and the one who just knowing the rough idea of the product he might be interested
Do-goal	Using specific technique for product taxonomy or categorization. Addition feature like ratings and reviews or more advanced technique like recommendation and featured product drastically change the customers into buyers
Motor-goal	• Effective navigation • Meaningful product categorization • Clear labels • Good visual design
Stage 3 : The product selection and purchase stage	
Be-goal	Accommodates many types of user during check out process, whether the user really intent to purchase the product or only satisfy the information seeking behavior. For example by providing direct add to cart or wishing list

Do-goal	Using the given principles of information architecture for check out process; However do not put the registration form as mandatory step. Beside put this as optional, for example provides option for guest check out without login first.
Motor-goal	Determine the two type of user checkout process : one-page check out process or multiple-page check out process. Focused on the optimization principle by make it as simple as it can, but do not forget about the performance to prevent from platform crash during the check out process.

5 Conclusions and Future Research Directions

In this paper, we come up with a scenario based testing approach to assess the design of e commerce platform. We think that scenario based approach is fit to the description of experience as episode or story of user dialogue with an interactive product such e commerce. The scenario is developed based on the user journey when they interact with e commerce platform. The scenario-based method can be used for analysis, ideation and dealing with the collaborative innovation of user experience design [35]. It has the benefit of being easier to understand compared to other methods. Even the user can follow it without any crucial difficulties. Likewise, the involvement of end users and multidisciplinary teams in design is also important.

We used Hassenzahl's method and expand it on the conceptual level to emphasize the criteria on Why, What and How technique by using a scenario based evaluation. The scenario is divided into five steps ; define the goal of the platform, define the user journey, develop the scenario test, evaluate the Hassenzahl's properties and generating result. We defined the concept of UX for each scenario and mapping the Hassenzahl's properties into perspective dimension. Therefore, in every scenario, we explain conceptually the implementation of Be-Goal, Do-Goal, and Motor-Goal. We also provides principles and some hints for each aspect to create e-commerce application which comply with user satisfaction.

Although from our perception model can contribute to provide improvement of the design of an e-commerce platform, however we think that a further research is needed to develop the testing tools then proof the measurement model using an appropriate

methodology. We acknowledge that a conceptual model is a representation of idea which can be perceive as a way to understand a process. Although representaion of idea on Hassenzahl' concept of user experience concept was developed through a systematic way of thinking, however it need to be broadly understood as a guideline in examining user experience. This model provide a comprehensive description of implementation of Hassenzahl's method for evaluating user experience in e -commerce platform, then further study is needed to develop a measurement model which can be implemented in various e-commerce platform and context. And as the complexity of technology growing rapidly, we believe that the user experience still be a key to fascinate the user, and creating scenario-based method will be an essential part of the development process to create a product that is efficient, handy, and engaging.

References

[1] DIS, "9241-210:2010. Ergonomics of human-system interaction - Part 210: Human-centred design for interactive systems (formerly known as 13407)," International Standardization Organization (ISO), Switzerland, 2010.

[2] J. Lehmann, M. Lalmas, E. Yom-Tov, and G. Dupret, "Models of user engagement," in *International Conference on User Modeling, Adaptation, and Personalization*, Berlin, Heidelberg: Springer, July 2012, pp. 164–175.

[3] P. Wright and M. Blythe, "User experience research as an inter-discipline: Towards a UX Manifesto," in *Proceedings of the Workshop on Towards a UX Manifesto*, E. Law, A. Vermeeren, M. Hassenzahl, and M. Blythe, Eds., Sept. 2007, pp. 65–70.

[4] E. Karapanos, R. Gouveia, M. Hassenzahl, and J. Forlizzi, "Wellbeing in the making: People's experiences with wearable activity trackers," *Psychology of Well-Being*, vol. 6, no. 1, p. 4, 2016.

[5] M. Laschke, S. Diefenbach, and M. Hassenzahl, "Annoying, but in a nice way: An inquiry into the experience of frictional feedback," *International Journal of Design*, vol. 9, no. 2, pp. 129–140, 2015.

[6] C. Jetter and J. Gerken, "A simplified model of user experience for practical application," in *NordiCHI 2006: The 2nd COST294-MAUSE International Open Workshop 'User eXperience - Towards a Unified View'*, Oslo, 2007, pp. 106–111.

[7] H. de Ridder and M. C. Rozendaal, "Beyond image quality: designing engaging interactions with digital products," *Proc. SPIE 6806, Human Vision and Electronic Imaging XIII*, vol. 68060F, Feb. 13, 2008. DOI: 10.1117/12.784146.

[8] V. Roto, M. Obrist, and K. Väänänen-Vainio-Mattila, "User experience evaluation methods in academic and industrial contexts," in *Proceedings of the Workshop UXEM*, vol. 9, Aug. 2009, pp. 1–5.

[9] L. Bonastre and T. Granollers, "A set of heuristics for user experience evaluation in e-commerce websites," in *7th International Conference on Advances in Computer-Human Interactions*, IARIA, Mar. 2014, pp. 27–34.

[10] L. J. Najjar, "Designing E-commerce User Interfaces," 2005.

[11] D. J. Mayhew, "User experience design: The evolution of a multi-disciplinary approach," *Journal of Usability Studies*, vol. 3, no. 3, pp. 99–102, 2008.

[12] R. Figueiredo and A. Paiva, "Persu: An architecture to apply persuasion in interactive storytelling," in *Proceedings of the 8th International Conference on Advances in Computer Entertainment Technology*, Nov. 2011, p. 36, ACM.

[13] M. Hassenzahl, "User experience and experience design," *The Encyclopedia of Human-Computer Interaction*, 2nd ed., 2013.

[14] K. Väänänen-Vainio-Mattila, V. Roto, and M. Hassenzahl, "Towards practical user experience evaluation methods," in *Meaningful Measures: Valid Useful User Experience Measurement (VUUM)*, 2008, pp. 19–22.

[15] A. Mital, A. Desai, A. Subramanian, and A. Mital, *Product Development: A Structured Approach to Consumer Product Development, Design, and Manufacture*. Elsevier, 2014.

[16] A. Chammas, M. Quaresma, and C. Mont'Alvão, "A closer look on the user centred design," *Procedia Manufacturing*, vol. 3, pp. 5397–5404, 2015.

[17] M. MandeepKaur and R. Kumar, "Scenarios uses to validate and test software systems: A survey," *International Journal of Technical Research*, vol. 2, 2013.

[18] Y. Halmø and G. A. Jenssen, "Scenario testing in a real environment - Key Card Administration System at the University Hospital in North Norway," Master's thesis, NTNU, 2006.

[19] A. Richardson, *Innovation X: Solutions for the New Breed of Complex Problems Facing Business*. Wiley, 2010.

[20] R. Mangiaracina and G. Brugnoli, "The e-commerce customer journey: A model to assess and compare the user experience of e-commerce websites," *The Journal of Internet Banking and Commerce*, vol. 14, no. 3, pp. 1–11, 1970.

[21] B. Kitchenham, *Procedures for Performing Systematic Reviews*, Keele University, Keele, UK, vol. 33, 2004, pp. 1–26.

[22] N. B. M. Suki, M. I. Ahmad, and V. Thyagarajan, "Motivation and concern factors for internet shopping: A Malaysian perspective," *The Electronic Journal for E-commerce Tools and Applications*, vol. 1, pp. 1–18, 2002

[23] W. Winn and K. Beck, "The persuasive power of design elements on an e-commerce web site," *Technical Communication*, vol. 49, no. 1, pp. 17–35, 2002.

[24] I. Michailidou, *Design the Experience First: A Scenario-Based Methodology for the Design of Complex, Tangible Consumer Products*, Doctoral dissertation, Universitätsbibliothek der TU München, 2017.

[25] J. Beaird, *The Principles of Beautiful Web Design*. SitePoint Pty. Limited, 2007.

[26] Y. Purwati, "Standard features of e-commerce user interface for the web," *Researchers World*, vol. 2, no. 3, p. 77, 2011.

[27] P. Katerattanakul and K. Siau, "Creating a virtual store image," *Communications of the ACM*, vol. 46, no. 12, pp. 226–232, 2003.

[28] S. N. Junaini and J. Sidi, "Improving product display of the e-commerce website through aesthetics, attractiveness, and interactivity," in *CITA*, Dec. 2005, pp. 23–27.

[29] B. Kitchenham, R. Pretorius, D. Budgen, O. P. Brereton, M. Turner, M. Niazi, and S. Linkman, "Systematic literature reviews in software engineering–a tertiary study," *Information and Software Technology*, vol. 52, no. 8, pp. 792–805, 2010.

[30] Altius Technologies, "Quality Product Content Matters to Increase E-commerce Sales," White Paper, 2019.

[31] P. H. Goddard, S. McLeary, and D. Gorney, "Five dimensions of user experience: Balancing business and user experience perspectives to create successful e-commerce sites," 2008.

[32] A. Malik, "An Innovative Information Architecture for the Shopping Cart," *International Journal of Technology, Knowledge and Society*, vol. 2, no. 1, pp. 175–180, 2006. DOI: 10.18848/1832-3669/CGP/v02i01/55541.

[33] M. Belk, P. Germanakos, A. Constantinides, and G. Samaras, "A human cognitive processing perspective in designing e-commerce checkout processes," in *IFIP*

Conference on Human-Computer Interaction, Cham: Springer, Sept. 2015, pp. 523–530.

[34] H. J. Wen, H. G. Chen, and H. G. Hwang, "E-commerce web site design: Strategies and models," *Information Management & Computer Security*, vol. 9, no. 1, pp. 5–12, 2001.

[35] E. Michailidou, S. Harper, and S. Bechhofer, "Visual complexity and aesthetic perception of web pages," in *Proceedings of the 26th Annual ACM International Conference on Design of Communication*, Sept. 2008, pp. 215–224, ACM.

[36] A. G. Close and M. Kukar-Kinney, "Beyond buying: Motivations behind consumers' online shopping cart use," *Journal of Business Research*, vol. 63, no. 9-10, pp. 986–992, 2010.

[37] M. Niemelä, V. Ikonen, J. Leikas, K. Kantola, M. Kulju, A. Tammela, and M. Ylikauppila, "Human-driven design: A human-driven approach to the design of technology," in *IFIP International Conference on Human Choice and Computers*, Berlin, Heidelberg: Springer, July 2014, pp. 78–91.

[38] M. B. Cano, P. Perry, R. Ashman, and K. Waite, "The influence of image interactivity upon user engagement when using mobile touch screens," *Computers in Human Behavior*, vol. 77, pp. 406–412, 2017.

[39] K. Finstad, "Response interpolation and scale sensitivity: Evidence against 5-point scales," *Journal of Usability Studies*, vol. 5, no. 3, pp. 104–110, 2010.

[40] D. Dwiniasih, J. Jaja, and J. F. Raharjo, "An analysis of principals' digital literacy capabilities as instructional leaders in Indonesia," Int. J. Appl. Sci. Smart Technol., vol. 6, no. 2, pp. 267-276, 2024. DOI : https://doi.org/10.24071/ijasst.v6i2.8843.

IJASST International Journal of Applied Sciences and Smart Technologies

Volume 07
Issue 01

p-ISSN 2655-8564, e-ISSN 2685-943, pp. 129-144, 2025

Effect of Hyperparameter Tuning on Performance on Classification model

Muhammad Sholeh*[1], Uning Lestari[1], Dina Andayati[2]

[1] *Informatics Study Program, Faculty of Science and Information Technology, Universitas AKPRIND Indonesia*
[2] *Retail Management Study Program, Faculty of Communication and Business, Universitas AKPRIND Indonesia*
[*]*Corresponding Author: muhash@akprind.ac.id*

(Received 14-02-2025; Revised 05-03-2025; Accepted 06-03-2025)

Abstract

This research aims to analyze the effect of hyperparameter tuning on the performance of Logistic Regression, K-Nearest Neighbours, Support Vector Machine, Decision Tree, Random Forest, Random Forest Classifier, Naive Bayes algorithms. These six algorithms were tested both using hyperparameter tuning and not using hyperparameter tuning. The dataset used in this research is a public dataset, namely the heart datasheet. This datasheet contains information about features related to the diagnosis of heart disease. Hyperparameter tuning is performed using a grid search technique to determine the best combination of hyperparameter values that can improve model accuracy. Performance comparison is done by measuring the accuracy, precision, recall, and F1-score of each algorithm before and after tuning. The research method follows the stages in the Knowledge Discovery in Databases (KDD) methodology. The KDD methodology consists of several stages of data collection, data cleaning to remove errors, data integration from various sources, and data selection and transformation to be ready for analysis. Next, data mining is performed to find patterns or relationships in the data and evaluation and interpretation of the results to ensure their validity. The results show that hyperparameter tuning applied to the six algorithms does not necessarily improve performance. In the algorithm. SVM and decision tree algorithms, the performance results before hyperparameter tuning actually have a higher accuracy value. The performance of algorithms that experienced an increase after hyperparameter tuning was logistic regression and K-Nearest neighbours. The same performance results are generated in the Random Forest and Naive Bayes algorithms. Based on testing the six algorithms and using the heart datasheet, the hyperparameter tuning process does not always result in a better performance value.

Keywords: Algorithm, Datasheet Hyperparameter tuning, Grid search

1 Introduction

The data science process aims to find the best performance of the model used. This data science process is expected to produce the most accurate and effective model in predicting or classifying data from the datasheet processed. In the context of

This work is licensed under a Creative Commons Attribution 4.0 International License

classification, the best performance is the ability of the model to make correct predictions with a minimal error rate, and to generalize well to data that has never been seen before. The goals in finding the best performance include maximizing the benefits that can be obtained from the available data, by minimizing the bias and variance of the model. This process includes selecting the right algorithm, setting hyperparameters, and selecting relevant features [1],[2]. Classification models can be used to make predictions from a datasheet, [3] created a classification model to determine nutritional status and [4] created a classification model to predict whether patients have lung and colon cancer using the CNN (Convolutional Neural Network) algorithm. By finding the best performing model, the data science process can ensure that the results of data analysis provide more accurate and reliable insights for data-driven decision making, and optimize the resources available in the application of the model.

One of the processes used to improve model performance is Hyperparameter tuning [5]. The goal of finding the best performance in the data science process is to produce a model that is most accurate and effective in predicting or classifying the given data. In the context of classification, the best performance is the ability of the model to make correct predictions with a minimal error rate, and to generalize well to data that has never been seen before. One of the goals of finding the best performance is to maximize the benefits that can be obtained from the available data, by minimizing the bias and variance of the model. This process includes selecting the right algorithm, setting hyperparameters, and selecting relevant features [6]. By finding the best performing model, the data science process can ensure that the results of data analysis provide more accurate and reliable insights for data-driven decision making, as well as optimize the resources available in the application of the model.

Some previous studies have shown that hyperparameter tuning can improve the performance of classification algorithms [7], [8]. Research by Ilemobayo [9], applied hyperparameter tuning using the grid search method to improve accuracy. The results showed that with tuning, the accuracy of the model increased significantly compared to without tuning. [10], used hyperparameter tuning in Machine Learning to Predict Student Academic Achievement. The results showed that the comparison of the four hyperparameter techniques had almost the same MAE value. The range of MAE values

between techniques is not significant. GridSearchCV is a technique that has the lowest MAE value, but to achieve this value requires a large estimator value and depth and a very small learning_rate.

[11], This research focuses on analyzing the classification model using the Support Vector Machine (SVM) algorithm, with the aim of finding the optimal parameter value through two hyperparameter tuning techniques, namely Grid Search and Random Search. The research was conducted on seven different datasets, with an evaluation based on the accuracy value, memory usage, and the time required to test the validity of the best model from the two techniques.

Similar research has been conducted by [12]. which uses GridSearch to optimize the Random Forest model. In that study, optimization was performed using the GridSearchCV method to improve model accuracy. The evaluation results showed an increase in model performance, with accuracy reaching 89.61%, recall of 90.15%, precision of 88.72%, and F1-Score of 89.43%. This finding confirms that optimization with GridSearchCV can significantly improve model performance, not only in terms of accuracy but also in other evaluation metrics such as recall, precision, and F1-Score.

Research [13], using the Hyperparameter Tuning method implemented using the CRISP-DM framework. The result obtained is a stance detection model using the Support Vector Machine algorithm which has a micro f1-score value of 78.4%. The hyperparameters of the model are C of 10, max_features parameter from the feature extraction process using TF-IDF method of 10000, and using unigram features. It is concluded that the model has better performance with a micro f1-score value that is 6.6% greater than the stance detection model in previous research.

Research [14] uses the AdaBoost method to process science data with a classification model. The process to get a good accuracy value is done using Hyperparameter Optimization. AdaBoost has hyperparameters needed in the classification process, namely learning rate and n_estimator. The hyperparameter process in this study uses RandomSearchCV. RandomSearchCV is a hyperparameter search method for machine learning models that works by randomly trying hyperparameter combinations from a predefined search space. Unlike GridSearchCV, which tries all possible hyperparameter combinations in the search space, RandomSearchCV randomly

selects a certain number of combinations to test. The method is applied using cross-validation techniques to ensure the model's performance on various subsets of data.

Another study using RandomSearchCV on the Random Forest algorithm was conducted [15],, the main purpose of hyperparameter tuning conducted in this study was to improve accuracy in the Covid-19 diagnosis process. The process of finding the optimal hyperparameter value was carried out using two methods, namely Grid Search and Random Search. The results show that the Random Forest algorithm can be used to diagnose Covid-19 with an accuracy rate of 94%. Furthermore, the application of hyperparameter tuning proved effective in increasing the accuracy of this algorithm by 2%, thus providing more optimal results to support disease diagnosis.

In addition, research by [16] also shows that SVM with hyperparameter tuning produces much better performance in cancer classification compared to other algorithms such as Decision Tree and KNN. This study revealed that selecting the right kernel and setting the C and gamma parameters can provide a significant increase in performance in data classification. The average accuracy result obtained is 0.91 and the accuracy can be obtained in a short iteration. This research shows that the use of the PSO algorithm in SVM hyperparameter optimization in imbalanced digital image classification works effectively and efficiently in improving the accuracy obtained. Other research that uses the SVM algorithm and the hyperparameter process is carried out [17] with the aim of improving the classification accuracy of heart disease diagnosis, [18] using hyperparameter tuning to Optimize Stunting with Classification models and using KNN, SVM, and Naïve Bayes algorithms.

Meanwhile, in the KNN algorithm, hyperparameter tuning by selecting the right number of nearest neighbors can also improve prediction accuracy. A study by [19], showed that selecting the optimal number of neighbors gave a clear improvement to the classification results. [20], development of K Hyperparameter Optimization in K-Nearest Neighbor Using Particle Swarm Optimization (PSO). The purpose of PSO is to find the best solution by utilizing collective behavior and iteration between particles. [21], Research conducted using the K-Nearest Neighbor (KNN) algorithm to classify breast cancer, with the number of nearest neighbors (k) parameter determined as 7. To improve the performance of the algorithm, Hyperparameter Tuning is performed using the Grid

Search Cross Validation method. The evaluated performance includes accuracy, precision, and recall. The results showed that the KNN classification model achieved an accuracy rate of 83%, precision of 73%, and recall of 89%

From the literature review, it can be concluded that hyperparameter tuning is an important step in improving the performance of classification algorithms. By performing proper tuning, it can achieve better and more accurate performance in real-world applications, including in the classification of cancer datasets.

The research aims to analyze the effect of hyperparameter tuning on the performance of Logistic Regression, K-Nearest Neighbors, Support Vector Machine, Decision Tree, Random Forest, Random Forest Classifier and Naive Bayes algorithms in the classification of heart datasets using grid search techniques. |The research also aims to identify algorithms that have the best performance after hyperparameter tuning, as well as compare the performance of each algorithm before and after hyperparameter tuning.

2 Material and Methods

Data Analysis Technique

The research method used is Knowledge Discovery in Databases (KDD), which is a systematic process for identifying patterns, information, and useful knowledge from large data sets. The KDD stage begins with data selection, where data relevant to the research objectives are collected from various sources. Next, data cleaning is performed to remove noise, duplication, and inconsistencies that may affect the analysis results. The third stage is data transformation, where the data is converted into a format suitable for further analysis processes. After that, data mining is performed, which is the core process of KDD that involves applying algorithms and statistical techniques to extract hidden patterns or information. The final stage is evaluation and interpretation, where the data mining results are assessed to ensure their accuracy and relevance to the research objectives. [22]. The stages of the KDD methodology are presented in Fig. 1

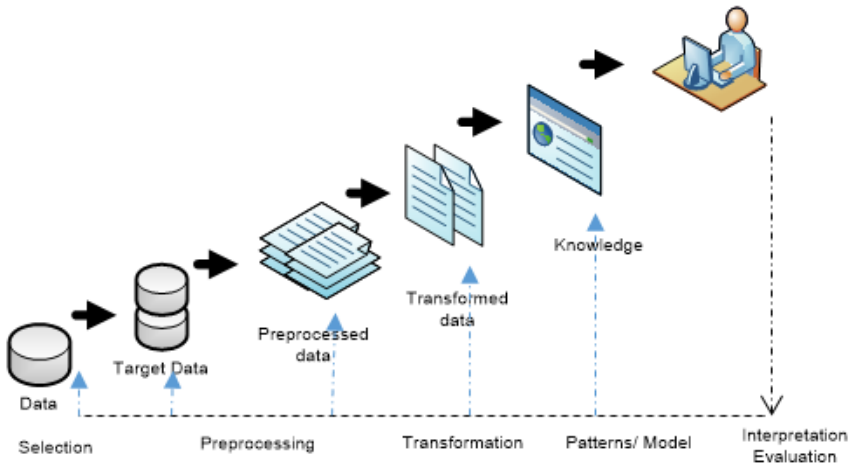

Figure 1. Stages in the Knowledge Discovery method [22]

Datasheet

The processed datasheet is a datasheet obtained from https://archive.ics.uci.edu. The datasheet used is a datasheet that contains data related to heart disease and is stored in a CSV file. The heart disease datasheet can be downloaded at https://archive.ics.uci.edu/dataset/45/heart+disease. The datasheet consists of 309 data and consists of 14 columns.

Hyperparameter Tuning with Grid Search

Hyperparameter tuning is the process of optimizing parameters that are not learned directly by the machine learning model during training, but are determined before the training process begins. The goal of hyperparameter tuning is to find the hyperparameter combination that produces the best model performance.

The hyperparameter tuning method used in this research is Grid Search. Grid Search is a systematic exploration technique where all possible hyperparameter combinations are tested within a predefined range. The process works by creating a "grid" of all combinations of hyperparameter values to be tested, then training the model for each of those combinations and evaluating its performance using metrics such as accuracy, F1-score. .

The main advantage of Grid Search is its ability to find the optimal hyperparameter combination thoroughly, as all possible combinations are tested. However, the disadvantage is that it is computationally expensive, especially when the number of

hyperparameters and their value ranges are large, as the number of combinations to be tested increases exponentially. The process of creating a gridsearchCV object is

```
Grid_search = GridSearchCV(
estimator=model, # Model to be tuned
param_grid=param_grid, # Grid hyperparameter c
v=5, # Cross-validation with 5 fold
scoring='accuracy', # Evaluation metric
verbose=1, # Display progress
n_jobs=-1 # Use all CPU cores
)
```

The required parameters are in GridSearchCV are:

- cv=5: Uses 5-fold cross-validation to evaluate each hyperparameter combination.
- scoring='accuracy': Uses accuracy as the evaluation metric.
- verbose=1: Displays the progress during the tuning process.
- n_jobs=-1: Uses all CPU cores to speed up computation.

3 Results and Discussions

Data Selection Stages

In the data selection stage, the dataset used is the Heart Disease Dataset which contains 303 samples with 14 attributes. These attributes include age, gender, chest pain type, blood pressure, cholesterol level, electrocardiogram results, maximum heart rate, and others. This data was chosen because it is relevant for predicting the presence of heart disease based on patient characteristics. The dataset was obtained from the UCI Machine Learning Repository public data repository.

Data Cleaning Stages

Data cleaning stage is performed to remove noise, missing values, and inconsistencies.

(1) Checking for empty data. This process is to ensure that the datasheet has no empty data. Fig. 2, the process for checking empty data. The result of the datasheet checking process is that there is no empty data.

(2) Checking twin data. This process is carried out to check the datasheet of the same data. If there is the same data, delete it. Fig. 3, the process of deleting the same.

(3) Checking outlier data. Outliers are data that have values that are significantly different from the majority of other data in a dataset. The presence of outliers can affect the statistical analysis and performance of data science models, so it is important to detect and handle outliers appropriately. Fig. 4, the process of checking outliers in the datasheet.

```
# prompt: perintah utuk cek data kosong

# Check for missing values in each column
print(df.isnull().sum())

# Check for empty strings in object columns
for col in df.select_dtypes(include=['object']):
    print(f"Empty strings in '{col}': {df[col].astype(str).str.len().eq(0).sum()}")
```

```
age         0
sex         0
cp          0
trestbps    0
chol        0
fbs         0
restecg     0
thalach     0
exang       0
oldpeak     0
slope       0
ca          0
thal        0
target      0
dtype: int64
```

Figure 2. Process for viewing empty data information

```
print("Jumlah duplikat sebelum dihapus:", df.duplicated().sum())
df.drop_duplicates(inplace=True)
print("Jumlah duplikat setelah dihapus:", df.duplicated().sum())
```

```
Jumlah duplikat sebelum dihapus: 723
Jumlah duplikat setelah dihapus: 0
```

Figure 3. The process for viewing empty data information

```
print("\nOutliers (using IQR method):")
for col in df.select_dtypes(include=np.number): # Check only numerical columns
    Q1 = df[col].quantile(0.25)
    Q3 = df[col].quantile(0.75)
    IQR = Q3 - Q1
    lower_bound = Q1 - 1.5 * IQR
    upper_bound = Q3 + 1.5 * IQR
    outliers = df[(df[col] < lower_bound) | (df[col] > upper_bound)]
    print(f"Column '{col}': {len(outliers)} outliers found")
```

```
Outliers (using IQR method):
Column 'age': 0 outliers found
Column 'sex': 0 outliers found
Column 'cp': 0 outliers found
Column 'trestbps': 9 outliers found
Column 'chol': 5 outliers found
Column 'fbs': 45 outliers found
Column 'restecg': 0 outliers found
Column 'thalach': 1 outliers found
Column 'exang': 0 outliers found
Column 'oldpeak': 5 outliers found
Column 'slope': 0 outliers found
Column 'ca': 24 outliers found
Column 'thal': 2 outliers found
Column 'target': 0 outliers found
```

Figure 4. The process of checking outlier data

Data TransformationStage

In the data transformation stage, several steps are taken to prepare the data for further processing. The process is to normalize numeric attributes such as age, blood pressure (trestbps), cholesterol (chol), thalach and oldpeak using the Min-Max Scaling method so that all attributes have a uniform scale. Fig. 5, Results of the data transformation process on attributes age, trestbps, chol, thalach and oldpeak.

```
# Select numerical features for scaling
numerical_features = ['age', 'trestbps', 'chol', 'thalach', 'oldpeak']

# Initialize MinMaxScaler
scaler = MinMaxScaler()

# Fit and transform the selected features
df[numerical_features] = scaler.fit_transform(df[numerical_features])
df
```

	age	sex	cp	trestbps	chol	fbs	restecg	thalach	exang	oldpeak	slope	ca	thal	target
0	0.479167	1.0	0.0	0.407895	0.351918	0.0	1.0	0.711559	0.0	0.250	2.0	2.0	3.0	0.0
1	0.500000	1.0	0.0	0.605263	0.315090	0.0	0.0	0.601273	1.0	0.775	0.0	0.0	3.0	0.0
2	0.854167	1.0	0.0	0.671053	0.196419	0.0	1.0	0.346766	1.0	0.650	0.0	0.0	3.0	0.0
3	0.666667	1.0	0.0	0.710526	0.315090	0.0	1.0	0.652174	0.0	0.000	2.0	1.0	3.0	0.0
4	0.687500	0.0	0.0	0.578947	0.687468	0.0	1.0	0.185578	0.0	0.475	1.0	2.5	2.0	0.0

Figure 5. Results of the data transformation process on attributes age, trestbps, chol, thalach and oldpeak.

Stages of model building

The model selection process begins with selecting an appropriate algorithm based on the type of problem and data characteristics. In this research, the algorithms used are Logistic Regression, K-Nearest Neighbors, Support Vector Machine, Decision Tree, Random Forest, Random Forest Classifier, Naive Bayes can. These six algorithms were tested both using hypertuning and not using hypertuning. Once the model is selected, the model training process is performed by optimizing the hyperparameters using techniques such as Grid Search or Random Search. The data is divided into training data (70%) and test data (30%), and validation methods such as 5-fold cross-validation are used to ensure the model is not overfitting. Grid Search will test all combinations of predefined hyperparameters, such as n_estimators (10, 50, 100) and max_depth (None, 10, 20), while Random Search will test combinations randomly. Each hyperparameter combination is tested by training the model on the training data and evaluating its performance using metrics such as accuracy or F1-score. The hyperparameter combination that gives the best performance is selected as the final configuration of the model. Thus, this process ensures that the resulting model has optimal performance and is ready to be used for prediction on new data. The model parameter settings are presented in Fig. 6.

Evaluation and interpretation stage

In the evaluation stage, the model that has been built is tested to measure its performance using metrics appropriate to the type of problem. The evaluation results are presented in Fig. 7.

```
# Inisialisasi model-model
models = {
    "Logistic Regression": LogisticRegression(),
    "K-Nearest Neighbors": KNeighborsClassifier(),
    "Support Vector Machine": SVC(),
    "Decision Tree": DecisionTreeClassifier(),
    "Random Forest": RandomForestClassifier(),
    "Naive Bayes": GaussianNB()
}

# Parameter Tuning untuk setiap algoritma
param_grids = {
    "Logistic Regression": {'C': [0.1, 1, 10]},
    "K-Nearest Neighbors": {'n_neighbors': [3, 5, 7]},
    "Support Vector Machine": {'C': [0.1, 1, 10], 'kernel': ['linear', 'rbf']},
    "Decision Tree": {'max_depth': [None, 10, 20]},
    "Random Forest": {'n_estimators': [50, 100, 200]},
    "Naive Bayes": {} # Tidak ada parameter yang perlu di-tuning
}
```

Figure 6. Model parameter settings

	Model	Akurasi Tanpa Tuning	Akurasi Dengan Tuning	Confusion Matrix (No Tuning)	Confusion Matrix (Tuning)
0	Logistic Regression	0.824176	0.835165	[[37, 11], [5, 38]]	[[39, 9], [6, 37]]
1	K-Nearest Neighbors	0.813187	0.857143	[[35, 13], [4, 39]]	[[38, 10], [3, 40]]
2	Support Vector Machine	0.857143	0.835165	[[36, 12], [1, 42]]	[[36, 12], [3, 40]]
3	Decision Tree	0.758242	0.736264	[[37, 11], [11, 32]]	[[37, 11], [13, 30]]
4	Random Forest	0.824176	0.824176	[[35, 13], [3, 40]]	[[36, 12], [4, 39]]
5	Naive Bayes	0.846154	0.846154	[[39, 9], [5, 38]]	[[39, 9], [5, 38]]

Figure 7. Model evaluation results

The figure Based on the Fig. 7, the results of analyzing the performance of six classification algorithms before and after hyperparameter tuning, several research results were obtained

1. Logistic Regression experienced a slight increase in accuracy from 0.824 to 0.835 after tuning. The change in confusion matrix showed improvement in classifying positive samples with a slight increase in the number of correct predictions.

2. K-Nearest Neighbors (KNN) showed a significant improvement from 0.813 to 0.857, indicating that tuning successfully found the optimal combination of the number of neighbors (k-value) that improved classification performance.
3. Support Vector Machine (SVM) experienced a slight decrease in accuracy from 0.857 to 0.835, possibly due to overfitting or inappropriate kernel parameter selection.
4. Decision Tree showed a decrease in performance after tuning, with accuracy dropping from 0.758 to 0.736. This indicates that tuning may have caused the model to become more complex without improved generalization.
5. Random Forest had a stable performance, with accuracy remaining at 0.824 before and after tuning, indicating that tuning did not have a significant impact on this model.
6. Naïve Bayes also had no change in performance, with a fixed accuracy of 0.846, indicating that this method is not significantly affected by hyperparameter tuning.

From these results it can be concluded that hyperparameter tuning does not always improve model accuracy. Algorithms such as Logistic Regression and KNN benefit from tuning, while SVM and Decision Tree experience performance degradation, and Random Forest and Naïve Bayes remain stable. This confirms that the effectiveness of tuning is highly dependent on the characteristics of the algorithm and the dataset used.

4 Conclusions

Based on this research, it can be concluded that hyperparameter tuning does not always significantly improve model performance. Tests were conducted on six classification algorithms, namely Logistic Regression, K-Nearest Neighbors (KNN), Support Vector Machine (SVM), Decision Tree, Random Forest, and Naïve Bayes, using the heart disease dataset. Evaluation is done by measuring accuracy, precision, recall, and F1-score before and after tuning using grid search technique to find the best hyperparameter combination.

The results show that the effectiveness of hyperparameter tuning is highly dependent on the algorithm and dataset characteristics. In Logistic Regression and KNN,

tuning successfully improves model performance by optimizing parameters such as the number of neighbors in KNN and regulation in Logistic Regression. In SVM and Decision Tree, tuning actually caused a decrease in accuracy and in Random Forest and Naïve Bayes, tuning did not make a significant change to model performance.

This study confirms that hyperparameter tuning does not always provide better results, and its application should be tailored to the characteristics of the dataset and the specific needs of each algorithm. In the process of data processing and modeling, a deep understanding of the algorithms used and directed experiments are needed to ensure that tuning really provides benefits in improving model performance.

References

[1] D. Cielen, A. D. B. Meysman, and M. Ali, *Introducing Data Science*. 2016.

[2] M. Arhami and M. Nasir, *Data Mining - Algoritma dan Implementasi*. Yogyakarta: Penerbit Andi, 2020.

[3] K. Pinaryanto, R. A. Nugroho, and Y. Basilius, "Classification of Toddler Nutrition Using C4 . 5 Decision Tree Method," *Int. J. Appl. Sci. Smart Technol.*, vol. 3, no. 1, pp. 131–142, 2021.

[4] B. L. Qasthari, E. Susanti, and M. Sholeh, "Classification of Lung and Colon Cancer Histopathological Images Using Convolutional Neural Network (CNN) Method on a Pre-Trained Models," *Int. J. Appl. Sci. Smart Technol.*, vol. 5, no. 1, pp. 133–142, 2023.

[5] M. Barlow, *Learning to Love Data Science*. Gravenstein Highway North, Sebastopol: O'Reilly Media, Inc, 2015.

[6] D. Sarkar, R. Bali, and T. Sharma, *Practical Machine Learning with Python*. Bangalore, Karnataka, India: Apress, 2018.

[7] D. N. Ardelia, H. D. Arifin, S. Daniswara, and A. P. Sari, "Klasifikasi Harga Ponsel Menggunakan Algoritma Logistic Regression," *J. INFORMATICS Electron. Eng.*, vol. 04, no. 01, pp. 37–43, 2024.

[8] R. A. Putri and N. S. Fatonah, "Perbandingan Metode Klasifikasi serta Analisis Faktor Akademis Pola Kelulusan Mahasiswa di Perguruan Tinggi," *J. Inform. J. Pengemb. IT*, vol. 7, no. 2, pp. 109–117, 2022, doi: 10.30591/jpit.v7i2.3082.

[9] J. A Ilemobayo *et al.*, "Hyperparameter Tuning in Machine Learning: A

Comprehensive Review," *J. Eng. Res. Reports*, vol. 26, no. 6, pp. 388–395, 2024, doi: 10.9734/jerr/2024/v26i61188.

[10] M. Arifin and S. Adiyono, "Hyperparameter Tuning in Machine Learning to Predicting Student Academic Achievement," *Int. J. Artif. Intelegence Res.*, vol. 8, no. 1, pp. 1–8, 2024.

[11] M. Fajri and A. Primajaya, "Komparasi Teknik Hyperparameter Optimization pada SVM untuk Permasalahan Klasifikasi dengan Menggunakan Grid Search dan Random Search," *J. Appl. Informatics Comput.*, vol. 7, no. 1, pp. 14–19, 2023, doi: 10.30871/jaic.v7i1.5004.

[12] N. Amalia and Asmunin, "Optimasi Algoritma Random Forest dengan Hyperparameter Tuning Menggunakan GridSearchCV untuk Prediksi Nasabah Churn pada Industri Perbankan," *Manaj. Inf.*, vol. 16, no. 1, pp. 1–9, 2024.

[13] A. Hamied Nababan and M. Y. Hutagalung, "Hyperparameter Tuning Pada Model Stance Detection Menggunakan GridSearchCV," *J. Sains dan Teknol.*, vol. 5, no. 1, pp. 205–209, 2023, [Online]. Available: https://doi.org/10.55338/saintek.v5i1.1505

[14] T. A. E. Putri, T. Widiharih, and R. Santoso, "Penerapan Tuning Hyperparameter Randomsearchcv Pada Adaptive Boosting Untuk Prediksi Kelangsungan Hidup Pasien Gagal Jantung," *J. Gaussian*, vol. 11, no. 3, pp. 397–406, 2023, doi: 10.14710/j.gauss.11.3.397-406.

[15] A. Baita, I. A. Prasetyo, and N. Cahyono, "Hyperparameter Tuning on Random Forest for Diagnose Covid-19," *JIKO (Jurnal Inform. dan Komputer)*, vol. 6, no. 2, pp. 138–143, 2023, doi: 10.33387/jiko.v6i2.6389.

[16] S. W. Lubis, P. P. Adikara, and B. Darma, "Optimasi Hyperparameter Support Vector Machine Dengan Particle Swarm Optimization Terhadap Klasifikasi Citra Digital Imbalanced," *J. Pengemb. Teknol. Inf. dan Ilmu Komput.*, vol. Vol 8 No 3, 2024, [Online]. Available: https://j-ptiik.ub.ac.id/index.php/j-ptiik/article/view/13508

[17] G. F. Fahrudin, S. Suroso, and S. Soim, "Pengembangan Model Support Vector Machine untuk Meningkatkan Akurasi Klasifikasi Diagnosis Penyakit Jantung," *J. Teknol. Sist. Inf. dan Apl.*, vol. 7, no. 3, pp. 1418–1428, 2024, doi: 10.32493/jtsi.v7i3.42254.

[18] W. Firgiawan, D. Yustianisa, and N. A. Nur, "Hyperparameter Tuning for Optimizing Stunting Classification with KNN , SVM , and Naïve Bayes Algorithms," *J. TEKNO KOMPAK*, vol. 19, no. 1, pp. 92–104, 2025.

[19] P. J. Deo and Y. B. D. Setianto, "K-Nearest Neighbor (KNN) Algorithm Performance In Diabetes Case Study," *PROXIES*, vol. 6, no. 1, pp. 93–102, 2022.

[20] M. Rizki, A. Hermawan, and D. Avianto, "Optimization of Hyperparameter K in K-Nearest Neighbor Using Particle Swarm Optimization," *JUITA J. Inform.*, vol. 12, no. 1, p. 71, 2024, doi: 10.30595/juita.v12i1.20688.

[21] N. Hendradinata, I. Gede, and S. Astawa, "Hyperparameter Tuning Algoritma KNN Untuk Klasifikasi Kanker Payudara Dengan Grid Search CV," *JNATIA Vol.*, vol. 1, no. November, pp. 397–402, 2022.

[22] S. Suraya, M. Sholeh, and D. Andayati, "Penerapan Metode Clustering Dengan Algoritma K-Means Pada Pengelompokan Indeks Prestasi Akademik Mahasiswa," *Skanika*, vol. 6, no. 1, pp. 51–60, 2023, doi: 10.36080/skanika.v6i1.2982.

This page intentionally left

IJASST
International Journal of
Applied Sciences and Smart Technologies

Volume 07
Issue 01

p-ISSN 2655-8564, e-ISSN 2685-943, pp. 145-158, 2025

Comparison of SVM, K-NN, RF, CART, and GNB Algorithms for Water Bodies Detection Using Sentinel-2 Level-2a Imagery in Nakhon Pathom, Thailand

Ni Putu Nita Nathalia[1*], Gede Andra Rizqy Wijaya [1,] Kadek Yota Ernanda Aryanto[1], Ni Putu Novita Puspa Dewi[1], Putu Hendra Saputra[1], Ni Putu Karisma Dewi[1], Mellisa Damayanti[1], Kadek Losinanda Prawira[1]

[1]*Engineering and Vocational Faculty/ Universitas Pendidikan Ganesha, Jl. Udayana Singaraja-Bali, 81116, Indonesia*
[*]*Corresponding Author: andra.rizqy@student.undiksha.ac.id*

(Received 14-02-2025; Revised 05-03-2025; Accepted 06-03-2025)

Abstract

Satellite imagery is utilized in various fields, one of which is land use and land cover (LULC) analysis. This study aims to classify water bodies using machine learning models such as SVM, K-NN, RF, CART, and GNB. The data source is obtained from the Google Earth Engine (GEE) platform using Sentinel-2 Level-2A satellite imagery, with a dataset of 5,514 data points per year. The Pixel-Based approach is used as the main method for data extraction, while CRISP-DM is applied as a structured methodology for data management. The parameter indices used include the BSI, NDBI, MNDWI, NDVI and AWEIsh. The results of these calculations serve as dataset features for training algorithms in the model development and training process. Each model has its own parameters, making parameter selection crucial in the training process. Model evaluation is conducted using a confusion matrix. Based on confusion matrix analysis, accuracy, precision, recall, and F1-score are calculated. Among the five models, SVM achieves the highest accuracy at 87%, followed by RF and K-NN. This indicates that the SVM model performs better in binary classification. Ground truth analysis is also conducted using the QGIS platform, which visualizes the classification results, with SVM providing the best visualization.

Keywords: CRISP-DM, Machine learning, Pixel-Based, S2L2A, Water bodies classification

1 Introduction

Water is the most essential element in life. Geographically, water refers to an element that shapes the Earth's surface, such as oceans, rivers, lakes, wetlands, snow, ice, and

This work is licensed under a Creative Commons Attribution 4.0 International License

water vapor[1]. Physiologically, water serves as a source of life on Earth, as all living organisms require water to survive[2]. However, the role of water is not limited to physiological aspects alone. It also plays a crucial role in economic, social, and environmental activities. For instance, water is used in agriculture for crop irrigation, in industry for production processes, and in recreational activities such as swimming or fishing. Therefore, the identification and monitoring of water areas are necessary to ensure optimal water resource management and to prevent the impacts of water-related disasters[3].

The identification and monitoring process can be carried out using data obtained from remote sensing in space, known as satellite imagery. This approach is chosen because image processing results can be measured in real-time at a relatively low cos. In digital image processing, the classification of water and non-water areas can be performed using a pixel-based image classification approach. Pixel-based image classification is one of the most commonly used methods in land use and land cover (LULC) analysis. This method utilizes digital values to identify each pixel, which is classified into predefined categories based on its characteristic values. A study conducted by Dervisoglu in 2020 on the Duden River in Turkey demonstrated that the pixel-based method has both advantages and disadvantages, depending on data characteristics and analysis objectives[4], [5], [6]. This study aims to analyze the capability of the pixel-based method in classifying water and non-water areas.

The development of machine learning (ML) enhances the data classification process, optimizing image processing for more accurate results. Several classification algorithms are commonly used, including Random Forest (RF), Support Vector Machine (SVM), k-Nearest Neighbors (k-NN), Gaussian Naïve Bayes (GNB), and Classification and Regression Tree (CART). Studies have shown that RF outperforms GNB, CART, and GBT in machine learning modelling [7], [8], [9], [10]. Several classification algorithms are commonly used, including Random Forest (RF), Support Vector Machine (SVM), k-Nearest Neighbors (k-NN), Gaussian Naïve Bayes (GNB), and Classification and Regression Tree (CART) [11], [12], [13]. [14] states that the use of the RF algorithm in machine learning modeling performs better than the GNB, CART, and GBT algorithms. [15] states that Google Earth Engine (GEE) has been proven to be an effective and fast

method for LULC mapping. This is demonstrated by the average accuracy of the SVM, RF, and CART models, which are 87.99%, 87.81%, and 84.72%, respectively. This study also shows that the SVM model exhibits better accuracy than other models. Therefore, the authors aim to reanalyze ML algorithms such as SVM, RF, k-NN, GNB, and CART in a different case study with a different dataset.

The case study used in this research is the classification of water and non-water areas in Nakhon Pathom, Thailand. Nakhon Pathom has ponds, rivers, and wetlands that serve as water retention areas. This advantage makes Nakhon Pathom the selected area of interest for obtaining the dataset used in the development of the machine learning (ML) model. This study aims to develop and compare the performance of several ML algorithms previously mentioned in classifying water and non-water areas using Sentinel-2 Level-2A satellite imagery data. The evaluation is based on the accuracy values produced by each model. In addition, an analysis is also conducted on the strengths and weaknesses of each model in the classification process.

Based on these objectives, the benefits of this study include creating an ML model capable of classifying water and non-water areas, as well as providing recommendations on ML algorithms to readers based on the analysis of the strengths and weaknesses of each algorithm used in this research. The evaluation process is carried out using a confusion matrix by calculating the values of true positive (TP), true negative (TN), false positive (FP), and false negative (FN) to derive precision, recall, and F1-score values, which are then used to determine the accuracy of the ML model. With this information, this study can provide readers with insights into the appropriate algorithm for similar case studies.

2 Material and Methods

2.1 Study Area

This study focuses on Nakhon Pathom Province, Thailand. Nakhon Pathom Province is located in the Central Region of Thailand, covering an area of approximately 2,168 square kilometres. Geographically, Nakhon Pathom Province lies between latitudes

13°46′00″N to 14°02′00″N and longitudes 100°00′00″E to 100°20′00″E (**Error! Reference source not found.**). The

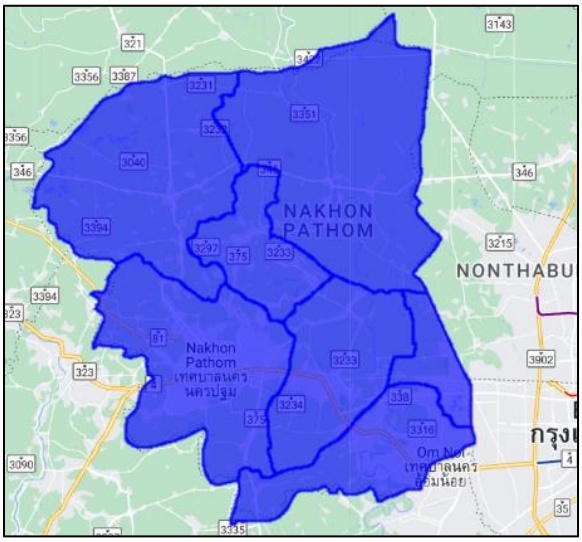

Figure 1. Nakhon Pathom Province, Thailand.

province is situated 56 kilometers west of Bangkok and is administratively divided into seven districts. This province contains water bodies such as rivers, ponds, lakes, and wetlands, making Nakhon Pathom a valuable area of interest for research related to water body classification.

2.2 Cross-Industry Standard Process for Data Mining

The Cross-Industry Standard Process for Data Mining (CRISP-DM) is used as a method to structure a framework for data management in this research (**Error! Reference source not found.**)[16]. The Business Understanding phase has been explained in the introduction section. In this phase, the author analyzes problems that could be caused by water, leading to the idea of forming a machine learning (ML) model capable of classifying water and non-water areas. In the Data Understanding phase, the author explores the necessary data and then collects the data to be processed in the data preparation phase (Table 1).

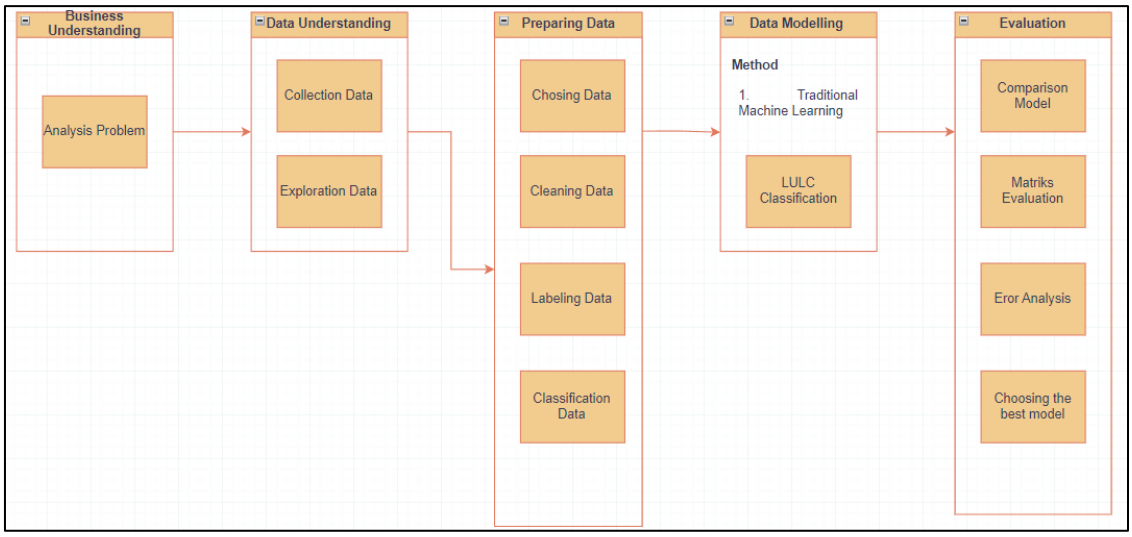

Figure 2. CRISP-DM workflow.

Table 1. Data in a single CSV file

Column	Description
Index	The serial numbers for the data start from 0_0 to 0_299 (for the water class) and 0_0 to 0_99 (for the vegetation and building classes). These numbers will adjust according to the data available.
Spectral Band	The extracted spectral bands include B1, B2, B3, B4, B5, B6, B7, B8, B8A, B9, B11, and B12.
Class	The data groups are classified as water (1), vegetation (2), and buildings (3).
Geo	The coordinate points correspond to the actual area.

The next phase is Data Preparation. In this phase, the data is cleaned to ensure that the data used is accurate and does not introduce significant bias into the machine learning (ML) model (Table 2. 3). The data is extracted based on classes (i.e., water and non-water classes). Since the data is obtained using Sentinel-2 Level-2A (S2L2A) satellites, the

extraction results consist of the band values available on S2L2A. These values are then calculated using the chosen parameter index, and the results of these calculations are used as dataset features for training the ML model (Table 2. 4). In the modeling phase, the five selected traditional ML algorithms are trained using the processed dataset, with each model having its own parameter tuning (Table 2. 5). The results of this training then move to the Evaluation phase using a confusion matrix (Table 3. 1). In this phase, the best model is selected based on the highest accuracy achieved.

2.3 Satellite Sentinel-2 Level-2A

In S2L2A, the extracted spectral bands consist of 12 bands. The obtained pointing data is then extracted and stored in CSV (comma-separated value) format, which is then processed into a dataset for the learning model (Table 1). This process falls under the category of Data Understanding.

In the Data Preparation phase, data collection was conducted from May 2023 to April 2024. The water data consisted of 300 points per month, vegetation data had 100 points per month, and building data had 100 points per month. The total sample data obtained was 500 points per month, or 6000 points over the course of one year (May 2023 – April 2024) (Table 2. 2). This data will be referred to as the initial data.

Before the extraction phase, we used the built-in feature of S2L2A, namely S2Cloudless, which aims to reduce the impact of clouds so that the values and characteristics of an area can be clearly captured by the satellite. This process is referred to as cloud masking. Therefore, the total sample data obtained after cloud masking is displayed in (Table 2. 3). The final data was then extracted using a Python notebook library within the Visual Studio Code framework. All data extraction was performed through Google Earth Engine (GEE).

Table 2. 2 The total sample points for the initial data

Water	Building	Vegetation	Total
3600	1200	1200	6000

Table 2. 3 Table of final data

Water	Building	Vegetation	Total
3306	1090	1118	5514

The data is then categorized into two classes: water class and non-water class. The band values contained in the downloaded CSV file are then calculated using parameters such as Bare Soil Index (BSI), Normalized Difference Built-up Index (NDBI), Modified Normalized Difference Water Index (MNDWI), Normalized Difference Vegetation Index (NDVI), and Automated Water Extraction Index (AWEIsh). Mathematically, this is written as follows:

$$BSI = \frac{(B11+B4)-(B8+B2)}{(B11+B4)+(B8+B2)} \quad (1)$$

$$NDBI = \frac{(B11-B8)}{(B11+B8)} \quad (2)$$

$$\text{MNDWI} = \frac{(B3-B8)}{(B3+B8)} \quad (3)$$

$$\text{NDVI} = \frac{(B8-B4)}{(B8+B4)} \quad (4)$$

$$\text{AWEIsh} = \frac{(B2+2.5*B3-1.5(B8+B11)-0.25*B12)}{B2+B3+B11+B12} \quad (5)$$

The selection of these five parameters is based on the representation of water, building, and vegetation values in the dataset. BSI and NDBI are used as parameters to help the model recognize buildings, NDVI is used as a parameter to help the model recognize vegetation, and MNDWI and AWEIsh are used as parameters to help the model recognize water. If the value of each parameter is 0.5, this can be interpreted as a situation where the measured characteristic is in the middle of the possible value range, indicating that accurate interpretation may be difficult. For example, an NDVI value of 0.5 may indicate the presence of vegetation in suboptimal conditions or a mix of vegetation and soil, while an MNDWI value of 0.5 may indicate uncertain water presence or areas with high soil moisture. After calculating the parameters, the format of the previous CSV file will change as shown in (Table 2. 4).

Table 2. 4 Dataset for modelling process

Column	Description
Index	The serial numbers for the data start from 0_0 to 0_299 (for the water class) and 0_0 to 0_99 (for the vegetation and building classes). These numbers will adjust according to the data available.
Spectral Bands	The extracted spectral bands include B1, B2, B3, B4, B5, B6, B7, B8, B8A, B9, B11, and B12.
Class	The data groups are classified as water (1), vegetation (2), and buildings (3).
Geo	The coordinate points correspond to the actual area.
Parameter Index	The values from the calculation of the parameters (BSI, NDBI, MNDWI, AWEIsh, and NDVI).

The next phase is the Modelling phase. The modelling process is carried out using five (5) different ML algorithms, namely SVM, K-NN, RF, CART, and GNB. The steps in the modelling process are almost the same for each model, including defining the x and y variables for the parameters and model class, searching for the best parameters for each model, classification, and performance evaluation. The distinction in the process lies in the selection of parameters (parameter tuning) for each model (Table 2. 5).

Table 2. 5 Parameter tuning for each algorithm

SVM	c: 100; class_weights: None; degree: 2; gamma: ‘scale’; kernel: ‘rbf’.
RF	leaf_size: 20; metric: ‘minkowski’; n_jobs: -1; n_neighbors: 20; p: 2; weights: ‘distance’.

k-NN	bootstrap: True; max_depth: None; min_sampes_leaf: 1; min_samples_spit: 5; n_estimators: 200; n_jobs: -1.
CART	criterion: ‘entropy’; max_depth: 10; min_samles_leaf: 10; min_samples_split: 10.
GNB	var_smoothing: 1e-09.

The final process is evaluation. The evaluation of the model is performed using evaluation matrices such as the confusion matrix. Analysis is carried out on the results based on the accuracy, precision, recall, and F1-score values of each algorithm. Below is the mathematical formulation for calculating accuracy, precision, recall, and F1-score.

$$\text{Accuracy} = \frac{\text{TP+TN}}{\text{TP+FP+TN+FN}} \quad (1)$$

$$\text{Precision} = \frac{\text{TP}}{\text{TP+FP}} \quad (2)$$

$$\text{Recall} = \frac{\text{TP}}{\text{TP+FN}} \quad (3)$$

$$\text{F1} - \text{Score} = \frac{2*\text{precision}*\text{recall}}{\text{precision+recall}} \quad (4)$$

Description : TP (True Positive), TN (True Negative), FP (False Positive), FN (False Negative).

In addition to the calculations above, ground truth is also used as a form of evaluation and comparison between the model results and the real-world conditions. Ground truthing is performed using the QuantumGIS (QGIS) software.

3 Results and Discussions

3.1 Model Analysis

Based on the results of the confusion matrix, with a dataset of 5514 data points, the model using the SVM algorithm successfully identified 2922 water class samples correctly as water. The model also correctly identified 1870 non-water class samples as non-water. On the other hand, the model incorrectly identified 384 non-water class samples as water, and 338 water class samples as non-water (Table 3. 1). The resulting ratio scale is 6.64:1, or approximately 7:1. Based on the values derived from the confusion

matrix analysis, the results shown in (Table 3. 2) indicate that the SVM model excels in classifying both water and non-water classes with a ratio of 6.64:1 and an accuracy of 87%, followed by the RF and k-NN models with an accuracy of 86%.

Table 3. 1 The acquisition of the confusion matrix values for each model.

	TP	TN	FP	FN	Ratio
SVM	2922	1870	384	338	6.64:1
k-NN	2916	1804	390	404	5.94:1
RF	2918	1822	388	386	6.12:1
CART	2769	1740	537	468	4.48:1
GNB	2663	1629	643	579	3.51:1

Table 3. 2 The calculation of the precision, recall, F1-Score, and accuracy values produced by the model.

Class	*Precision*	*Recall*	*F1-Score*	*Accuracy Model*
		SVM Model		
Water	0.90	0.88	0.89	0.87
Non-water	0.83	0.85	0.84	
		k-NN Model		
Water	0.88	0.88	0.88	0.86
Non-water	0.82	0.82	0.82	
		RF Model		
Water	0.88	0.88	0.88	0.86
Non-water	0.82	0.83	0.82	
		CART Model		
Water	0.86	0.84	0.85	0.82
Non-water	0.76	0.79	0.78	
		GNB Model		
Water	0.82	0.81	0.81	0.78

Non-water	0.72	0.74	0.73

3.2 Visualization of the results of each model using Quantum GIS (QGIS).

The comparison of the results from each model is done for a region in Nakhon Pathom. The blue colour indicates water areas, and the green colour represents non-water areas. Using a pixel-based method, it shows detailed results, but when viewed from a distance, it displays patches, indicating that adjacent areas have been classified into different classes.

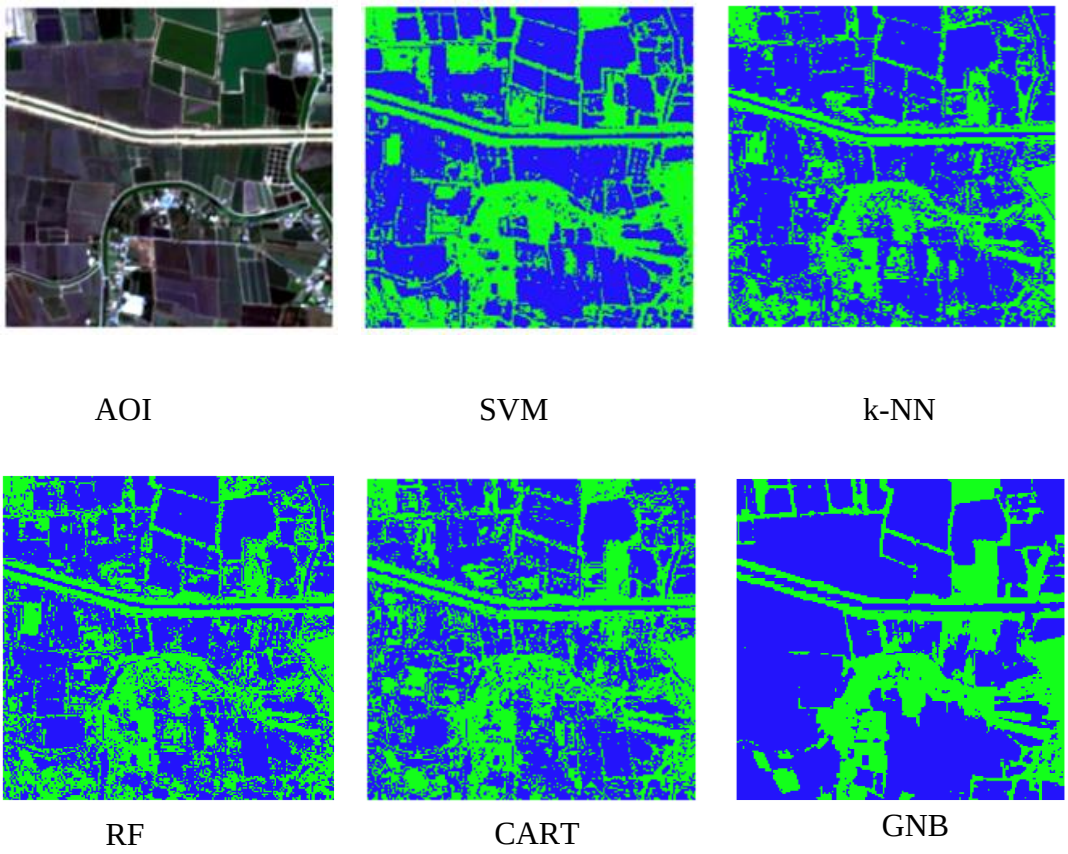

Figure 3. 1 Comparison of the classification results from each model.

The results show that, in the classification of water and non-water areas, the SVM model performs the best, followed by the RF and k-NN models. This can be confirmed based on the accuracy values Table 3. 1 - Table 3. 2 and the provided ground truth results. Therefore, SVM, RF, and k-NN are recommended algorithms for the classification of water and non-water areas.

4 Conclusions

In this study, we understand that the selection of data, algorithms, and methods is crucial to the success of building a machine learning (ML) model. For the classification of water and non-water areas, we recommend several supervised learning algorithms such as SVM, RF, and k-NN. The accuracies achieved by each model are 87%, 86%, and 86%, respectively. To improve the model's quality, it is necessary to increase the dataset size and split the non-water class into more specific classes, such as vegetation, barren land, and buildings. This would result in greater area variability. Future research could consider using deep learning methods like Convolutional Neural Networks (CNNs), which are better at handling the complexity of image data. Additionally, testing the model on datasets from different regions or in varying environmental conditions could provide further insights into the model's generalization ability.

Acknowledgements

The author would like to express gratitude to the supervisor and colleagues who have contributed and assisted the author throughout the process of this research.

References

[1] H. Ghosh, M. A. Tusher, I. S. Rahat, S. Khasim, and S. N. Mohanty, “Water Quality Assessment Through Predictive Machine Learning,” in *Lecture Notes in Networks and Systems*, Springer Science and Business Media Deutschland GmbH, 2023, pp. 77–88. doi: 10.1007/978-981-99-3177-4_6.

[2] W. Jiang *et al.*, “A new index for identifying water body from sentinel-2 satellite remote sensing imagery,” in *ISPRS Annals of the Photogrammetry, Remote Sensing and Spatial Information Sciences*, Copernicus GmbH, Aug. 2020, pp. 33–38. doi: 10.5194/isprs-Annals-V-3-2020-33-2020.

[3] A. Tassi and M. Vizzari, "Object-oriented lulc classification in google earth engine combining snic, glcm, and machine learning algorithms," *Remote Sens (Basel)*, vol. 12, no. 22, pp. 1–17, Nov. 2020, doi: 10.3390/rs12223776.

[4] A. Dervisoglu *et al.*, "Comparison of Pixel-Based and Object-Based Classification Methods in Determination of Wetland Coastline," *International Journal of Environment and Geoinformatics (IJEGEO)*, vol. 7, no. 2, pp. 213–219, 2020, doi: 10.30897/ijegeo.

[5] L. Qu, Z. Chen, M. Li, J. Zhi, and H. Wang, "Accuracy improvements to pixel-based and object-based LULC classification with auxiliary datasets from google earth engine," *Remote Sens (Basel)*, vol. 13, no. 3, Feb. 2021, doi: 10.3390/rs13030453.

[6] H. Ouchra, A. Belangour, and A. Erraissi, "A Comparative Study on Pixel-based Classification and Object-Oriented Classification of Satellite Image," *International Journal of Engineering Trends and Technology*, vol. 70, no. 8, pp. 206–215, Aug. 2022, doi: 10.14445/22315381/IJETT-V70I8P221.

[7] D. W. Triscowati and A. W. Wijayanto, "Peluang Dan Tantangan Dalam Pemanfaatan Teknologi Penginderaan Jauh Dan Machine Learning Untuk Prediksi Data Tanaman Pangan Yang Lebih Akurat," *Seminar Nasional Official Statistics*, vol. 2019, no. 1, 2020, doi: 10.34123/semnasoffstat.v2019i1.230.

[8] F. Traoré, S. Palé, A. Zaré, M. K. Traoré, B. Ouédraogo, and J. Bonkoungou, "A Comparative Analysis of Random Forest and Support Vector Machines for Classifying Irrigated Cropping Areas in The Upper-Comoé Basin, Burkina Faso," *Indian J Sci Technol*, vol. 17, no. 8, pp. 713–722, Feb. 2024, doi: 10.17485/IJST/v17i8.78.

[9] D. M. Abdullah and A. M. Abdulazeez, "Machine Learning Applications based on SVM Classification: A Review," *Qubahan Academic Journal*, vol. 3, no. 4, pp. 206–218, Nov. 2023, doi: 10.48161/Issn.2709-8206.

[10] M. C. R. Cordeiro, J.-M. Martinez, and S. Peña-Luque, "Remote Sensing of Environment," vol. 253, p. 112209, 2021, doi: 10.1016/j.rse.2020.112209ï.

[11] C. Avci, M. Budak, N. Yagmur, and F. B. Balcik, "Comparison between random forest and support vector machine algorithms for LULC classification," *International Journal of Engineering and Geosciences*, vol. 8, no. 1, pp. 1–10, Feb. 2023, doi: 10.26833/ijeg.987605.

[12] D. Danuri and M. Mohd Pozi, "Machine Learning Approaches for Fish Pond Water Quality Classification: Random Forest, Gaussian Naive Bayes, and Decision Tree Comparison," European Alliance for Innovation n.o., Feb. 2024. doi: 10.4108/eai.21-9-2023.2342964.

[13] H. R. Bittencourt and R. T. Clarke, "Use of Classification and Regression Trees (CART) to Classify Remotely-Sensed Digital Images," in *International Geoscience and Remote Sensing Symposium (IGARSS)*, 2003, pp. 3751–3753. doi: 10.1109/igarss.2003.1295258.

[14] S. Bayas, S. Sawant, I. Dhondge, P. Kankal, and A. Joshi, "Land Use Land Cover Classification Using Different ML Algorithms on Sentinel-2 Imagery," in *Lecture Notes in Electrical Engineering*, Springer Science and Business Media Deutschland GmbH, 2022, pp. 761–777. doi: 10.1007/978-981-19-0840-8_59.

[15] E. M. Sellami and H. Rhinane, "A New Approach For Mapping Land Use / Land Cover Using Google Earth Engine: A Comparison Of Composition Images," in *International Archives of the Photogrammetry, Remote Sensing and Spatial Information Sciences - ISPRS Archives*, International Society for Photogrammetry and Remote Sensing, Feb. 2023, pp. 343–349. doi: 10.5194/isprs-archives-XLVIII-4-W6-2022-343-2023.

[16] C. Schröer, F. Kruse, and J. M. Gómez, "A systematic literature review on applying CRISP-DM process model," in *Procedia Computer Science*, Elsevier B.V., 2021, pp. 526–534. doi: 10.1016/j.procs.2021.01.199.

IJASST International Journal of Applied Sciences and Smart Technologies

Volume 07
Issue 01

p-ISSN 2655-8564, e-ISSN 2685-943, pp. 159-168, 2025

Analysis of Spiral Pump Head Based on Water Wheel Parameters

Hengky Luntungan[1*], Stenly Tangkuman [1], Benny L. Maluegha[1]

[1]*Mechanical Engineering Department, Sam Ratulangi University,*
Jl. Kampus Unsrat, Bahu, 95115, Indonesia
[*]*Corresponding Author: st75@unsrat.ac.id*

(Received 14-02-2025; Revised 05-03-2025; Accepted 06-03-2025)

Abstract
Water supply is a crucial factor for farmers in managing agricultural land, especially those relying on river water sources. The lower position of rivers and the considerable distance from the fields often pose challenges, making water pumps powered by electricity or fuel a common choice, despite their high operational costs. To address this issue, the utilization of renewable energy through the use of a spiral pump powered by a water wheel is proposed. The spiral pump is considered an environmentally friendly technology as it does not require electricity or fossil fuels. This study aims to analyze the head of a spiral pump based on the parameters of an undershot water wheel as preparation for the design of the spiral pump. In this study, a significant decrease in discharge value was observed from a head of 0.5 m up to a head of 3 m; in contrast, from a head of 3 m to 10 m, the discharge value decreased gradually. For small agricultural land or household needs, this spiral pump water wheel would be suitable at a maximum head of 5 m with a discharge value of 0.53 L/s. The results show a negative correlation between the head of the spiral pump and the discharge produced, where an increase in head results in a lower discharge.

Keywords: fluid flow, head pump, spiral pump, water discharge, water wheel

1 Introduction

The spiral pump is a type of water pump that operates without electricity or fossil fuels, making it often considered environmentally friendly. The spiral pump consists of two main components: a spiral pipe (or spiral hose) and a driving mechanism, which is generally a water wheel [1]. The spiral pipe is placed in the water and rotates with the wheel, transporting water into the spiral. The spiral pump utilizes the kinetic energy of the water that drives the wheel, so it does not require additional energy. For this reason,

This work is licensed under a Creative Commons Attribution 4.0 International License

the spiral pump is ideal for areas far from power sources or where fuel resources are limited.

The spiral pump, initially invented by H. A. Wirtz in 1746 [2], was originally powered by horses. This invention remained largely forgotten for approximately 240 years until it was revived and advanced by Peter Morgan, who transformed it into an eco-friendly technology by using a water wheel instead of horse power to drive the pump. Spiral pumps offer valuable support to communities, particularly in agriculture, as they operate without needing electricity or fuel.

The water wheel converts the kinetic energy of the water flow into mechanical power to rotate the spiral pump [3]. The higher the speed and volume of the water flow hitting the wheel, the greater the power generated, which then increases the spiral pump's rotation and its efficiency in raising water. A well-designed water wheel can maximize the use of energy from the water flow, thereby optimizing the spiral pump's performance [4]. Factors such as wheel size, number of blades, and blade angle affect how efficiently the water flow energy is transferred to the spiral pump. Overall, the performance of the spiral pump largely depends on the design and performance of the water wheel [5]. For the spiral pump to operate optimally, the water wheel should be designed to match the flow conditions and energy needs at a specific location [6].

Therefore, it is necessary to conduct research on the water wheel of the spiral pump. This study aims to analyze the head of a spiral pump based on the parameters of an undershot water wheel as preparation for the design of the spiral pump.

2 Theoretical Background

The wetted cross-sectional area refers to the area of the blade or paddle cross-section of the water wheel that is in direct contact with or submerged by the water flow. This area is important because it indicates how much of the wheel is receiving pressure or force from the water flow, which affects the efficiency and power generated by the wheel. For d as the water depth on the wheel and w as the width of the wheel, the wetted cross-sectional area (A) can be calculated using the following equation (Equation 1).

$$A = d.w \quad (1)$$

The input power of the water wheel is influenced by the density (ρ), wetted cross-sectional area (A), and water flow velocity (V). The following equation (Equation 2) can be used to calculate the input power of the water wheel [7][8].

$$P_{in} = ½.\ \rho.\ A.\ V^3 \quad (2)$$

Only about 30% - 50% of the water power calculated above can be converted into the output power of the water wheel. This value is known as the water wheel's efficiency. In this study, the midpoint value of 40%, or 0.4, is used. The choice of 40% efficiency is also based on three main considerations. First, in practice, even under good conditions, there are unexpected losses due to turbulence, friction, misalignment, and non-ideal flow. Choosing 40% instead of assuming a higher 50% helps account for these typical inefficiencies without requiring complex adjustments. Second, selecting a slightly conservative value like 40% ensures that the system is more reliable. It prevents overestimating the pump's capability, which is important if the water flow rate or environmental conditions change. Finally, since this study did not engage in detailed optimization (such as adjusting blade shapes or angles), assuming a moderate efficiency like 40% simplifies the calculations while maintaining a realistic approach. Therefore, the output power of the water wheel P_{out} can be calculated using the following equation (Equation 3).

$$P_{out} = \eta.\ P_{in} \quad (3)$$

The power generated is also directly proportional to the density (ρ), gravitational acceleration (g), water discharge (Q), and pump head (H), which can be formulated as follows.

$$P_{out} = \rho.\ g.\ Q.\ H \quad (4)$$

If the desired pump head value has been determined, the pump discharge can be calculated using Equation 4, with slight adjustments to the formula. Therefore, the pump discharge can be calculated using the following equation (Equation 5).

$$Q = \frac{P_{out}}{\rho.g.H} \quad (5)$$

3 Method

The analysis of the spiral pump head based on the parameters of the water wheel consists of five steps: measuring the water flow velocity, modeling the water wheel, calculating the wetted cross-sectional area of the wheel, calculating the input and output power of the water wheel, and analyzing the head relative to the pump flow rate. These five sections will be explained further in sections 4.1 to 4.5. Through these steps, the head of the spiral pump can be analyzed by utilizing the performance of the water wheel as the driving mechanism. The numerical software used in this study was Solidworks.

4 Application and Results

4. 1 Measurement of Water Flow Velocity

The measurement of water flow velocity in this study is relatively simple. The tools used include a cylindrical float made of wood and a stopwatch to measure the time [9]. The procedure involves releasing the float over a distance of 10 meters, then measuring the time it takes to travel that distance using the stopwatch. From this measurement, the average flow velocity of the river water was determined to be 0.896 m/s.

4.2 Water Wheel Modeling

Creating a model of the spiral pump for this study provides an understanding of the behavior and performance of the spiral pump. Through this model, researchers can identify influencing factors such as efficiency, design more optimal configurations, and develop performance prediction methods for real-world applications [10]. Specifically,

in this study, the pump head analysis was conducted using the spiral pump model as shown in Fig. 1.

4.3 Calculation of Wetted Cross-Sectional Area of the Water Wheel

The wetted cross-sectional area can be calculated using Equation 1. For a water depth on the wheel (d) of 0.3 m and a wheel width (w) of 0.6 m, the wetted cross-sectional area (A) is:

$$A = 0.3m.\ 0.6m = 0.18\ m^2. \quad (6)$$

4.4 Calculation of Input & Output Power of the Water Wheel

If the density (ρ) is known to be 1000 kg/m³, the wetted cross-sectional area (A) is 0.18 m², and the water flow velocity (V) is 0.896 m/s, then using Equation 2, the input power of the water wheel (P_{in}) can be calculated as follows.

$$P_{in} = ½.\ 1000\ kg/m^3.\ 0.18\ m^2.\ (0.896m/s)^3 = 64{,}738\ Watt. \quad (7)$$

Meanwhile, the output power of the water wheel can be calculated using Equation 3 by assuming the wheel's efficiency to be 40%. The output power of the water wheel (Pout) is then calculated to be 25.895 watts.

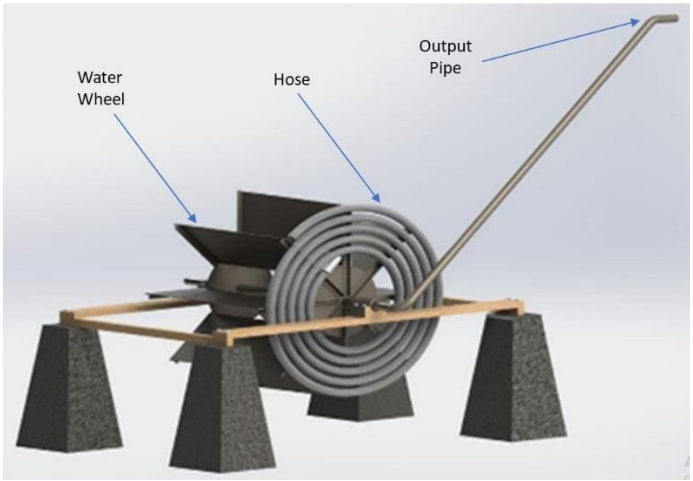

Figure 1. The spiral pump model under study

4.5 Spiral Pump Head Analysis

By determining the desired pump head, the pump discharge can be calculated using Equation 5. For example, if the pump head is set to 0.5 m, the pump discharge is:

$$Q = \frac{25.895 \text{ Watt}}{1000kg/m^3.9.81m/s^2.0.5m} = 0.00528 \text{ m}^3/\text{s} = 5.28 \text{ L/s.} \quad (8)$$

Based on the data from the calculation of the water discharge against the head, a graph is then created to facilitate the interpretation of the change in water discharge with respect to the head. Below are the Table 1 and Fig. 2 showing the relationship between the head and water discharge of the spiral pump.

In Fig. 2, the head of the spiral pump is varied from 0.5 m to 10 m with an interval of 0.5 m. A significant decrease in flow rate occurs until the head reaches 3 m, whereas from 3 m to 10 m, the flow rate decreases gradually. For small agricultural land needs or household purposes, a pump with a minimum flow rate of 0.5 L/s is required. Based on Fig. 2, the maximum head that meets this requirement is 5 m. Overall, the highest discharge (5.28 L/s) occurs at a head of 0.5 m, while the lowest discharge (0.26 L/s) occurs at a head of 10 m.

Table 1. Head versus discharge of pump

No	*Head (m)*	Discharge Q (m^3/s)	Discharge (L/s)
1	0.5	0.00528	5.28
2	1	0.00264	2.64
3	1.5	0.00176	1.76
4	2	0.00132	1.32
5	2.5	0.00105	1.05
6	3	0.00088	0.88
7	3.5	0.000754	0.75
8	4	0.00066	0.66
9	4.5	0.000587	0.59
10	5	0.000528	0.53

11	5.5	0.00048	0.48
12	6	0.00044	0.44
13	6.5	0.000406	0.41
14	7	0.000377	0.38
15	7.5	0.000352	0.35
16	8	0.00033	0.33
17	8.5	0.00031	0.31
18	9	0.00029	0.29
19	9.5	0.000278	0.28
20	10	0.000264	0.26

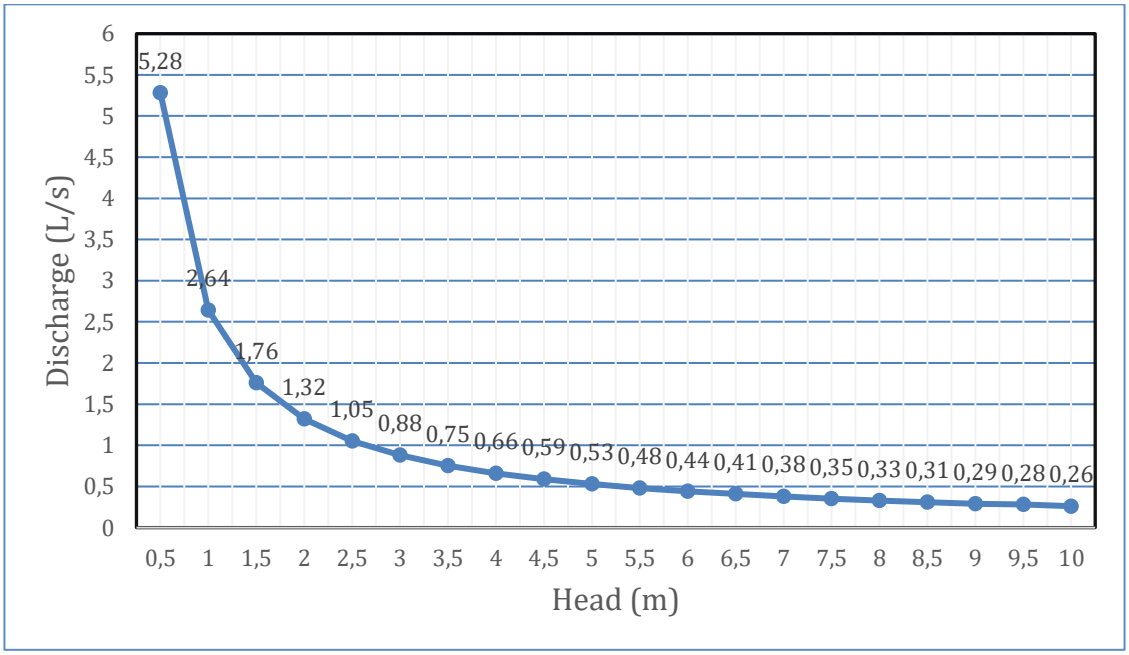

Figure 2. Head vesus discharge of pump

5 Conclusions

This study shows that a significant decrease in discharge occurs from a head of 0.5 m to a head of 3 m, whereas from 3 m to 10 m, the decrease in discharge is more gradual. For small agricultural land needs or household use, the water wheel pump for

this spiral pump will be suitable for a maximum head of 5 m with a discharge of 0.53 L/s. Overall, the highest discharge (5.28 L/s) occurs at a head of 0.5 m, while the lowest discharge (0.26 L/s) occurs at a head of 10 m. The analysis shows that the higher the head of the spiral pump, the lower the discharge obtained.

Although this study identifies a maximum head of 5 meters as suitable for small-scale applications, examining the scalability of the spiral pump design is crucial to extend the applicability and impact of the findings. Adapting the spiral pump for larger capacities would involve modifications to key design parameters such as coil diameter, the number of turns, pipe size, and the driving mechanism (e.g., using larger water wheels or optimizing rotational speed). Increasing the pipe diameter and the overall scale of the spiral can enhance the volume of water transported per cycle, while adjustments to the number of turns can increase the achievable head. For instance, if a two-fold increase in head is desired, the pipe diameter and water wheel diameter may need to increase by a factor of approximately 1.5 times.

Furthermore, larger systems would need to address additional engineering challenges such as higher mechanical stresses, increased frictional losses, and the need for structural stability. Material selection becomes more critical to ensure durability under greater operational loads. By exploring these adaptations, this study could provide valuable insights into how the fundamental principles of the spiral pump can be applied not only to small-scale rural water supply projects but also to medium- to large-scale agricultural irrigation systems or decentralized industrial water distribution systems.

Acknowledgements

This research was funded by Sam Ratulangi University in 2024 through a basic research scheme (RDUU-K2, SP DIPA-023.17.2.677519/2024).

References

[1] Luntungan Hengky, Stenly Tangkuman, dan I Nyoman Gede, 2023. Analysis of Spiral Pump Discharge Based on Simulation of Fluid Flow In Hoses. *International Journal of Applied Sciences and Smart Technologies*, Volume 5, Issue 2, pages 355–364.

[2] Peter Tailer, *The Spiral Pump A High Lift Slow Turning Pump*, 1986, https://lurkertech.com/water/pump/tailer/

[3] Kumar Fanesh, J. Sinha, Kamalkant, et al, Design and Development of a Spiral Tube Water Wheel Pumping System: A Review, *AgricultureAssociation of Textile Chemical and Critical Reviews Journal*, 2023, 217 – 222.

[4] Patel Priyankkumar R., et al, Design Of Spiral Tube Agriculture Water Wheel Pump. *International Journal Of Applied Research In Science And Engineering*, 2017, pp.560-565.

[5] Satish H. Patil et al, A Review Paper on Spiral Tube Water Wheel Pump, *International Journal of Advance Research in Science and Engineering*, Vol. 6 Issue. 08, 2017, pp 1123-1125.

[6] Mukhtar Anas and Gatut Rubiono, Spiral Pumping Wheel Turbine Application Concept for Irrigation with Different Altitudes, *Gandrung: Jurnal Pengadian Kepada Masyarakat*, Vol. 3, No.2, 2022, pp.626-632.

[7] R. Eko, Agung Fauzi Hanafi, I. G. N. A. Satria Prasetya D.Y., and Enggar Priyadi, Design And Manufacture Of Undershot Waterwheel As A Spiral Pump Driven For Agricultural Irrigation, *SJMEkinematika*, vol. 8, no. 1, pp. 13-24, Jun. 2023.

[8] Diaz Eddisney, Carlos Trinchet and Javier Vargas, Design and Simulation of a Spiral Hydraulic Pump Based on Multi-Objective Optimization, *ARPN Journal of Engineering and Applied Sciences*, Vol.15, No.5, 2020, pp. 657-663.

[9] Kumar Fanesh, Jitendra Sinha and Kamalkant, Development and Testing of a Spiral Type Water Wheel Pumping System, *Internasional Journal of Current Microbiology and Applied Sciences*, Vol. 9, No. 5, 2020, pp. 3061-3069.

[10] Lee Man Djun, J.Y.Chan, J.Ling and P.S.Lee, Design and Development of Zero Electricity Water Pump for Rural Development, *Universal Journal of Mechanical Engineering*,

IJASST International Journal of Applied Sciences and Smart Technologies
Volume 07
Issue 01
p-ISSN 2655-8564, e-ISSN 2685-943, pp. 169-180, 2025

Determination of Premium Reserves for Whole Life Insurance Using the Canadian Method with Varying Premium Payment Periods

Illuminata Wynnie[1*], Yefan[1]

[1]*Actuarial Science Study Program, Hasanuddin University, Perintis Kemerdekaan Street, 90245, Indonesia*
[*]*Corresponding Author: illuminataw@unhas.ac.id*

(Received 07-05-2025; Revised 11-05-2025; Accepted 13-05-2025)

Abstract

Premium reserves are essential funds prepared by insurance companies, particularly in life insurance, to cover potential future claims. These reserves are calculated based on premiums paid by policyholders and must be sufficient to meet all projected claim-related expenses. A lower reserve implies reduced financial liability and typically correlates with more affordable premium rates for policyholders. This study aims to analyze the determination of premium reserves using the Canadian and Prospective methods in traditional life insurance products, specifically whole life insurance, focusing on different premium payment periods. The Indonesian Population Mortality Table (TMPI) 2023 and the Bank Indonesia interest rate of 5.57% (as of April 2025) as the calculation basis. The results show that the Canadian method produces lower reserve values compared to the Prospective method and indicate a decreasing trend in reserve values as the premium payment period increases in both methods.

Keywords: Canadian Method, Premium Reserves, Prospective Method, Whole Life Insurances

1 Introduction

Insurance is a financial program designed to reduce risk through an agreement between two parties, in which one party pays a premium and the other party provides full coverage in the event of an incident as specified in the agreement [1]. One of the most commonly offered types of insurance in Indonesia is life insurance. In simple terms, life

This work is licensed under a Creative Commons Attribution 4.0 International License

insurance can be understood as a program that provides financial protection to an individual or their family in the event of life-related risks, such as death or permanent disability due to an accident [2]. Based on the duration of its coverage, life insurance can be classified into three types: term life insurance, whole life insurance, and endowment insurance [3].

A premium is a sum of money paid by the policyholder (insured) to the insurer as predetermined [4]. The company calculates the premium to be paid by the policyholder to obtain the agreed-upon benefits. However, sometimes the set premium is not sufficient to cover the company's expenses. Therefore, to cover this shortfall, the company must have a reserve fund called a premium reserve. A premium reserve is the money that must be set aside by the company to cover risks, which, in the case of endowment insurance, includes compensation to the insured or their beneficiary [5]. Premium reserves are usually based on the premiums received from policyholders and must cover all potential costs associated with future claim payments. A smaller premium reserve indicates that the insurance company estimates lower future liabilities. This can be due to factors such as a younger age of the insured or a shorter insurance period. As a result, the premiums offered to customers are also lower because the risks borne by the insurance company are smaller. Conversely, if the premium reserve is large, the company must allocate more funds to meet future claims, resulting in higher premiums charged to customers [6].

With technological advancements, actuaries have introduced many calculation methods to optimize premium reserves, such as the prospective, retrospective, Zillmer, New Jersey, and Canadian methods. The Canadian method is an extension of the prospective method, which equates the initial modified premium with the net premium and the difference between the policy’s net premium and natural premium. One advantage of this method is that it extends the modification period to cover the entire premium payment duration, thus reducing losses in the early years of premium reserve calculation [5].

Previous studies have examined various calculation methods to optimize premium reserves in whole life insurance. Sari [7] applied the Canadian method to calculate premium reserves for endowment life insurance and found that the reserve value obtained at the end of the coverage period matched the compensation value provided. Additionally,

Ekawati [5] showed that the Canadian method is very useful in creating joint life insurance reserve tables. Furthermore, according to Kele [8] premium reserves calculated using the Canadian method increase with the age of the insured. The prospective method has become the standard in setting life insurance premiums, with a focus on estimating future risks and claims.

On the other hand, the Canadian method, as an extension of the prospective approach, offers added advantages by accounting for premium modifications and extending the modification period. This study will adopt a comparative approach to evaluate the premium reserve values between the prospective and Canadian methods, taking into account different premium payment periods. This scheme is regarded as attractive from an actuarial and policyholder perspective, as it allows the insured to pay premiums over a limited number of years while still being entitled to death benefits throughout their entire lifetime. By comparing these two methods, the study aims to identify differences in the resulting premium reserve values whole life insurance.

2 Material and Methods

Mortality Table

A mortality table contains several components, such as l_x, which represents the number of people alive at age x, d_x which indicates the number of people who die at age x and q_x which denotes the probability that a person aged x will die between age x and$x + 1$. Mortality tables are used by insurance companies to calculate premiums, as they include key components that are essential in determining premium rates. To facilitate calculations within the mortality table, commutation functions are commonly used. These functions are typically applied in the calculation of annuities, actuarial present values, premium reserves, and related computations [9].

$$D_x = v^x . l_x \quad (1)$$

$$C_x = v^{x+1} . d_x \quad (2)$$

$$N_x = \sum_{i=0}^{n} D_{x+i} \quad (3)$$

$$M_x = \sum_{i=1}^{n} C_{x+i} \tag{4}$$

Actuarial Present Value for Whole Life Insurance

The net single premium for whole life insurance is a one-time lifetime premium payment for a policyholder aged x, denoted by A_x, and is expressed using commutation symbols as follows [8]:

$$A_x = \frac{M_x}{D_x} \tag{5}$$

Life Annuity

An annuity is a series of fixed payments made at regular intervals, such as monthly, quarterly, semi-annually, or annually. A life annuity includes a survival factor, meaning it is contingent upon the policyholder's life expectancy [10]. The present value of a life annuity, with payments made at the beginning of each year, is denoted as:

$$\ddot{a}_x = \frac{N_x}{D_x} \tag{6}$$

$$\ddot{a}_{x:\overline{n}|} = \frac{N_x - N_{x+n}}{D_x} \tag{7}$$

Whole Life Insurance Premium

A premium is the amount of money paid by the insured to the insurer, as predetermined in the insurance agreement [5]. The annual whole life insurance premium for a person aged x is calculated as:

$$P_x = \frac{A_x}{\ddot{a}_x} = \frac{M_x}{N_x} \tag{8}$$

Premium payments can also be made over a certain period h, and are denoted as:

$$_hP_x = \frac{A_x}{\ddot{a}_{x:\overline{h}|}} = \frac{M_x}{N_x - N_{x+h}} \tag{9}$$

Prospective Premium Reserves

The prospective premium reserve is calculated based on the present value of all future income and outgoings [11]. The reserve at time n is the difference between the present value of total future benefits (claims) and the present value of total future premiums at time n. If x is the age of the insured at the start of the contract, then the prospective reserve at the end of year k is given by [14]:

$$ {}_{k}^{h}V_x = \begin{cases} A_{x+k} - {}_hP_x\ddot{a}_{x+k:\overline{h-k|}} & k < h \\ A_{x+k} & k \geq h \end{cases} \tag{10} $$

Canadian Premium Reserves

The Canadian reserve method calculates reserves by aligning the modified initial premium with the net premium, adjusted by the difference between the net premium and the natural premium. The modified premium is denoted by α for the first year and β for subsequent years [15].

The modified first-year premium in the Canadian method is:

$$ \alpha = {}_hP_x - \left(P_x - \frac{C_x}{D_x}\right) $$

Here, $\frac{C_x}{D_x}$ represents the natural premium, which is a renewable one-year term premium, extended annually over a specific premium payment period. The present value of the total net premiums at the start of the insurance contract equals the present value of the total expected gains from the contract.

$$ {}_hP_x\ddot{a}_{x:\overline{h|}} = \alpha + \beta\left(\ddot{a}_{x:\overline{h|}} - 1\right) $$

The extended modified premium β is expressed as:

$$ \beta = {}_hP_x + \frac{P_x - \frac{C_x}{D_x}}{\ddot{a}_{x:\overline{h|}} - 1} \tag{11} $$

The β is used as the annual premium in Canadian reserve calculations, which are influenced by the number of payments h

$$ {}_{k}^{h}V_{x}^{can} = \begin{cases} A_{x+k} - \beta \ddot{a}_{x+k:\overline{h-k}|} & k < h \\ A_{x+k} & k \geq h \end{cases} \quad (12) $$

Research Parameters

This study uses a fixed interest rate of 5.75%, as set by Bank Indonesia in April 2025 [12]. The mortality data used in the calculations is sourced from the 2023 Indonesian Male Mortality Table (TMPI 2023)[13].

Methods

1. Define the age of the policyholder (insured), which is 25 years.
2. Determine the probability of death and the remaining unknown elements of the mortality table.
3. Calculate the commutation values.
4. Compute the actuarial present values.
5. Calculate the initial annuity values for whole life insurance.
6. Compute the whole life insurance premiums for different premium payment periods ($h = 5,10,20$)
7. Calculate the prospective premium reserves for different payment durations ($h = 5,10,20$)
8. Determine the modified premiums α and β for the Canadian method with various premium payment periods.
9. Calculate the Canadian premium reserves for each duration.
10. Analyze and compare the results from the prospective and Canadian reserve methods

3 Results and Discussions

In the calculation of premium reserves for whole life insurance, an insured individual aged 25 is selected. The researcher chooses the age of 25 because policyholders at this age are generally at their peak performance, both in terms of health and work. In addition, the researcher uses data from Indonesian Male Mortality Table (TMPI 2023) [13] and interest rates from Bank Indonesia (5,57% in April 2025) [12].

The calculation of the commutation value D_x or the present value of payments for the number of insured individuals alive at age x, using a constant interest rate, is performed using Equation (1). The calculation of the present value of payments, or C_x or the number of insured individuals who die at age x = 25 to x = 110, is done using Equation (2). The value N_x is the accumulation of D_{x+i} for $i = 0$ up to $\omega = 110$. Equation (3) is used to calculate N_x. The value M_x is the accumulation C_{x+i} for $i = 0$ up to $\omega = 110$. Equation (4) is used to calculate M_x. The results of the commutation values are shown in Table 1.

The present value of whole life insurance is calculated using Equation (5) and is shown in Table 2. After obtaining the present value of whole life insurance, the calculation of whole life annuities and term life annuities can be carried out using Equations (6) and (7), as shown in Tables 3 and 4. The value of the term annuity increases as the premium payment period lengthens, with $h = 20$ having the highest term annuity value.

Table 1. Commutation Values, N_x, C_x, M_x

x	D_x	N_x	C_x	M_x
25	24.027,8	403.218	24,4481	1.785,73

Table 2. Actuarial Present Value

x	A_x
25	0,08754

Table 3. Whole Life Annuity

x	$\ddot{a}_x$
25	16,7813

Table 4. Term Annuity

x	h	$\ddot{a}_{x:\overline{h}\|}$
25	5	4,4754
	10	7,8371
	20	12,2385

. After obtaining the present value of whole life insurance and life annuities, the premium value of whole life insurance and the premium value of whole life insurance paid over a period of h are calculated using Equations (8) and (9), as shown in Tables 5 and 6. The value of the whole life premium decreases as the premium payment period lengthens, with $h = 20$ having the lowest premium value.

Table 5. Whole Life Premium

x	P_x
25	0,00522

Table 6. Premium payment over a period of h year

x	h	${}_hP_x$
25	5	0,01956
	10	0,01117
	20	0,00715

Before determining the premium reserves using the Canadian method, the prospective reserve value is also calculated for comparison using Equation (10). The reserves are calculated over a 10-year period, from $t = 0$ to $t = 10$. The results of the prospective reserves for various premium payment periods are shown in Table 7. Subsequently, the calculation of the value of β which is the modified premium, is carried out using Equation (11), as shown in Table 8. After obtaining the modified premium, the calculation of premium reserves using the Canadian method can be performed using Equation (12). The reserves are also calculated over a 10-year period, from $t = 0$ to $t = 10$.

Table 9 shows a decrease in premium reserve values as the premium payment period increases. In addition, the reserve value from the Canadian method is lower than the prospective method. The Canadian method uses a modified premium reserve, which is based on a modified premium β, as the foundation for reserve calculation. With higher premiums charged in the early years, the reserve during that period become smaller. Overall, the smaller reserve values under the Canadian method do not indicate that the method is less reliable, but rather reflect a different funding strategy in premium reserve formation.

Table 7. Prospective Premium Reserves

k	${}^{5}_{k}V_{25}$	${}^{10}_{k}V_{25}$	${}^{20}_{k}V_{25}$
0	0	0	0
1	0,01963	0,01075	0,00650
2	0,04036	0,02207	0,01332
3	0,06224	0,03400	0,02047
4	0,08535	0,04656	0,02799
5	0,10976	0,05980	0,03588
6	0,11484	0,07376	0,04418
7	0,12015	0,08848	0,05289
8	0,12570	0,10399	0,06204
9	0,13151	0,12034	0,07166
10	0,13759	0,13759	0,08176

Table 8. Modified premium

x	α	h	β
25	0,00697	5	0,02077
		10	0,01178
		20	0,00753

Table 9. Canadian Premium Reserves

k	${}_{k}^{5}V_{25}^{can}$	${}_{k}^{10}V_{25}^{can}$	${}_{k}^{20}V_{25}^{can}$
0	-0,00541	-0,00481	-0,00457
1	0,01518	0,00630	0,00205
2	0,03693	0,01801	0,00901
3	0,05989	0,03035	0,01631
4	0,08414	0,04335	0,02397
5	0,10976	0,05705	0,03202
6	0,11484	0,07150	0,04049
7	0,12015	0,08674	0,04938
8	0,12570	0,10279	0,05872
9	0,13151	0,11973	0,06853
10	0,13759	0,13759	0,07884

4 Conclusions

The findings demonstrate differences between the Canadian method and the Prospective method in calculating premium reserves for whole life insurance. Reserve values calculated using the Canadian method are lower than the Prospective method, primarily due to the modified premium structure. Additionally, the analysis indicates a decreasing trend in reserve values as the premium payment period increases. This reduction in reserve requirements implies advantageous for actuaries and policymakers aiming to promote affordability and broaden insurance coverage, but it requires careful risk management to maintain solvency.

Acknowledgements

I would like to extend my sincere gratitude to the Big Data Laboratory, Department of Mathematics, Hasanuddin University, for providing the academic environment and resources that facilitated the successful execution of this research. I am also deeply thankful to my beloved family, whose sincere prayers, unwavering support, encouragement, and wise advice have sustained me throughout this journey. Finally, I would like to acknowledge any individual or organization not explicitly mentioned here but who has contributed, directly or indirectly, to the successful completion of this research.

References

[1] B. J. Siregar, A. Saragih, H. Maryani, and A. Halim, "Aspek Hukum Terkait Dengan Perjanjian Asuransi Menurut Kitab Undang-Undang Hukum Perdata," *Jurnal Rectum: Tinjauan Yuridis Penanganan Tindak Pidana*, vol. 5, no. 3, p. 299, Aug. 2023, doi: 10.46930/jurnalrectum.v5i3.3641.

[2] H. Darmawi, *Manajemen Risiko*. 2022.

[3] W. H. Sadli, "Penentuan Cadangan Premi Asuransi Jiwa Dwiguna dengan Metode Zillmer dan Metode Illinois pada Kasus Joint Life," 2023.

[4] D. Badruzaman, "Perlindungan hukum tertanggung dalam pembayaran klaim asuransi jiwa," *Amwaluna: Jurnal Ekonomi dan Keuangan Syariah*, pp. 96–118, 2019.

[5] Darma Ekawati and Fardinah, "Penentuan Cadangan Premi Asuransi Jiwa Bersama Dwiguna dengan Metode Canadian," *Journal of Mathematics: Theory and Applications*, pp. 1–4, Aug. 2020, doi: 10.31605/jomta.v2i1.748.

[6] A. Olivieri and E. Pitacco, *Introduction to Insurance Mathematics*, Second Edition. Springer, 2015.

[7] D. P. Sari and D. Ekawati, "Cadangan Canadian Asuransi Jiwa Dwiguna dengan Penerapan Hukum Mortalitas De Moivre," *Journal of Mathematics: Theory and Applications*, pp. 35–39, 2022.

[8] F. Pasriyane Kele, T. Manurung, D. Tineke Salaki, K. Kunci, and A. Jiwa Semur Hidup Cadangan Premi Metode Canadian, "Penentuan Cadangan

Premi Asuransi Jiwa Seumur Hidup Menggunakan Metode Canadian." [Online]. Available: https://ejournal.unsrat.ac.id/index.php/decartesian

[9] F. S. Ibrahim, "Penentuan Cadangan Premi pada Asuransi Jiwa Berjangka Status Joint Life Menggunakan Metode Canadian," *Journal of Mathematics UNP*, vol. 7, no. 1, p. 19, Mar. 2022, doi: 10.24036/unpjomath.v7i1.10870.

[10] S. Fatimah, N. Satyahadewi, and S. Martha, "Penentuan Nilai Anuitas Jiwa Seumur Hidup Menggunakan Distribusi Gompertz," 2016.

[11] M. R. Oktavian, D. Devianto, and F. Yanuar, "Kajian Metode Zillmer, Full Preliminary Term, Dan Premium Sufficiency Dalam Menentukan Cadangan Premi Pada Asuransi Jiwa Dwiguna."

[12] "BI-Rate Tetap 5,75%: Mempertahankan Stabilitas, Mendukung Pertumbuhan Ekonomi." Bank Indonesia. https://www.bi.go.id/id/publikasi/ruang-media/news-release/Pages/sp_278425.aspx (accessed May 1st 2025)

[13] "Tabel Mortalitas dan Morbiditas Penduduk Indonesia Tahun 2023 dari BPJS Kesehatan". The Society of Actuaries of Indonesia. https://www.aktuaris.or.id/page/news_detail/251/tabel-mortalitas-dan-morbiditas-penduduk-indonesia-tahun-2023-dari-bpjs-kesehatan (accessed March 4th 2025)

[14] N. L. Bowers, H. U. Gerber, J. C. Hickman, D. A. Jones, and C. J. Nesbitt, *Actuarial Mathematics*, Second Edition. The Society of Actuaries, 1997.

[15] N. Hasnah, "Kajian Metode Commissioners, Illinois dan Canadian dalam Menentukan Cadangan Pada Asuransi Jiwa Dwiguna," *Jurnal Matematika UNAND*, vol. 4, no. 4, pp. 99–106, Jul. 2019, doi: 10.25077/jmu.4.4.99-106.2015.

IJASST International Journal of Applied Sciences and Smart Technologies

Volume 07
Issue 01

p-ISSN 2655-8564, e-ISSN 2685-943, pp. 181-192, 2025

A Green Pathway to Advanced Cobalt Oxide Materials: Dye Integration and Phytochemical Modification

Otah P. B[1, 2], C. I. Nworie[1, 2*], A. O. Ojobeagu[1, 4], A. O. Chikwendu[1, 3], Nwigwe G.C[1, 2], and Akande P. I[5]

[1]*Department of Industrial and Medical Physics, David Umahi Federal University of Health Sciences (DUFUHS), Uburu Ebonyi State, Nigeria*
[2]*International Institute for Machine Learning, Robotics & Artificial Intelligence Research, (DUFUHS) Ebonyi State, Nigeria*
[3]*International Institute of Oncology and Cancer Research, (DUFUHS) Ebonyi State, Nigeria*
[4]*International Institute for Infectious Disease, Biosafety and Biosecurity research, (DUFUHS) Ebonyi State, Nigeria*
[5]*Department of Industrial Physics, Ebonyi State University, Abakaliki, Nigeria*
[*]*Corresponding Author: nworieikechukwuc@gmail.com*

(Received 31-01-2025; Revised 09-03-2025; Accepted 15-03-2025)

Abstract

This study investigated the impact of natural dyes derived from three plant sources (Eupatorium odoratum, Ageratum conyzoides, and Pueraria phaseoloides) on the bandgap energies of cobalt oxide (CoO) thin films thin films were synthesized using a chemical bath deposition technique at 80-85°C and subsequently annealed at 100, 150, and 200 °C. The incorporation of these natural dyes significantly influenced the bandgap energies of the CoO films, with values ranging from 3.80 eV to 4.12 eV depending on the dye and annealing temperature with the as-grown films exhibiting bandgap energies ranging from 3.80 eV to 4.00 eV. Moderate heat treatment typically increased the bandgap of the films, but at higher temperatures, the behavior became more complex, with some dyes demonstrating a substantial reduction in bandgap. These findings demonstrate the potential of utilizing natural dyes to effectively tailor the electronic structure of CoO, offering a sustainable and eco-friendly approach to materials modification.

Keywords: Bandgap, chemical bath deposition, Cobalt oxide, natural dyes, phytochemicals

This work is licensed under a Creative Commons Attribution 4.0 International License

1 Introduction

Cobalt oxide (CoO) is a significant p-type semiconductor with direct optical band gaps ranging from 1.48 eV to 2.19 eV, making it a material of interest for applications in gas sensing, solar energy absorption, and environmental purification [1]. CoO thin films have also found extensive use in lithium-ion battery electrodes, catalysts, ceramic pigments, field-emission materials, and magnetic applications [2]. Its unique electronic and optical properties, coupled with its abundance and low cost, make it an attractive candidate for technological advancements. However, the intrinsic limitations of CoO, such as its relatively low conductivity and limited light absorption range, hinder its full potential.

For optoelectronic applications, a wide band gap is essential to achieve high transmittance in the visible and solar spectral ranges [3, 4]. Researchers have explored various strategies, including doping, nanostructuring, and composite formation to improve its quality. Doping these materials enhances their electrical conductivity, metallic properties, and infrared reflection capabilities for specific plasma wavelengths. Various metal oxides, including zinc, cadmium, tin, lead, and their alloys, are often doped with foreign elements to achieve these properties. Such doping improves chemical and mechanical stability, which is a key advantage for these semiconductors [5, 6]. In recent years, there has been growing interest in utilizing natural dyes as a sustainable and eco-friendly approach to modify the properties of semiconductor materials. Natural dyes, derived from plants, offer a rich source of organic compounds with diverse functional groups, which can interact with the semiconductor surface, leading to significant changes in its electronic and optical properties.

Traditional methods of producing cobalt oxide coatings, such as chemical vapor deposition and sputtering, are costly and require complex setups [7]. Conversely, chemical bath deposition offers a cost-effective and scalable alternative for producing high-quality, large-area metal oxide films suitable for solar control, decorative coatings, and optoelectronic applications [8, 9, 10, and 11] demonstrated the surface reactivity and structural stability of cobalt oxides, highlighting facile interconversion between CoO and Co_3O_4 and their ability to undergo hydroxylation under ultra-high vacuum conditions,

crucial for partial oxidation catalysis. [12] Studied CoO thin films deposited at varying pH levels, revealing that films with lower pH had high transmittance and potential for antireflection coatings, while those with higher pH exhibited properties suitable for solar cells and anti-dazzling applications.

This study investigated the impact of natural dye integration on the optical properties of CoO thin films, incorporating natural dyes extracted from *Eupatorium odoratum*, *Ageratum conyzoides*, and *Pueraria phaseoloides*, to enhance the light absorption properties of CoO and potentially tune its bandgap. This novel and green approach not only provides an environmentally friendly pathway but also offers a sustainable and cost-effective alternative to conventional methods of semiconductor modification.

2 Material and Methods

Fresh leaves of *Eupatorium Odorata*, *Ageratum Conyzoides*, and *Pueraria Tuberosa* were harvested and thoroughly washed. These were labeled as Dyes A, B, and C, respectively. Ten grams of each plant material were immersed in 100 mL of distilled water and extracted at 80-85°C for one hour. The resultant dye extracts were used for subsequent experiments. A reaction bath containing 10 mL of 0.2 M $CoCl_2$, 5 mL of thiourea, 20 mL of distilled water, and 0.4 mL of a specific dye extract was prepared for each film deposition. Thoroughly cleaned glass slides were vertically immersed in the respective bath and heated at 80-85°C for one hour. After deposition, the slides were rinsed with distilled water, air-dried, and annealed at 100°C, 150°C, and 200°C. The optical properties of the cobalt thin films were characterized using a spectrophotometer. The absorbance and transmittance data were used to calculate the optical absorption coefficient using Lambert's law [13]

3 Results and Discussions

Analysis of Phytochemical Content in Plant Leaf Extracts

The summary of the Phytochemical Contents of the dyes used is as presented in Fig. 1. The three plant species, *Eupatorium odoratum*, *Ageratum conyzoides*, and *Pueraria phaseoloides*, were found to contain a diverse range of phytochemicals. These

compounds are known for their potential biological activities, including antioxidant, anti-inflammatory, and antimicrobial properties capable of fighting bacteria [14].

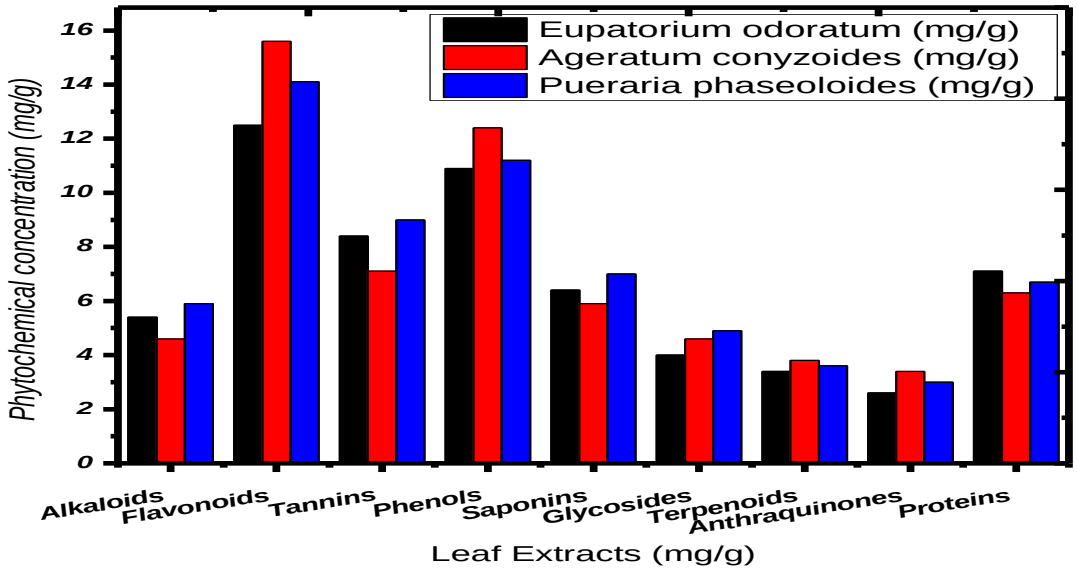

Figure 1. Comparative Chart of Phytochemical Composition in Plant Leaf Extracts

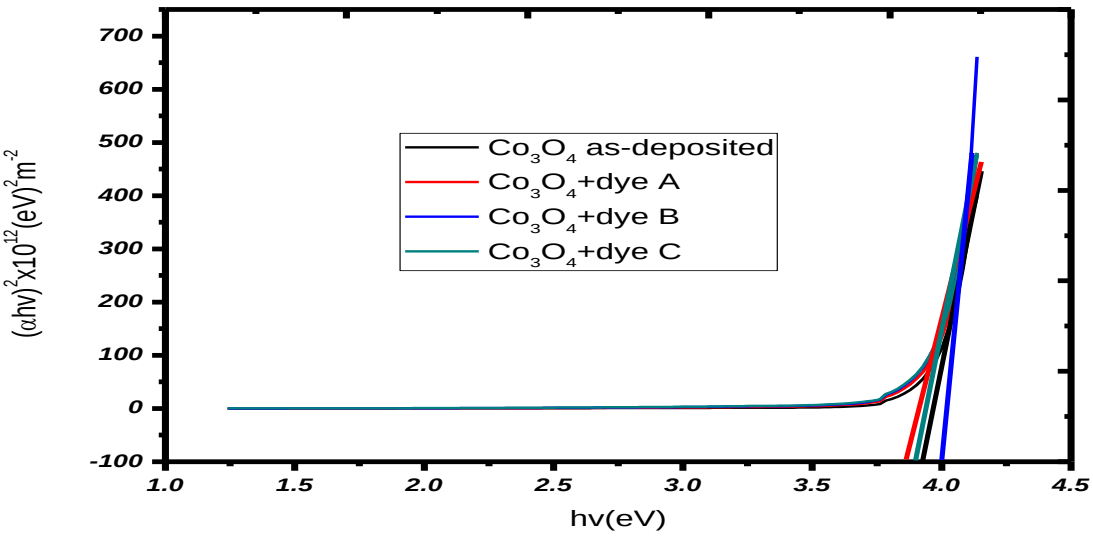

Figure 2. Plot of $(\alpha hv)^2$ Versus hv for As-grown and Dye Samples of CoO Thin Films

Fig. 1 reveals that all three plant species, Eupatorium odoratum, Ageratum conyzoides, and Pueraria phaseoloides, contain significant levels of flavonoids and phenols, both of which are known for their potent antioxidant properties [15]. Ageratum conyzoides exhibited the highest concentrations of both these compounds. Additionally, Pueraria phaseoloides was found to have the highest levels of tannins and alkaloids. Tannins are associated with astringent properties and antioxidant activity [16], while alkaloids are known for their diverse biological activities, including analgesic and anti-inflammatory effects [17]. The bandgap energies of the films with and without dye, annealed and unannealed are as displayed in Figs. 2 to 5. The band gap of the CoO thin films generally increased with increasing annealing temperature. This is in line with that obtained by [18, 19, and 20].

However, there are notable exceptions, particularly with CoO+dye B and CoO+dye C at higher temperatures (200°C). The presence of the dyes significantly impacts the band gap values compared to the as-deposited CoO film. Film CoO+dye A showed a decrease in band gap with increasing annealing temperature, suggesting a potential reduction in band gap due to the dye incorporation. This is trend to that obtained by [21] and indicates that annealing improves the films. Film CoO+dye B had an initial increase followed by a sharp decrease at 200°C.

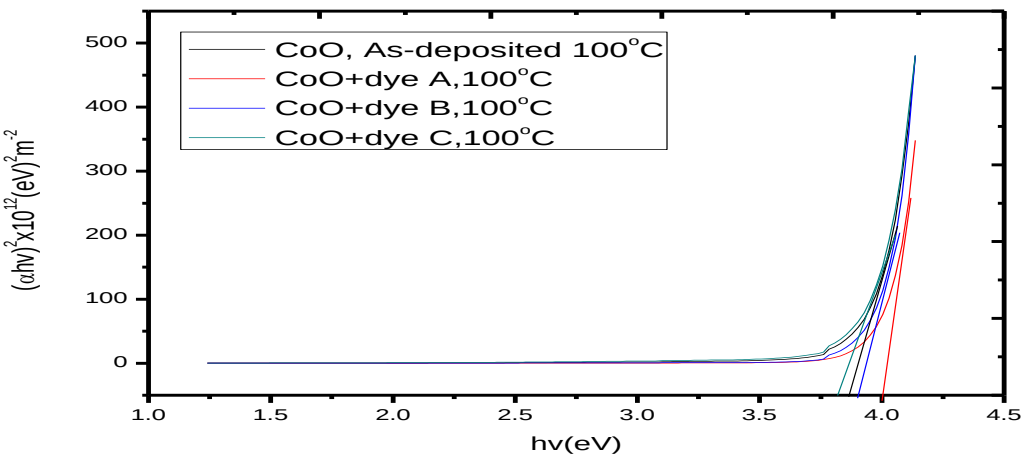

Figure 3. Plot of $(\alpha hv)^2$ versus hv for As-grown and Dye Samples of CoO Thin Films Annealed at 100^o

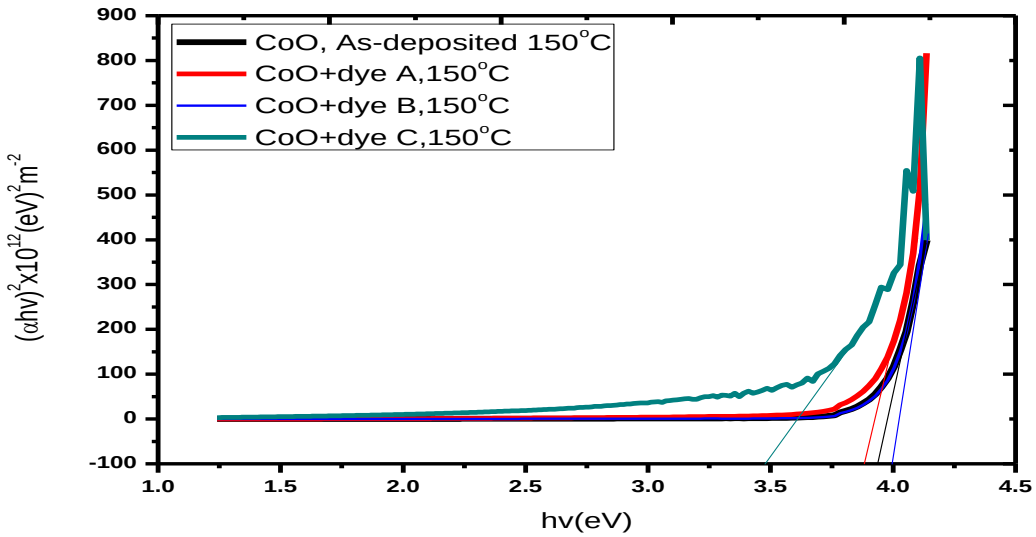

Figure 4. Plot of $(\alpha hv)^2$ versus hv for As-grown and Dye Samples of CoO Thin Films Annealed at 150ºC

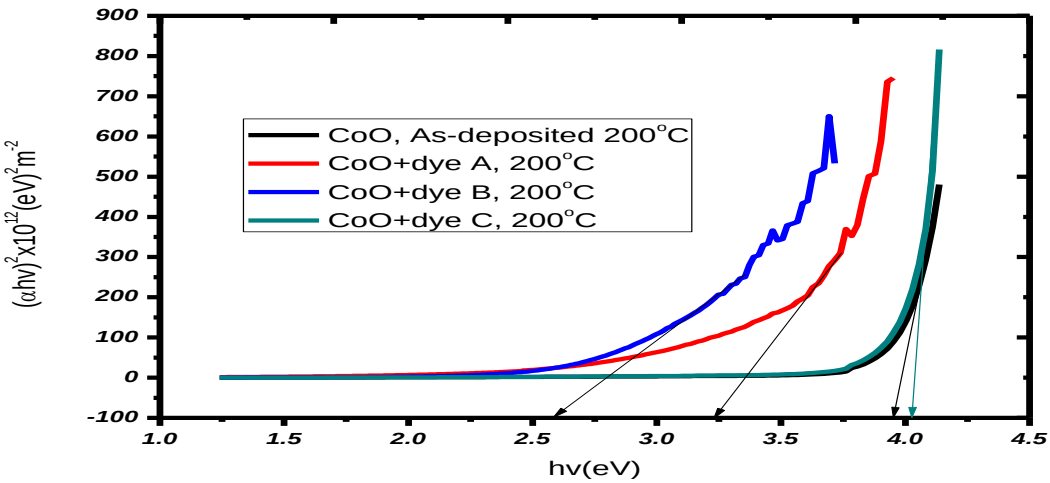

Figure 5. Plot of $(\alpha hv)^2$ versus hv for As-grown and Dye Samples of CoO Thin Films Annealed at 200ºC

For Film CoO+dye C, it was an initial slight increase followed by a significant decrease at 200°C. At room temperature in Fig. 2, Dye A exhibited the lowest band gap (3.80 eV), suggesting strong light absorption, while Dye B showed the highest (4.0 eV),

indicating weaker interaction with CoO. Dye C displayed an intermediate band gap (3.88 eV). Annealing at 100°C as displayed in figure 3 generally increased band gaps due to improved molecular order within the dye-CoO interface. However, higher temperatures (150–200°C) in Figs. 4 and 5 led to diverse responses, likely due to dye degradation or structural reorganization. Notably, Dye B exhibited a significant band gap narrowing to 2.60 eV at 200°C probably due to its high Phenols and tannins content functioning as primary photoreceptors [22], while Dye C's band gap increased to 4.12 eV, suggesting stabilization at elevated temperatures. The presence of tannins and saponins in the extracts, with their strong chelating and amphiphilic properties [23], facilitated strong dye-CoO interactions. Meanwhile, flavonoids and phenols contributed significantly to light absorption and charge transfer processes. These findings suggest that the developed dye-sensitized CoO composites hold promise for applications in solar cells, optoelectronics, and photocatalysis, where tunable optical properties are crucial.

4 Conclusions

This research explores a sustainable approach to enhancing cobalt oxide (CoO) materials by incorporating natural dyes extracted from three plant species. Using a solution growth technique, CoO thin films were successfully doped with these dyes. The study found that these plant-based dyes, rich in bioactive compounds, significantly influenced the optical properties of CoO, particularly the bandgap energy. While moderate heat treatment generally increased the bandgap, higher temperatures led to more complex behavior, with some dyes causing significant narrowing. These findings demonstrate the potential of utilizing natural dyes to tune the properties of CoO, opening promising avenues for the development of advanced CoO-based materials for applications such as solar cells and other optoelectronic devices.

For large-scale applications in mainstream optoelectronics and photovoltaics, further optimization and standardization of the materials and processes are essential. For niche applications where sustainability and cost-effectiveness are paramount, this method may be feasible on a smaller scale. Future research should focus on deeply understanding how dyes interact with CoO using techniques like FTIR, Raman spectroscopy, and XPS to identify chemical bonds and interactions between dyes and CoO, examining the CoO

film's microstructure and morphology changes due to dye incorporation and annealing using TEM and AFM

Acknowledgements

The authors wish to express their sincere thanks to those who supplied the materials used in this research.

Disclosure of Conflict of Interest:

The authors declare that they have no conflicts of interest.

Data Availability Statement:

The data used in this study are available upon reasonable request from the corresponding author.

Statement of informed consent:

All participants gave their informed consent.

References

[1]. Gulino, A., Dapporto, P., Rossi, P., & Fragalà, I. (2003). A novel self-generating liquid MOCVD precursor for Co3O4 thin films. *Chemistry of materials*, *15*(20), 3748-3752. https://pubs.acs.org/doi/full/10.1021/cm034305z

[2]. Jiang, J., & Li, L. (2007). Synthesis of sphere-like Co3O4 nanocrystals via a simple polyol route. *Materials Letters*, *61*(27), 4894-4896. https://doi.org/10.1016/j.matlet.2007.03.067

[3]. Woods-Robinson, R., Han, Y., Zhang, H., Ablekim, T., Khan, I., Persson, K. A., & Zakutayev, A. (2020). Wide band gap chalcogenide semiconductors. *Chemical reviews*, *120*(9), 4007-4055. https://pubs.acs.org/doi/abs/10.1021/acs.chemrev.9b00600

[4]. Shi, J., Zhang, J., Yang, L., Qu, M., Qi, D. C., & Zhang, K. H. (2021). Wide bandgap oxide semiconductors: from materials physics to optoelectronic devices. *Advanced materials*, *33*(50), 2006230. https://advanced.onlinelibrary.wiley.com/doi/abs/10.1002/adma.202006230

[5]. Scaccabarozzi, A. D., Basu, A., Aniés, F., Liu, J., Zapata-Arteaga, O., Warren, R., & Anthopoulos, T. D. (2021). Doping approaches for organic semiconductors. *Chemical Reviews*, *122*(4), 4420-4492. https://pubs.acs.org/doi/abs/10.1021/acs.chemrev.1c00581

[6]. Ele, U. S., Nworie, I. C., Ojobeagu, A. O., Otah, P. B., & Nwulegu, E. N. (2024). Influence of Magnesium Doping Concentrations and annealing on the Transmittance and Energy Band-gap of Sb2S3 Thin Films Deposited via Chemical Bath Deposition Technique. *Nigerian Journal of Physics*, *33*(1), 23-27. https://doi.org/10.62292/njp.v33i1.2024.185

[7]. Sathish, M., Radhika, N., & Saleh, B. (2023). Current status, challenges, and future prospects of thin film coating techniques and coating structures. *Journal of Bio-and Tribo-Corrosion*, *9*(2), 35. https://link.springer.com/article/10.1007/s40735-023-00754-9

[8]. Nnabuchi, M. N. (2005). Bandgap and optical properties of chemical bath deposited magnesium sulphide (MgS) thin films. *Pacific Journal of Science and*

Technology, *6*(2), 105-110. https://www.akamai.university/files/theme/AkamaiJournal/PJST6_2_105.pdf

[9]. Bhosale, C. H., Kambale, A. V., Kokate, A. V., & Rajpure, K. Y. (2005). Structural, optical and electrical properties of chemically sprayed CdO thin films. *Materials Science and Engineering: B*, *122*(1), 67-71. https://doi.org/10.1016/j.mseb.2005.04.015

[10]. Nworie, I. C., Ele, U. S., Otah, P. B., Ojobeagu, A. O., Mbamara, C., Brown, N. W., & Ishiwu, S. M. U. (2024). Interdependence of Deposition Time, Doping concentration, and annealing on the optical behavior of Mg-Doped Antimony Sulphide (Sb_2S_3) Thin Films. *The Journals of the Nigerian Association of Mathematical Physics*, *67*(2), 105-112. https://nampjournals.org.ng/index.php/home/article/view/386

[11]. Petitto, S. C., Marsh, E. M., Carson, G. A., & Langell, M. A. (2008). Cobalt oxide surface chemistry: The interaction of CoO (1 0 0), Co3O4 (1 1 0) and Co3O4 (1 1 1) with oxygen and water. *Journal of Molecular Catalysis A: Chemical*, *281*(1-2), 49-58. https://doi.org/10.1016/j.molcata.2007.08.023

[12]. Ilenikhena, P. A. (2008). Optical characterization and possible solar energy applications of improved solution grown cobalt oxide (CoO) thin films at 300K. *The African Review of Physics*, *2*(1). http://lamp.ictp.it/index.php/aphysrev/article/viewFile/91/42

[13]. Kalu, P. N., Onah, D. U., Agbo, P. E., Augustine, C., Chikwenze, R. A., Anyaegbunam, F. N. C., & Dike, C. O. (2018). The Influence of Deposition Time and annealing Temperature on the Optical Properties of Chemically Deposited Cerium Oxide (Ceo) Thin Film. *Journal of Ovonic Research Vol*, *14*(4), 293-305. https://openurl.ebsco.com/EPDB%3Agcd%3A12%3A25135036/detailv2?sid=ebsco%3Aplink%3Ascholar&id=ebsco%3Agcd%3A132977781&crl=c&link_origin=scholar.google.com

[14]. Zainullah, M., Setiana, M. D., Fatimah, V. N., Fitriana, I., & Kurniawan, R. (2024). Characterization The Flavonoids Extract of Tridax Procumbens l. Leaves and Betel Lime as Materials for Open Wound Analgesic Ointment. *International*

Journal of Applied Sciences and Smart Technologies, *6*(2), 229 240. https://ejournal.usd.ac.id/index.php/IJASST/article/view/7915

[15]. Kaurinovic, B., & Vastag, D. (2019). *Flavonoids and phenolic acids as potential natural antioxidants* (pp. 1-20). London, UK: IntechOpen. https://books.google.com.ng/books?hl=en&lr=&id=vHH8DwAAQBAJ&oi=fnd&pg=PA127&dq=flavonoids+and+phenols+are+known+for+their+potent+antioxidant+properties.+&ots=OO4ewUoWvq&sig=1RjZ7nOqhaBKsMJturKm68j2g_8&redir_esc=y&output=html_text

[16]. Soares, S., Brandão, E., Guerreiro, C., Soares, S., Mateus, N., & De Freitas, V. (2020). Tannins in food: Insights into the molecular perception of astringency and bitter taste. *Molecules*, *25*(11), 2590. https://www.mdpi.com/1420-3049/25/11/2590

[17]. Bai, R., Yao, C., Zhong, Z., Ge, J., Bai, Z., Ye, X., ... & Xie, Y. (2021). Discovery of natural anti-inflammatory alkaloids: Potential leads for the drug discovery for the treatment of inflammation. *European Journal of Medicinal Chemistry*, *213*, 113165. https://doi.org/10.1016/j.ejmech.2021.113165

[18]. Maity, R., & Chattopadhyay, K. K. (2006). Synthesis and characterization of aluminum-doped CdO thin films by sol–gel process. *Solar energy materials and solar cells*, *90*(5), 597-606. https://doi.org/10.1016/j.solmat.2005.05.001

[19]. Nnabuchi, M. N., & Augustine, C. (2018). Mn3O4/PbS thin films: preparation and effect of annealing temperature on some selected properties. *Materials Research Express*, *5*(3), 036414. https://iopscience.iop.org/article/10.1088/2053-1591/aab589/meta

[20]. Anyaegbunam, F. N. C., & Augustine, C. (2018). A study of optical band gap and associated urbach energy tail of chemically deposited metal oxides binary thin films. *Digest Journal of Nanomaterials and Biostructures*, *13*(3), 847-856. https://chalcogen.ro/847_AugustineC.pdf

[21]. Patil, V., Joshi, P., Chougule, M., & Sen, S. (2012). Synthesis and characterization of Co 3 O 4 thin film. *Soft Nanoscience Letters*, *2*(01), 1-7. https://doi.org/10.4236/snl.2012.21001

[22]. Christian, N. I., Ekuma, A. P., & Osondu, N. (2022). Phytochemical, Optical and FTIR Studies of ZnSe Thin Films for Solar Energy Applications. https://www.researchgate.net/publication/379285061_Phytochemical_Optical_and_FTIR_Studies_of_ZnSe_Thin_Films_for_Solar_Energy_Applications

[23]. Liu, Z., Li, Z., Zhong, H., Zeng, G., Liang, Y., Chen, M., ... & Shao, B. (2017). Recent advances in the environmental applications of biosurfactant saponins: a review. *Journal of environmental chemical engineering*, *5*(6), 6030-6038. https://doi.org/10.1016/j.jece.2017.11.021

IJASST International Journal of Applied Sciences and Smart Technologies

Volume 07
Issue 01

p-ISSN 2655-8564, e-ISSN 2685-943, pp. 193-206, 2025

The Effect of Flexible Resin and Standard Resins Mixtures Variations on Dimensional Accuracy Using SLA 3D Printing

Gilang Argya Dyaksa[1*], Felix Krisna Aji Nugraha[2], Achilleus Hermawan Astyanto[1,3], Stefan Mardikus[1], Michael Seen[1], Rines[1], Y.B. Lukiyanto[1], Doddy Purwadianto[1], Heryoga Winarbawa[1], Wibowo Kusbandono[1], Budi Sugiharto[1], Oktavianus Nekson Hermawan[1], Mahendra Pratama Putra[1]

[1,]*Department of Mechanical Engineering, Faculty of Science & Technology, Sanata Dharma University, Paingan Maguwoharjo Depok Sleman Yogyakarta, 55282, Indonesia*
[2]*Faculty of Vocational Mechatronics Engineering, Sanata Dharma Paingan Maguwoharjo Depok Sleman Yogyakarta, 55282, Indonesia*
[3]*Centre for Smart Technology Studies, Universitas Sanata Dharma Kampus III USD Maguwoharjo, Sleman, DI Yogyakarta, 55282, Indonesia*
[*]*Corresponding Author: gilangad@dosen.usd.ac.id*

(Received 06-05-2025; Revised 13-05-2025; Accepted 15-05-2025)

Abstract

The present study investigates the effect of the concentration of flexible resin on the dimensional accuracy of mixtures product manufactured by 3D printing using SLA technology. Specimens were designed and according to the ASTM D412 standard. Ten variations of resin mixtures were examined. The concentrations of the flexible resins were varied from 10% to 100%. Measurements of accuracy dimension were conducted on the fabricated specimens, and the average deviation was used to estimate the dimensional accuracy. The study reveals the least deviation in dimensions in the 10% flexible resin containing mixture and the highest in the 60% flexible resin containing mixture. The results explain the fabrication tendency of flexible resins in dimensional accuracy for 3D printing.

Keywords: Dimensional accuracy, Flexible resin, SLA

This work is licensed under a Creative Commons Attribution 4.0 International License

1 Introduction

Rapid prototyping or also known as 3D Printing is a method of rapidly creating three-dimensional objects from digital data, which is different from conventional manufacturing. If conventional manufacturing uses the subtractive principle by cutting material, rapid prototyping works with the additive principle, adding material layer by layer [1]. A three-dimensional (3D) printing technology has both undergone a rapid development in recent years, and been widely used in various fields such as manufacturing [2], medical [3], as well as education [4]. Furthermore, since various materials are now available to meet specific needs in industries, a flexible resin is of large interest in 3D printing. Here, the flexible resin has a partial characteristic of an elastomer in which its high elongation offers the ability to be bent or stretched without being easily broken. Therefore, the flexible resin can be utilized in many applications such as prototypes, functional objects, and components that require a high elasticity. Hence, if the products of flexible resin 3D printing are used as functional objects, then the required aspect is not only the elongation but also its dimensional accuracy [5]. As a result, the dimensional accuracy is then a major challenge in the application of flexible resins since it has not widely been discussed on various reference of 3D printing.

The dimensional accuracy is important during manufacturing to assess the level of precision of an object [6]. Herein, a dimensional deviation may cause the product to be malfunction or not function optimally in high-precision manufacturing [7] especially in industries that require very high tolerances such as automotive, medical device, and aerospace [8]. In 3D printing using stereolithographic (SLA) technology, the dimensional accuracy is affected by many factors such as the printing parameters [9], curing process [10], and the properties of the material [11] The flexible resins, with their high elasticity properties, have the challenge of maintaining dimensional accuracy after the molding process. Therefore, it is important to conduct a dimensional accuracy testing on the product of flexible resin 3D printing to ensure the quality of products.

This present study experimentally investigates the effect of the concentration of a flexible resin on the dimensional accuracy of the mixture produced using SLA 3D printer. The results provide more in-depth insights into the limitations and potential uses of

flexible resins in various industrial applications, as well as an overview of flexible resin 3D printing with optimal concentration of the flexible resin to achieve accurate and precise printing products.

2 Material and Methods

The methodology carried out in the present work includes the process 3D model designs using computer aided design (CAD) software, variations in the composition of resin mixtures, printing processes, and geometrical measurements of the specimens to evaluate the level of dimensional accuracy. Here, the geometry of specimen was designed following the ASTM D412 standard for tensile testing on thermoplastic elastomer materials [11]. The geometry and dimensions of the selected specimen is depicted in Fig 1. The specimen was designed using a computer software namely Solid Edge Community Edition computer-aided design. For dimensional accuracy measurement, the specimen has a total length of 115 mm (L-115), a total width of 25 mm (W-25), and a thickness of 3 mm (T-3). The position of the printed specimen at the time of resin printing is used to identify the movement of the nozzle and table during the printing process.

The resin used in this study uses resins that are already available in stores and online marketplaces to consider their availability. Standard resins use anycubic standard resins and flexible resins use Esun eResin–Flex. The physical and mechanical properties for both resins can be seen in Table 1.

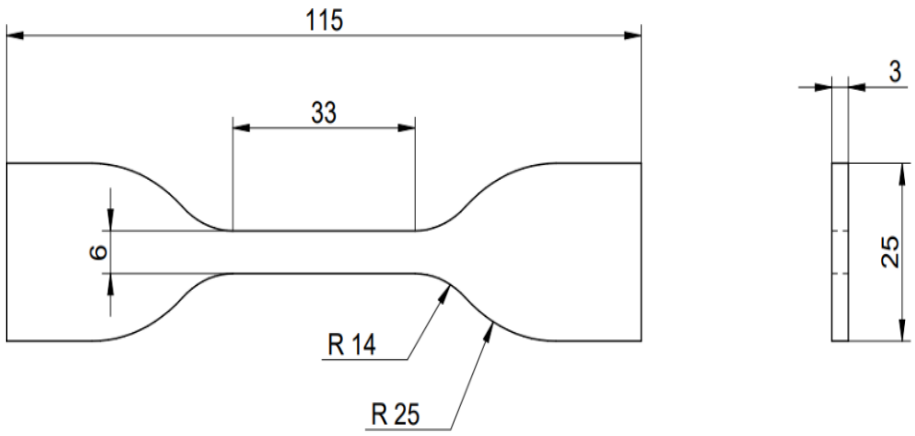

Figure 1. ASTM D412 standard specimen geometry (units in millimeters).

In this study, testing was conducted on specimens with 10 variations of a mixture of flexible resin and standard resin, which was marked with RF notation followed by a number indicating the percentage of flexible resin content in the mixture. Resin mix variations range from RF10 to RF100, with RF10 containing 10% flexible resin and RF100 being a pure flexible resin. Each variation was printed with 3 specimens, so that the total number of specimens printed was 30 pieces [12]. The concentration of the mixture of flexible resin and standard resin in each specimen can be seen in Table 2.

Tabel 1. Physical properties of standard and flexible resins used in research.

Parameter	Esun eResin-Flex	Anycubic Resin Standard
Viscosity (mPa.s)	600 – 1400	150 – 200
Density (g/cm3)	1.02 – 1.05	1.05 – 1.25
Tensile Strength (MPa)	4 – 10	36 – 45
Elongation (%)	100 – 350	8 – 12
Hardness (D)	60 – 90	82
Flexural strength (MPa)	-	50 – 65

Table 2. Concentration of a standard and flexible resin mixture on the specimen.

Specimen Notation	Standard resin (%)	Flexible resin (%)
RF10	90	10
RF20	80	20
RF30	70	30
RF40	60	40
RF50	50	50
RF60	40	60
RF70	30	70
RF80	20	80
RF90	10	90
RF100	0	100

The specimen was printed using an SLA technology machine, namely Anycubic Photon Mono X with specifications that can be seen in Table 3. Specimens were printed in a total of 3 for each variation of the mixture, so that the total number of specimens printed was 30 specimens. All specimens of flexible resin mixture variations and standard resins are printed using the same printing parameters to ensure consistency in the printing process. This is done so that the difference in dimensional accuracy produced is only influenced by variations in resin composition, not by differences in printing parameter settings. The printing parameters can be seen in Table 4.

Table 3. Specification of Anycubic Mono Photon X printer machine.

Specifications	Dimension	Unit
Machine Size	270 × 290 × 475	mm
Bed Size	192 × 120 × 245	mm
Lightsource	High quality filament (wavelength 405 nm)	
XY Resolution	0.050 (3840 × 2400)	mm
Z Resolution	0.01	mm
Layer Resolution	0.01 – 0.15	mm
Print speed	Max 60	mm/h
Material	405 (UV Resin)	nm
Technology	LCD-Based SLA	

Table 4. Specimen printing parameters.

Parameter	Value	Unit
Exposure Time	10	s
Bottom Layer Count	5	layer
Bottom Exposure Time	55	s
Lifting Distance	10	mm
Lift Speed	50	mm/min
Retract Speed	100	mm/min

The printing parameters of the specimens were set up using Chitubox software as shown in Fig. 2. The tilt position for the workpiece specimen is 450 with a dimension of length 115 with the resultant of the X axis and the Y axis, the width dimension is the resultant of the Y axis and the Z axis. The selection of printing parameters in Table 4 is a recommendation for printing parameters from the material supplier. In this study, we tried to print the recommended parameters to find out the results of the dimensional accuracy. The results of this study will be our preliminary data for further research if needed for optimization of dimensional accuracy results using flexible resins.

For the dimensional accuracy a measurement of L-115, W-25, T-3 utilized a Mitutoyo 505-730 dial caliper with a measurement range of 0-150 mm and an accuracy level of 0.02 mm. The data from each specimen are tabulated in a table showing the measurement results for each dimension as well as deviations from the initial design dimensions. The dimensional accuracy was analyzed by calculating the mean deviation. The analysis was performed to compare the variations of flexible resins to identify the trend line between the flexible resin mixture and the standard resin on the dimensional accuracy of the specimens.

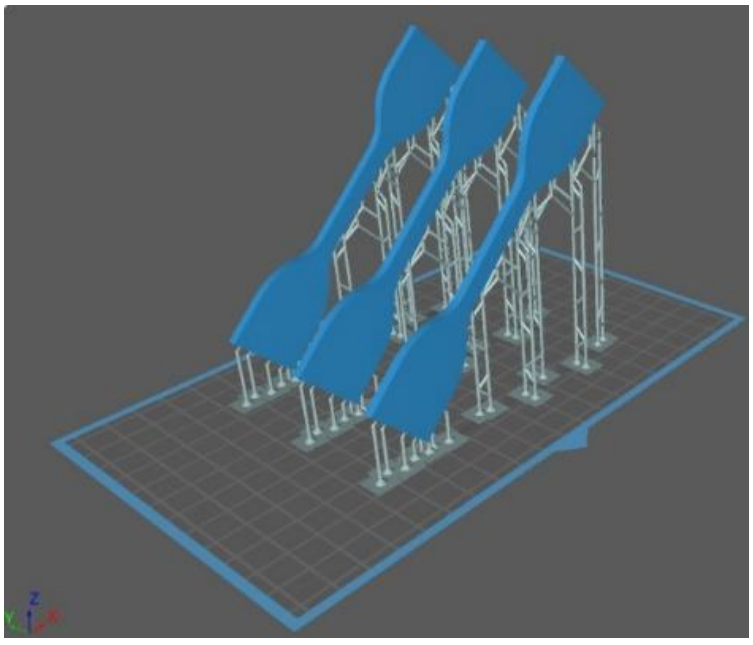

Figure 2. Position of workpiece specimens in Chitubox software.

3 Results and Discussions

The printed specimens are seen in Fig. 3. The test specimen of the print result is visible in comparison with the dimensions of the CAD design. On each dimension of the test specimen is measured at three points. From the three measurements on each of the dimensions, the average dimension was obtained and listed in Table 5.

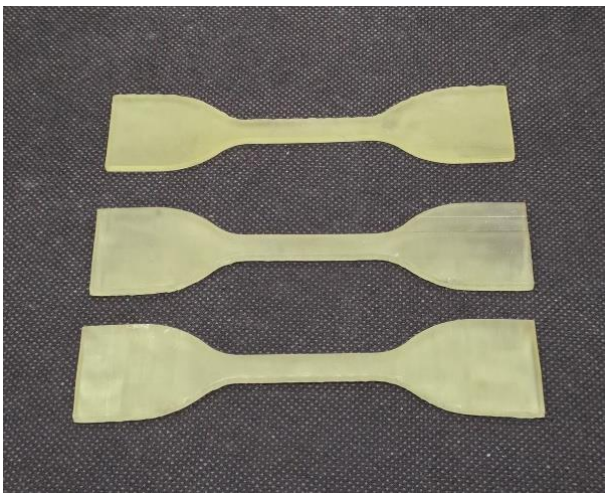

Figure 3. Test specimen prints.

Table 5. Average dimensions of the test specimen.

Specimen Notation	Dimension 3	Dimension 25	Dimension 115
RF 10	3.25	25.12	115.26
RF 20	3.44	25.30	115.70
RF 30	3.34	25.19	115.45
RF 40	3.43	25.36	115.81
RF 50	3.39	25.24	115.71
RF 60	3.38	25.39	119.26
RF 70	3.46	25.54	116.66
RF 80	3.37	25.22	116.48
RF 90	3.45	26.04	116.66
RF 100	3.63	25.23	116.79

Fig. 4 depicts the dimensional accuracy of L-115. From the results of the measured dimensions of the printed specimens, it can be seen that in each dimension deviations from the desired dimensions. The actual dimensions of the printed specimen and the tolerance amount according to the ISO with the medium can be seen in the following graph, at the Length 115 mm the medium general tolerance of ±0.3 mm is used to give the corresponding range of printed specimen dimensions. From the results of the specimen printing on the material composition, RF 10 enters the good dimensions. The largest deviation in the composition of RF 60 is 4.6 mm.

In the dimensional accuracy of W-25, there are two material compositions that are still within the tolerance of the specified dimensions there are RF 10 and RF 30 as shown in Fig. 5. The largest deviation is 1.04 mm of RF 90 composition.

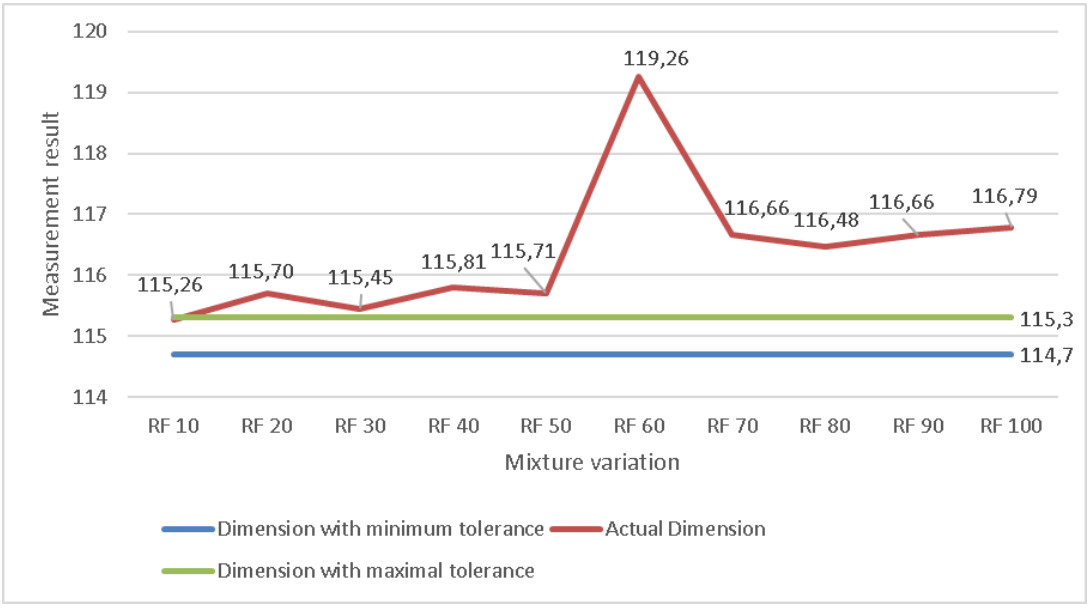

Figure 4. Dimensional accuracy test results of L-115.

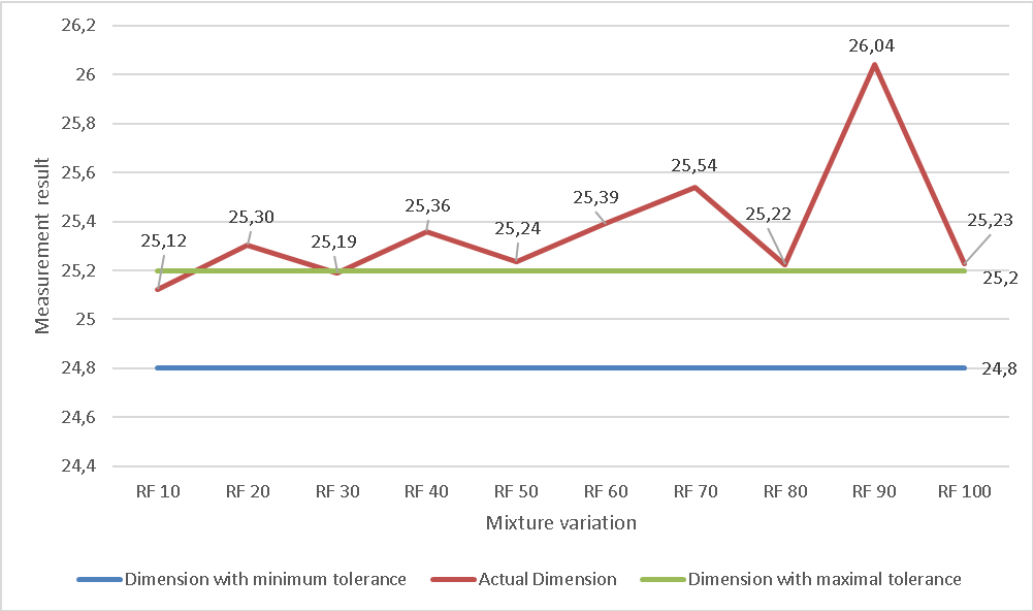

Figure 5. Dimensional accuracy test results of W-25.

Fig. 6 depicts the dimensional accuracy of L-3. From the figure it is revealed that all material compositions cannot meet the expected dimensions or fall within the predetermined tolerances. In this composition the smallest deviation is 0.24 mm and the largest deviation is 0.63 mm.

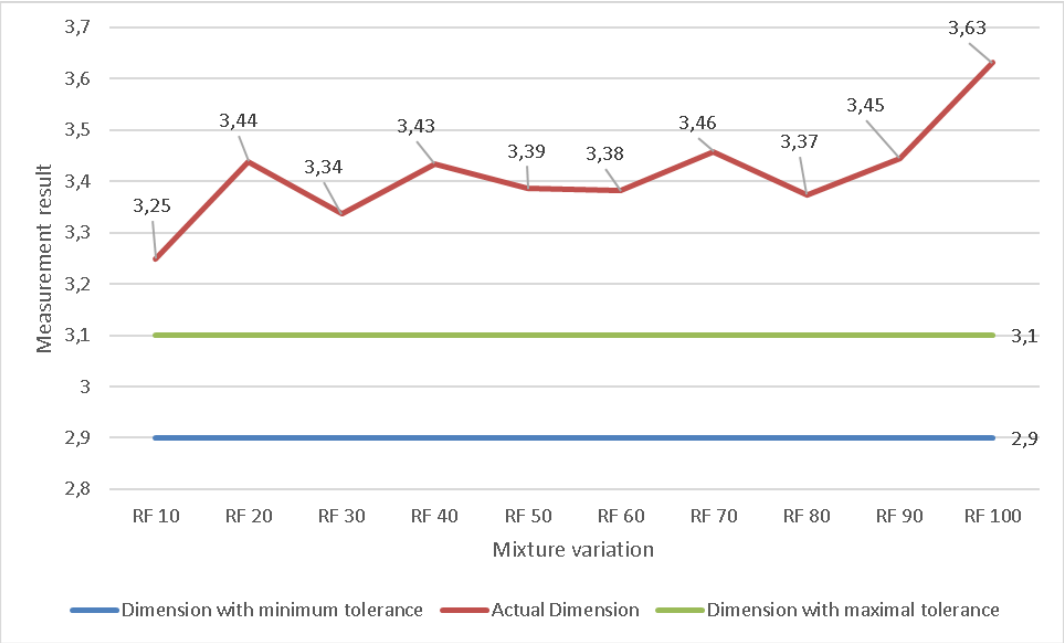

Figure 6. Dimensional accuracy test results of T-3.

Moreover, from Table 6, it can be seen the deviation of each variation of RF 10 to RF 100 for L-115, W-25, and T-3. From the rightmost column, the average deviation of the three dimensions measured is obtained. The deviation of the specimen ranges from the 0.211 mm to 1.678 mm. The smallest deviation was found in the RF 10 specimen and the largest deviation was found in RF 60. Here, RF 10 has a small deviation due to the low elasticity properties of only 10% of the flexible resin mixture, thus making the RF 10 specimen have a fairly good dimensional accuracy [13] [14].

The range of RF 10 to RF 50 has a maximum deviation value at RF 40 which is 0.535 mm. The RF 50 has an average deviation of 0.443 mm, which means that even if the mixture between flexible resin and standard resin has the same amount, it still cannot produce a deviation that is within the general tolerance.

Table 6. Average dimensions of the test specimen.

Specimen Notation	Dimension 115 (mm)	Dimension 25 (mm)	Dimension 3 (mm)	Average of Deviations (mm)
RF 10	0.262	0.123	0.249	0.211
RF 20	0.697	0.304	0.439	0.480
RF 30	0.452	0.191	0.337	0.327
RF 40	0.810	0.360	0.434	0.535
RF 50	0.706	0.237	0.386	0.443
RF 60	4.262	0.391	0.381	1.678
RF 70	1.661	0.540	0.458	0.886
RF 80	1.476	0.223	0.374	0.691
RF 90	1.661	1.041	0.446	1.049
RF 100	1.786	0.227	0.631	0.881

4 Conclusions

The process of printing product specimens has dimensional deviations. At each dimension, the smallest deviation occurs in the material composition of RF 10. As for the largest deviation in each, each test dimension differs in its material composition. The smallest deviation occurred in the composition of RF 10 of 0.211 mm, while the mean of the largest deviation in the composition of RF 60 was 1.678 mm. The machine parameters in the printing process in this study have not been the composition of the parameters. In order to have a more comprehensive picture of the influence of printing parameters on flexible resin materials, further research is needed to produce flexible resins that are more precise but do not reduce their elasticity.

Acknowledgements

The author would like to express a deepest gratitude to The Institute for Research and Community Service (LPPM) of Sanata Dharma University has provided research funds so that this research can be carried out, along with assistance from the beginning to the end of the research. Also thanks to Mr. Martono Dwiyaning Nugroho for the technical assistances during this study. We also appreciate the valuable 3D printing technology support from Garasi 3D Print. In addition, the author would also like to acknowledge both Mechanical Engineering and Vocational Mechatronics Department lecturers for their constructive discussions and inputs that have enriched our understanding in this study.

References

[1] F. K. A. Nugraha, "Shrinkage of Biocomposite Material Specimens [HA/Bioplastic/Serisin] Printed using a 3D Printer using the Taguchi Method," *International Journal of Applied Sciences and Smart Technologies*, vol. 4, no. 1, pp. 89–96, 2022, doi: https://doi.org/10.24071/ijasst.v4i1.4205.

[2] G. T. Mark, "Footwear fabrication by composite filament 3D printing," *US Patent 10,226,103*, no. Query date: 2023-07-13 11:40:45, 2019, [Online]. Available: https://patents.google.com/patent/US10226103B2/en

[3] J. Garcia, Z. L. Yang, R. Mongrain, R. L. Leask, and K. Lachapelle, "3D printing materials and their use in medical education: A review of current technology and

trends for the future," *BMJ Simul Technol Enhanc Learn*, vol. 4, no. 1, pp. 27–40, 2018, doi: 10.1136/bmjstel-2017-000234.

[4] Z. Shen *et al.*, "The process of 3D printed skull models for anatomy education," *Computer Assisted Surgery*, pp. 1–14, 2019, doi: 10.1080/24699322.2018.1560101.

[5] D. Andriyansyah, A. Jamaldi, I. Taufik, P. Studi Teknik Mesin, and A. Teknologi Warga Surakarta, "Evaluasi Akurasi Dimensi Pada Objek Hasil 3D Printing," Magelang, Mar. 2021. Accessed: Sep. 26, 2024. [Online]. Available: https://jurnal.untidar.ac.id/index.php/mechanical/index

[6] M. Lestari, Subkhan, and Pritiansyah, "Pengaruh Parameter Proses 3D Printing Terhadap Akurasi Dimensi Filament PETG (Polyethylene terephthalate Gylacol)," Bangka Belitung, Aug. 2021.

[7] A. Ahmed, A. Majeed, Z. Atta, and G. Jia, "Dimensional quality and distortion analysis of thin-walled alloy parts of AlSi10Mg manufactured by selective laser melting," *Journal of Manufacturing and Materials Processing*, vol. 3, no. 2, Jun. 2019, doi: 10.3390/jmmp3020051.

[8] S. Gruber *et al.*, "Comparison of dimensional accuracy and tolerances of powder bed based and nozzle based additive manufacturing processes," *J Laser Appl*, vol. 32, no. 3, Aug. 2020, doi: 10.2351/7.0000115.

[9] A. Komjaty, E. S. Wisznovszky (Muncut), and L. I. Culda, "Study on the influence of technological parameters on 3D printing with sla technology," *MATEC Web of Conferences*, vol. 343, p. 01003, 2021, doi: 10.1051/matecconf/202134301003.

[10] Y. S. Zeng, M. H. Hsueh, and T. C. Hsiao, "Effect of ultraviolet post-curing, laser power, and layer thickness on the mechanical properties of acrylate used in stereolithography 3D printing," *Mater Res Express*, vol. 10, no. 2, Feb. 2023, doi: 10.1088/2053-1591/acb751.

[11] A. C. Uzcategui, A. Muralidharan, V. L. Ferguson, S. J. Bryant, and R. R. McLeod, "Understanding and Improving Mechanical Properties in 3D printed Parts Using a Dual-Cure Acrylate-Based Resin for Stereolithography," *Adv Eng Mater*, vol. 20, no. 12, Dec. 2018, doi: 10.1002/adem.201800876.

[12] T. Appalsamy, S. L. Hamilton, and M. J. Kgaphola, "Tensile Test Analysis of 3D Printed Specimens with Varying Print Orientation and Infill Density," *Journal of Composites Science*, vol. 8, no. 4, Apr. 2024, doi: 10.3390/jcs8040121.

[13] N. Majca-Nowak and P. Pyrzanowski, "The Analysis of Mechanical Properties and Geometric Accuracy in Specimens Printed in Material Jetting Technology," *Materials*, vol. 16, no. 8, Apr. 2023, doi: 10.3390/ma16083014.

[14] C. Savin, M.-E. Antohe, A. Balan, A. Sirghe, and L. Gavrila, “Study Regarding the Elastic Impression Biomaterials Dimensional Stability,” Bucharest, 2019. [Online]. Available: http://www.revistadechimie.ro797

This page intentionally left

IJASST International Journal of Applied Sciences and Smart Technologies

Volume 07
Issue 01

p-ISSN 2655-8564, e-ISSN 2685-943, pp. 207-218, 2025

Topology Optimization of Rear Sprocket of Electric Prototype Vehicle

Heryoga Winarbawa[1, *]

[1]*Departement of Mechanical Engineering, Faculty of Science and Technology, Sanata Dharma University, Yogyakarta, Indonesia*
[*]*Corresponding Author: heryoga@usd.ac.id*

(Received 15-05-2025; Revised 22-05-2025; Accepted 23-05-2025)

Abstract

Kompetisi Mobil Hemat Energi (KMHE) competes for energy efficient vehicles, which are composed of integrated energy-saving systems. One of the systems that is required to be energy efficient is transmission. The transmission discussed in this study is the sprocket chain transmission system. The rear sprocket is an object that needs to be optimized to obtain a lighter mass, thus efficient in terms of overall weight. Using topology optimization via CAD software, rear sprocket mass can be reduced. The results of topology optimization are used as a reference for changing the shape of the sprocket face, to make it easier in terms of fabrication. These results were then re-tested with static simulations to ensure its strength. The conclusion is that the latest sprocket design has a mass reduction of 66% of its original version and the von Misses stress was only 55% of the yield strength at most.

Keywords: KMHE, sprocket, topology optimization

1 Introduction

The increasing number of motorized vehicles in urban areas has become a major contributor to exhaust emissions that have a negative impact on air quality and public health. Emissions from fossil fuels used by vehicles produce pollutants such as carbon monoxide (CO), nitrogen oxides (NOx), and particulates (PM), which contribute to global warming and respiratory diseases. Although vehicle technology is increasingly developing, the rate of vehicle growth still exceeds the capabilities of emission control systems. Therefore, there needs to be stricter policies and the development of environmentally friendly fuels and technologies to reduce these emissions.

This work is licensed under a Creative Commons Attribution 4.0 International License

The impact analysis of electric vehicle use in the road transportation sector is used to evaluate energy demand and CO_2 emissions in Indonesia [1]. Using the Modified Mobility Model (MoMo) and PUCE method, this study projects that by 2040, a moderate electric vehicle adoption scenario can reduce energy consumption by 6% and CO_2 emissions by 4.8%. Meanwhile, a high adoption scenario shows a potential reduction in energy consumption by 14% and CO_2 emissions by 8.8%. These findings emphasize that increasing the adoption of electric vehicles can contribute significantly to reducing greenhouse gas emissions in the Indonesian transportation sector.

Kompetisi Mobil Hemat Energi (KMHE) is a vehicle competition focusing on energy saving in Indonesia. This competition is a response to issues related to the decreasing availability of energy [2]. KMHE tests the ability of a group of students to design a vehicle that uses as little energy as possible. Students are asked to design and build energy-efficient vehicles that comply with KMHE regulations. Vehicles must be designed as light as possible to achieve the most efficient energy consumption. The use of carbon fiber and aluminum is widespread in this competition vehicle.

The use of static simulation with CAD software provides significant benefits in the engineering design and analysis process. With this simulation, designers can evaluate the strength and resistance of a component to static loads before a physical prototype is made. This not only saves time and production costs but also minimizes the risk of design errors. In addition, CAD simulation allows visualization of stress distribution and deformation, so that design improvements can be made more precisely. As in the study related to the design of a prototype vehicle chassis with CAD software, it was found that the maximum deformation was 2.5 mm [3]. The chassis was then fabricated and tested with the same load, but no deformation was visually found. The topology optimization feature in CAD software also supports material efficiency by producing a lightweight but strong structural shape based on the results of the load analysis. Therefore, the integration of static simulation in the design process is very important to produce safe, efficient and reliable products.

Apart from materials which are the main factor in reducing vehicle weight, the application of topology optimization can be used to reduce the weight of vehicle components further. Topology optimization is a method that distributes initial mass in

each 3D space to create the best possible shape for mechanical construction. It gives efficient geometry by concentrating on material volume. Topology optimization has been proven to reduce the weight of electric motor high-speed stator to 20.2% [4], motorcycle engine cover to 16% [5], 125 cc sport bike rear sprocket to 27% [6], Formula Student car front upright to 60.43% [7], steering shaft support bracket to 34,25% [8], and motorcycle swingarm to 30% [9].

One of the crucial parts of this vehicle is the transmission system. The use of chain and sprocket transmission systems is intended to achieve high power transfer efficiency. Under correct lubrication and installation conditions, the chain drive's mechanical efficiency was 98,4 – 98,9 % [10].

With optimization topology, reducing the mass of a component can reduce the total mass of the vehicle, with the aim of increasing fuel efficiency. In a study, increasing the battery capacity from 10.5 kWh to 21 kWh caused an increase in vehicle weight of 125 kg. This resulted in an increase in energy use of 5.8% [11]. Based on the results of this study, it is necessary to reduce weight through topology optimization of the rear sprocket of the electric prototype vehicle

2 Material and Methods

The rear sprocket, which is the subject of the research, is designed to accommodate the RS-35 chain. The steps in this research can be shown in Figure 1. The first step is to create a 3D model of the 92 teeth rear sprocket via CAD software, SolidWorks. Aluminum 7075-T6 mechanical properties (Table 1) were added to the model. Aluminum 7075-T6 was chosen because it is widely used as a sprocket for motorbikes, go-karts, and all-terrain vehicles. The sprocket model is then subjected to topology optimization inside SolidWorks. The results of the topology optimization are then exported into a separate file. At the re-design phase, the results of both the default and the topology optimization of the rear sprocket model are compared. The default rear sprocket model was then redesigned by tracing the hollow parts from the results of the topology optimization model. The redesigned default model is saved as a lightweight version. This lightweight version is then subjected to static simulation to ensure its safety. Both forces that act on

each sprocket tooth for topology optimization and static simulation are generated from the torque of the 500-Watt DC motor that that drives this vehicle.

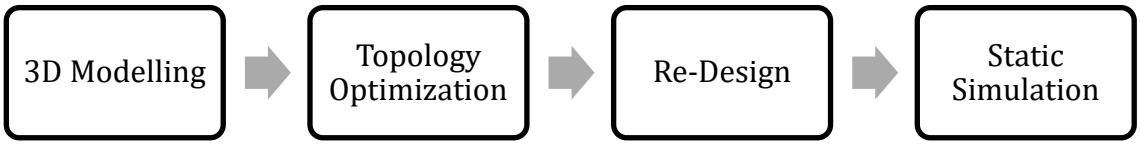

Figure 1. Lightweighting rear sprocket process

Table 1. Mechanical properties of aluminum 7075-T6

Mechanical properties	Value
Elastic Modulus (N/m^2)	7.19×10^{10}
Poisson's Ratio	0.33
Tensile Strength (N/m^2)	5.7×10^{8}
Yield Strength (N/m^2)	5.05×10^{8}

3 Results and Discussions

3.1. 3D Modelling

Through the SolidWorks Toolbox add-in, a model of the 92-tooth RS35 rear sprocket can be created, by entering the options as shown in **Figure 2**a. Next, the model can be edited to add features such as 6 – Ø6 mm holes equally spaced in Ø92 mm PCD, and a bore diameter of 88 mm to match the rear wheel hub, as shown in **Figure 2**b.

3.2. Topology Optimization

3.2.1. Force of each sprocket tooth

The force acting on each sprocket tooth is caused by the tension, F. The tension F is a combination of effective circumferential force, F_1; the centrifugal force tension, F_e; and the sag of the loose side tension, F_f.

A. Effective Circumferential Force, F_1

It is known that the torque of the 500-Watt DC motor is 0.5 N.m, and the diameter of the rear sprocket is 0.56 m, thus F_1 can be calculated using the following formula.

$$F_1 = \frac{M_2}{r_1} = \frac{M_1}{r_2} \quad \textbf{(1)}$$

where,

F_1 : effective circumferential force (N)

M_1 : motor sprocket torque (N.m)

M_2 : rear sprocket torque (N.m)

r_1 : motor sprocket radius (m)

r_2 : rear sprocket radius (m)

Thus,

$$F_1 = \frac{M_1}{r_2}$$

$$= \frac{0.55}{0.28} = 1.96\ N$$

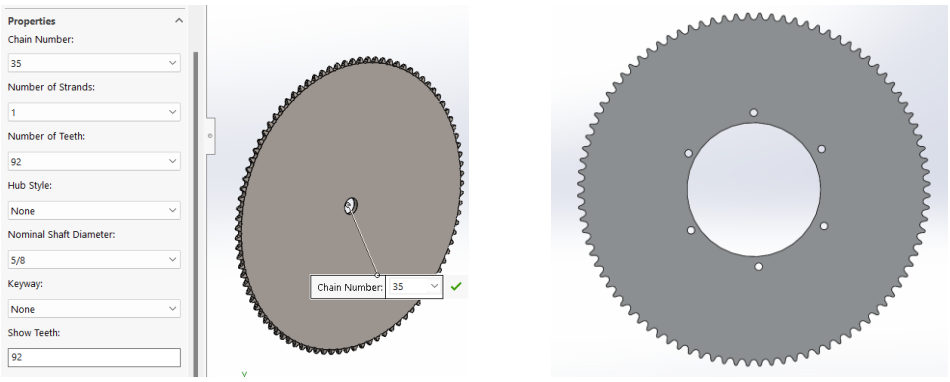

(a) **(b)**

Figure 2. Rear sprocket modeling

B. Centrifugal Force Tension, F_e

Using RS35 chain pitch, 9.525 mm; 10 teeth motor sprocket, weight per meter, 0.33 kg; and the 500-Watt DC motor could reach 10000 RPM, centrifugal force tension F_e can be calculated as follows:

$$v = \frac{p \times N \times n}{60 \times 1000} \quad \textbf{(2)}$$

$$F_e = q \times v^2 \quad \textbf{(3)}$$

where,

v : chain speed (m/s)

p : chain pitch (mm)

N : number of teeth of motor sprocket

n : rotational speed of motor (RPM)

F_e : centrifugal force tension (N)

q : chain weight per meter (kg)

Thus,

$$v = \frac{9.525 \times 10 \times 10000}{60 \times 1000} = 15.87\, m/s$$

$$F_e = 0.33 \times (19.05)^2 = 83.11\, N$$

C. Sag of The Loose Side Tension, F_f

The design of the chain sprocket is required to be slightly loose. The lower part is made a little loose when the chain transmits power. This looseness also creates a force, which can be calculated by

$$F_f = g \times K_f \times q \times a \quad (4)$$

where,

F_f : sag of the loose side tension (N)

g : gravitational force (m/s^2)

K_f : coefficient (6-7 for horizontal chain arrangement)

q : chain weight per meter (kg/m)

a : center distance of chain (m)

Thus,

$$F_f = 9.8 \times 6 \times 0.33 \times 0.34 = 6.59\ N$$

3.2.2. Topology optimization parameter

The first step in the topology optimization stage is to determine the location of the fixture, in this case 6 bolt holes. The next step is to place the force on each sprocket tooth, which is $F = F_1 + F_e + F_f \approx 92\ N$. Then determine the goals and constraints, in this case, the mass constraint is 90% reduction. The next step is to determine the preserved region in the manufacturing control section. The preserved region is the area where the part must not be lost due to the overall topology optimization stage. The last step is to mesh and run the topology.

3.2.3. Topology optimization result

After going through the process above, the results of the optimization topology are obtained as shown in **Figure 3**. On the right side of the image there is a description showing the parts of the component that are OK to remove (blue color region) and must be kept (yellow color region). The results of this topology optimization are then exported into a separate file to be compared with the original file.

3.3. Re-Design

The re-design begins by combining the topology optimization result files with the original files in an assembly. The next step is to create a hole pattern on the original file by tracing the hole pattern on the topology optimization result file, as shown in Figure 4a. A 5 mm radius fillet was added to the hole pattern to reduce stress concentration. The hole pattern is then extruded cut, and the file is saved as a re-design edition, as shown in Figure 4b. The re-design version has a mass of 194.56 grams compared to the original version, 578.71 grams.

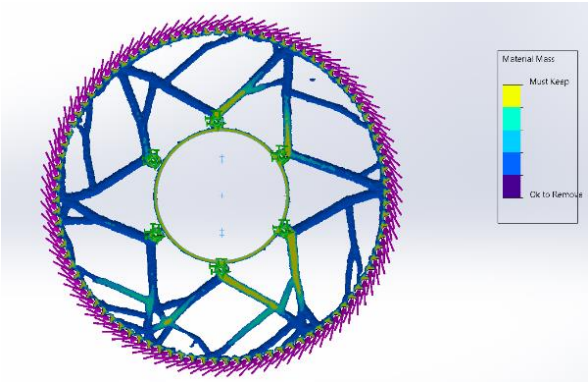

Figure 3. Topology optimization result

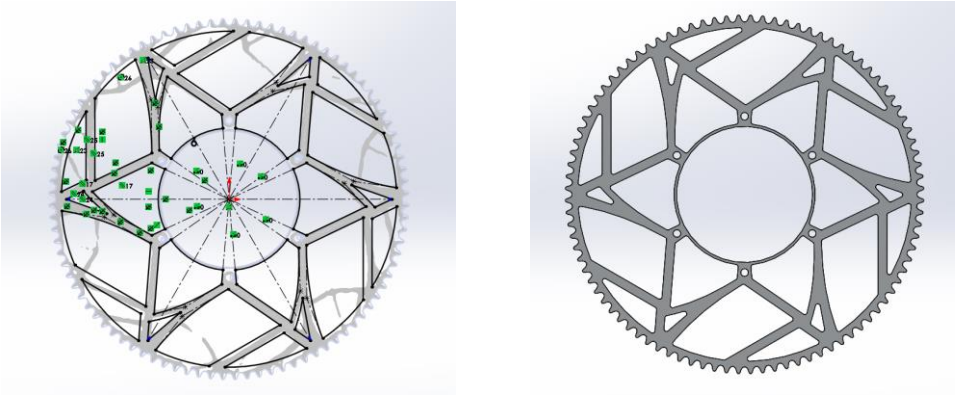

(a) **(b)**

Figure 4. Redesign process (a) hole pattern tracing, and (b) re-design result

Static Simulation

The static simulation stage is used to verify that the redesign results have the same strength. The simulation parameters are the same as those in the topology optimization stage. The static simulation results show that the maximum von Misses stress is valued at 2.256×10^8 N/m^2, about 55% below yield strength, 5.050×10^8 N/m^2, as shown at Figure 5. The results of this static simulation show that the redesigned version is considered strong enough to receive the appropriate forces.

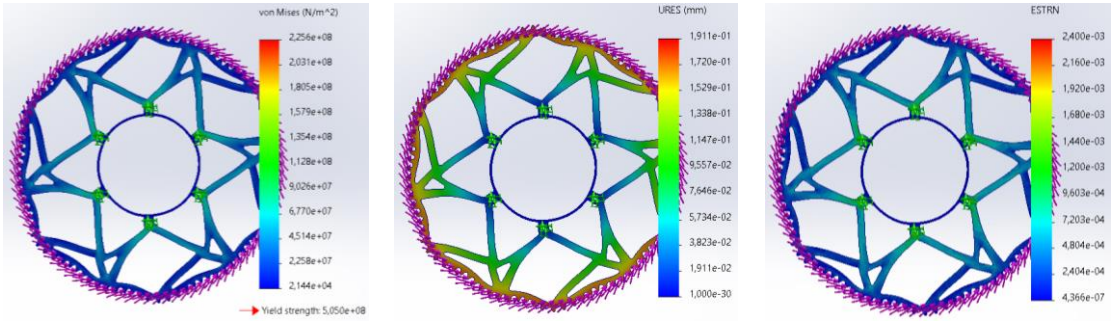

(a) (b) (c)

Figure 5. Static simulation (a) von Mises, (b) displacement, and (c) strain result of re-design sprocket

4 Conclusions

The topology optimization process with manual tracing resulted in a sprocket design with a mass reduction of 66% of its original version. After being retested with static simulation, the von Misses stress was only 55% of the yield strength at most. This result is considered good for later production and use in electric prototype vehicles. Although it is rated as good in terms of software, the rear sprocket needs to be fabricated from the same material and tested under appropriate loads before being finally installed on the vehicle.

Acknowledgements

This research is completely compiled by the author independently. All forms of analysis, interpretation, and writing are the result of personal thoughts without direct involvement of other parties.

References

[1] A. Y. W. Kurniawan, A. A. Setiawan, and A. Budiman, “The Impact of Electric Vehicle on Road Transportation in Indonesia: Energy Demand and CO2 Emission,” *JPSE (Journal Phys. Sci. Eng.*, vol. 5, no. 2, pp. 36–45, 2020, doi: 10.17977/um024v5i22020p036.

[2] F. Saleh *et al.*, “Pedoman Kontes Mobil Hemat Energi (KMHE) Perguruan Tinggi 2024,” 2024.

[3] A. H. Astyanto, Y. R. Yanto, and A. B. W. Adi, “A Study of Statics on Driyarkara Electric Automobile Chassis Prototype,” *Int. J. Appl. Sci. Smart Technol.*, vol. 2, no. 1, pp. 35–44.

[4] B. Lizarribar, B. Prieto, M. Martinez-Iturralde, and G. Artetxe, “Novel Topology Optimization Method for Weight Reduction in Electrical Machines,” *IEEE Access*, vol. 10, no. May, pp. 67521–67531, 2022, doi: 10.1109/ACCESS.2022.3185741.

[5] H. Nagamoto, K. Kobayashi, and H. Fujita, “Stiffness optimization process using topology optimization techniques and lattice structures,” *SAE Tech. Pap.*, pp. 92–97, 2022, doi: 10.4271/2022-32-0078.

[6] Y. Zhang, “Topology Optimization of a Chain Drive’s Sprocket of Aprilia RS 125 Sport Bike,” *Int. J. Front. Sociol.*, vol. 2, no. 9, pp. 35–47, 2020, doi: 10.25236/IJFS.2020.020906.

[7] J. Li, J. Tan, and J. Dong, “Lightweight Design of front suspension upright of electric formula car based on topology optimization method,” *World Electr. Veh. J.*, vol. 11, no. 1, 2020, doi: 10.3390/WEVJ11010015.

[8] D. A. Tristanto, S. Mulyadi, M. N. Kustanto, A. Triono, and I. Hardiatama, “Analisis optimasi topologi desain support bracket pada steering main shaft mobil TITEN EV-2,” *Turbo J. Progr. Stud. Tek. Mesin*, vol. 12, no. 1, pp. 63–69, 2023, doi: 10.24127/trb.v12i1.2388.

[9] B. Ardjuna, B. Setiyana, and I. Haryanto, “Optimasi Desain Swingarm Tipe Monoshock Dua Lengan Dengan Software Solidworks,” *J. Tek. Mesin S-1*, vol. 12, no. 2, pp. 1–10, 2024.

[10] B. R. Duke, *Mechanical Power Transmission.*, vol. 26, no. 295. 1979. doi:

10.4324/9781315737973-28.

[11] D. Berjoza, I. Jurgena, and R. Millers, “Effect of electric vehicle mass change on energy consumption and the range,” *Agron. Res.*, vol. 22, no. 3, pp. 1089–1097, 2024, doi: 10.15159/AR.24.052.

This page intentionally left

IJASST
International Journal of
Applied Sciences and Smart Technologies
p-ISSN 2655-8564, e-ISSN 2685-943

AUTHOR GUIDELINES

Author guidelines are available at the journal website:
http://e-journal.usd.ac.id/index.php/IJASST/about/submissions#authorGuidelines

IJASST
International Journal of
Applied Sciences and Smart Technologies
p-ISSN 2655-8564, e-ISSN 2685-943

This page intentionally left blank